

**OPERATIONAL SEASONAL CLIMATE FORECAST METHODS
AND SKILLS OVER THE SAHELIAN REGION OF WEST AFRICA**

BY

**SITTA, AISSATOU
Eng., MSc. (Agrometeorology, Biosystems Engineering)
MET/20/7730**

June, 2025

**OPERATIONAL SEASONAL CLIMATE FORECAST METHODS
AND SKILLS OVER THE SAHELIAN REGION OF WEST AFRICA**

BY

SITTA, AISSATOU

Eng., MSc. (Agrometeorology, Biosystems Engineering)

MET/20/7730

A Thesis of the Doctoral Research Programme of the West African Climate System Under the West African Science Service Centre on Climate Change and Adapted Land Use (WASCAL) in the Department of Meteorology and Climate Science submitted to
the School of Postgraduate Studies in partial fulfilment of the requirements for the award of the degree of Doctor of Philosophy in Meteorology and Climate Science of the Federal University of Technology, Akure, Nigeria.

June, 2025

DECLARATION

I hereby declare that this Thesis was written by me and is a correct record of my own research work. It has not been presented in any previous application for any degree of this or any other University. All citations and sources of information are clearly acknowledged by means of references.

Candidate's Name

Sitta, Aissatou

Signature:

Date:

CERTIFICATION

We certify that this Thesis entitled “Operational Seasonal Climate Forecast Methods and Skills Over The Sahelian Region of West Africa” is the outcome of the research carried out by Sitta, Aissatou in the Department of Meteorology and Climate Science, The Federal University of Technology, Akure, Nigeria.

Major Supervisor's Name

Dr. S.B. Traore

Signature:



Date:

Co-Supervisor's Name

Prof. I. A Balogun

Signature:

Date:

Co-Supervisor's Name

Prof. H. Paeth

Signature:

Date:

Advisor's Name

Dr. P. Laux

Signature:

Date:

ABSTRACT

In the context of increasing climate change and variability, reliable climate seasonal forecasts play critical role in agricultural planning. Recurring droughts, erratic rainfall, and limited adaptive capacity in the Sahel have highlighted the need for timely and usable climate information to enhance resilience among smallholder farmers. The West African Regional Climate Outlook Forums (WARCOF or PRESASS in French) forecasting system, predicts annually the rainy season key parameters (*season cumulative rainfall, onset date, cessation date and length of dry spells*). The WARCOF often shows significant percentage of forecast mismatches with observation. Thus, it urges to evaluate the performance and practical relevance of the WARCOF/PRESASS approach that has been used since 2011. The research aimed to assess the technical skill of the forecasting system, identify pathways to improve prediction accuracy, and examine how farmers access and utilize forecast information. Specifically, it was achieved through: first by the evaluation of the forecast skills for onset, cessation, and dry spells; then by the research on alternative predictors and statistical methods for forecast enhancement; and finally by the investigation on the dissemination and adoption of forecasts information among smallholders farmers. The guiding research question was: how can seasonal climate forecasts be improved and effectively communicated to strengthen smallholders' adaptive strategies in West Africa? A mixed-methods approach was adopted. Quantitative forecast verification techniques (such as reliability diagrams, ROC curves, and Brier scores) were used to analyze historical forecasts against observed data from 1991 to 2023. The Climate Predictability Tool (CPT) was applied for statistical modelling using sea surface temperature (SST) anomalies, precipitation hindcasts, and newly tested predictors like April-May-June (AMJ) cumulative

rainfall and wet-day frequencies. Additionally, qualitative data obtained from a baseline survey of 619 farmers and quantitative data from two-year demonstration trials in four municipalities of southwest Niger were used. Key findings indicate that in the WARCOF/PRESASS approach, onset forecasts demonstrated higher skill and reliability compared to cessation and dry spells, particularly when using precipitation hindcasts (e.g., NASA and CFSv2) as predictors. Incorporating wet-days and AMJ rainfall totals as alternative predictors significantly improved forecast skill. However, dry spell forecasts exhibited low discrimination ability. The field-level study revealed that only 42.3% of farmers had access to forecasts, and those who fully applied the information achieved measurable yield gains (up to 234 kg/ha) compared to traditional practices, validating the forecast's real-world utility. The positive impact of the forecast information on yield was more noticeable in drought prone areas (trials sites in Sahelian and Sudano-Sahelian zones) compared to wetter areas in the Sudanian zone; showing the relevance of climate information dissemination in the most vulnerable area. The study concludes that enhancing the PRESASS forecasting system requires scientific recalibration using high-performing predictors and user-oriented communication strategies. Co-production of forecasts, capacity building, and integration with local agricultural calendars are essential to maximize uptake and effectiveness. The findings contribute to climate resilience strategies and support SDGs 1 (No Poverty), 2 (Zero Hunger), and 13 (Climate Action), as well as WASCAL's priorities on sustainable agriculture and climate risk reduction.

ACKNOWLEDGMENTS

The German Ministry of Education and Research (BMBF) through the West African Science Center on Climate Change and Adapted Land Use (WASCAL) sponsored the entire doctoral program. I am very thankful to BMBF and WASCAL for providing me this opportunity and the financial support to achieve my study objectives. Similar appreciation goes to the AGRHYMET Regional Climate Center for West Africa and the Sahel for hosting and facilitating my field data collection work, for providing complementary funding to support this field work through the collaboration with the intra ACP/GFCS/ClimSA project, and for giving me access to data and technical support essential for the analytical components of this work. My sincere thanks also go to the Mawazo Institute that offered partial financial support to my 2nd year field trials and allowed me to attend several relevant online courses enhancing our research and leadership skills through its fellowship program supporting African female PhD students in order to reach a critical number of women scientists over the continent.

I'm grateful to the Niger government for giving me the authorization to seize this chance, for providing the climate stations data used in this work and for the logistic support during some of my field trips. In particular, I would like to express my gratitude to the Director of the Niger National Meteorological Service, Mr. Katiellou Gaptia Lawan and to the former Minister of Transportation, the late Alma Oumarou, may his soul rest in peace, who did not hesitate to grant the study leave with their encouragement to me as the first female staff in the history of the Meteorological Service willing to undertake PhD level studies.

I would like to express my sincere gratitude to the Director and staff of the WASCAL Headquarter in Accra, Ghana; the Director and the staff of the WASCAL DRP-WACS,

FUTA, Nigeria for their efforts in making this program successful. My thanks also go to Prof. Debo Adeyewa, the former DRP-WACS Director for his encouragement and support. I'm grateful to all the Climatology Working Group and the Earth Observation Research Cluster at the Department of Geography, University of Wuerzburg, especially Drs. Michael Thiel, Sabine Oppman, Felix Pollinger, Luzia Keupp, Fredy, Daniel, Katrin for their assistance during my research stay there. My special regards to Mrs. Angelika Scharl, coordinator of the group "Get-together for Visiting Academics" of the University of Wuerzburg and her team for periodical socialization meetings at the University guesthouse and the guided monthly field trips around Wuerzburg that made our stay very pleasant and informative. My regards also to her husband Christoph for his kindness and hospitality.

I would like to express my heartfelt gratitude to my major supervisor, Dr. Seydou B. Traore, and co-supervisors, Prof. Ifeoluwa A. Balogun, Prof. Heiko Paeth, and Dr. Patrick Laux for their invaluable guidance, encouragement, and constructive feedback throughout this research journey. Their mentorship has been instrumental in shaping the direction and quality of this dissertation

I extend my appreciation to the colleagues Dr. Tinni Halidou Seydou, Mahamadou Dan Ladi from AGRHYMET Center, and M. Kossomi Mahamadou, Allassane Mayaki Abdoullahim, Ibrahim Mamane, Iladaoula Drague from the Niger Meteorological Service for their key role in the data collection process. Special thanks go to colleagues from the National Institute for Agronomic Research (INRAN) for facilitating the access to millet seeds and the soil data collection and analysis, the colleagues from ICRISAT Niger for yield data lab analysis, the experiments data collectors and extension agents Mr. Moussa Oumarou, Mariama Amadou, Oumarou Nameywa, Youssouf Djibrilla, Abdoulaye Amadou

in the municipalities of Guéchémé, Tounouga, N'Dounga, and Kiota, whose dedication enabled the successful implementation of fieldwork and demonstration trials.

I am deeply grateful to the 619 farmers and the 60 pilot farmers in Niger who generously shared their time, insights, and land for this research. Their trust and cooperation are the backbone of this study.

My appreciation also goes to my fellow WASCAL students, particularly Dr. Laouali Ibrahim Tanimoun from the 4th batch for his relevant advices and those in the 5th batch of DRP-WACS for the great memories and for making our stay in Akure enjoyable despite the frustrations of being far from home.

I am extremely grateful to Prof. Kolawole T. Gbadamosi from FUTA and his wife Alhaja Kudirat Abosedo Gbadamosi for their kindness, hospitality and continuous support.

Special thanks to my whole family and friends for their unwavering emotional and moral support. Your encouragement has been a source of strength during the most challenging phases of this work. I particularly appreciate very much the great support from my sister, brother, children and my dearest husband, Prof. Rabani Adamou whose continuous care, academic advices and various support throughout this journey have paved my way.

I acknowledge the institutions and colleagues whose work I have built upon and cited throughout this dissertation. This work is also a reflection of the collaborative efforts of researchers committed to advancing climate services and agricultural resilience in West Africa.

Above all this, I thank Allah, the Almighty, the Merciful, for granting me grace, health, wisdom, and the strength to pursue my studies to this point. All praises go to Him.

DEDICATION

This dissertation is dedicated:

To the cherished memory of my beloved parents, whose sacrifices, values, and dreams for me laid the foundation for all my achievements. Your absence has been deeply felt throughout this journey, but your spirit has remained my greatest strength and your legacy continues to guide and inspire me.

To my dear siblings, friends and colleagues for your endless encouragement, prayers, and belief in me.

To my loving husband and our wonderful children, thank you for your love, patience, and understanding during the many months and miles that separated us. Your unwavering support gave me the courage and motivation to persevere while studying far from you.

This work is for you all—with all my heart.

TABLE OF CONTENTS

DECLARATION	i
CERTIFICATION	ii
ABSTRACT	iii
ACKNOWLEDGMENTS	v
DEDICATION.....	viii
TABLE OF CONTENTS	ix
LIST OF TABLES	xiii
LIST OF FIGURES	xiv
LIST OF ACRONYMS AND ABBREVIATIONS.....	xxi
CHAPTER ONE	1
INTRODUCTION	1
1.1. Background and Context.....	2
1.2. Problem Statement / Justification	3
1.3. Aim and Objectives of the Research	4
1.4. Research questions	5
1.5. Research scope.....	6
1.6. Contribution to knowledge	6
1.7. Structure of the document	7
CHAPTER TWO	8
LITERATURE REVIEW.....	8
2.1. Conceptual review	8
2.2. Empirical review of the existing seasonal forecast systems over West Africa	9
2.3. Theoretical review: Importance and predictability of rainfall intraseasonal parameters for agriculture	15
2.3.1. Onset predictability	15
2.3.2. Cessation date forecast	19
2.3.3. Dry spell duration forecast	21
2.4. Overview on the WARCOF forecasting system	25
2.4.1. Brief description of the PRESASS forecasting system	25
2.4.2. Towards new generation of WARCOF forecasting system and forecast information communication.....	27
2.4.3. Existing gap in literature	27

CHAPTER THREE.....	31
METHODOLOGY.....	31
3.1. Overall Research approach	32
3.2. Description of the study areas	32
3.2.1. Study area for assessment of forecast information use.....	35
3.3. Data	38
3.3.1. Climate observational data.....	38
3.3.2. Global Circulation Model output data and forecast maps	41
3.3.3. Field data	0
3.3.3.1. Survey data.....	0
3.3.3.2. Field experiments data.....	0
3.3.3.3. Soil data.....	1
3.4. Methods	3
3.4.1. Forecast verification	3
3.4.2. Improvement of the season parameters prediction process	4
3.4.3. Assessment of forecast information dissemination and use.....	5
3.4.3.1. Field survey sampling method and implementation	5
3.4.3.2. Field trials data collection and analysis methods.....	9
CHAPTER FOUR.....	15
RESULTS AND DISCUSSION	15
4.1. Performance assessment of the PRESASS method regarding the forecast of season onset date, cessation date and dry spells	15
4.1.1. Assessment of the statistical aspects of the PRESASS forecasting system regarding season characteristics forecast.....	15
4.1.1.1. Assessment of correlation between SST anomalies and season parameters using regression models	15
4.1.1.2. Verification of statistical forecast using CPT based on best combinations of predictor and predictand.....	20
4.1.2. Assessment of the PRESASS overall approach in forecasting season characteristics	60
4.2. Possible ways to improve the dynamical aspects of the forecasting system	67
4.2.1. Using wet days as predictors to forecast season onset dates, cessation dates and dry spell duration.....	68

4.2.1.1.	Assessment of the correlation between wet days and season parameters forecast over Sahel	68
4.2.1.2.	Verification of forecasts made based on wet days frequency as predictors....	71
4.2.2.	Using cumulative rainfall to forecast season onset dates over Niger	87
4.2.2.1.	Assessment of the correlation between cumulative rainfall and season onset dates	87
4.2.2.2.	Verification of forecast made using AMJ cumulative rainfall as predictors	88
4.3.	Forecast information dissemination and on-farm use: Current state and perspectives	95
4.3.1.	Current state of the forecast information use from survey outcomes in Southwest Niger	95
4.3.1.1.	Forecast information dissemination	96
4.3.1.2.	Perception and use of the forecast products and other climate services.....	99
4.3.1.3.	Major constraints to agriculture productivity and crop yield	100
4.3.1.4.	Needs Assessment for Further Climate Services.....	101
4.3.2.	Assessing the impacts of forecast information use on crop yield through on-farm demonstration trials	108
4.4.	General Discussion	117
4.4.1.	Forecast performance and predictability of season parameters	118
4.4.1.1.	Current predictor and model performance	118
4.4.1.2.	Reliability and discrimination of forecasts	119
4.4.2.	Added value of potential new predictors: wet days frequency and cumulative rainfall	120
4.4.3.	Forecast dissemination and user engagement for forecast information use	120
CHAPTER FIVE	124
CONCLUSIONS AND RECOMMENDATIONS	124
5.1.	Conclusions	124
5.2.	Recommendations	125
5.3.	Contributions to Knowledge	127
5.4.	Limitations, suggestions and implications for Further Studies	129
REFERENCES	131
APPENDICES	139
Appendix A:	Field Survey questionnaire.....	139
Appendix B:	Experiments data collection forms	145

Appendix B1: Farmers and plots identification form	145
Appendix B2: Plots monitoring form	149
Appendix B3: Cropping activities monitoring form	150
Appendix B4: Yield data collection form	151
Appendix C: Goodness indices from the cross-validation regressions runs using CPT	152
Appendix D: Correlation coefficients from the regression between the actual onset dates and the rainfall totals over various time windows within the season at station level in Niger	187

LIST OF TABLES

Table 3.1: Summary of Global Circulation Models (GCMs) and Systems used	0
Table 3.2: Background information of the targeted municipalities	8
Table 4.1: SST domains used to build and run the regression models	17
Table 4.2 : Pearson correlation coefficients from regression models between SST hindcasts and season parameters	19
Table 4.3: Summary of the key findings from the skill maps analysis for onset date forecasting	22
Table 4.4 : Summary of the key findings from the skill maps analysis for cessation date forecasting	28
Table 4.5 : Summary of the key findings from the skill maps analysis for the early season dry spell duration	34
Table 4.6 : Summary of the key findings from the skill maps analysis for the end season dry spell duration	41
Table 4.7 : Forecast verification metrics for (a) Onset date, (b) Cessation date, (c) Early season dry spells duration, (d) End of season dry spells duration	61
Table 4.8 : Pearson correlation coefficient (r) between wet days monthly / seasonal frequency and onset dates / early season dry spells duration (ESDS) duration	69
Table 4.9: Pearson correlation coefficient (r) between wet days monthly / seasonal frequency and cessation date / late season dry spells duration (LSDS) duration	70
Table 4.10 : Information reception status through the various dissemination channels	97
Table 4. 11 : Preferred information dissemination channels by farmers	98
Table 4.12: ANOVA Table comparing the 3 treatments	113
Table 4. 13: Tukey HSD test results	115

LIST OF FIGURES

Figure 3.1. Mean annual precipitation in West Africa and bioclimatic zones	34
Figure 3.2. Field work study area: municipalities of Kiota, N'Dounga, Guéchémé, and Tounouga in red color	36
Figure 3. 3. Interannual variability of rainfall in the study area over the period 1981-2020	37
Figure 3. 4. Glocalization of rain gauges stations used in the study area	39
Figure 3. 5. Experiments design at village level	10
Figure 4.1. Skill maps (a = pearson correlations and b = hit skill score) for onset retroactive forecast using sst anomaly hindcast from nasa model (initialized in april with lead time july) as predictor and onset date historical data	23
Figure 4.2. Skill maps (a = pearsons correlation and b = hit skill score) for onset retroactive forecast using precipitation hindcast from cfsv2 model (initialized in april with lead time july) as predictor and onset date historical data	24
Figure 4.3. Skill maps (a = pearsons correlation and b = hit skill score) for onset retroactive forecast using sst anomaly hindcast from cfsv2 model (initialized in april with lead time may) as predictor and onset date historical data	25
Figure 4.4. Skill maps (a = pearsons correlation and b = hit skill score) for onset retroactive forecast using sst anomaly hindcast from cmc1 (initialized in april with lead time jja) as predictor and onset date historical data	26
Figure 4.5. Skill maps (a = pearsons correlation and b = hit skill score) for cessation retroactive forecast using precipitation hindcast from nasa model (initialized in april with lead time son) as predictor and cessation date historical data	29
Figure 4.6. Skill maps (a = pearsons correlation and b = hit skill score) for cessation retroactive forecast using sst anomaly hindcast from cmc1 model (initialized in april with lead time august) as predictor and cessation date historical data	30
Figure 4.7. Skill maps (a = pearsons correlation and b = hit skill score) for cessation retroactive forecast using sst anomaly hindcast from cmc2 model (initialized in april with lead time august) as predictor and cessation date historical data	31
Figure 4.8. Skill maps (a = pearsons correlation and b = hit skill score) for cessation retroactive forecast using sst anomaly hindcast from nmme model (initialized in april with lead time aso) as predictor and cessation date historical data	32
Figure 4.9. Skill maps (a = pearsons correlation and b = hit skill score) for early season dry spells duration retroactive forecast using sst anomaly hindcast from cmc1 model (initialized in april with lead time jja) as predictor and early season dry spells duration historical data	35

- Figure 4.10. Skill maps (a = pearsons correlation and b = hit skill score) for early season dry spells duration retroactive forecast using precipitation hindcast from nasa model (initialized in april with lead time july) as predictor and early season dry spells duration historical data 36
- Figure 4.11. Skill maps (a = pearsons correlation and b = hit skill score) for early season dry spells duration retroactive forecast using sst anomaly hindcast from cmc2 model (initialized in april with lead time may) as predictor and early season dry spells duration historical data 37
- Figure 4.12. Skill maps (a = pearsons correlation and b = hit skill score) for early season dry spells duration retroactive forecast using sst anomaly hindcast from gfdl (initialized in april with lead time july) as predictor and early season dry spells duration historical data 38
- Figure 4.13. Skill maps (a = pearsons correlation and b = hit skill score) for early season dry spells duration retroactive forecast using precipitation hindcast from nasa model (initialized in april with lead time mjj) as predictor and early season dry spells duration historical data 39
- Figure 4.14. Skill maps (a = pearsons correlation and b = hit skill score) for end season dry spells duration retroactive forecast using sst anomaly hindcast from gfdl (initialized in april with lead time jas) as predictor and end season dry spells duration historical data 42
- Figure 4.15. Skill maps (a = pearsons correlation and b = hit skill score) for end season dry spells duration retroactive forecast using sst anomaly hindcast from nmme model (initialized in april with lead time jas) as predictor and late season dry spells duration historical data 43
- Figure 4.16. Skill maps (a = pearsons correlation and b = hit skill score) for end season dry spells duration retroactive forecast using sst anomaly hindcast from cfsv2 (initialized in april with lead time september) as predictor and end season dry spells duration historical data 44
- Figure 4.17. Skill maps (a = pearsons correlation and b = hit skill score) for end season dry spells duration retroactive forecast using sst anomaly hindcast from cfsv2 (initialized in april with lead time august) as predictor and late season dry spells duration historical data 45
- Figure 4.18. Skill maps (a = pearsons correlation and b = hit skill score) for end season dry spells duration retroactive forecast using precipitation anomaly hindcast from nasa model (initialized in april with lead time october) as predictor and late season dry spells duration historical data 46
- Figure 4.19. Reliability diagrams (a) and roc curves (b) for onset forecast using sst anomaly hindcast from the nasa model initialized in april for july lead time. 52

- Figure 4.20. Reliability diagrams (a) and roc curves (b) for onset forecast using precipitation hindcast from the cfsv2 model initialized in april for july lead time. 53
- Figure 4.21. Reliability diagrams (a) and roc curves (b) for cessation date forecast using precipitation hindcast from the nasa model initialized in april for son lead time. 54
- Figure 4.22. Reliability diagrams (a) and roc curves (b) for cessation date forecast using sst anomaly hindcast from the cmc1 model initialized in april for august lead time. 55
- Figure 4.23. Reliability diagrams (a) and roc curves (b) for early season dry spell duration forecast using sst anomaly hindcast from the cmc1 model initialized in april for jja lead time. 56
- Figure 4.24. Reliability diagrams (a) and roc curves (b) for early season dry spell duration forecast using sst anomaly hindcast from the nasa model initialized in april for july lead time. 57
- Figure 4.25. Reliability diagrams (a) and roc curves (b) for late season dry spell duration forecast using sst anomaly hindcast from the gfdl model initialized in april for jas lead time. 58
- Figure 4.26. Reliability diagrams (a) and roc curves (b) for late season dry spells duration forecast using sst anomaly hindcast from the nmme model initialized in april for jas lead time. 59
- Figure 4.27. Reliability diagrams (a), sharpness histograms (b) and roc curves (c) for onset date forecast. In subfigure a), the thick colored lines show the reliability curves of the 3 forecast categories, the dash thin diagonal represents the line of perfect reliability 62
- Figure 4.28. Reliability diagrams (a), sharpness histograms (b) and roc curves (c) for cessation date forecast. In subfigure a), the thick colored lines show the reliability curves of the 3 forecast categories, the dash thin diagonal represents the line of perfect reliability 63
- Figure 4.29. Reliability diagrams (a), sharpness histograms (b) and roc curves (c) for early season dry spell duration forecast. In subfigure a), the thick colored lines show the reliability curves of the 3 forecast categories, the dash thin diagonal represents the line of perfect reliability 64
- Figure 4.30. Reliability diagrams (a), sharpness histograms (b) and roc curves (c) for end season dry spell duration forecast. In subfigure a), the thick colored lines show the reliability curves of the 3 forecast categories, the dash thin diagonal represents the line of perfect reliability 65
- Figure 4.31. Reliability diagrams (a) and roc curves (b) for onset forecast using wet days frequency during june as predictor. 72
- Figure 4.32. Reliability diagrams (a) and roc curves (b) for onset forecast using wet days frequency during july as predictor. 73

Figure 4.33. Reliability diagrams (a) and roc curves (b) for onset forecast using wet days frequency during jja as predictor.	74
Figure 4.34. Reliability diagrams (a) and roc curves (b) for early season dry spells duration forecast using wet days frequency during may as predictor.	76
Figure 4.35. Reliability diagrams (a) and roc curves (b) for early season dry spells duration forecast using wet days frequency during june as predictor.	77
Figure 4.36. Reliability diagrams (a) and roc curves (b) for early season dry spells duration forecast using wet days frequency during amj season as predictor.	78
Figure 4.37. Reliability diagrams (a) and roc curves (b) for cessation forecast using wet days frequency during aso as predictor.	80
Figure 4.38. Reliability diagrams (a) and roc curves (b) for cessation forecast using wet days frequency during son period as predictor.	81
Figure 4.39. Reliability diagrams (a) and roc curves (b) for cessation forecast using wet days frequency during october as predictor.	82
Figure 4.40. Reliability diagrams (a) and roc curves (b) for end season dry spells duration forecast using wet days frequency during august as predictor.	84
Figure 4.41. Reliability diagrams (a) and roc curves (b) for end season dry spells duration forecast using wet days frequency during september as predictor.	85
Figure 4.42. Reliability diagrams (a) and roc curves (b) for end season dry spells duration forecast using wet days frequency during aso period as predictor.	86
Figure 4.43. Reliability diagrams (a) and roc curves (b) for onset forecast made by using amj rainfall hindcast from cfsv2 as predictor.	89
Figure 4.44. Reliability diagrams (a) and roc curves (b) for onset forecast made by using amj rainfall bias corrected hindcast from cfsv2 as predictor.	90
Figure 4.45. Reliability diagrams (a) and roc curves (b) for onset forecast made by using gpcc rainfall observation data cumulated over amj period as predictor.	92
Figure 4. 46. Reliability diagrams (a) and roc curves (b) for onset forecast made by using chrips rainfall observation data cumulated over amj period as predictor.	93
Figure 4.47. Reliability diagrams (a) and roc curves (b) for onset forecast using station rainfall data cumulated over amj period as predictor.	94
Figure 4.48. Farmer’s perception of the different types of climate information provided to them	102
Figure 4.49. Farmer’s appreciation of the different types of seasonal forecast products.	103
Figure 4.50. Application of climate information to on-farm activities.	104

Figure 4.51. Farmers' appreciation of seasonal forecast products.	105
Figure 4.52. Major constraints encountered during the growing season.	106
Figure 4.53. Additional climate services needed by farmers	107
Figure 4.54. Average millet grain yield (kg/ha) a) per treatment and per municipality over the 2 years of experiments; b) per treatment, per year and per municipality	111
Figure 4. 55. Average millet yield (kg/ha) per treatment and per year at tounouga	112
Figure 4.56. Yield differences across treatments and municipalities	116

LIST OF PLATES

Plate 3. 1 : Soil sampling for soil fertility analysis	2
Plate 3. 2 : Dissemination of crop inputs kits, forecast information and recommendations at NDounga, Guecheme and Tounouga to farmers during field trip before the starting of the rainy season	13
Plate 3. 3 : Millet harvesting and weighing at Tounouga	14
Plate 4. 1: Millet crops in experiment plot (left) and control plot (right) during the cropping cycle at Tounouga	110

LIST OF EQUATIONS

Equation (3. 1): Probabilistic forecast resolution Estimation equation	3
Equation (3. 2): Sloven formula	5
Equation (3.3): Equation to estimate the size of the agricultural population of the municipality	6

LIST OF ACRONYMS AND ABBREVIATIONS

ACMAD	African Center for Meteorological Applications for Development
AGRHYMET	Agro-Hydro-Meteorology
AGRHYMET CCR-AOS	AGRHYMET Centre Climatique Régional pour l'Afrique de l'Ouest et le Sahel (AGRHYMET Regional Climate Center for West Africa and the Sahel)
ANADIA	Climate Change Adaptation, Disaster Prevention and Agricultural Development for Food Security
CCA	Canonical Correlation Analysis
CCMS3	Community Climate System Model 3
CFSv2	Climate Forecast System Version 2
CMC2	Canadian Meteorological Centre version 2 (CMC2)
CPT	Climate Predictability Tool
C3S	Copernicus Climate Change Service
DMN	Direction de la Météorologie Nationale, Niger
ECMWF	European Centre for Medium-Range Weather Forecasts
ESDS	Early Season Dry Spells
GCM	Global Circulation Model

GPCC	Global Precipitation Climatology Center
CHRIPS	Climate Hazards Group InfraRed Precipitation with Station data
GFDL	Geophysical Fluid Dynamics Laboratory
GloSea4	Global Seasonal Forecasting System version 4
GPCs	Global Producing Centers
GPC-LRF	Global Predicting Centers - Long Range-Forecast
HSS	Hit Skill Score
IFDC	International Fertilizer Development Center
INRAN	Institut National de la Recherche Agronomique du Niger (National Institute for Agronomic Research of Niger)
INS	Institut National de la Statistique (National Institute for Statistics)
IRI	International Research Institute for Climate and Society
ITCZ	Intertropical Convergence Zone
LSDS	Late Season Dry Spells
MF3	Météo France version 3
MSC	Meso-Scale Convective

NCEP	National Center for Environmental Prediction
NMHS	National Meteorological and Hydrological Services
NMME2	North American Multi-Model Ensemble phase 2
PASEC	Projet d'Appui à la Sensibilisation et la Promotion de l'Agriculture Sensible aux Risques Climatiques (World Bank Climate Smart Agriculture Support Project)
PRESASS	Prévisions Climatiques Saisonnières en Afrique Soudano Sahélienne
PyCPT	Python Interface to the Climate Predictability Tool
RCOFs	Regional Climatic Outlook Forums
RENALOC	Répertoire Nationale des Localités du Niger
ROC	Relative Operating Characteristic
RPSS	Ranked Probability Skill Score
SPSS	Statistical Package for the Social Sciences
SST	Sea Surface Temperature
S2S	Sub-seasonal to Seasonal
TRMM	Tropical Rainfall Measuring Mission
WAM	West-African Monsoon

WARCOF	West Africa Regional Climate Outlook Forum
WASCAL	West African Science Service Centre on Climate Change and Adapted Land Use
WMO	World Meteorological Organization
WRF	Weather Research and Forecasting

CHAPTER ONE

INTRODUCTION

Agriculture in many regions of the world is heavily dependent of weather and climate conditions. Rainfed agriculture is the main component of food production in Africa, contributing over 90% of the continent's agricultural output and sustaining the livelihoods of the majority of rural populations. It is especially crucial in sub-Saharan Africa, where irrigation infrastructure is limited and most smallholder farmers rely almost entirely on seasonal rainfall for crop cultivation. However, its high dependence on seasonal and often erratic rainfall patterns makes it highly vulnerable to climate variability and change, posing significant risks to agricultural productivity and livelihoods (Rockström et al., 2010). Generally, in West Africa and in the Sahel in particular, the adverse effects of extreme weather conditions on Agriculture and food security are becoming recurrent as a result of climate change. The rapid population growth, progressive environmental change and natural resources degradation exacerbate those adverse effects of climate change (Adamou et al., 2021). The low adaptive capacity of farmers and the lack of climate-resilient infrastructure further emphasize these vulnerabilities (Rockström et al., 2010; Cooper et al., 2008; FAO, 2015). Seasonal climatic forecast has the potential as a key adaptation strategy to climate change negative impacts in Agriculture sector. However, the shortcomings related to the forecast method need to be assessed and reduced in order to let it play reliably its mitigating role.

This research aims to evaluate the skills of the West Africa Regional Outlook Forum (WARCOF) forecast method and identify strategies for more utilization of forecast information in farming system in Sahelian West Africa.

This chapter will introduce the study by discussing first the background and context, followed by the research problem, the research aims, the specific objectives and questions, the significance of the research, the limitations and the contributions to knowledge.

1.1. Background and Context

The major climatic risks observed in the West African Sahel are mainly droughts and floods (related to the spatio-temporal variability of rainfall), heat waves and sand storms. Indeed, in the large part of the West African sub-region, the climate is hot and semi-arid with a short rainy season (from June to October) and a long dry season (from November to May). The rainfall regime is characterized by a high spatial and temporal variability and depends on the behavior of the West African Monsoon (Tearfund, 2008). Hess et al. (1995); Bello (1996); Tarhule & Lamb (2003), found an inter-annual variability of the yearly totals ranging between 20 to 80% for the Sahel Savannah. This variability results in irregularity in rainfall patterns, random season onset and cessation dates, with occurrences of more or less long dry spells often happening at crucial stages of crop development. In the Sahel, the observed climate change and variability negative effects are huge in terms of intensity and spatial scale of the impacts.

Crops yield and smallholders' income are determined mostly by the quality of the rainy season. Well distributed rainfall conditions often result in better crops yield whereas prolonged dry spells, late onset or early cessation impact negatively the agriculture production and threaten the food security (Rauch et al., 2019). Knowing earlier the characteristics of the upcoming rainy season can help farmers and other actors in food security sector adapt to the negative effects of climate fluctuation. Reliable forecast information is therefore crucial in the decision-making process for good adaptation of Agriculture and food security to climate change and variability in West Africa where the welfare of communities relies heavily on rain-fed agricultural production.

Several adaptation strategies have been implemented through research and extension services for the resilience of the agricultural sector to these extreme weather events. These methods include the development of improved seeds, including drought-resistant varieties, short-cycle varieties (Mertz et al., 2009), the promotion of good farmer practices (Nyong et al., 2007), Assisted Natural Regeneration (ANR), climate services for the agricultural sector based on seasonal climate forecast, and numerical weather forecast (Sissoko et al., 2011).

Seasonal forecasts allow farmers adopt strategies according to the expected characteristics of the season, and thus make the right choice of crops and varieties, optimal periods for sowing in order to avoid false starts, better planning of cultivation operations according to the optimum periods.

1.2. Problem Statement / Justification

While several forecast systems have been developed for forecasting seasonal cumulative rainfall in Sudano-Sahelian Africa over the years, there are very few methods for predicting its intra-seasonal distribution, despite of the importance of that in Agriculture. Only few studies have been conducted on the predictability of the season onset and dry spells during the season (Sultan et al., 2020).

Currently, the best known and most used seasonal forecast method for rainfall intra-annual distribution characteristics in the region is the one that has been used since 2011 (AGRHYMET, 2011) during the West African Regional Climate Outlook Forums (WARCOF). This method provides probabilities of occurrence for four (4) key parameters of the rainy season which are the onset date, the cessation date, the durations of the longest dry spells during the early stage of the cropping season and at the end of the season. These seasonal forecast products are increasingly becoming essential decision support tools for rural producers (Bacci et al., 2020; Daron et al.,

2021). However, the forecast verification often shows significant percentage of forecast mismatching with observation. The biases and uncertainties related to the WARCOF forecasting system may stem from the challenges to predict the high variable west Africa monsoon rainfall system, the scarcity and quality of the observed rainfall data used as input of the model, the criteria used to define rainy season parameters as stated by Fitzpatrick et al., (2015) for the season onset definition, the forecasting models performance, biases related to forecasters risk aversion i.e. their fearing to give incorrect forecast as shown by Mason and Chidzambwa (2009), the subjective component in the forecast process (Mason and Chidzambwa, 2009; confirmed by Bliefernicht et al., 2019), the unappropriated verification procedures often used to evaluate that probabilistic forecast (Rauch et al., 2019), etc. Another shortcoming of the West Africa Regional Climate Outlook Forum (WARCOF) forecast is its broad regional scale which is not suitable for local application. All those factors make the farmers skeptical vis-a-vis the forecast products and they are mostly reluctant to use them in their cropping season planning. Therefore, it urges to find the way to reduce the observed biases and uncertainties and to make it usable by small scale farmers in order to help them trust the forecast outputs and adapt to climate change and variability.

1.3. Aim and Objectives of the Research

The aim of this study is to assess the operational seasonal climate forecast methods that have been used by AGRHYMET Regional Climatic Centre and West African Meteorological Services during the WARCOF to forecast rainy season parameters in order to improve the forecast products and to make it usable for small scale farmers adaptation to climate change and variability.

The specific objectives of the research are:

- evaluate the performance of the WARCOF forecast methods for forecasting rainfall onset and cessation dates, as well as dry spell durations over Sahelian countries;
- investigate ways to improve the WARCOF method by reducing the biases sources effects; and
- assess the forecast products at local level and identify strategies to engage smallholders for more on-farm use of the forecast information.

1.4. Research questions

In summary, considering that early knowledge about upcoming rainy season characteristics is very relevant to small scale farmers in the Sahel region, there is a need for a better understanding of biases and uncertainties related to the forecast of rainfall intra-seasonal characteristics over West Africa in general and over the Sahel region in particular. More specifically, the following research questions need to be addressed:

1. what are the typical skills and biases related to the forecast method used over the region to predict season onset, cessation and dry spells durations?
2. how to reduce the level of uncertainty in rainy season characteristics forecast in order to improve the WARCOF intraseasonal products?
3. which forecast products are needed locally and the strategies to engage small holder farmers for an extensive use of the seasonal forecast products?

The overall research question remains how we can unify outcomes from these three questions to propose an improved operational seasonal forecast method in order to support Sahelian farmers with more reliable forecast products.

1.5. Research scope

This research will assess the WARCOF / PRESASS forecasting system regarding three forecast products which are rainy season onset, cessation and dry spells and investigate the strategies for improved utilization of forecast information by farmers. The assessment aspects of the study will cover the whole Sahelian region of West Africa using observational dataset covering the period 1991 – 2021 while the end user’s engagement will be conducted through field surveys in four municipalities (N’Dounga, Guecheme, Tounouga and Kiota) of southwest Niger, and 2-years (2023-2024) on-farm demonstration trials implemented in three of the four municipalities.

The farmers are the main communities targeted in this study, however, the forecasters and researchers involved in the West Africa seasonal forecast may benefit also from the outcomes of the research.

1.6. Contribution to knowledge

The outcomes from this study will help improve the forecast of intraseasonal rainfall parameters performed by AGRHYMET Regional Climatic Center (A specialized Center of the Permanent Inter-State Committee for Drought Control in the Sahel (CILSS) and West African Meteorological Services. The output will strengthen the capacity of these institutions to provide more reliable forecast information that will be beneficial to end-users which are mainly smallholders farmers in the study area.

This research work will contribute to three of the United Nations Sustainable Development Goals (UN SDGs) which are SDG 1 No Poverty, SDG 2 Zero Hunger, SDG 13 Climate Action. The study is also in line with the WASCAL Priority Research Themes 2 and 4 which are respectively Risks and Vulnerability to Climate Extremes; Sustainable Agriculture / Climate Smart Landscape Nexus.

1.7. Structure of the document

The present document is structured around five chapters outlined as follows:

1. in Chapter One, the context of the study has been introduced. The research objectives and questions have been identified, and the value of such research discussed. The scope of the study has also been established;
2. in Chapter Two, the existing literature surrounding the seasonal forecast performance and limitations over West Africa and the forecast information use in Agriculture will be reviewed. The progress made in the improvement of the forecasting system and the gap from existing research will be highlighted;
3. in Chapter Three, the data and methods used will be presented. Specifically, the broader research design will be discussed, the limitations and the methodological choices will be justified, and the geographical area covered by the research will also be shown;
4. Chapter Four will present and interpret the research findings from data collection to data analysis processes; then the key results will be discussed accordingly by taking into account previous studies.
5. Chapter Five will draw conclusions and present recommendations and perspectives from this research.

CHAPTER TWO

LITERATURE REVIEW

This chapter will give a brief overview of the scholarly context about the main challenges surrounding the seasonal forecast of the rainfall variables that are important for Agriculture over West Africa in general and in the Sahel region in particular.

2.1. Conceptual review

Seasonal forecasts of cumulative rainfall and its related intraseasonal variables have become key decision-support and droughts/floods early warning information in climate sensitive sectors such as Agriculture, food security, water resources management. The regional climatic outlook forums (RCOFs) have been providing this information across many regions worldwide (Ogallo et al. 2008). The West Africa Regional Climatic Outlook Forum (WARCOF) locally named by the French acronyms PRESAO (Previsions saisonnières en Afrique de l'Ouest) in its early years, then PRESASS (Prévisions Climatiques Saisonnières en Afrique Soudano-Sahélienne) later, has been releasing forecast of the season cumulative rainfall since 1998 and extend its forecast products to season onset, cessation and dry spells from 2011 (AGRHYMET, 2011). However, the verification of the previous year forecast performed annually at the beginning of the subsequent WARCOF session has mostly shown mismatching between the observational data and the forecast.

Limited research has been carried out on the evaluation of the WARCOF products (Hansen et al, 2011). Very few of the studies have investigated on the predictability of the season onset and dry spells (Sultan et al, 2020) despite their high importance for rainfed Agriculture in the Sahel region (Sivakumar, 1992). Those studies have linked the forecasts biases to various challenges, including the complexity of predicting the highly variable West African monsoon rainfall system, the

performance of the forecasting models, the scarcity and reliability of observed rainfall data used as model inputs, and the criteria employed to define rainy season parameters, particularly for determining the season's onset (Fitzpatrick et al., 2015). Additionally, some of those studies have attributed the forecast shortcomings to biases stemming from forecasters' risk aversion, that is, their fearing to give incorrect forecast as shown by Mason and Chidzambwa (2009). Other limiting factors identified include the subjective nature of the forecasting process (Mason & Chidzambwa, 2009), as confirmed by Bliefernicht et al. (2019) and the use of inappropriate verification procedures when assessing probabilistic forecasts (Rauch et al., 2019).

Dynamical and statistical forecasting methods to predict intra seasonal rainfall variables such as season onset, cessation and dry spells, over the region are rarely represented in scientific literature (Rauch et al., 2019; N'diaye, 2010). Further investigation is needed to better understand the biases sources of the WARCOF products in order to enhance the forecast system performance and to meet the small-scale farmers' needs in the region.

2.2. Empirical review of the existing seasonal forecast systems over West Africa

Cyclic droughts periods observed over the Sahel region in the early 1970's and 1980's were the triggering factors to the development of several coping strategies. Early landmark studies have laid the foundation for the seasonal forecast and applications in Agriculture over sub-saharian Africa. Cane & Eshel (1994) found a strong correlation between Pacific Sea Surface Temperatures, associated with the El Niño/Southern Oscillation (ENSO), with maize (*Zea mays*) yields in Zimbabwe. Some other previous studies (Rowell, 2001, 2013; Graham et al., 2012; Fontaine et al., 2011) identified teleconnections between some domains of the tropical sea surface temperatures and Africa's rainfall patterns. Glantz (1977) investigated the constraints seasonal forecasts

application could be faced in the West African Sahel if they were available during the severe drought of early 1970's.

Several climate forecast systems and models have been developed for cumulative rainfall prediction over West Africa. Among the most popular one are the UK Met Office (GloSea4) which was found to have modest skill at 2–3 months' lead time, with ROC scores of 0.6–0.8 (Vellinga et al., 2013); North American Multi-Model Ensemble phase 2 (NMME-2) (Wanders et al., 2018); ECMWF-S4, the coupled Global Circulation Model (GCM) of the European Centre of Medium-Range Weather Forecasts (ECMWF), the Climate Forecast System version 2 (CFSv2) from National Center for Environmental Prediction (NCEP) (Siegmund et al., 2015); Météo-France 3 (MF3); Community Climate System Model 3 (CCSM3); GFDL; The Canadian Meteorological Centre version 2 (CMC2), etc.

The skills of several dynamical and statistical models and forecast systems have been assessed over West Africa through previous studies but there is no a clear-cutting conclusion showing the most performing over the region. However, some of the evaluation studies (Wanders et al. 2018; Rauch et al., 2019 agree on the stronger skills of some models in West African Monsoon (WAM) onset prediction over the Guinean Zone compared to the Sahel region. Rodrigues et al., 2014 found that only a fraction of the models captures the rainfall signal at the north of 10°N and that only S4 has significant correlation when predicting both Guinean and Sahelian WAM regimes, MF3 performs well when predicting the Guinean regime and GFDL when predicting the Sahelian regime. Barnston et al. (2010) examined the quality of seasonal probabilistic forecasts of near-global temperature and precipitation issued by the International Research Institute for Climate and Society (IRI) from late 1997 through 2008 and found average skills of SST higher in the tropics than extra tropics (Figure 2.1) and good skills for JAS (July – August – September) and ASO

(August – September – October precipitation over the Sahel (Figures 2.2 and 2.3). Through this study we will focus on some of the models which outputs are used in the WARCOF forecasting system. Those GCMs are CFSv2, CMC1, CMC2, GFDL, NCAR_CCSM4, and NMME.

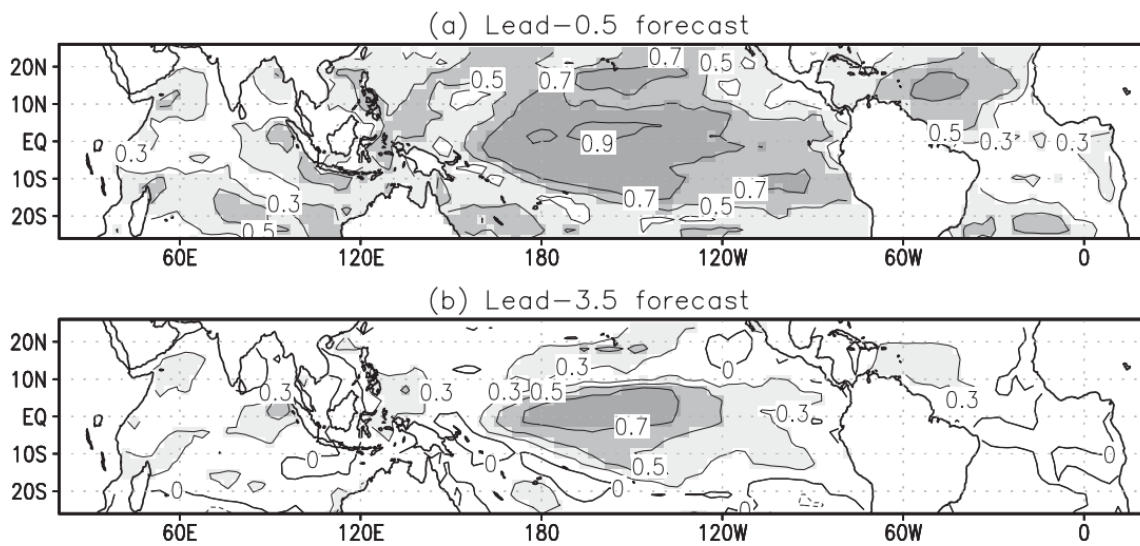


Figure 2.1. Skills of IRI SST forecasts made over the period 1997 - 2008 for all seasons at: (a) lead time - 0.5 and (b) lead time - 3.5 (Source: Barnston et al., 2010)

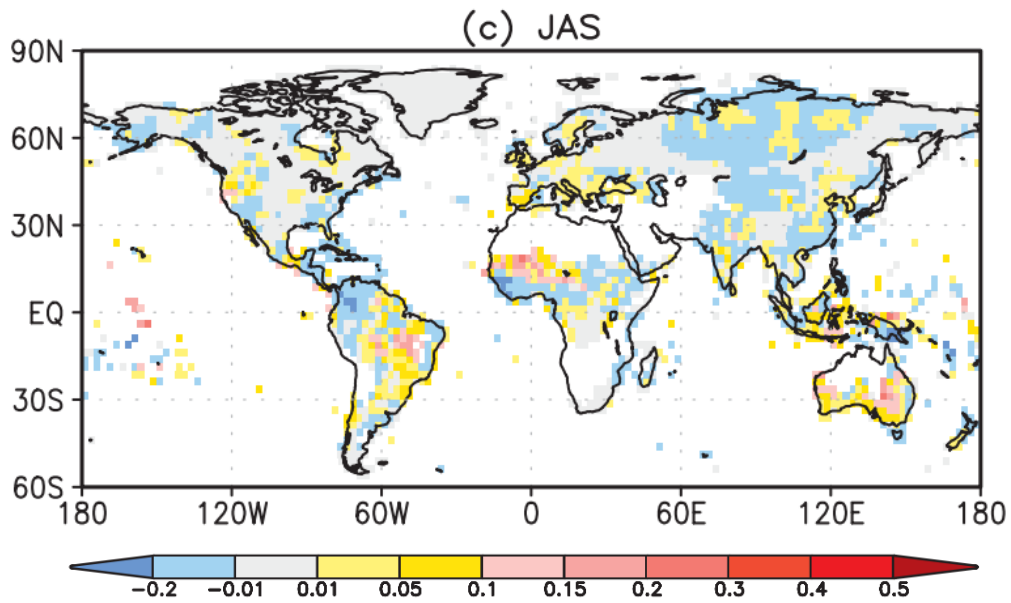


Figure 2.2. Skills (RPSS) of IRI JAS precipitation forecasts made over the period 1997 - 2008
Lead time – 0.5 (Source: Barnston et al., 2010)

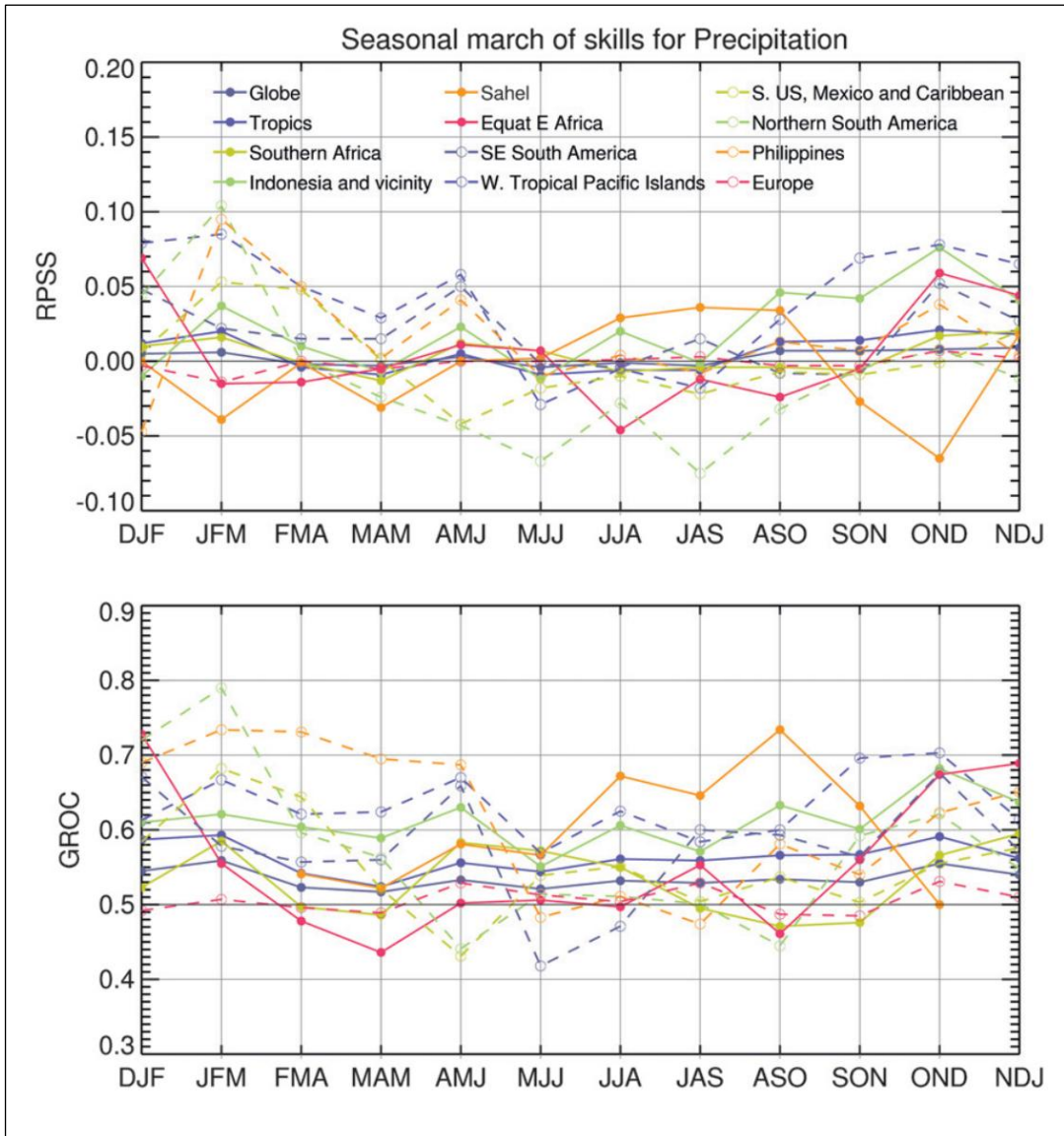


Figure 2. 3. Seasonal distribution of mean skill (1997–2008) for precipitation at 0.5-month lead time for selected regions, using RPSS (top) and GROC (bottom) (Source: Barnston et al., 2010)

2.3. Theoretical review: Importance and predictability of rainfall intraseasonal parameters for agriculture

Rainy season onset and cessation dates and the intra-seasonal distribution (dry/wet spells durations) are determinant in sahelian rainfed Agriculture. Many studies (Tearfund, 2008; Hess et al., 1995; Bello, 1996; Tarhule & Lamb, 2003) have given evidences that rainfall varies erratically both at spatial scale (even within few kilometres as shown over west Niger by Graef et al., 2000) and temporal scale (annual, monthly and daily) over sahelian west Africa (Laux et al., 2008 & 2009).

The rainfall spatial and temporal high variability has made droughts recurrent and affected considerably crop yields and small-scale farmers' incomes. The timing of the onset date varies from year to year and is a key determining factor for the duration of the growing season. Sivakumar (1988) has analysed daily long-term rainfall data for 58 locations in southern Sahelian and Sudanian zones and found that early onset resulted in a longer crop growing season whereas delayed onset reduced considerably its duration. N'Diaye (2010) has reported for sites near Niamey, that in years with an early onset of rainfall, dry matter production of millet reached 7 t/ha while late onset of rains resulted in only 3 t/ha. Dry spells play also a key role in the season duration as they are more frequent at the early stages and the end of the rainy season (Laux et al., 2009; Fall et al., 2021). Dry spells during crucial phases of crop reproduction can cause considerable yield damage. Graef et al. (2000) have reported that severe climate limitations occur in one out of three years and often lead to a total loss of millet yield at Chical in the western part of Niger. Therefore, beyond the season cumulative rainfall, information on the intraseasonal parameters are needed by farmers for a better field and crop management.

2.3.1. Onset predictability

Depending on the northward ITCZ movement and the WAM dynamics, the rainy season onset dates in West Africa is characterized by a high spatio-temporal variability (Vellinga et al., 2013). That makes its predictability very challenging. Onset can be analysed regionally, locally, or over a designated intermediate scale. Many onset dates definitions have been established for the region. At least 18 distinct definitions of the WAM onset exist in publication according to Fitzpatrick et al. (2015) who investigated those definitions and found poor interannual agreement between onsets calculated using different datasets although there is mean patterns agreement among them. The sensitivity of the interannual variability of onset date resulting from different datasets implies forecast evaluation skills are tied to observations data against which the model is being evaluated.

The multiple factors controlling the WAM rainfall regime and its own high spatio-temporal variability make difficult the predictability of season onset dates specially over the Sahel region. Wanders et al. (2018) found that NMME2 ensemble shows a significant skill in forecasting the onset of the rainy season over West Africa, however model skill is lower in the Sahel where the observational data are scattered. Their assessment showed good skill in the wetter zone of Niger, Chad and Mali but less performance of the models in the northern parts of those countries where annual precipitation is less than 200 mm; that may be related to the high interannual variability of rain onset in that region. Another source of uncertainty in onset predictability is the lack of agreement between the regional scale onset and the local one. The results from Marteau et al. (2009) showed a lack of agreement between local onset dates and large-scale monsoon jump that needs further investigation.

In the WARCOF approach, the onset of the coming season is predicted by statistical correlation of the actual onset dates calculated over the 30-years climatological normal in date (1991-2020 is currently used) with a number of parameters derived from dynamical coupled ocean-atmosphere

models as predictors. Those parameters include observed or predicted sea surface temperatures from different oceanic basins (Nino3.4 in the Pacific, Gulf of Guinea, northern and southern Atlantic, western Indian Ocean and Mediterranean), precipitable water in the atmosphere, upper air wind velocities at 850mb level, etc. The actual onset dates are estimated based on a combined onset definition criteria from Stern (1981), Sivakumar (1988), and Diallo et al. (2014).

Figure 2.4 shows an example of the forecast product resulting from that process. It represents the forecast of the 2024 rainy season onset dates. The figure indicates predicted early season onset over Burkina Faso, West of Niger, East of Mali, Northwest of Nigeria, Northern Benin, Togo and Cote d'Ivoire (orange zone on the Map). Over the remaining part of the Sahel, the season it is expected to observe near normal onset.

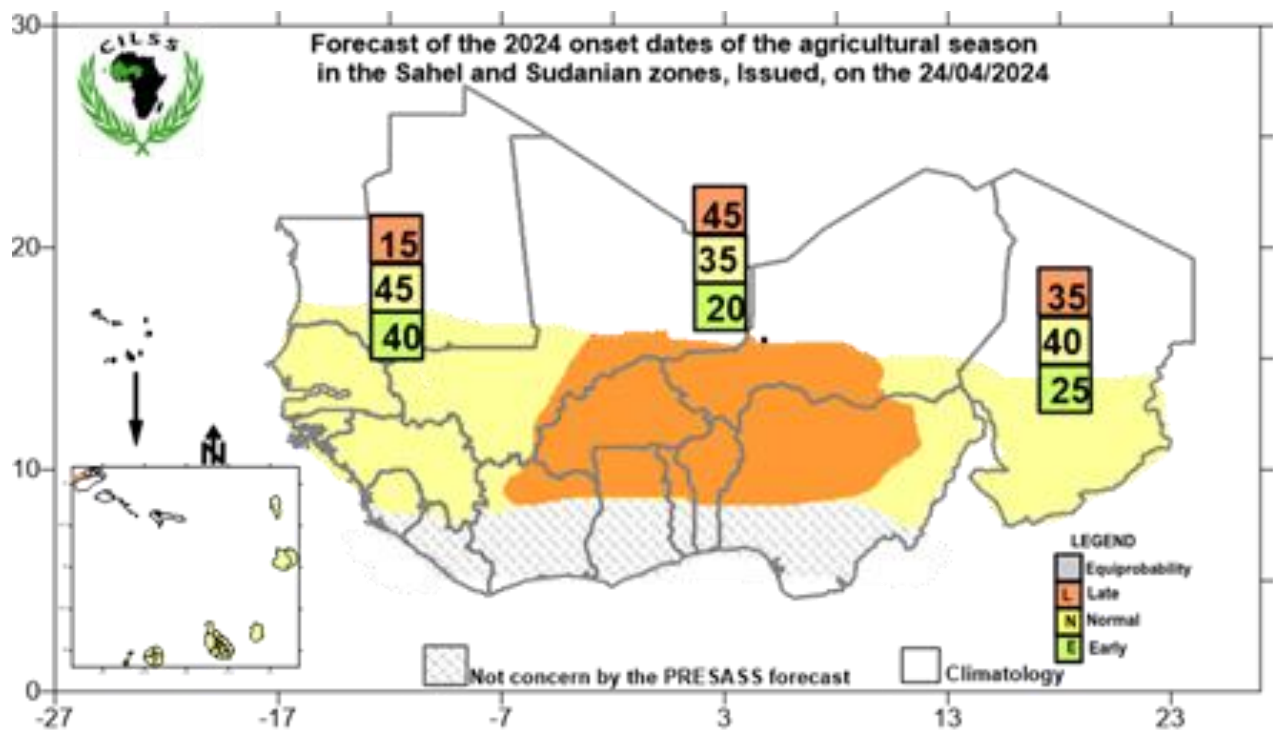


Figure 2. 4. Predicted onset dates for the rainy season 2024. The values in the upper, middle and lower boxes represent the probability to have have late season onset, normal onset and early onset respectively.

(Source: AGHYMET regional Center)

2.3.2. Cessation date forecast

As described in the previous section, rainy season duration, and indirectly crop yield depend on the season cessation date in the Sahel region. However, less research investigated on that season parameter, hence limited definition criteria and estimation method exist in the literature. Dunning et al., (2016) presented a method using satellite-base rainfall data and reanalysis data to determine cessation dates in regions such as horn of Africa, that may be applicable in other parts of Africa with some limitations for application for operational purpose.

In the WARCOF process, similarly to the onset dates forecast, the actual cessation dates are first estimated based on daily rainfall data and cessation date definition criteria.

Then, the cessation of the coming season is predicted using statistical correlation between the calculated actual cessation dates and a number of parameters derived from dynamical coupled ocean-atmosphere models as predictors. The 2024 forecast of cessation dates is shown in Figure 2.5. The figure indicates predicted late season cessation all over the Sahelian zone as the highest probability (45%) range in the above normal category.

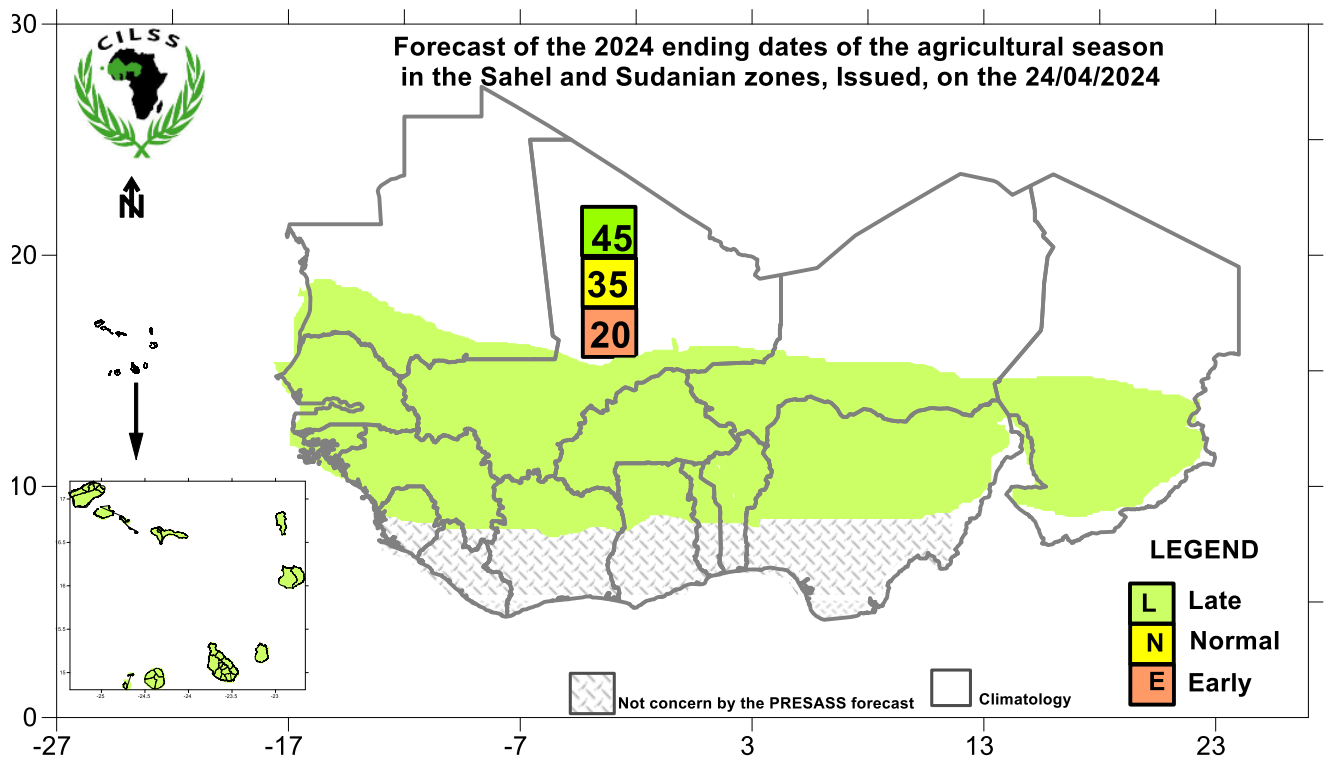


Figure 2. 5. Predicted cessation dates for the rainy season 2024

(Source: AGHRYMET regional Center)

2.3.3. Dry spell duration forecast

Dry spells, based on their occurring time during the growing season could be prejudicial for crop yield. Prolonged dry spells at the early stages of the season can cause false start and considerable economic losses (waste of seed, yields reduction) for low-income farmers in the Sahel region. They could also shorten the season duration when they occur in September and prevent the crops to complete their normal life cycle.

The WARCOF currently provides only qualitative probabilistic forecast of occurring of long, short or normal duration dry spells for the starting and ending periods of the season (Figures 2.6 & 2.7). These probabilities of occurrence are given over large spatial patches delimited consensually among forecasters without taking into account local specificities that could influence a lot that variable. The WARCOF approaches to correlate large scale predictors to local intraseasonal modulation of rainfall could be also a bias. In that extend, the seasonal forecast acts as a spatiotemporal filter that increases the rainfall predictability by enhancing the slow SST-forced larger-scale component of rainfall variability while hiding the smaller scale unpredictability of weather variability (Maron et al., 2013). The Sahel region rainfall regime has a dominant component of Meso-Scale Convective (MSC) systems and their frequency may affect rainfall intraseasonal distribution more than a large-scale SST. Some evidences have been shown by Douville et al. 2001; Clark et al. 2004; Dirmeyer et al. 2009, that soil moisture anomalies and gradients have positive feedback on MSC formation and intensity over Sahel toward the end of the season, that could be an insight to improve the subseasonal predictability during the second part of the rainy season.

Moron et al. (2013) proposed a new method combining the empirical orthogonal function of both interannual and subseasonal variations with a fuzzy k means clustering captures that could be an

approach to reduce the noises in capturing the rainfall variables at shorter spatio-temporal scales. Hence the approach provides insight into the seasonal predictability of long dry spells and heavy daily rainfall events at local scale and their subseasonal modulation.

Fall et al., (2021) also found spatialized data via kriging necessary for dry spells detection rather than direct gauge data over Senegal and suggested TRMM data as a favourite alternative to scale up their results to West Africa.

Figures 2.6 and 2.7 show the 2024 forecast of the durations of the longest dry spells respectively at early stage of the season and towards the end of the season.

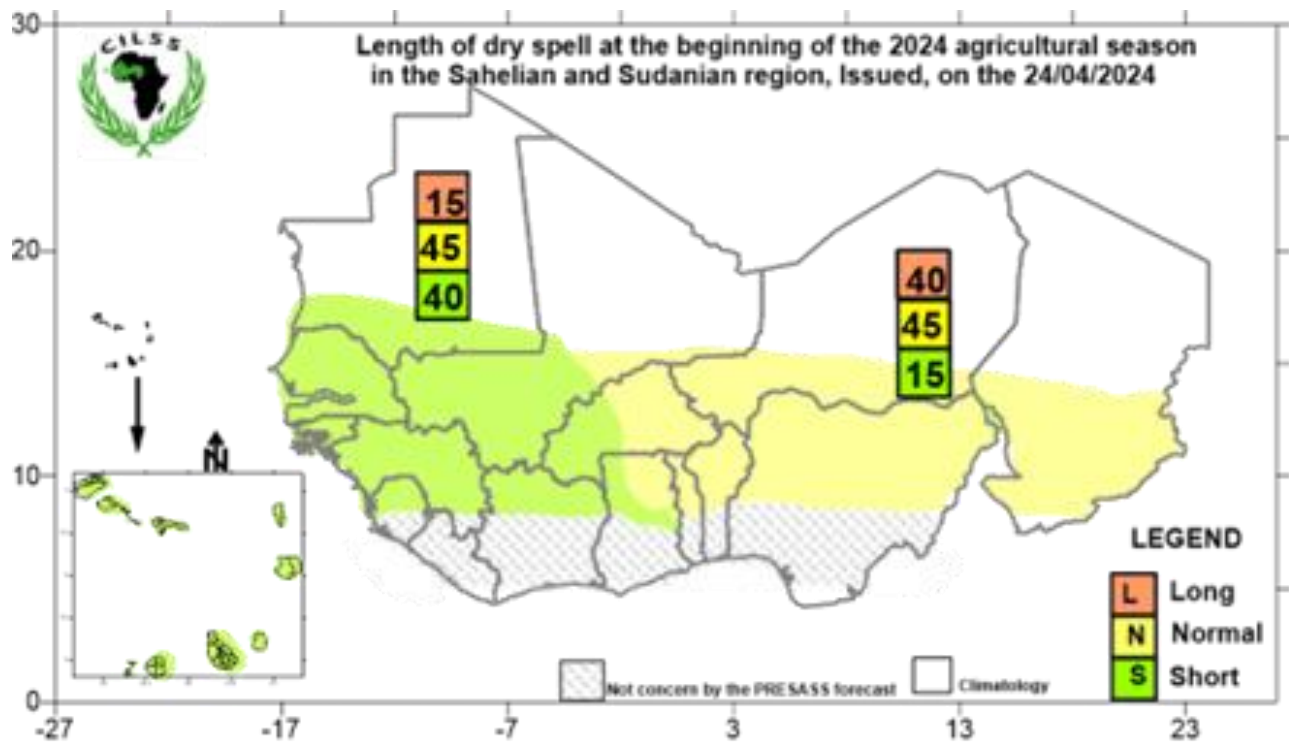


Figure 2. 6. Predicted dry spell duration map at the beginning of rainy season 2024
(Source: AGHYMET regional Center)

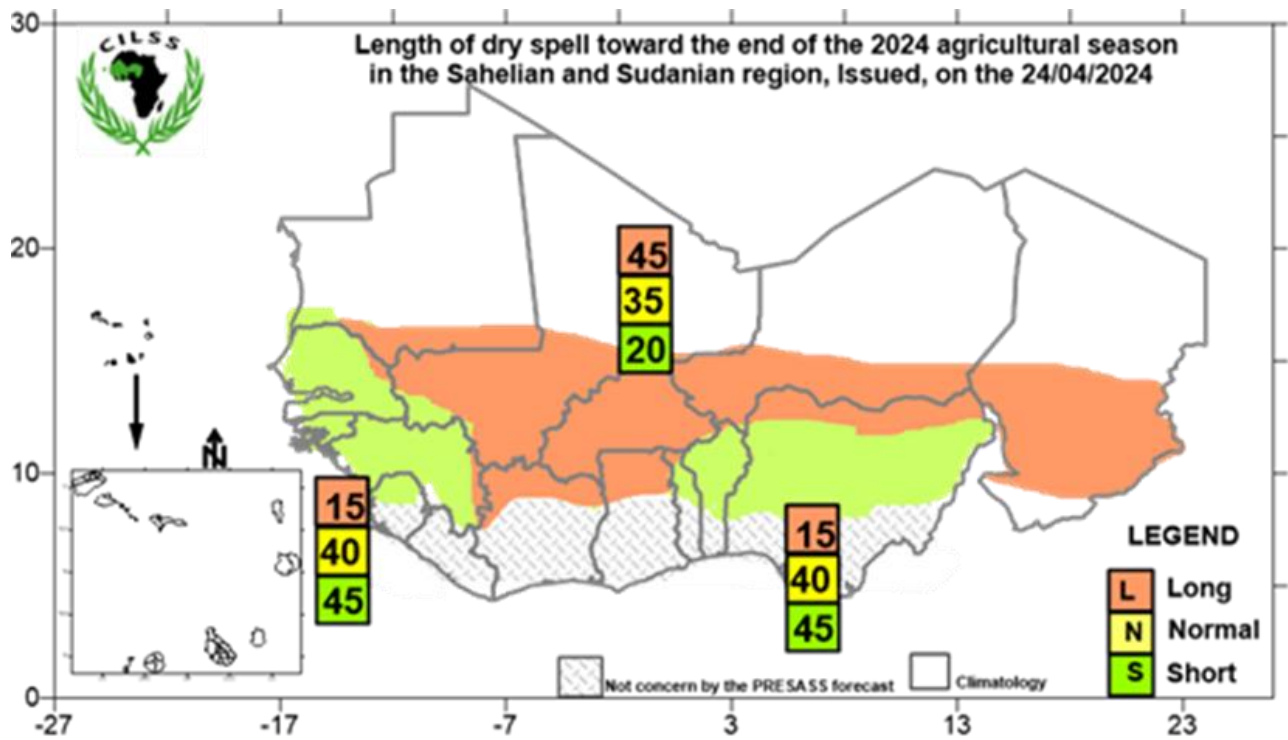


Figure 2.7. Predicted dry spells map at the end of rainy season 2024

(Source: AGHRYMET regional Center)

2.4. Overview on the WARCOF forecasting system

According to Ogallo et al. 2008, the precipitation outlook provided by the WARCOF is one of the earliest RCOF products. Hansen et al. (2011), also stated that Sub-Saharan Africa has the longest continuous records of RCOFs in history of anywhere in the World and the forums timing has been initially defined based on Agriculture needs. The WARCOF is a forecasting initiative of the national weather and hydrological services of West African and some central African countries (Chad and Cameroon), coordinated by the African Centre of Meteorological Applications for Development (ACMAD) and the Centre Regional de Formation et d'Application en Agrométéorologie et Hydrologie Opérationelle (AGRHYMET Regional Centre). The forum meets annually and is usually complemented by experts from several Global Producing Centres for Long-Range Forecasts and other climate specialists (Bliefernicht et al., 2019). Detailed overview of the information and methods used by the West African RCOF to provide seasonal precipitation outlooks is given in the study by Mason and Chidzambwa (2009).

2.4.1. Brief description of the PRESASS forecasting system

The PRESASS method is a complex and hybrid operational forecasting system combining dynamical, statistical and consensual forecasting approaches. The overall process can be described in 2 steps as follow:

Step 1

GCM outputs as predictors and historical observed season parameters data as predictands are used in Canonical Correlation Analysis (CCA) through Climate Predictability Tool (CPT, a tool developed by International Research Institute for Climate and Society (IRI)) by the experts from the National Meteorological and Hydrological Services (NMHSs) and the Regional Climate

Centers (ACMAD and AGRHYMET) to perform statistical forecasts of the season's characteristics over their respective countries. At this stage, as described by Graham et al. (2012), stepwise regression is used to select the best model, and this model is used with the latest observed predictor values to generate a forecast. Sea surface temperatures (SST) in different ocean areas (NINO3, North Atlantic, Gulf of Guinea, Indian Ocean, Mediterranean, etc.), ensemble means of precipitation forecasts or wind fields from models are mainly the predictors used in the process.

Step 2

Following step 1, all experts (from NMHSs, Regional Climatic Centers and invited experts) meet to analyze and compare different sources of information and forecasting methods in order to establish a convergence of evidence to agree on the different forecasts resulting from previous step. Judgments and knowledge of forecasters are taken into account during this process. Then, consensual conclusions are drawn at the end of this step.

Main sources of forecast used to make the consensus forecast are:

- a) Forecasts developed from statistical models by country experts (national scale) and regional experts from AGRHYMET and ACMAD (regional scale);
- b) Dynamic model forecasts from Global Producing Centers (GPCs) consolidated through the North American Multi-Model Ensemble (NMME) platforms (<https://iri.columbia.edu/our-expertise/climate/forecasts/seasonal-climateforecasts/>), Copernicus Data Store (C3S), IRI Data Library, WMO-GPC... (<https://wmo.org/>);
- c) Expert analysis of the status of factors influencing the characteristics of the West African rainy seasons in the Sahel (configuration of the SST, the MJO...).

At the end of this consultation, the forecasts are consolidated and validated by consensus. The results are presented in the form of probabilities of occurrence for the three categories: average, above average and below average, as illustrated in Figures 2.4, 2.5, 2.6 and 2.7 for agroclimatic characteristics of the season. The reference climatological period currently used is the 1991-2020 climatological normal.

2.4.2. Towards new generation of WARCOF forecasting system and forecast information communication

The WARCOF / PRESASS forecasting system has undergone continuous improvements over the decades. Recent developments resulted in new generation of forecasting systems (NextGen) that offers solutions to the issues related to conventional seasonal forecasts (Hansen et al., 2022). The NextGen approach is implemented using PyCPT, a Python Interface to the Climate Predictability Tool (CPT) which is the tool used so far in the conventional method.

2.4.3. Existing gap in literature

There are limited studies on the WARCOF evaluation. Review of current knowledge on regional climate revealed that in Sudano-Sahelian West Africa, climate predictability remains limited (Traoré et al., 2007). A first assessment of the WARCOF by Mason and Chidzambwa in 2009 covered the period 1998-2007 found some positive skills for below and above normal categories but showed a lack of sharpness. However, they found a strong overcasting of the near normal category due to the forecasters' risk aversion for producing wrong forecasts. Lack of skill for near normal is a typical limitation for tercile based seasonal forecasts, but there is insufficient detailed analysis of this failure (Bliefernicht et al., 2019). There are also few developments of operational seasonal forecast models to complement the WARCOF, despite the efforts made in downscaling of meteorological variables for the region (Paeth et al., 2011). The review of the WARCOF

methods by Bliefernicht et al. (2019) revealed that it is a complex forecasting procedure based on various state-of-the art approaches and information sources and experts' knowledge but it needs to be complemented and improved.

Operational downscaling of forecast products for agricultural purposes

The regional scale of the WARCOF forecast remains a challenge for application at small scale farm level. Forecast probabilities are typically provided as maps of tercile probabilities that are homogeneous over large areas, without any information about the spatial and interannual variability of the underlying local climate (Hansen et al., 2019). At country level, meteorological services have tried to provide the forecast information to farmers at a finer scale but without any research proved downscaling method being applied for that purpose. A survey carried out by Hansen et al. (2011) revealed that while several countries provide forecasts at a finer resolution than the RCOFs, none of the respondents reported downscaling to individual stations.

Many downscaling approaches have been proposed by studies implemented in that field of research. Siegmund et al., (2015) experimented a performance analysis of a dynamical downscaling approach on the CFSv2 forecast products for West Africa by transferring the twenty-two CFSv2 ensemble members initialized in February 2013 to a resolution of 10 km × 10 km using the Weather and Research Forecasting (WRF) model. Their results showed that the downscaling approach (CFSv2-WRF) can reduce the CFSv2 uncertainty (up to 69%) for monthly precipitation and the onset of the rainy season but has still strong deficits regarding the northward progression of the rain belt. They suggested further studies for a more robust assessment of the techniques applied to confirm their promising outcomes. Hansen et al. (2019), suggested a statistical downscaling of seasonal forecasts onto local historical observations; and presenting the forecasts as full probability distributions, in probability-of-exceedance format, along with the historical

climate distribution. Rauch et al. (2019) proposed a better operational downscaling and less computational approach applicable to onset date forecasting for developing countries where bandwidth and computing power are often limited.

Forecast dissemination and use

The current forecast products dissemination and use needs also to be improved. The limiting factors to the forecast information dissemination may include the weakness and technical incapacity of extension agents to present probabilistic predictions in any form useful to farmers, farmers' illiteracy, inaccessibility to other forms of media in rural areas, the multilingual communication way needed to touch a larger number of users. Feedback and perceptions from farmers about the quality of the forecast products need to be assessed as well. According to Blench (1999), there is no systematic survey on users' needs or the impact of the information released.

From the foregoing, it has become evident that more investigation is needed to update the status of seasonal forecast information used by rural communities in Sahelian West Africa and to identify strategies to engage farmers for a larger use of the information in their activities.

In conclusion, it came out that only few studies have analysed the reliability of the WARCOF forecasts (Siegmond et al., 2015). Based on those studies, the shortcomings of the WARCOF approach can also be the reason of the low uptake of forecast information in spite of their importance for agricultural applications cannot be underestimated. The forecasting system provides the 3-months cumulative rainfall without giving clear distribution on smaller time resolution that is needed in Agriculture. Widespread use and benefits from seasonal prediction among smallholder farmers are limited due to constraints such as legitimacy, salience, access,

understanding, capacity to respond and data scarcity related to the forecast products (Hansen et al., 2011).

Rauch et al. (2019) also reported that the WARCOF produces just qualitative forecasts for rainy season variables in spite of their importance in Agriculture and in other economic sectors. In the WARCOF process, pre-monsoonal and post-monsoonal periods are not fully covered. It provides only information about the cumulative precipitation over JAS and formulates, for a lead time limited to one-month, subjective qualitative statements for the season onset and other rainfall intra-seasonal characteristics such as the dry spells' duration and the rainy season cessation. For all these reasons, the ongoing forecast procedures concerning rainfall intraseasonal variables need to be improved to provide more precise information that meet end-users needs. Our study will assess the WARCOF process with regards to the prediction of onset, cessation dates and dry spell durations and investigate the strategies for a better dissemination and use of those forecast information.

CHAPTER THREE

METHODOLOGY

The West Africa Regional Climate Outlook Forum (WARCOF or PRESASS in French) forecast method has been used for more than a decade to provide probabilities of occurrence for rainy season key parameters like the onset date, the cessation date, the length of dry spells during the early stage of the cropping season and the length of dry spells at the end of the season. It is currently the best known and most used forecast method in the subregion

Unlike the cumulative rainfall method, there has been insufficient evaluation of the WARCOF/PRESASS approach regarding the forecast of intraseasonal parameters in spite of its use for over a decade by AGRHYMET and West African Meteorological agencies.

This research aims to assess and improve the operational seasonal forecast production and use over Sahelian West Africa. The research was implemented in several stages in order to achieve the specific objectives which are : (i) the assessment of the forecasting system skills and performance, (ii) the exploration of ways for possible improvements of the method, and (iii) the evaluation of the on-farm use of the forecast products. Hence, the purpose of this chapter is to describe the research approach, the research design, the sampling strategy, the data collection and analysis techniques adopted to assess the skills of the WARCOF/PRESASS regarding the forecasting of onset, cessation and dry spells at a first stage, then secondly to investigate the good predictors for a better forecast of rainfall intraseasonal parameters and finally to engage farmers for more uptake of seasonal forecast information.

Canonical Correlation Analysis through cross-validation and retroactive verification were implemented using the Climate Predictability Tool (CPT) to assess and verify the statistical

component of the forecasting system. Thereafter, the consensual part of the forecasting system was evaluated through Reliability diagrams, ROC curves, Brier and AUC scores computed based on actual season parameters dataset from over 400 rain gauge stations disseminated over the Sahel region and the PRESASS forecast maps dataset from 2013 to 2023. The on-farm assessment was implemented through field surveys and 2-years demonstration trials.

3.1. Overall Research approach

Both qualitative and quantitative research approaches were adopted across multiple phases of the study to achieve the specific objectives. This methodology allowed to collect and analyze qualitative and quantitative data using structured data collection instruments such as survey, experiments, or existing datasets.

At a first stage, existing forecast datasets of onset and cessation and existing observational dataset were used to verify the skill and quality of the forecast. In the perspective of investigating the ways to improve the forecast process at the second stage, historical Global circulation Model (GCM) outputs, used as predictors, were also correlated with actual datasets through linear regression to identify the good predictors among those used in the WARCOF forecasting system for a skillful forecast of those season parameters. At the third stage, data were collected through field work including field survey and 2-years on-farm demonstration trials to assess the seasonal forecast information dissemination and use in the farming system over the Southwest of Niger.

3.2. Description of the study areas

3.2.1 Geographical coverage for forecast skills assessment

The Sahel region in general is a semi-arid area along the southern boundary of the Sahara Desert from the Atlantic coast to Ethiopia (Lu & Delworth, 2005). The forecast skills assessment and

investigation for good predictors to improve the onset and cessation forecast through PRESASS forecasting system were performed over the Sahelian part of West Africa and Chad extending from 10°–20°N, 20°W–30°E. The region of interest includes Burkina Faso, Cape Verde, The Gambia, Guinea-Bissau, Mali, Mauritania, Niger, Senegal and the northern parts of Benin, Ghana, Guinea, Ivory Coast, Liberia, Nigeria, Sierra Leone, and Togo (Figure 3.1).

The area has a semi-arid climate dominated by the West African Monsoon (WAM) characterized by a unimodal rainfall regime with a long dry season extending from October to April and a short rainy season from May to September. The summer monsoon rainfall results from a complex interaction between several atmospheric features including monsoon flow, African Easterly Jet (AEJ), Tropical Easterly Jet (TEJ), African Easterly Waves and Mesoscale Convective Systems (Diallo et al, 2013). The high interannual, intra-annual and interdecadal variability of the Sahelian rainfall regime has caused recurrent drought episodes (Nicholson et al, 2001) making it the most sensitive climate in the world (Nicholson, 2018). The average annual minimum and maximum temperatures fluctuate respectively between 16 - 20°C and 27-35°C depending on the proximity of the ocean (Mouhamed et al., 2013).

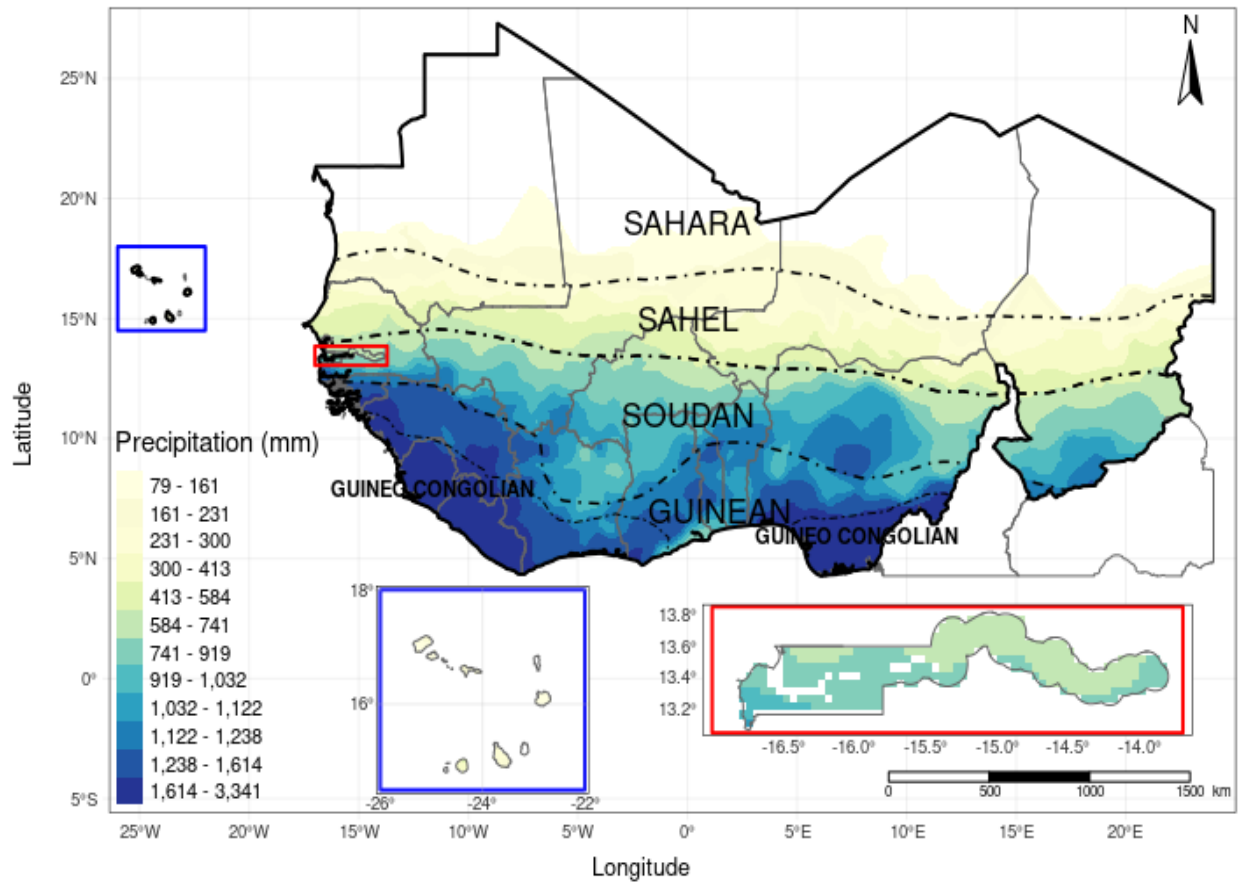


Figure 3.1. Mean annual precipitation in West Africa and bioclimatic zones

(Source: AGRHYMET Regional Center)

3.2.1. Study area for assessment of forecast information use

The field activities, namely the survey and the 2-years field experiments were conducted in the southwest of Niger. The study area is located in two main agroclimatic zones where rainfed Agriculture is practiced.

The field survey was implemented in 16 villages of four municipalities (Guecheme, Tounouga, N'Dounga and Kiota) (Figure 3.1) and concerned a sample of 619 farmers. The field experiments were carried out in 12 villages located in the first three municipalities and involved 60 farmers. The sites of N'Dounga and Kiota are located in the Sahelian Zone with an annual rainfall total varying from 400 to 600 mm (Issoufou et al., 2012). Tounouga is located at the borders with Benin and Nigeria in the sudanian zone where the annual rainfall is greater than 600 mm. Guecheme is located at the boundary of the two agricultural zones. The rainfall regime is driven by the atmospheric features interacting in the WAM; therefore, it is characterized by high inter and intraseasonal variability (Figure 3.2). The farming system is millet-based system either in pure form or intercropped with cowpea, groundnut, sorghum, sesame or roselle like in the rest of rainfed agricultural zone in Niger (Wezel & Haigis, 2002). The dominance of food crops over cash crops makes the cropping system in the study area more subsistent than business-oriented.

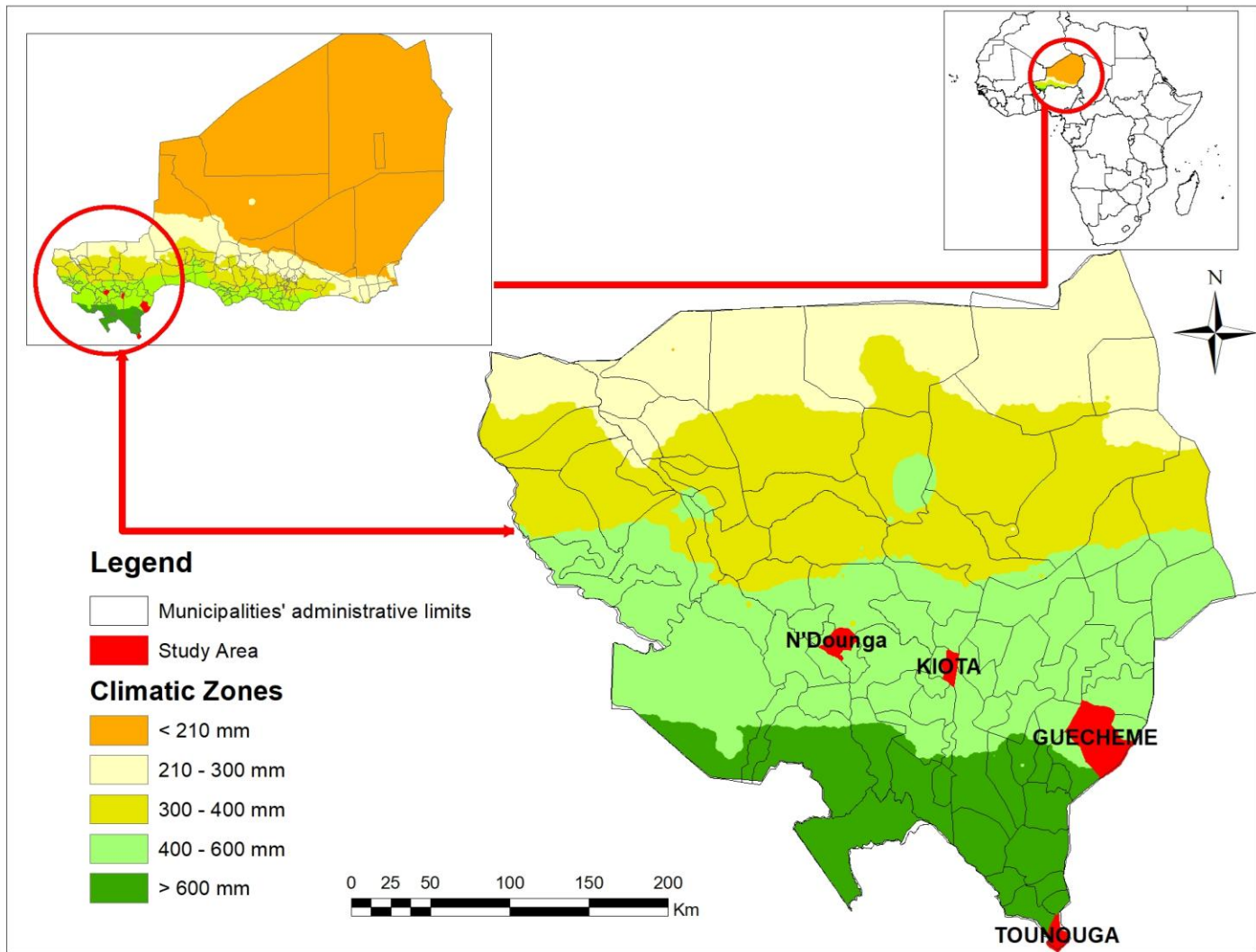


Figure 3.2. Field work study area: municipalities of Kiota, N’Dounga, Guéchémé, and Tounouga in red color

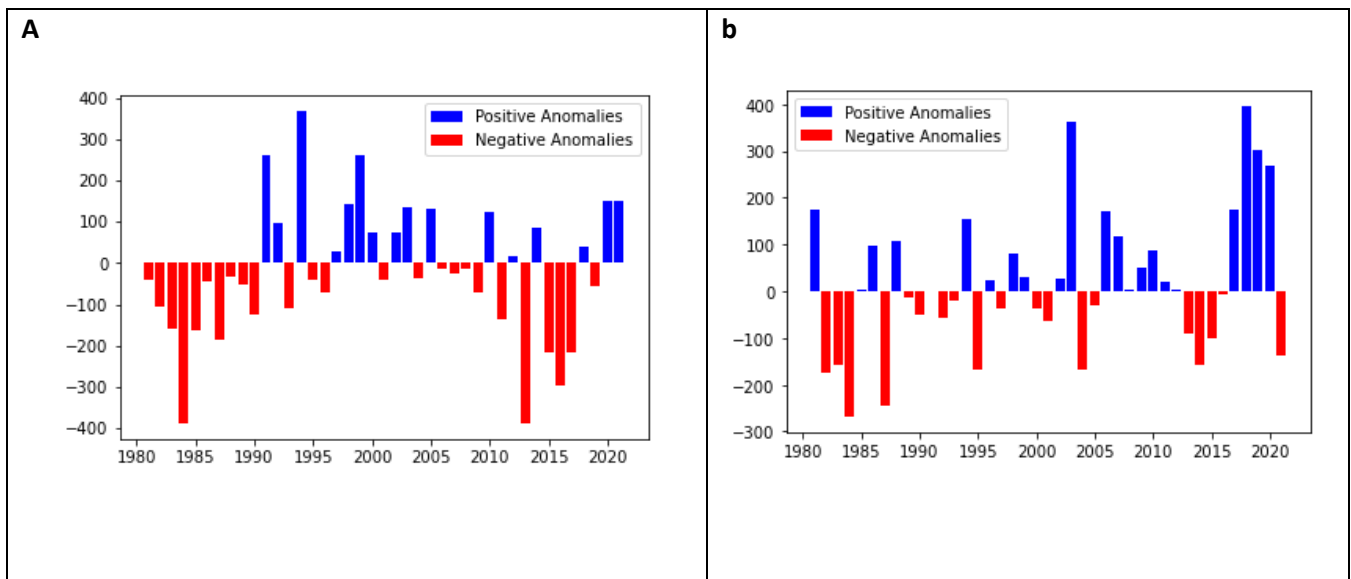


Figure 3. 3. Interannual variability of rainfall in the study area over the period 1981-2020

Rainfall anomalies at: a) Guéchémé, b) Gaya (a nearby station of Tounouga)

Data source: Niger National Meteorological Service, 2021

3.3. Data

3.3.1. Climate observational data

Climate observation data were collected from the Niger National Meteorological Service and from IRI data library. The datasets downloaded from IRI data library include GPCP, CHRIPS, and CFSv2 cumulative rainfall over AMJ season and CRU monthly wet days frequency data. The database collected from the Meteorological Service encompasses daily precipitation data (mm) from 50 rain gauges located in Niger. The data cover the period from 1981 to 2021. Actual onset and cessation dates, dry spells duration during early stage and end season, derived from daily rainfall data for 449 stations over Sahelian countries within the period from 1981 to 2023, were collected from AGRHYMET Regional Center. Figure 3.4 shows the localization of the rain gauges stations. The rainfall data used to generate the actual season parameters are from gauges located in Burkina Faso, The Gambia, Guinea-Bissau, Mali, Mauritania, Niger, Senegal and the northern parts of Benin, Ghana, Guinea, Côte d'Ivoire, Liberia, Nigeria, Sierra Leone, and Togo. The cumulative rainfall and wet days frequency observation data were used to perform the test related to the research for new predictors. The actual season parameters data were used as predictands to run the Climate Predictability Tool (CPT) in the WARCOF forecasting process.

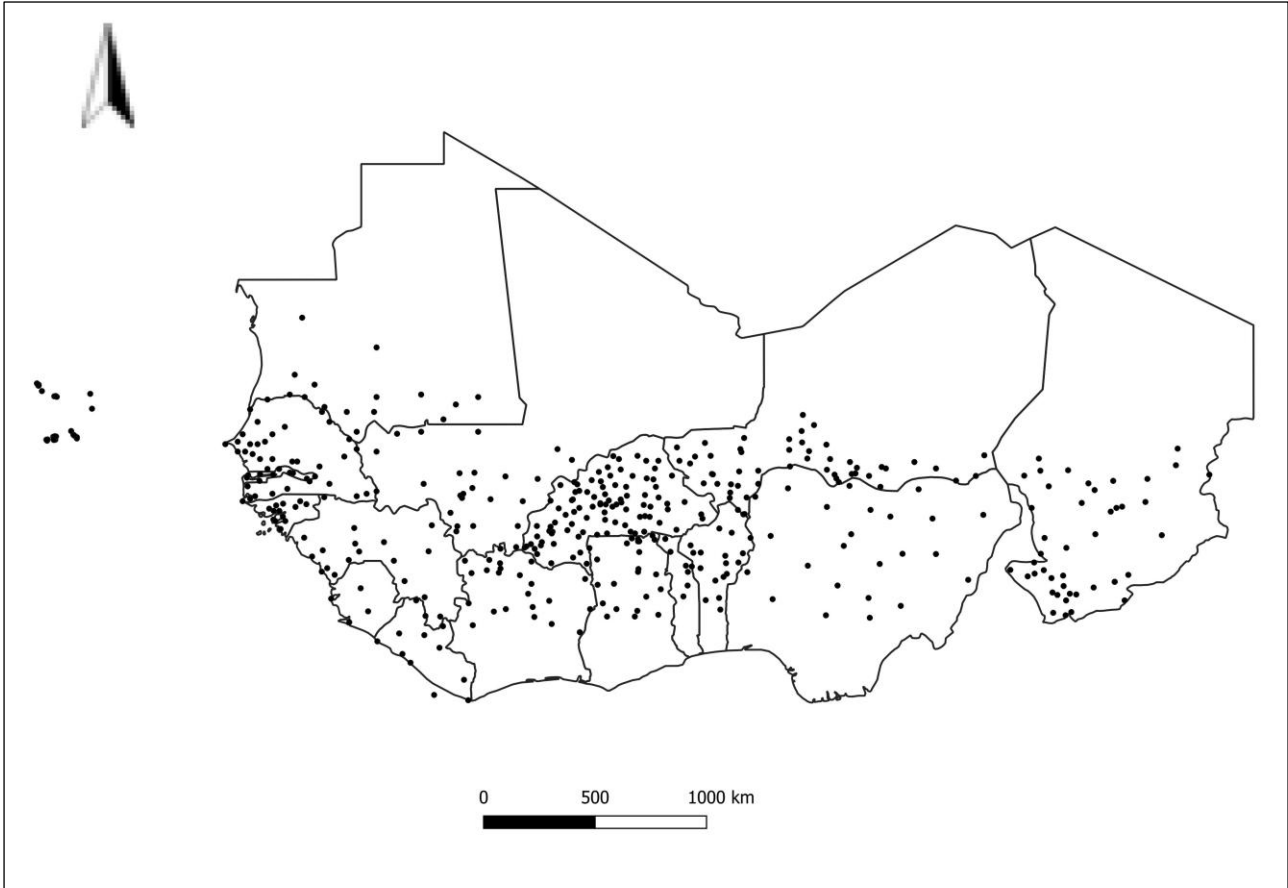


Figure 3. 4. Glocalization of rain gauges stations used in the study area

Data source used to make the map: AGRHYMET Regional Climatic Center, 2024

According to the zone of the study area where the stations are located the actual onset date is defined as follow:

For Sahelian countries with a unimodal regime the season onset date corresponds to the date after March 15, from which a cumulative rainfall of at least 20 mm is recorded for 1 to 3 consecutive days and without a dry spell exceeding 20 days during the following 30 days. For stations located beyond the isohyet 400 mm northward, the threshold considered is 15 mm recorded from May 1st during 1 to 3 consecutive days, without a dry spell exceeding 20 days during the following 30 days.

For costal countries in the Guinea Gulf, for monomodal regime (Latitude greater than 8°N), the rainy season starts from 15 March, when at least 20 mm of rain is recorded in 01 to 03 consecutive days and this without dry spells of more than 10 days in the following 30 days. For bimodal regime (Latitude less than 8°N), in the southern areas of these countries, there are two rainy seasons, the long (the main) season and the short one. For the onset of the main season, the same criterion as the northern zones is adopted, i.e. at least 20 mm of rain recorded in 01 to 03 consecutive days from 1st February, without dry spells of more than 10 days in the following 30 days. As for the short rainy season, it starts when from August 15, more than 10 mm is recorded in 3 consecutive days.

The actual agronomic cessation date of the season is observed once the soils dry out. It is different from the end of the rains events in that it is based on the depletion of the useful water reserve of the soil. It is defined as follows according to the zones:

For Sahelian countries with monomodal rainfall regime, the end date of the season occurs when after September 1st, a soil with 70 mm of useful water holding capacity dries out completely by

daily evapotranspiration of 5 mm. For the western parts of the Sahelian zone (western Mali, Senegal, Mauritania, Gambia and Guinea Bissau), the search is triggered from 15 September to take into account the relatively late end of the season in these areas, compared to the eastern part of the Sahel and in accordance with local practices that allow the conduct of agricultural activities (rainfed crops).

In northern areas of the Gulf of Guinea countries with monomodal rainfall regime, the end of the rainy season is observed when from 1 September a soil with a useful water reserve of 70 mm dries out completely by daily evapotranspiration of 4 mm.

In the southern areas, the same criteria as those in the northern areas are used, except that the calculations are triggered starting from July 1st for the main season. As for the end of the short season, calculations are triggered starting from October 15th.

3.3.2. Global Circulation Model output data and forecast maps

West Africa Regional climatic Outlook Forum (WARCOF) forecast products (onset dates, cessation dates, and dry spells forecast maps) were provided by AGRHYMET Regional Center. They cover the period from 2013 to 2023. Figures 2.4, 2.5, 2.6 and 2.7 show examples of those types of maps.

Global Circulation Models (GCMs) hindcast data and forecast data in the format they can be used in the forecasting tool, that is CPT, were collected from AGRHYMET and partially downloaded from IRI data portal. The dataset covered the period from 1991 to 2023 for the hindcast data and 2023-2024 for the forecast data. Those GCM outputs are used as predictors in the forecasting process. The predictors are usually sea surface temperatures (SST) in different ocean areas (NINO3, North Atlantic, Gulf of Guinea, Indian Ocean, Mediterranean, etc.), ensemble means of

precipitation forecasts or wind fields from models run through Global Predicting Centers Long Range-Forecast (GPC-LRF). The GCMs which outputs are used include CFSv2, CMC1, CMC2, GFDL, NCAR_CCSM4, and NMME. Table shows brief description of those models and systems.

Table 3.1: Summary of Global Circulation Models (GCMs) and Systems used

Model/System	Developer	Type	Purpose	Key Features	Reference
CFSv2	NOAA/NCEP (USA)	Fully coupled atmosphere-ocean-land-ice model	Operational seasonal and sub-seasonal forecasts	Daily initialization; MOM4 ocean; NOAA operational model	Saha et al. (2014)
CMC1	Environment and Climate Change Canada (ECCC)	Coupled atmosphere-ocean model	Seasonal forecasting	Based on CanCM3; GEM atmospheric model; CanOM3 ocean model	Merryfield et al. (2013)
CMC2	Environment and Climate Change Canada (ECCC)	Coupled atmosphere-ocean model	Seasonal forecasting	Based on CanCM4; improved resolution and coupling	Merryfield et al. (2013); Kharin et al. (2012)
GFDL	NOAA/GFDL (USA)	Suite of global coupled climate models	Climate and seasonal forecasting, climate change research	Modular design (e.g., GFDL-CM2.x, FLOR); MOM ocean model	Delworth et al. (2006); Vecchi et al. (2014)
NCAR_CCSM4	NCAR (USA)	Coupled atmosphere-ocean-land-ice model	Climate research and seasonal forecasting	CAM4 atmosphere; POP2 ocean; CLM4 land; CICE4 sea ice	Gent et al. (2011); Hurrell et al. (2013)
NMME2	Multi-agency (NOAA, NASA, NCAR, ECCC, etc.)	Multi-model ensemble system	Seasonal forecasting (probabilistic)	Combines multiple models (CFSv2, CMC1/2, GFDL, CCSM4, etc.); North American operational forecasts	Kirtman et al. (2014); Becker et al. (2014)

3.3.3. Field data

3.3.3.1. Survey data

Socio-economic data related to the dissemination means and the use of forecast information in the farming system were collected from 619 farmers within the study areas. The data include information characterizing the survey sample (respondents' age, level of education, gender etc), the cropping systems in place, farmers access to forecast information, their perception of the information, the proportion of farmers using the information, the intensity rate at which it is used in farmers decision-making process, the potential benefits and value gained related to forecast information use, the level of uptake of climate services in Agriculture, and the farm activities requiring forecast information, users preference and interest according to the type of information and dissemination channels. The survey questionnaire is presented in Appendix A.

3.3.3.2. Field experiments data

Data were collected during the two-years demonstration trials from 60 farms disseminated through 12 villages within the 3 municipalities representing the study area. Data collected can be classified in four groups as follow:

- a) Plots and farmers identification data including site/village name, farm owner's name, age, gender, plot identification number, plot area, plot characteristics (soil type and texture, type of fertilisation applied before and during the experiment, topography, type of land tillage), type of crop and variety used, planting dates, planting density;
- b) Farm activities monitoring data: dates when activities such as soil preparation, seeds preparation, planting, weeding, fertilizers and pesticides applications, harvesting were implemented and methods used to carry them out;

- c) Crop monitoring data: phenology, dates of occurrences of damages related to pest, diseases, climate risks (floods, drought, wind gusts, etc...);
- d) Crop postharvest data: yield data for grain, straw and ears.

3.3.3.3. Soil data

Existing soil data were collected for the sites located within municipalities of Guecheme and Tounouga from an IFDC data based hosted at the National Institute for Agronomic Research (INRAN). The data include soil pH, phosphorus, potassium, magnesium, sulphur, sodium, iron, zinc, organic carbon, nitrogen and its composition in silt, sand, and clay. For sites located in N'Dounga where existing data were not available, field soil sampling (plate 3.1) and fertility analysis have been done at the laboratory to generate soil data.



Plate 3. 1 : Soil sampling for soil fertility analysis

3.4. Methods

3.4.1. Forecast verification

The method used for that purpose was built on the *Guidance on Verification of Operational Seasonal Climate Forecasts*, WMO-No. 1220 (Mason, 2018). To assess the WARCOF approach which is probabilistic, the forecast products quality was verified using mainly reliability diagram and ROC. The resolution skill of the probabilistic seasonal forecast is obtained from the equation (3.1):

$$\bar{y}_k = \frac{1}{n_k} \sum_{i=1}^{n_k} y_{k,i} \quad (3.1)$$

where n_k is the number of forecasts of the k^{th} forecast probability, and $y_{j,i}$ is 1 if the i^{th} observation was an event, and is 0 otherwise. Equation (3.1) is akin to a hit score, which is the number of hits divided by the number of forecasts. The observed relative frequency for the k^{th} forecast probability,

\bar{y}_k , is the number of times an event occurred divided by the number of times the respective probability value was forecasted.

Metrics to assess the forecast discrimination ability and reliability were estimated after making retroactive forecasts based on relatively best predictors fields (domains) chosen among the domains of the tropical seas' temperature found to be teleconnected with rainfall patterns over Sahel region according to previous studies and the domains used by experts during the WARCOF meetings. To validate statistical forecast quality, two metrics were analyzed: (i) the Reliability Diagrams that assess the forecast probability calibration and the (ii) ROC Curves that measure the forecast discrimination ability (distinguishing events vs. non-events). Additionally, the Area Under ROC Curves, Brier' scores and sharpness histograms were analyzed to verify the final forecast

products, that is the forecast resulting from the WARCOF experts meetings following the statistical forecast process.

3.4.2. Improvement of the season parameters prediction process

In the perspective to improve the WARCOF procedure for onset forecast, the onset predictability was investigated using seasonal and monthly cumulative rainfall as predictors. The research approach for that purpose involve 3 main steps. At the first stage, rainfall stations data from 50 stations of Niger were used to check the correlation between different monthly and seasonal cumulative rainfall surrounding the season onset period. At this step, correlation was checked between onset date and monthly rainfall totals for April, May, June, July, then between onset dates and the seasonal moving rainfall cumulated over the periods April-May-June (AMJ), May-June-July (MJJ), June-July-August (JJA) and the annual total rainfall. In the second step, bias correction was applied on the CFS predicted rainfall over the period of the best potential predictor resulting from the investigation done at the first step. At the third and last step, the bias corrected CFS predicted rainfall total was used as predictor to build a linear regression model that will allow to predict the season onset. The onset dates obtained from the whole process were compared to the actual onset date to check whether the onset prediction could be improved by that procedure.

The performance of AMJ cumulative rainfall based on observational datasets from CFSv2, GCPC, CHRIPS and station data were also assessed as predictors to forecast the onset, cessation and dry spells at regional level. Besides, the wet days frequency over various time windows of the season generated from CRU wet days dataset was tested as predictor to forecast season onset, cessation and dry spells at regional level.

3.4.3. Assessment of forecast information dissemination and use

In order to achieve that goal, field work including a baseline survey and 2-years on farm demonstration trials were implemented in the Southwest of Niger.

3.4.3.1. Field survey sampling method and implementation

The sampling method for selecting villages and individuals to be surveyed consisted first, in applying the Sloven formula (Equation 3.2) to determine the sample size (Tejada & Punzalan, 2012),. This method allows us to draw, with the same probability, a sample that will be considered representative of the municipality. Thus, 156 individuals were selected for each of the municipalities of Guéchémé and Tounouga and 155 for the municipalities of Kiota and N'Dounga.

$$n = \frac{N}{1 + (N * e^2)} \quad (3.2)$$

With:

n: sample size

e: accuracy level = 0.08

N: total agricultural population of the municipality

N is estimated by weighing the total population of the municipality over the number of agricultural households assuming only the same average household size for agricultural households and non-agricultural households. Thus, the size of the agricultural population of the municipality was obtained by the following Equation (3.3):

$$N = \frac{P \times H_{agr}}{H}$$

(Equation 3. 3)

With

P: total population of the municipality

Hagr: number of agricultural households

H: total number of the municipality's households

The total population of each municipality as well as the number of households are extracted from the national register of localities of Niger (RENALOC) resulting from the 2012 population census (INS, 2014). An annual population growth rate of 0.03% was applied to update the population in 2021 and 2022.

The total number of villages to be surveyed was calculated by dividing the sample size by the total number of farmers who participated in the forecast results restitution workshops at the level of each municipality. After calculating the weight of the population of the villages that benefited from the dissemination of seasonal forecasts to the total agricultural population of the municipality, this number of villages to be surveyed was divided between the 2 categories (direct beneficiary and indirect-beneficiary villages of seasonal forecast results restitution workshops) each according to the weight of its population to the overall agricultural population of the municipality. The individuals to be surveyed were thus divided into those two categories of villages. The background information used to determine the sample size are given in Table 3.2.

The survey was administered from the end of November through early December 2022. At each of the 16 villages visited, targeted farmers were interviewed individually based on the

questionnaire according to the instructions given to the investigators through the survey protocol and Terms of References.

After the survey implementation, SPSS was used for data entry and the data analysis was performed using both SPSS and Excel.

Table 3.2: Background information of the targeted municipalities

Regions	Departments	Municipalities	Municipality's total population in 2012	Municipality's total population in 2022 (projection made with annual grow rate of 0.3%)	Municipality's agricultural population estimated in 2022	Climatic zones	Mean annual cumulative rainfall (mm)
Dosso	Dogondoutchi	Guéchémé	108778	138148	127718	South-sahelian	609
	Gaya	Tounouga	42849	54418	47830	Sudano-Sahelian	838
	Boboye	Kiota	25282	32108	26362	North-Sahelian	572
Tillabéry	Kollo	N'Dounga	22341	28373	25833	North-Sahelian	550

3.4.3.2. Field trials data collection and analysis methods

The main objective of the field experiments was to assess the crop yield benefits related to the use of seasonal forecast products at farm level. The field experiments were implemented in 3 municipalities (Tounouga, N'Dounga and Guecheme) in the southwest of Niger Republic over two consecutive growing seasons and it involved 60 pilot farmers over 12 villages; i.e. 5 farmers per targeted village. The 60 engaged farmers with age ranging between 35 and 81 years old, either male or female were selected among the group of farmers surveyed in 2022. Basic knowledge about on-farm demonstration or some experience in collaborating in such kind of project was used as an additional asset in farmers selection.

Three (3) treatments, i.e. seasonal forecast with full technologies package (T_1), seasonal forecast information only combined to farmers' practices (T_2), and farmer's practices or business as usual (T_0) as control treatment was applied over the fields of five (5) farmers in each of the 12 targeted villages. A plot of 0.25 ha was delimited obviously and randomly to receive the treatments T_1 and T_2 . The control plot (treatment T_0 or operating business as usual) was delimited discretely in the rest of the field to avoid farmer misbehaviors that can corrupt data integrity. Millet is the main crop considered in this study, therefore the fields to host the experiments were chosen based on that. Farmers involved in this study were identified within villages in collaboration with the local agricultural extension agents in each municipality. The scheme of the experiments design at each of the 12 villages is shown in Figure 3.5.

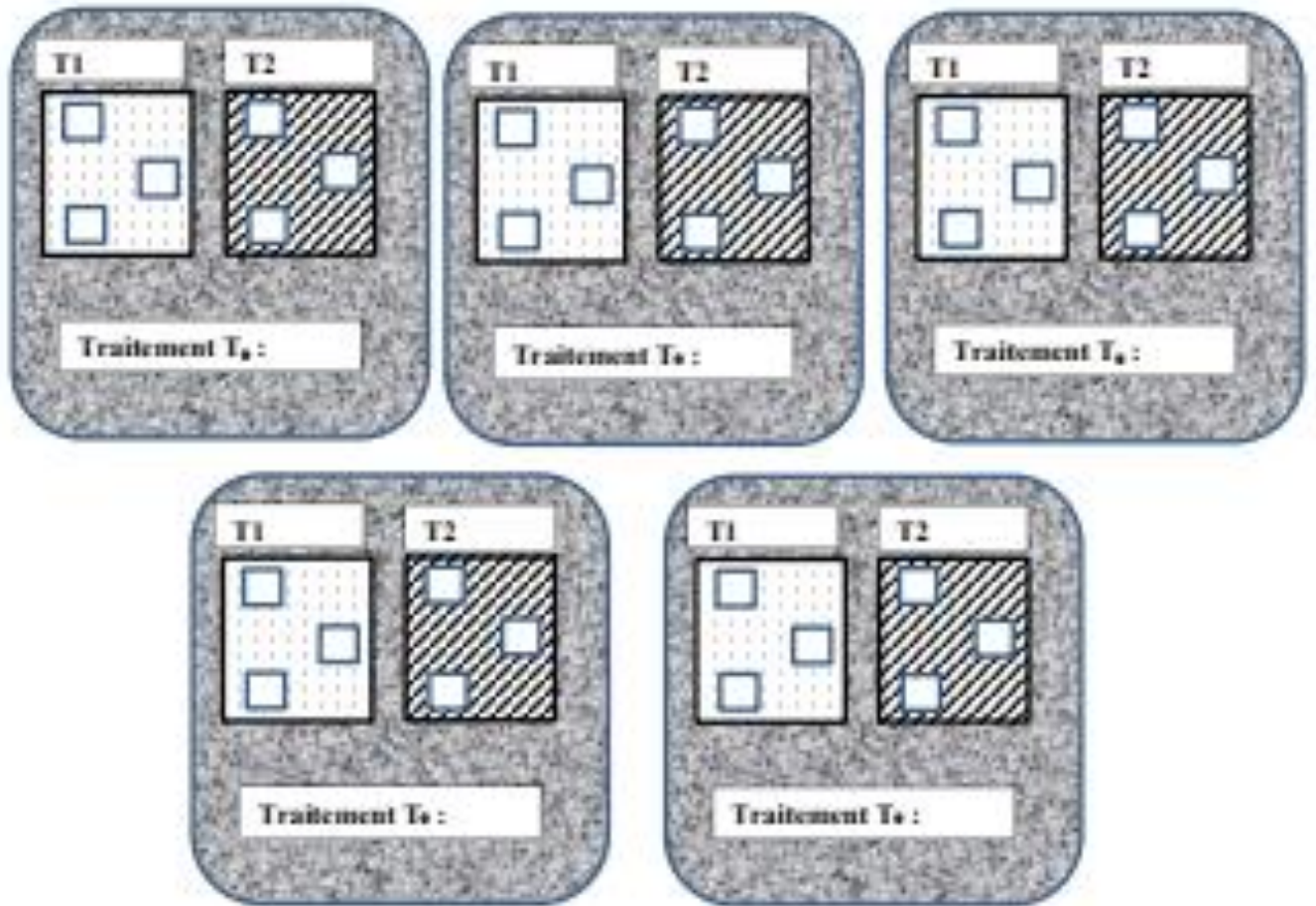


Figure 3. 5. Experiments design at village level

Legend :

T₀ = Control treatment (pure farmers' practices),

T₁ = seasonal forecast with full technologies package,

T₂ = Seasonal forecast information combined with farmers' practices

The experiments data were collected periodically and it included information about crop development (phenology, number of heads), crop environment (rainfall, soil type, diseases and pest attacks during the crop cycle), crop technical itinerary (sowing and harvest dates, fertilizer/pesticide application dates, type of fertilizer / pesticide used), crop yield. Data collection template was used for this purpose. For each year, two field trips was implemented over the 12 experiments sites. Statistical analysis was applied to the data collected to assess the gain that could result from the use of seasonal forecast information. The perception and experience of end users about the whole process collected from the mini-survey administrated to the 60 pilot farmers was analyzed and strategies to scale-up the experience to other regions and farmers were developed based on the trial's outcomes.

During the experiments' implementation, four field trips were carried out totally (two field trips per year). The first trip in the year was conducted in early May before the growing season start, just after the release of the WARCOF results. The aim of that trip is to share the forecast information and recommendations to farmers and the inputs (seeds, fertilizers, fungicide), train the data collectors (plate 3.2), disseminate data collection forms (Appendix B) and set the experiments plots on the farms. The second field trip was realized from the end of August to early September and it aims to set the plan for plots harvesting and yield data collection scheme (plate 3.3.). Three yield plots of 10m x 10m each are delimited in each of the treatment to measure data yield (grain, ears and straw weight).

The experiments were assimilated to a randomized complete block design (RCBD), hence as statistical methods, analysis of variance (ANOVA), Tukey's Honestly Significant Difference (HSD) test and linear regression were applied to analyze the endpoints.

This chapter started by restating the research objective and question, thereafter presenting a stepwise theoretical framework in response to the research question. Both qualitative and quantitative methodological approaches were argued for based on the socio-economic and correlational nature of the study, access to data, and contextual suitability. The next chapter will present, interpret and discuss key research findings using existing recent and current literatures.



Plate 3. 2 : Dissemination of crop inputs kits, forecast information and recommendations at NDounga, Guecheme and Tounouga to farmers during field trip before the starting of the rainy season



Plate 3. 3 : Millet harvesting and weighing at Tounouga

CHAPTER FOUR

RESULTS AND DISCUSSION

The purpose of this chapter is to present and discuss the main findings from the research and draw some perspectives based on the study outcomes. The chapter is organized around four main sections corresponding to the forecast skills assessment, potentials for improvement of the forecast method, evaluation of the forecast products dissemination and on-farm use, then finally the discussion section.

4.1. Performance assessment of the PRESASS method regarding the forecast of season onset date, cessation date and dry spells

As described at section 2.8 in chapter two, the PRESASS method is a complex and hybrid operational forecasting system involving both dynamical and statistical forecast methods completed by a consensual analysis by experts. The approach uses (GCM) outputs in a Models Output Statistics process through CPT software to build a statistical forecast, then products resulting from this process pass through a consultative analysis between experts from meteorological agencies, regional centers, guest experts from Long Range Forecasting – Global Producing Centers (LRF-GPC) and other scientists in climate-related fields to build a consensual forecast at the end.

4.1.1. Assessment of the statistical aspects of the PRESASS forecasting system regarding season characteristics forecast

4.1.1.1. Assessment of correlation between SST anomalies and season parameters using regression models

In the PRESASS forecasting system, CPT tool is used to assess the teleconnections between SST anomalies and rainfall patterns through statistical correlation, then regression models are used to quantify the relationships between them and thereafter the best model is used to forecast the

predictands (onset, cessation and dry spells for this case study) for the upcoming season. In the present study, to assess the performance and skill, several CPT experiments (1078 in total) correlating the predictands to different domains (grid boxes) of GCM outputs were run. The purpose of that is to test and identify the scenarios that provide the best goodness index. Table 4.1 shows the seven (7) domains of SST used within the tested scenarios. The selection of SST domains was guided by previous studies (Rowell et al., 2001, 2013; Graham et al., 2012; Fontaine et al., 2011) that identified teleconnections between some domains of the tropical sea surface temperatures and Africa's rainfall patterns, as well as by the domains usually utilized by experts to perform the statistical forecasting process during the PRESASS pre-forum.

For each of those domains of SST, regressions models were built using hindcasts from 8 GCMs (CFSV2, CMC1, CMC2, GFDL, NASA, NCAR_CCSM4, NMME) as predictors and the onset date, cessation date, dry spells duration at early stage and at the end of the season as predictands. Hindcasts time series used at this step cover the period 1991-2020. The same climatological normal is used also as training period for the regression models.

GCMs were initiated in April for 6 monthly lead times (May, June, July, August, September, October) and 5 seasonal lead times (MJJ, JJA, JAS, ASO, SON) to produce the hindcasts used as predictors. The hindcasts at lead times May, June, July, MJJ, JJA, JAS were correlated with early season parameters (Onset dates, early season dry spells duration) whereas those at lead times August, September, October, ASO and SON were correlated with end season parameters (cessation date and end of season dry spells).

Table 4.1: SST domains used to build and run the regression models

N ^o	Domain name	Domain coordinates	GCMs output variable used as predictor
1	NINO 3.4	5N-5S, 170W - 120E	SST
2	Central Eastern Tropical (CET) pacific	10S-10N, 150W-90N	SST
3	Tropical Northern Atlantic (TNA)	5N-24N, 50W - 15E	SST
4	Tropical Southern Atlantic (TSA)	20S-0, 30W-10E	SST
5	Equatorial Atlantic	3N-3S, 20W-0	SST
6	Domain of SST reportedly used during PRESASS	30N-30S, 0W-360E	SST
7	Domain of precipitation usually used during PRESASS	30N - 0, 30W - 30E	Precipitation

The goodness indices resulting from all the cross-validation regressions runs are listed in Appendix C. Table 4.2 is an excerpt from this appendix and it shows the scenarios giving relatively best goodness index coefficients (r). It comes out from those results that for season onset dates prediction, July precipitation hindcasts from CFSv2, May SST from CFSv2 at Equatorial Atlantic domain, July SST anomalies within TSA domain from NASA, JJA SST anomalies from CMC1 have the highest scores with r absolute value = 0.432. For the cessation date, September-October-November (SON) precipitation hindcast from NASA model and the August SST hindcast from CMC1 model picked out from the sample considered with r value respectively equal to 0.473 and 0.469. The dry spells duration at season early stage and at the end are well correlated respectively with SST hindcast over the June-July-August period from CMC1 and SST hindcast from GFDL during July-August-September period.

Table 4.2 : Pearson correlation coefficients from regression models between SST hindcasts and season parameters

Predictand Y	GCM name	Hindcast Achronym in PRESASS forecasting System	Predictor X	GCM output lead time	Domain used for prediction	r
Onset date	nasa	nasa_sst_hcst_Apric_7_1991	SST	July	4	-0,432
	cfsv2	cfsv2_precip_hcst_Apric_7_1991	precip	July	7	-0,432
	nasa	nasa_sst_hcst_Apric_6-8_1991-2020	SST	JJA	4	-0,431
	cfsv2	cfsv2_sst_hcst_Apric_5_1991	SST	May	5	-0,430
	cmc1	cmc1_sst_hcst_Apric_6-8_1991-2020	SST	JJA	6	-0,429
ESDS	cmc1	cmc1_sst_hcst_Apric_6-8_1991-2020	SST	JJA	6	-0,441
	nasa	nasa_precip_hcst_Apric_7_1991	precip	July	7	-0,439
	cmc2	cmc2_precip_hcst_Apric_5_1991	precip	May	7	-0,438
	gfdl	gfdl_sst_hcst_Apric_7_1991	SST	July	4	-0,437
	nasa	nasa_sst_hcst_Apric_5-7_1991-2020	SST	MJJ	6	-0,435
Cessation date	nasa	nasa_precip_hcst_Apric_9-11_1991-2020	precip	SON	7	-0,473
	cmc1	cmc1_sst_hcst_Apric_8_1991	SST	Aug	3	-0,469
	cmc2	cmc2_sst_hcst_Apric_8_1991	SST	Aug	3	-0,465
	nmme	nmme_sst_hcst_Apric_8-10_1991-2020	SST	ASO	4	-0,465
	cmc1	cmc1_sst_hcst_Apric_7-9_1991-2020	SST	JAS	3	-0,464
	nmme	nmme_sst_hcst_Apric_9-11_1991-2020	SST	SON	5	-0,464
LSDS	gfdl	gfdl_sst_hcst_Apric_7-9_1991-2020	SST	JAS	5	-0,446
	nmme	nmme_sst_hcst_Apric_7-9_1991-2020	SST	JAS	3	-0,444
	cfsv2	cfsv2_sst_hcst_Apric_9_1991	SST	Sept	5	-0,442
	cfsv2	cfsv2_sst_hcst_Apric_8_1991	SST	Aug	1	-0,428
	ncar_ccsm4	ncar_ccsm4_sst_hcst_Apric_8_1991	SST	Aug	3	-0,427
	nasa	nasa_precip_hcst_Apric_10_1991	precip	Oct	7	-0,427

ESDS: Early Season Dry Spells

LSDS: Late Season Dry Spells

4.1.1.2. Verification of statistical forecast using CPT based on best combinations of predictor and predictand

In order to perform the verification of statistical forecasts, CPT was run in retroactive mode to create the forecasts dataset to be verified. Based on scenarios with higher goodness index coefficients (r), resulting from the previous section (Table 4.2), retroactive validation was performed for the 4 season parameters. Then skill maps resulting from the retroactive validation were retrieved. Pearson's correlation and hit skill scores are the two skill parameters that were used to verify the forecast skills.

Figures 4.1, 4.2, 4.3, and 4.4 show Pearson's correlation and hit skill scores maps for the CPT experiments (scenarios in Table 4.2) that showed the relative highest correlation scores with the onset. Figures 4.5 to 4.8 show those performances metrics for cessation dates forecast. Figures 4.9 to 4.13 are skills maps for the early season dry spells duration and Figures 4.14 to 4.17 show the skills maps for the late season dry spell duration.

Pearson's correlation in these skill maps indicates how well the predictors (SST anomalies and precipitation hindcasts) align with historical onset and cessation dates or dry spell durations. Higher positive correlations (closer to +1) suggest that the climate predictor provides a strong linear relationship with the observed historical data. Negative correlations (closer to -1) indicate an inverse relationship, meaning the predictor might signal an opposite effect on the climate variable. Near-zero correlations indicate weak or no linear relationship, suggesting the predictor may not be reliable for forecasting.

Hit Skill Score (HSS) measures how well the categorical forecast (for instance early onset, normal onset, late onset) predicts the actual observed events. Higher HSS values (closer to 1.0) indicate that the forecast model performs significantly better than random predictions. $HSS = 0$ suggests

that the forecast is no better than random chance. Negative HSS values indicate that the forecast model performs worse than random chance, meaning it might be misleading for decision-making.

If a model consistently shows higher Pearson correlation and HSS, it is a better predictor for onset/cessation dates and dry spells. If correlations and HSS vary significantly across models, it suggests some models have stronger predictability than others depending on seasonality or lead time.

a) Interpretation of skills maps resulting from the retroactive validation for:

Onset date forecasting

Figure 4.1. shows that NASA SST anomaly (April initialized, lead time July) presents good Pearson Correlations over large regions with moderate HSS, however there are some scattered regions of poor correlation, possibly due to local variability. Precipitation predictors capture onset signals well, slightly better than SST for localized onset patterns as shown in Figure 4.2. presenting the performance of CFSv2 precipitation hindcasts (April initialized, lead time July), specially over Burkina Faso, Northern Senegal, Southern Mauritania and Southern Niger, but their performance remains moderate at regional level. SST anomalies from both CFSv2 (Figure 4.3.) and CMC1 models (Figure 4.4) show overall moderate performance for onset date forecasting.

Table 4.3 summarize the key findings that come out from the analysis of Figures 4.1. to 4.4 presenting the skill maps from the CPT experiments runs that have shown the relative highest correlation scores between the predictors and the onset date.

Table 4.3: Summary of the key findings from the skill maps analysis for onset date forecasting

Predictor Type	Initialization / Lead	Overall Skill (Pearson Correlation & Hit Skill)	Key Observations
SST (NASA model)	April Init. / July Lead	Good Pearson Correlations over large regions; Hit Skill moderate in most of the areas	Good skill but scattered regions of poor correlation, possibly due to local variability.
Precipitation (CFSv2)	April Init. / July Lead	Moderate to good	Precipitation predictors capture onset signals well, slightly better than SST for localized onset patterns.
SST (CFSv2)	April Init. / May Lead	Moderate but earlier lead time reduces skill slightly	Early signals weaker; still decent for some coastal zones.
SST (CMC1)	April Init. / JJA Lead	Overall moderate but stronger skill for JJA onset	Wider regional coherence in skill; JJA lead captures seasonal moisture buildup effectively.

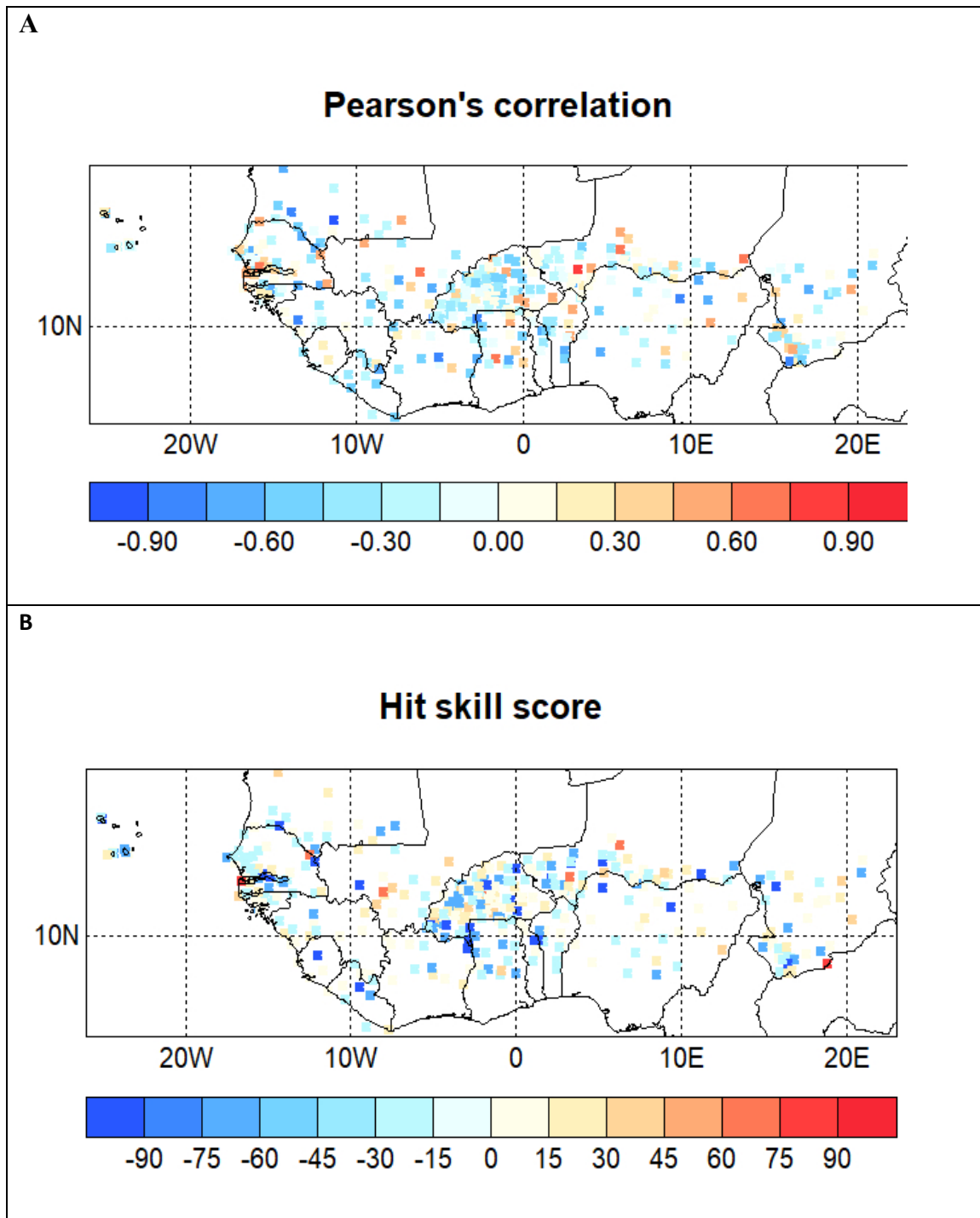


Figure 4.1. Skill maps (A = Pearson Correlations and B = Hit Skill Score) for onset retroactive forecast using **SST anomaly hindcast from NASA model (initialized in April with lead time July) as predictor** and **onset date** historical data

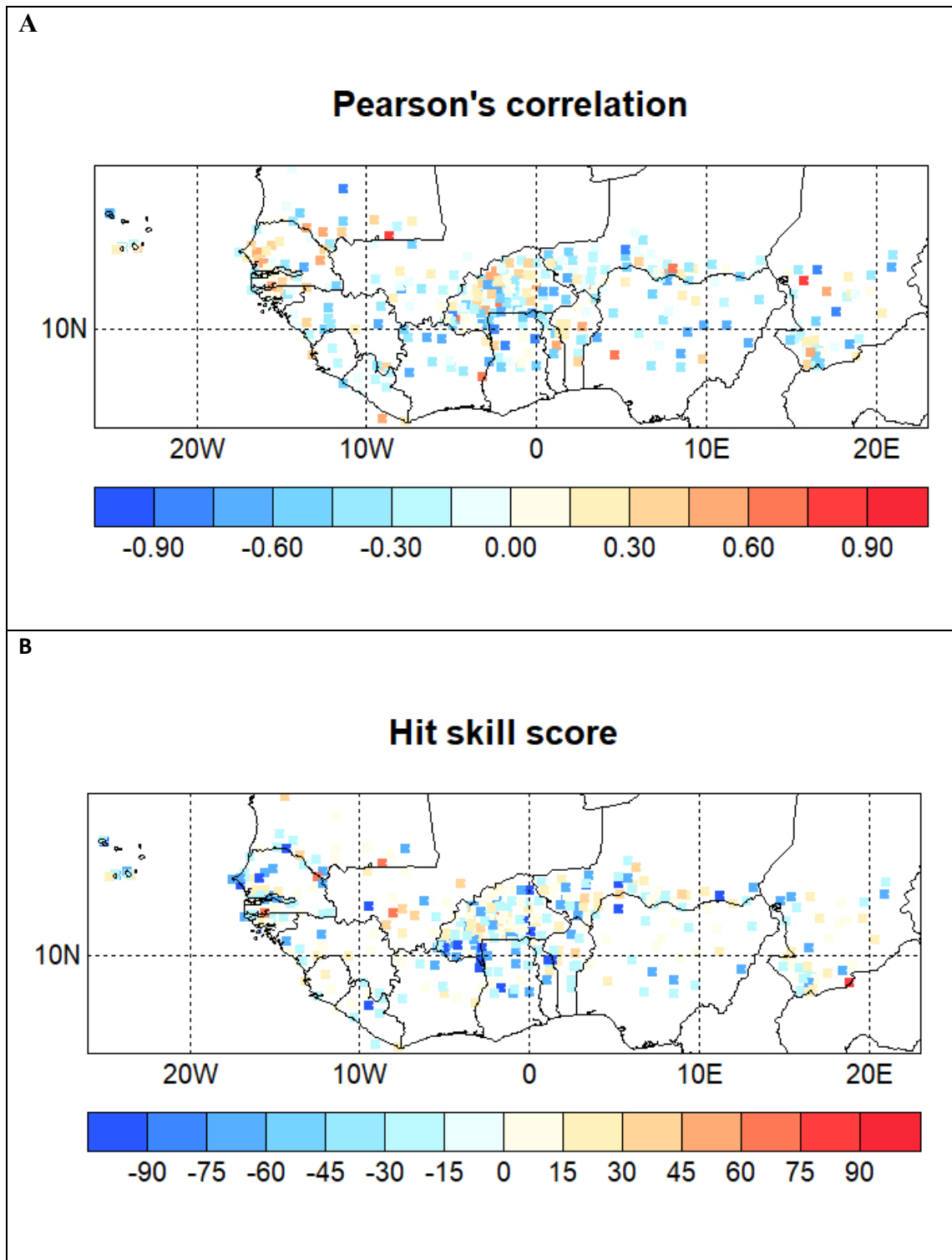


Figure 4.2. Skill maps (A = Pearsons Correlation and B = Hit Skill Score) for onset retroactive forecast using **precipitation hindcast from CFSv2 model (initialized in April with lead time July) as predictor** and **onset date** historical data

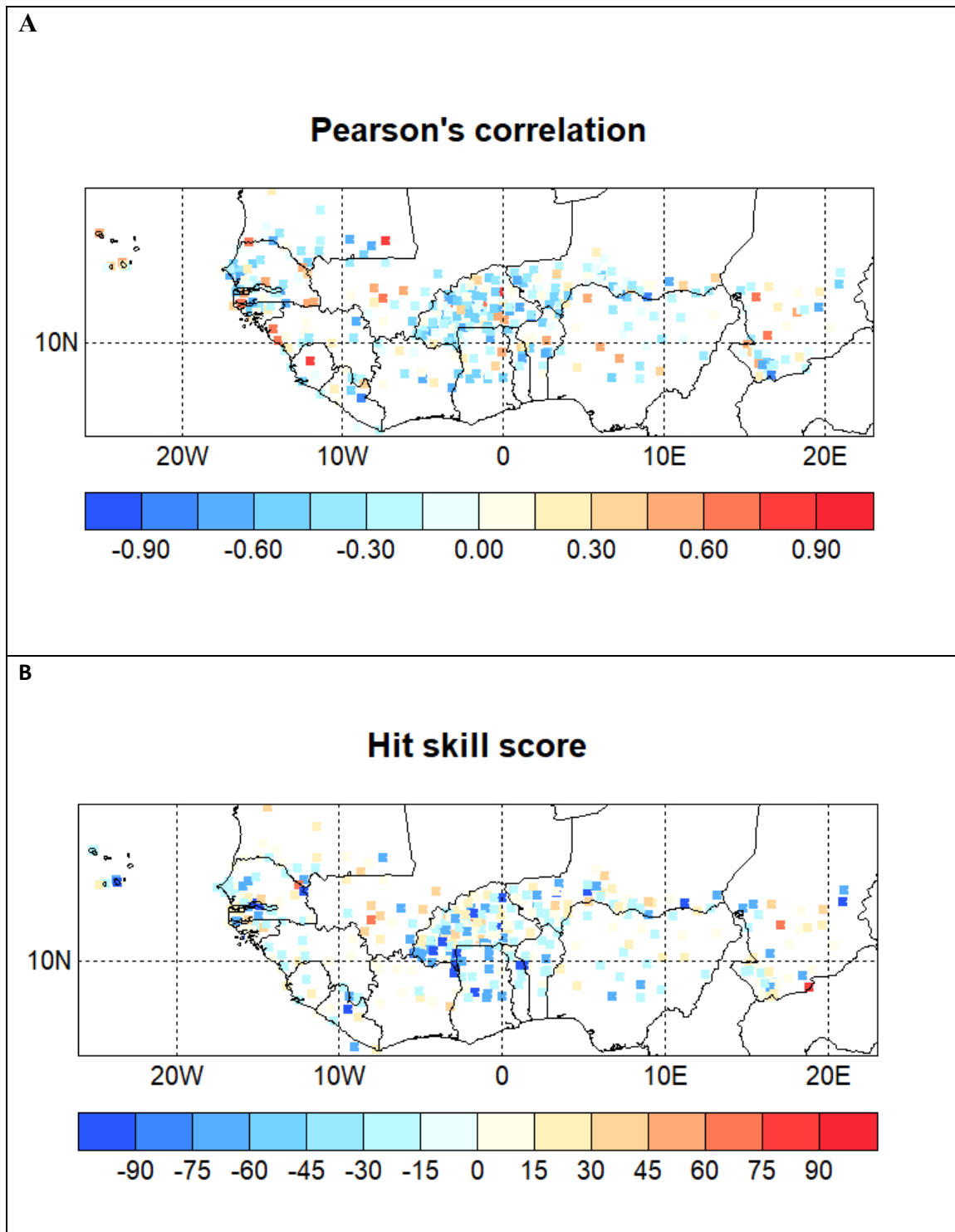


Figure 4.3. Skill maps (A = Pearson's Correlation and B = Hit Skill Score) for onset retroactive forecast using **SST anomaly hindcast from CFSv2 model (initialized in April with lead time May) as predictor and onset date historical data**

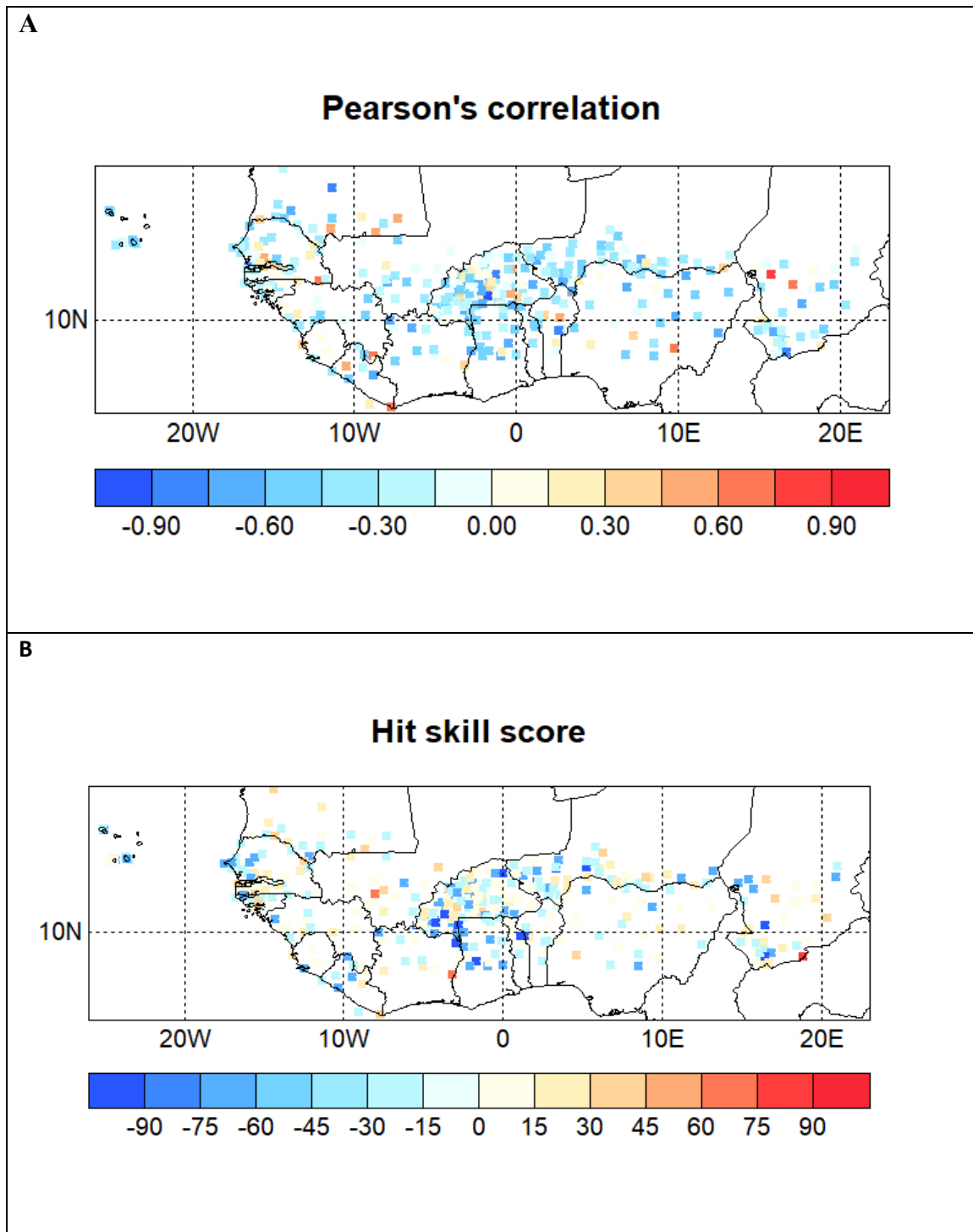


Figure 4.4. Skill maps (A = Pearsons Correlation and B = Hit Skill Score) for onset retroactive forecast using **SST anomaly hindcast from CMC1 (initialized in April with lead time JJA) as predictor and onset date historical data**

- **Cessation date forecasting**

Figure 4.5 shows that NASA precipitation (April initialized, lead time SON) presents high Pearson correlation and strong HSS. SST predictors alone are less effective for cessation dates forecasting as shown in Figures 4.6 and 4.7 presenting moderate performance of SST anomaly from CMC1 and CMC2 models initialized in April with August lead time. However, combining multiple models' ensemble SST forecasts may improve skill coverage as noticed with NMME SST anomaly (April initialized, lead time ASO) in Figure 4.8.

Table 4.4 summarizes the main results out from the analysis of Figures 4.5 to 4.8 presenting the skill maps from the CPT experiments runs that have shown the relative highest correlation scores between the predictors and the cessation date.

Table 4.4 : Summary of the key findings from the skill maps analysis for cessation date forecasting

Predictor Type	Initialization / Lead	Overall Skill	Key Observations
Precipitation (NASA model)	April Init. / SON Lead	Good correlation; moderate to strong Hit Skill Score.	Precipitation predictors good for cessation forecasts.
SST (CMC1)	April Init. / August Lead	Moderate	Some localized skill; however, SST predictors alone are less effective for cessation.
SST (CMC2)	April Init. / August Lead	Similar to CMC1	Cessation skill remains patchy when using SST alone at this lead.
SST (NMME)	April Init. / ASO Lead	Moderate to good	Combining multiple model ensemble SST forecasts improves skill coverage.

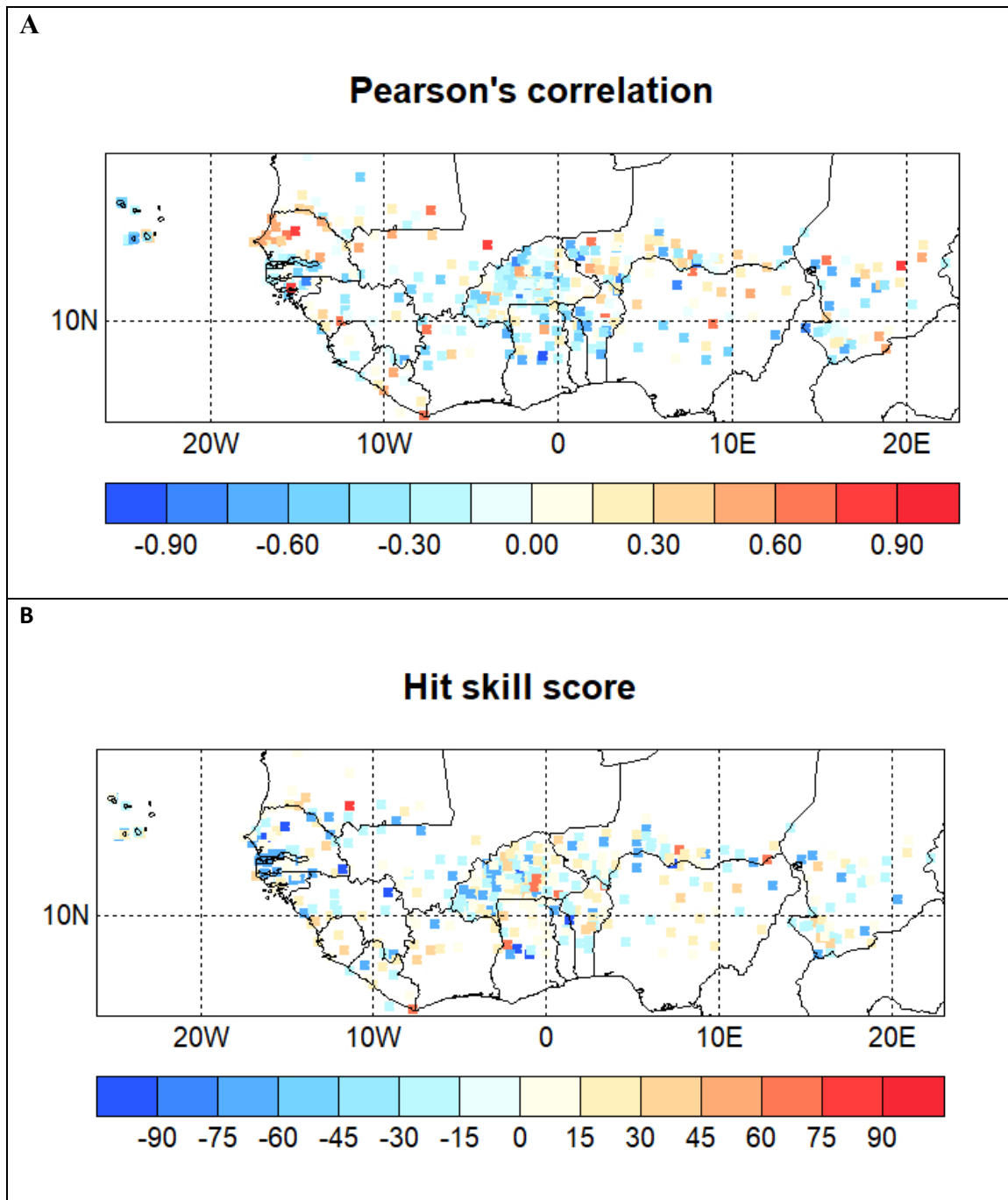


Figure 4.5. Skill maps (A = Pearsons Correlation and B = Hit Skill Score) for cessation retroactive forecast using **precipitation hindcast from NASA model (initialized in April with lead time SON) as predictor** and **cessation date historical data**

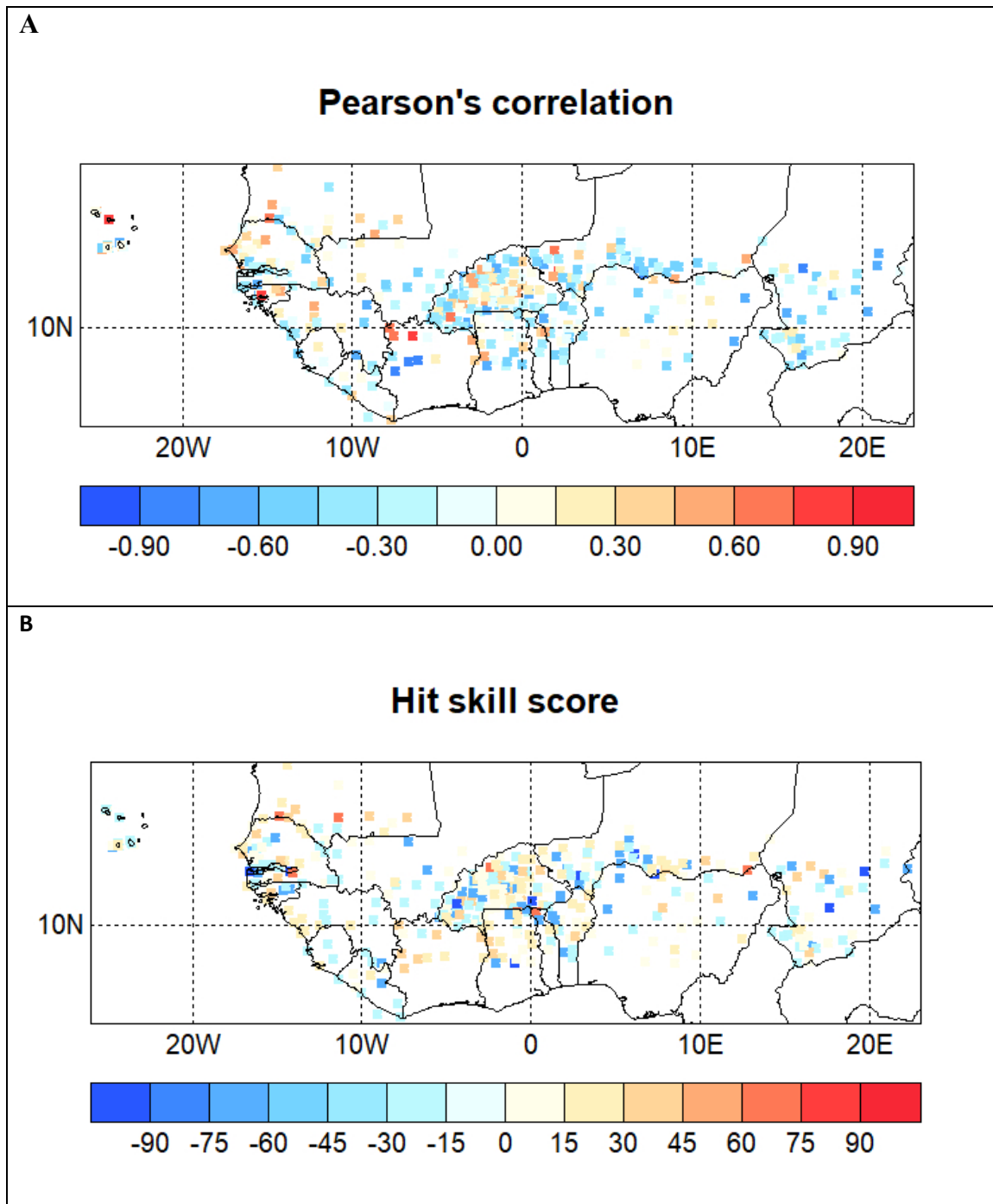


Figure 4.6. Skill maps (A = Pearsons Correlation and B = Hit Skill Score) for cessation retroactive forecast using **SST anomaly hindcast from CMC1 model (initialized in April with lead time August) as predictor** and **cessation date** historical data

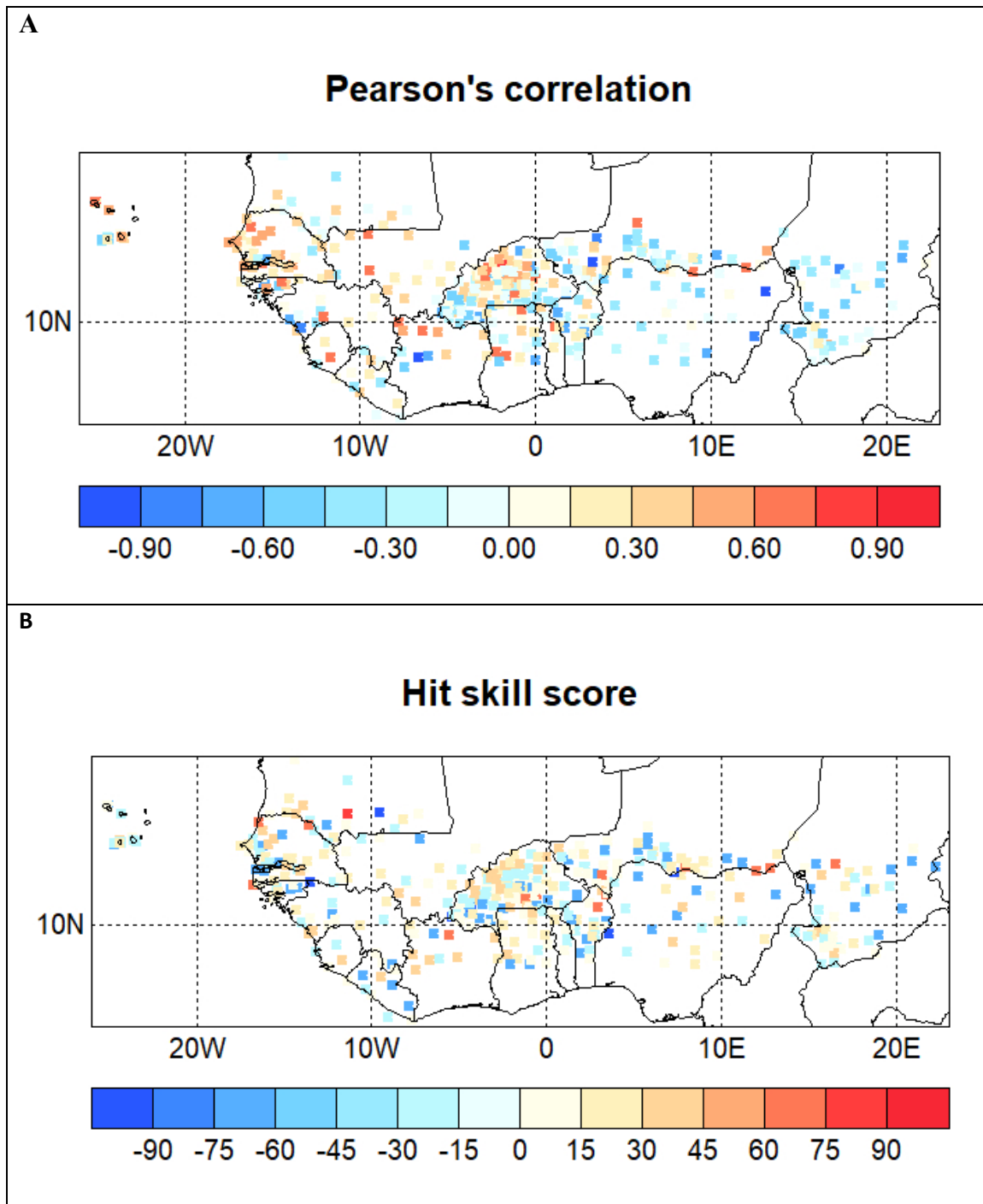


Figure 4.7. Skill maps (A = Pearsons Correlation and B = Hit Skill Score) for cessation retroactive forecast using SST anomaly hindcast from CMC2 model (initialized in April with lead time August) as predictor and cessation date historical data

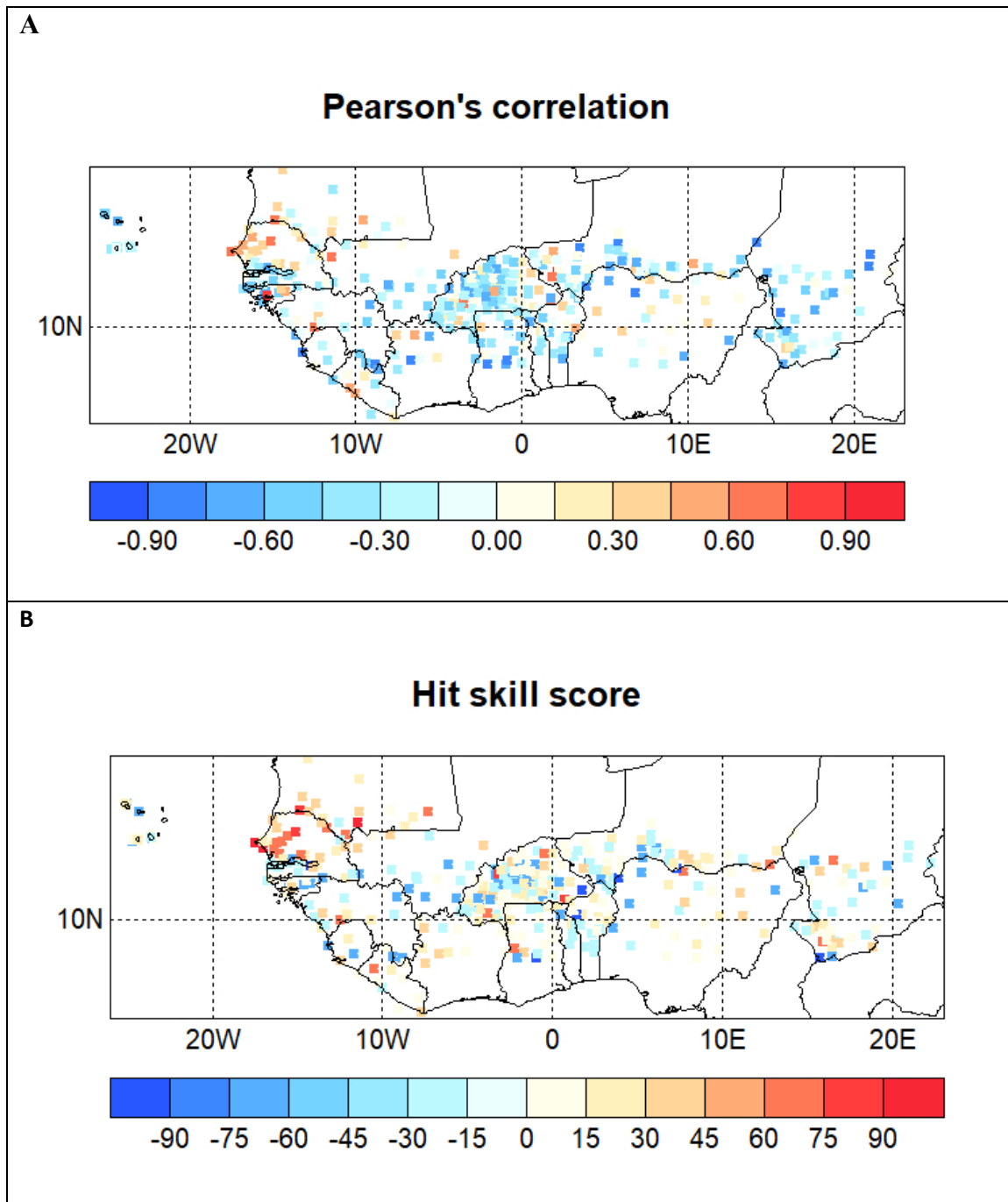


Figure 4.8. Skill maps (A = Pearsons Correlation and B = Hit Skill Score) for cessation retroactive forecast using SST anomaly hindcast from NMME model (initialized in April with lead time ASO) as predictor and cessation date historical data

- **Early season dry spells duration forecasting**

SST anomaly from CMC1 at lead time JJA show moderate Pearson's correlation coefficient with better Skill over wetter areas (Figure 4.9). SSTs from GFDL capture early dry spell patterns well, especially over coastal zones. Indeed, SST anomaly from that model initialized in April with July lead time shows good Pearson correlation coefficient and HSS (Figure 4.12). Precipitation hindcasts from NASA at MJJ and July lead times present respectively good and moderate to good skill scores (Figures 4.10 and 4.13). This confirms that early season forecasts are sharper when precipitation hindcasts are used as predictors instead of SSTs. The correlation coefficient and the HSS are lower for SST anomaly from CMC2 at lead time May (Figure 4.11). The low performance of this predictor here may be related to the early lead time as usually early lead forecasts carry lower skill.

Table 4.5 recapitulates the main take away messages from the analysis of Figures 4.9 to 4.13 showing the skills maps from the scenarios that showed the best correlation between the predictors and the early season dry spells duration.

Table 4.5 : Summary of the key findings from the skill maps analysis for the early season dry spell duration

Predictor Type	Initialization / Lead	Overall Skill	Key Observations
SST (CMC1)	April Init. / JJA Lead	Moderate	Skill better over wetter zones; weaker over semi-arid areas.
Precipitation (NASA)	April Init. / July Lead	Moderate to good	Precipitation anomalies are a good predictor for early season dry spells.
SST (CMC2)	April Init. / May Lead	Moderate	Early lead forecasts carry lower skill.
SST (GFDL)	April Init. / July Lead	Good	GFDL SST forecasts capture early dry spell patterns well, especially over coastal zones.
Precipitation (NASA)	April Init / MJJ Lead	Good	Early season forecasts are sharper when precipitation hindcasts are used instead of SSTs.

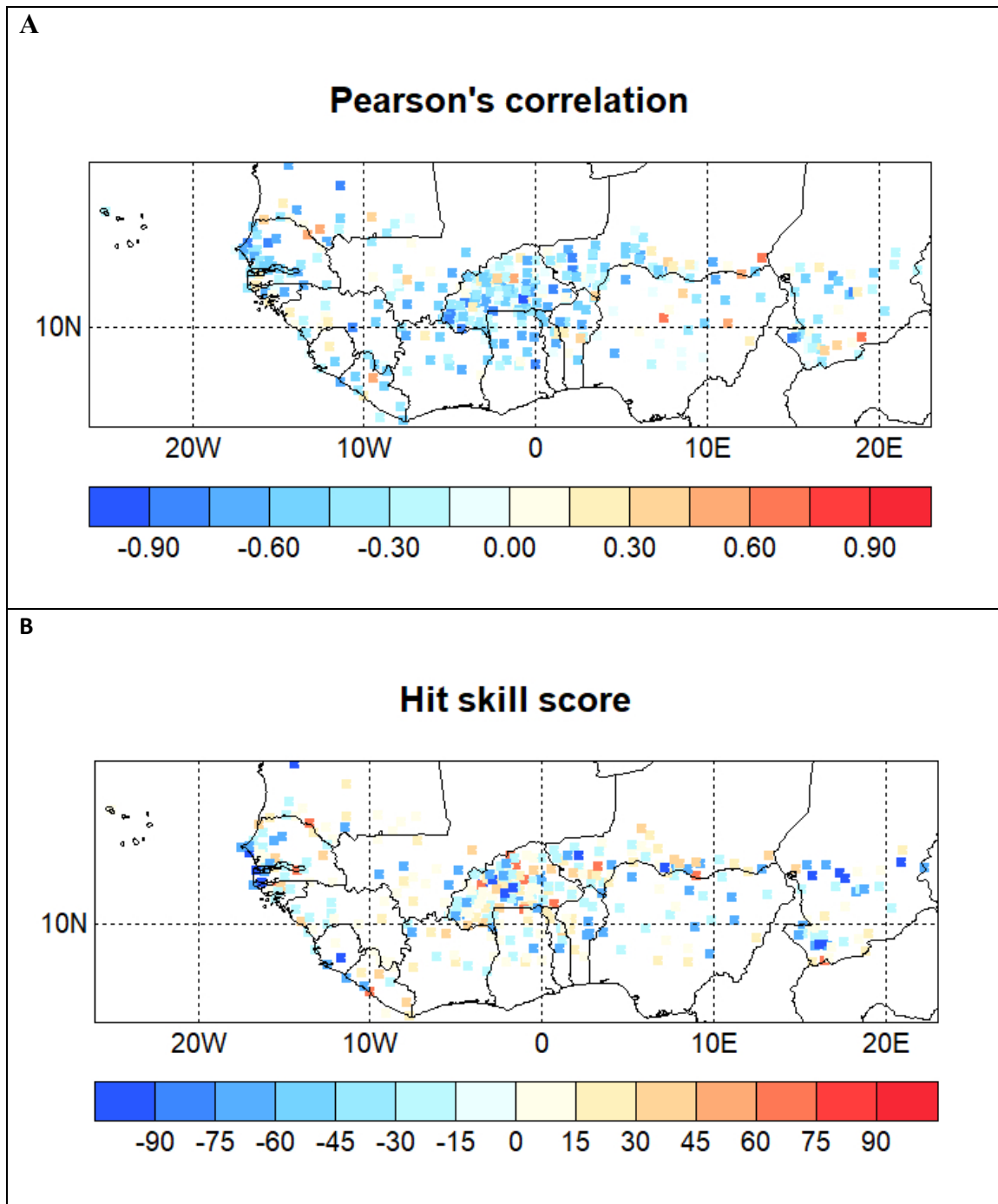


Figure 4.9. Skill maps (A = Pearsons Correlation and B = Hit Skill Score) for early season dry spells duration retroactive forecast using **SST anomaly hindcast from CMC1 model (initialized in April with lead time JJA)** as predictor and **Early Season Dry Spells duration** historical data

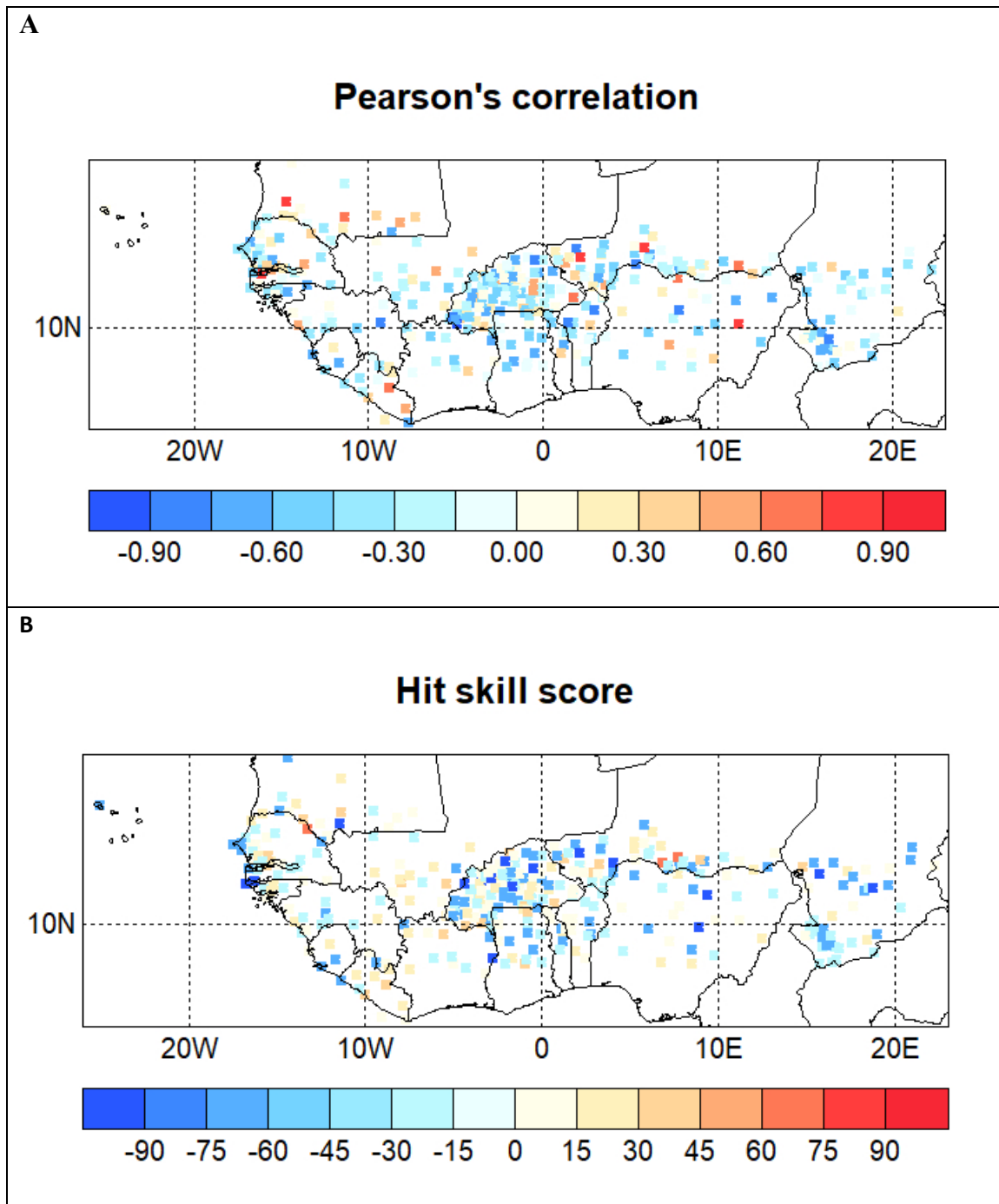


Figure 4.10. Skill maps (A = Pearsons Correlation and B = Hit Skill Score) for early season dry spells duration retroactive forecast using **precipitation hindcast from NASA model (initialized in April with lead time July)** as predictor and **Early Season Dry Spells duration** historical data

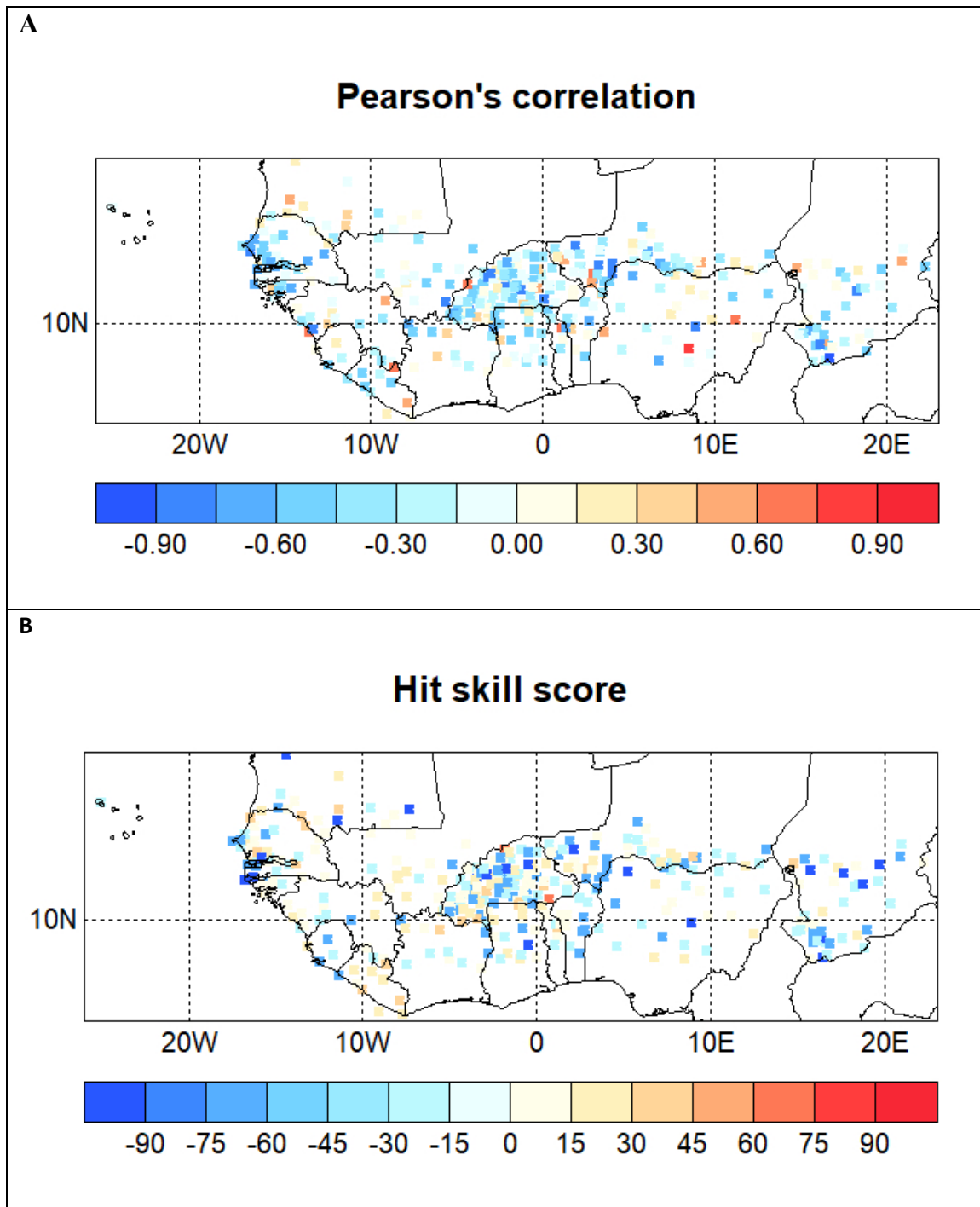


Figure 4.11. Skill maps (A = Pearsons Correlation and B = Hit Skill Score) for Early season dry spells duration retroactive forecast using **SST anomaly hindcast from CMC2 model (initialized in April with lead time May) as predictor** and **Early Season Dry Spells duration historical data**

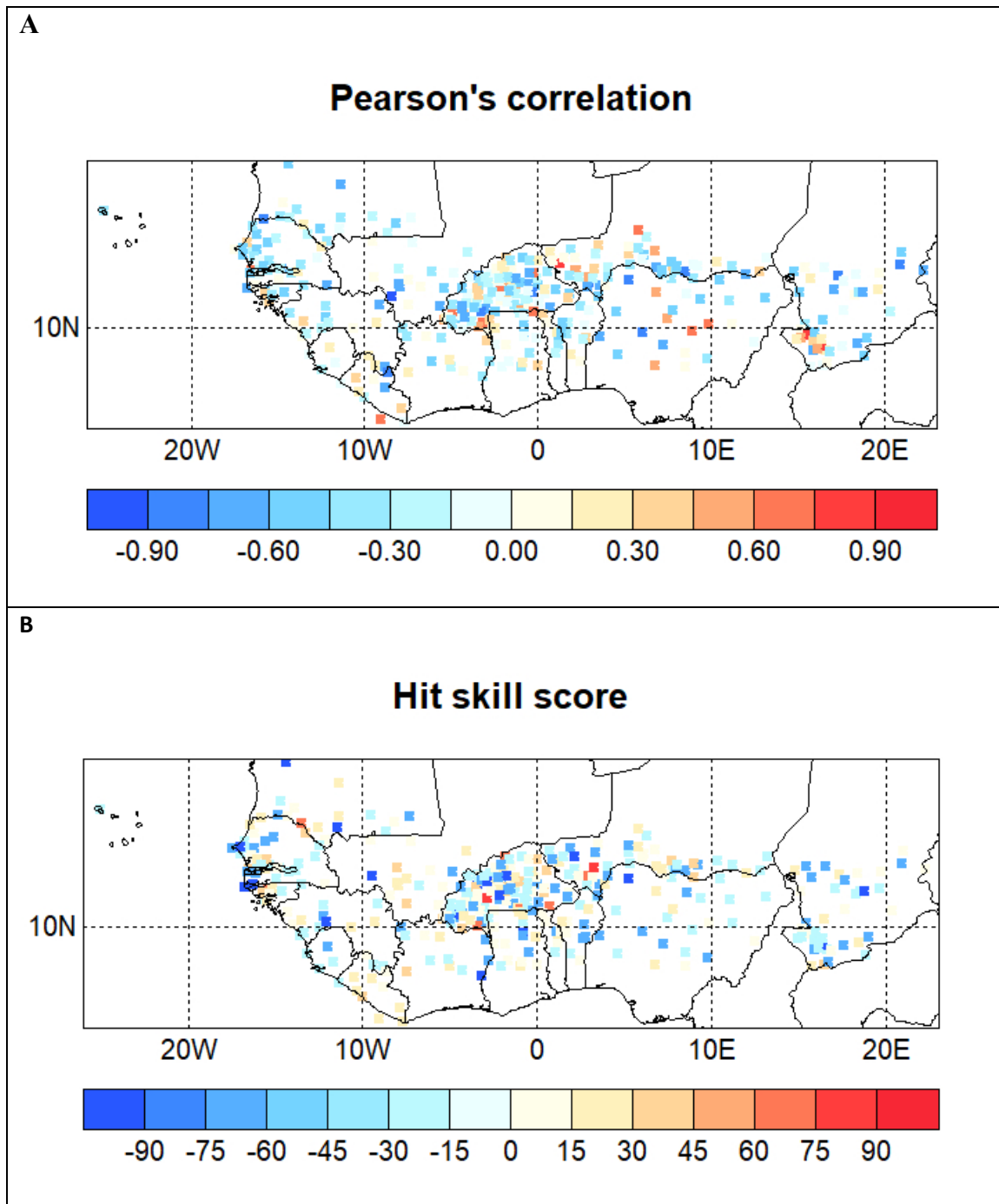


Figure 4.12. Skill maps (A = Pearsons Correlation and B = Hit Skill Score) for Early season dry spells duration retroactive forecast using **SST anomaly hindcast from GFDL (initialized in April with lead time July) as predictor** and **Early Season Dry Spells duration** historical data

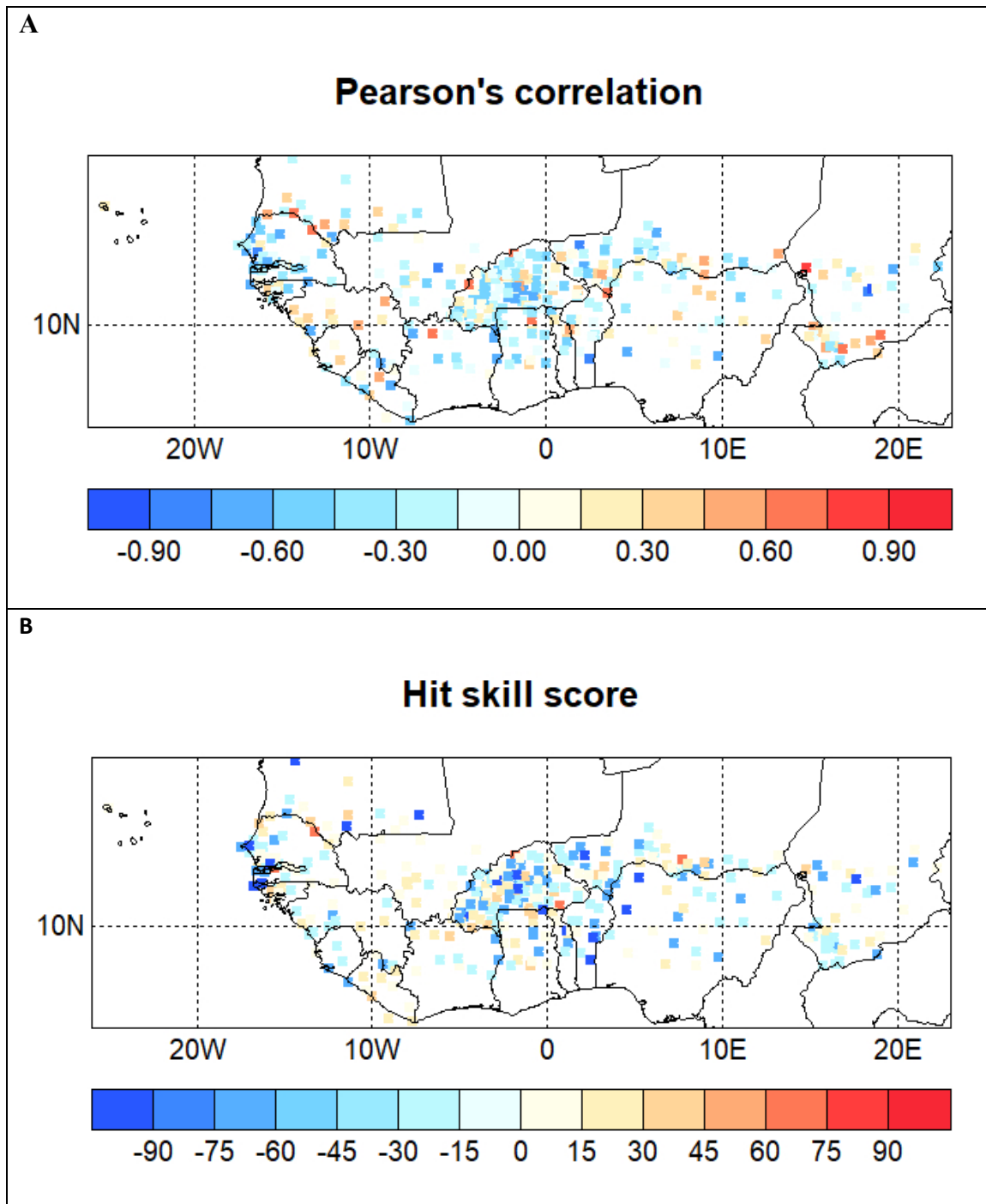


Figure 4.13. Skill maps (A = Pearsons Correlation and B = Hit Skill Score) for early season dry spells duration retroactive forecast using **precipitation hindcast from NASA model (initialized in April with lead time MJJ) as predictor** and **Early Season Dry Spells duration** historical data

- **End of season dry spell duration forecasting**

Consistent skills were observed with SST anomaly from GFDL model at JAS lead time (Figure 4.14) which shows higher Pearson's correlation coefficient and stronger HSS compared to the other indicators. SSTs from NMME model at lead time JAS (Figure 4.15) and August SST from CFSv2 (Figure 4.16) show moderate Pearson's coefficient and HSS. September SST from Cfsv2 (Figure 4.17) and October precipitation hindcast from NASA (Figure 4.18) show weak skill scores, suggesting the weaker predictive ability of those indicators for late dry spells.

Table 4.6 : Summary of the key findings from the skill maps analysis for the end season dry spell duration

Predictor Type	Initialization / Lead	Overall Skill	Key Observations
SST (GFDL)	April Init / JAS Lead	Good to moderate	Consistent skill across core monsoon retreat zones.
SST (NMME)	April Init / JAS Lead	Moderate	Multi-model SST improves late season dry spell prediction.
SST (CFSv2)	April Init / September Lead	Weak to Moderate	Somewhat degraded skill at longer lead times.
SST (CFSv2)	April Init / August Lead	Moderate	August lead time offers better skill compared to September lead.
Precipitation (NASA)	April Init / October Lead	Poorer skill	October precipitation hindcast has weaker predictive ability for late dry spells.

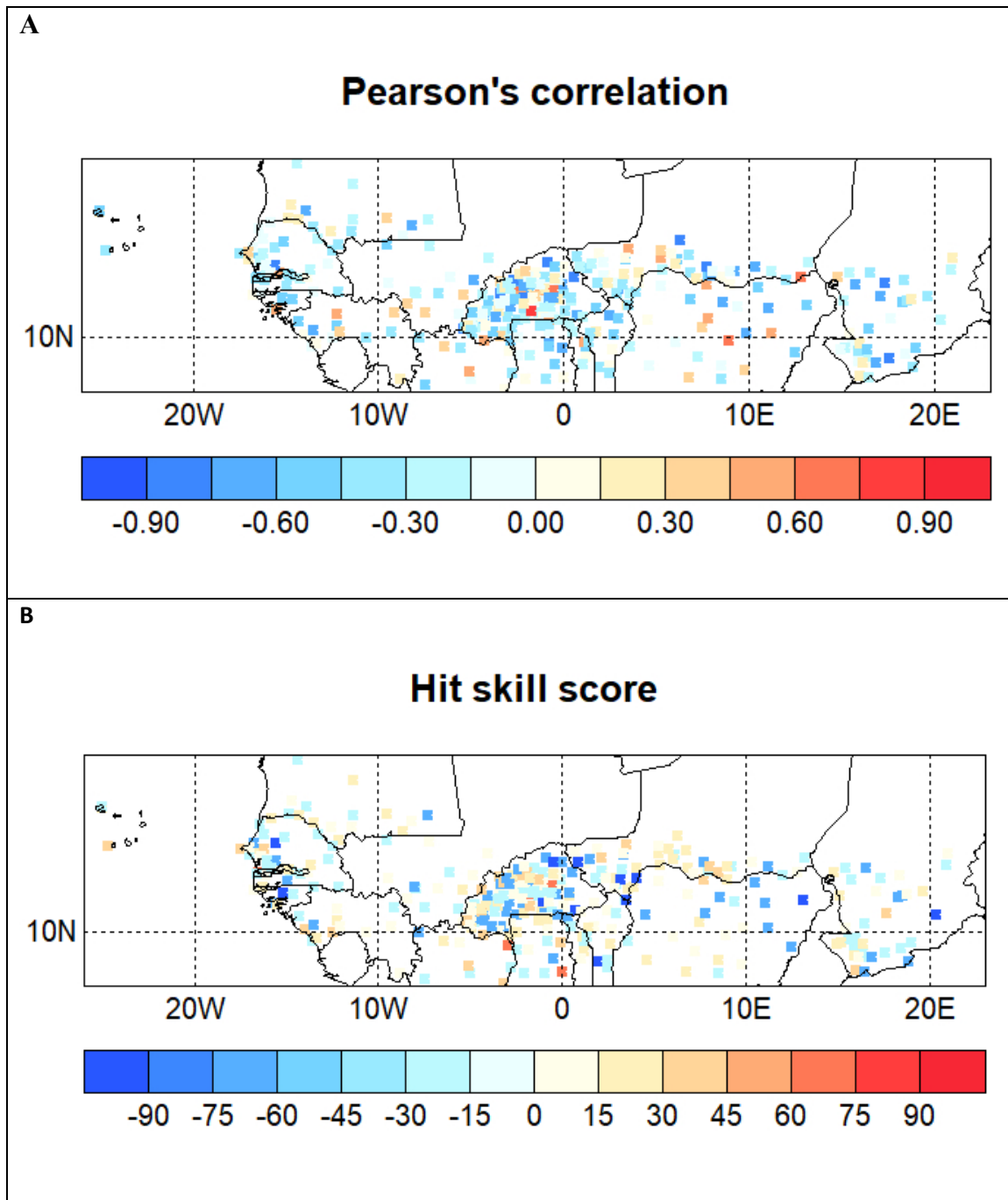


Figure 4.14. Skill maps (A = Pearsons Correlation and B = Hit Skill Score) for End season dry spells duration retroactive forecast using **SST anomaly hindcast from GFDL (initialized in April with lead time JAS)** as predictor and **End Season Dry Spells duration** historical data

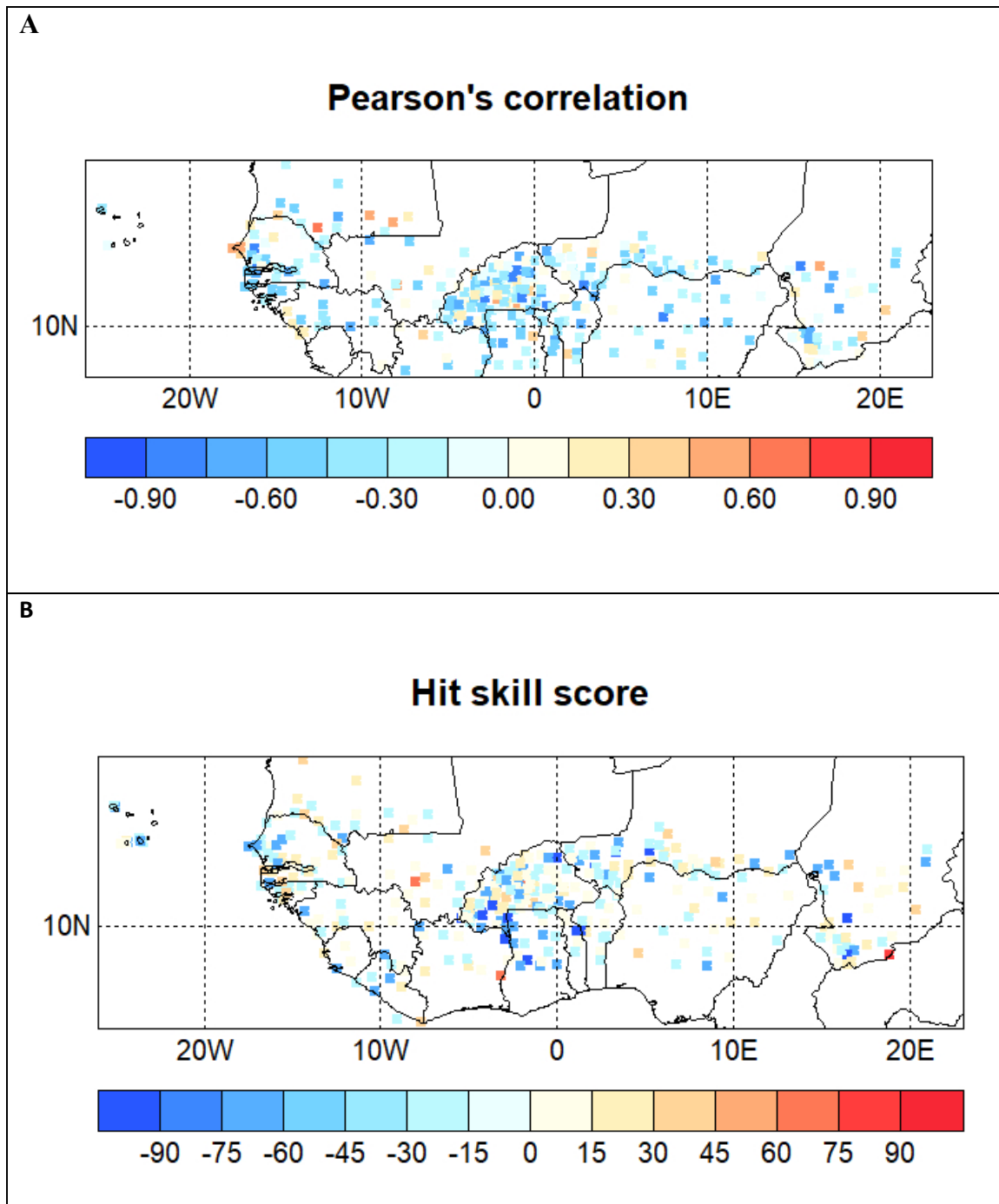


Figure 4.15. Skill maps (A = Pearsons Correlation and B = Hit Skill Score) for End season dry spells duration retroactive forecast using **SST anomaly hindcast from NMME model (initialized in April with lead time JAS)** as predictor and **Late Season Dry Spells duration** historical data

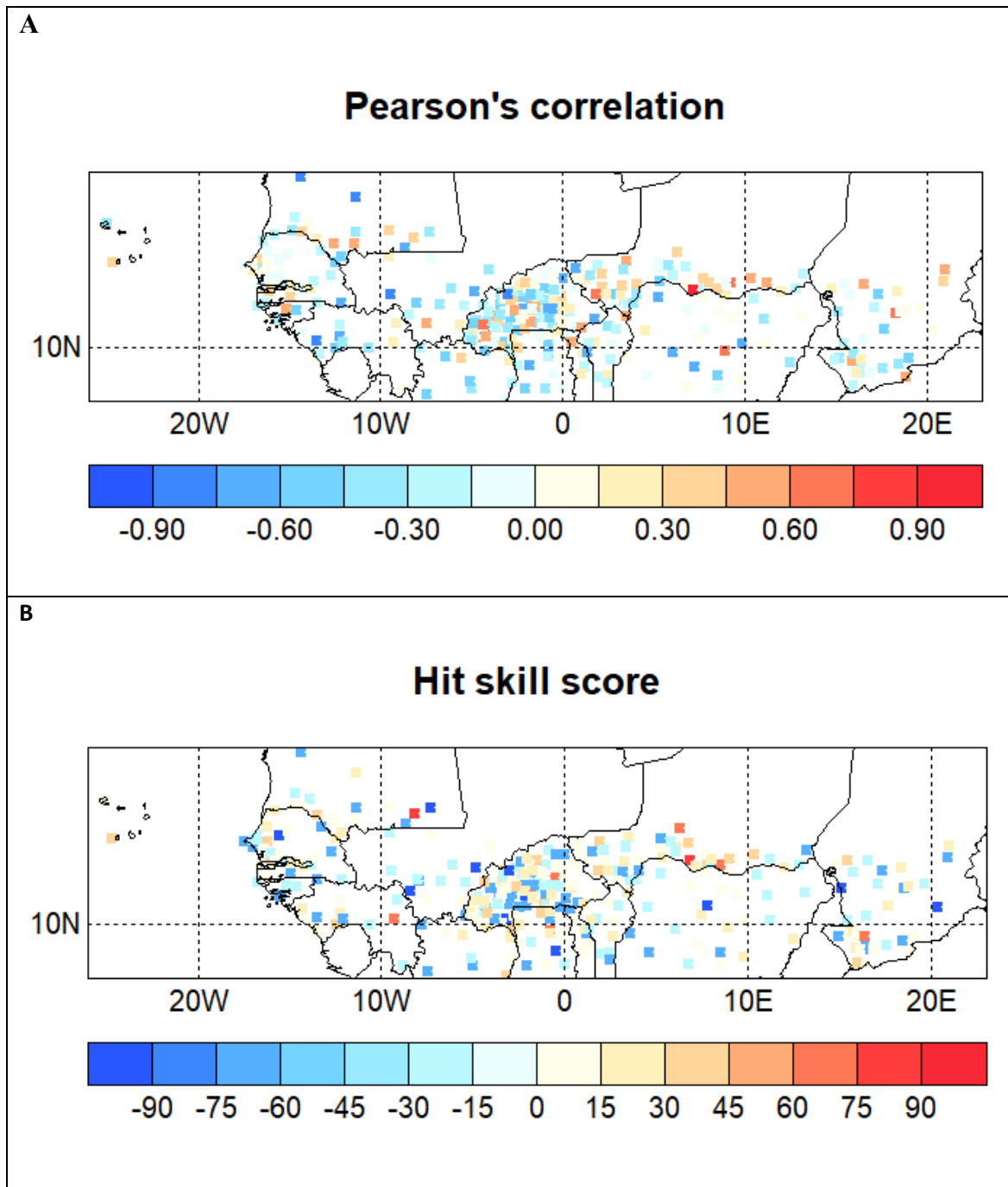


Figure 4.16. Skill maps (A = Pearsons Correlation and B = Hit Skill Score) for End season dry spells duration retroactive forecast using **SST anomaly hindcast from CFSv2 (initialized in April with lead time September) as predictor** and **End Season Dry Spells duration** historical data

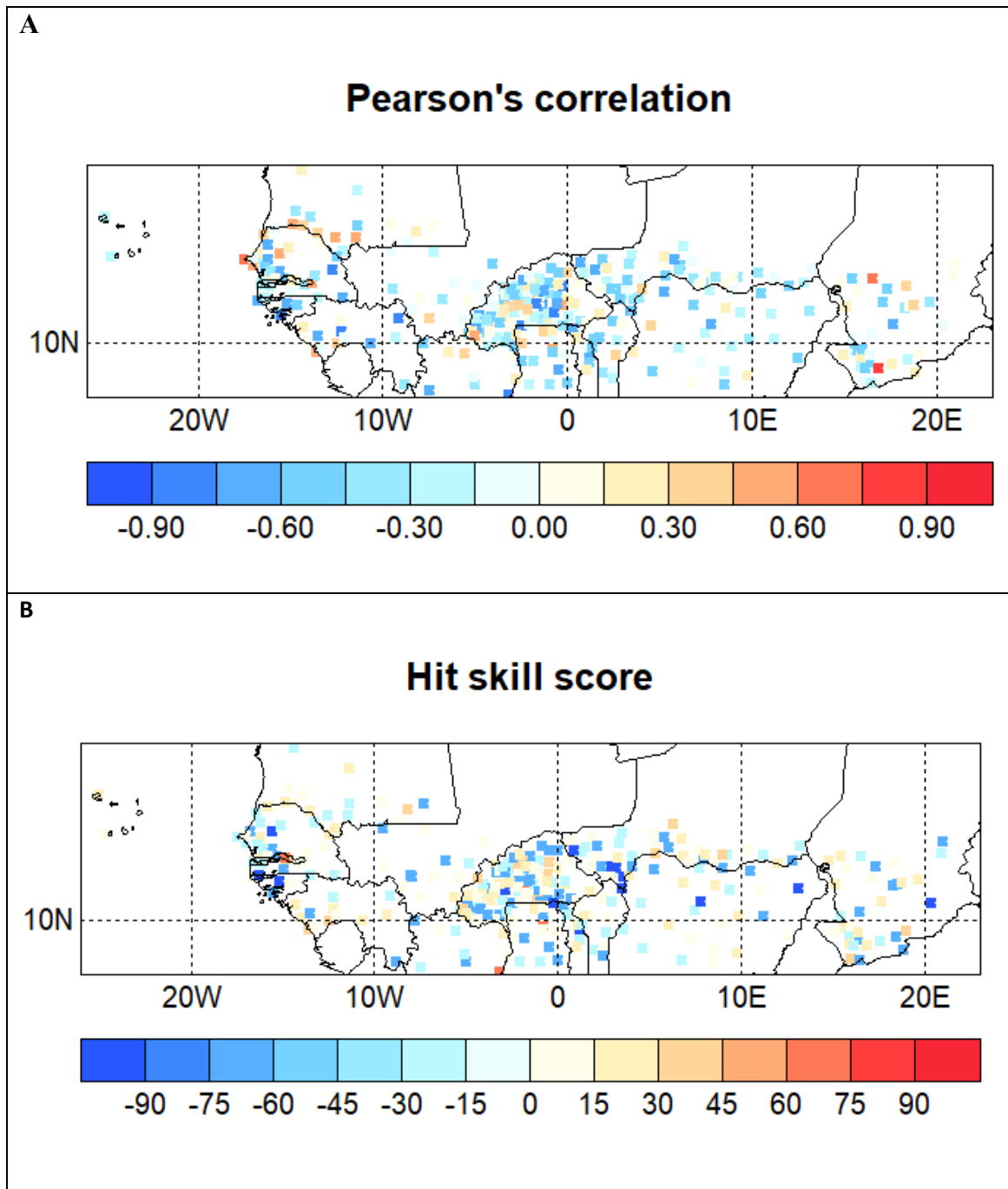


Figure 4.17. Skill maps (A = Pearsons Correlation and B = Hit Skill Score) for End season dry spells duration retroactive forecast using **SST anomaly hindcast from CFSv2 (initialized in April with lead time August)** as predictor and **Late Season Dry Spells duration** historical data

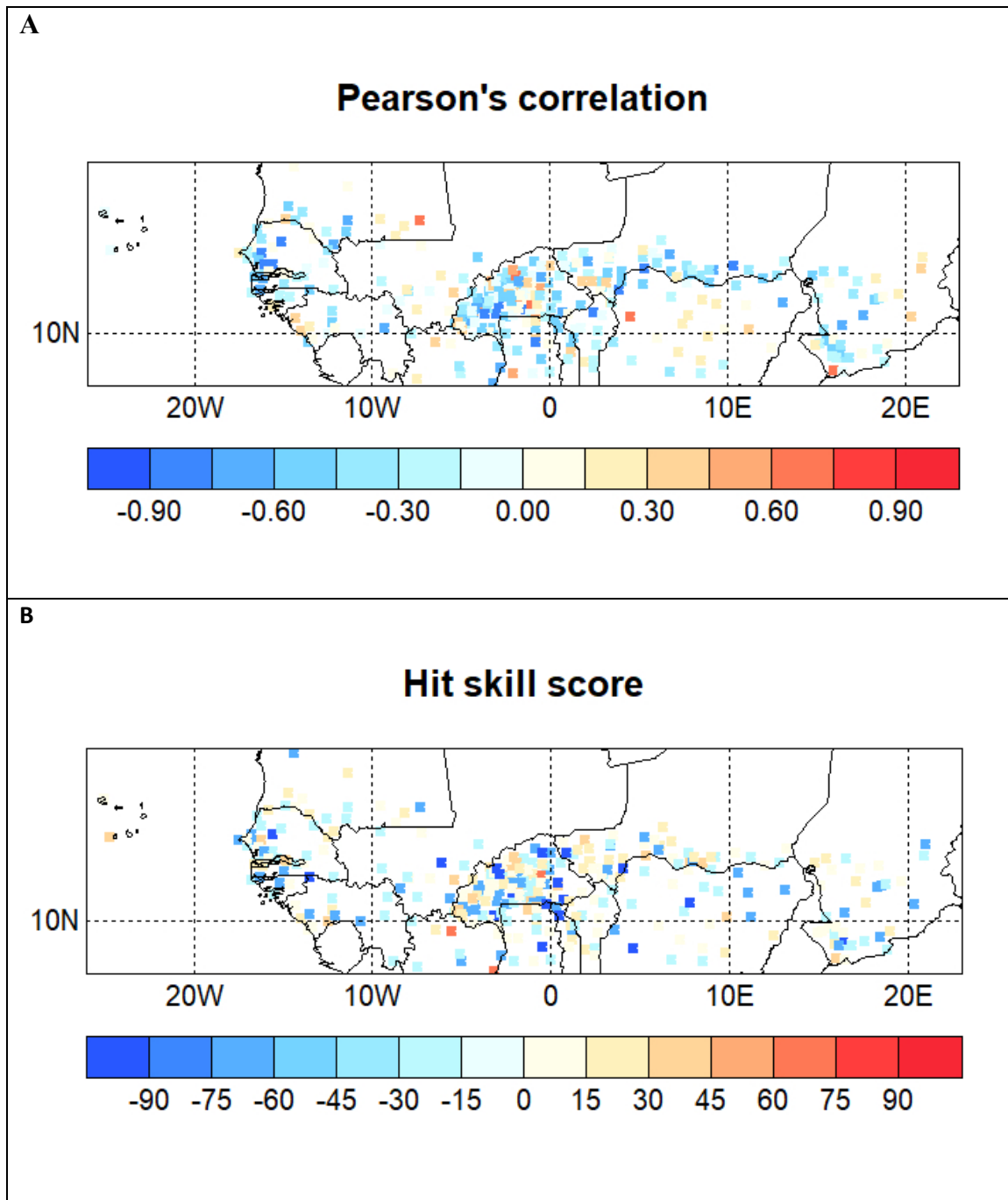


Figure 4.18. Skill maps (A = Pearsons Correlation and B = Hit Skill Score) for End season dry Spells duration retroactive forecast using **precipitation anomaly hindcast from NASA model (initialized in April with lead time October)** as predictor and **Late Season Dry Spells duration** historical data

Conclusions on the evaluation of predictors used in PRESASS process

Based on the results described above, it can be retained that:

Precipitation hindcasts generally offer better localized skills than SST hindcasts for both onset and dry spell forecasts and are therefore more useful for forecast at local level. SST anomalies are useful, but skill improves significantly when seasonal windows are better matched (e.g., JJA or ASO periods respectively for early season parameters and end season parameters). Early lead times (April initialization for May prediction) reduce skill; forecasts farther to event time (e.g., April initialization for July/August) perform better. Multi-model ensembles (e.g., NMME) tend to enhance skill compared to single model predictors. Late season dry spells are more predictable than early season dry spells, particularly when using SST predictors from high-performing models like GFDL.

From the predictors' assessment outcomes, the following recommendations are suggested:

- i) Use precipitation predictors (hindcasts) where possible for operational localized (e.g., country level) forecasting, especially for early and late season dry spells and SST anomaly hindcasts for regional level forecasting.
- ii) Rely on multi-model SST anomaly fields (e.g., NMME) rather than relying on a single model
- iii) For critical dates like onset and cessation, JJA and ASO periods provide better initialization windows.

b) Verification of the Statistical forecasts

This section summarizes the verification of statistical part of the probabilistic seasonal forecasts made using the Climate Predictability Tool (CPT) as implemented in the PRESASS forecasting system. As described in section 3.4.1., the statistical forecasts were verified following WMO

guidelines. The verification used metrics such as reliability diagrams and ROC evaluating respectively the calibration and discrimination skill of retroactive forecasts made for Onset Date, Cessation Date, Early and Late Dry Spells Duration. The retroactive forecasts were made based on relatively best predictors fields described previous section (see Tables 4.1. and 4.2). Figures 4.19 to 4.26 show the Reliability diagrams and ROC curves elaborated for each of the statistical forecasts of the season parameters (onset, cessation and dry spells).

Elements to consider in Reliability diagrams and ROC curves interpretation

According to the WMO guidelines for probabilistic forecast verification, the key facts to consider while interpreting reliability diagrams are:

- i) Diagonal 45° line indicates perfectly calibrated forecast.
- ii) Curves Above the diagonal indicates underconfidence (forecasted probabilities are too low).
- iii) Curves below the diagonal indicates overconfidence (forecasted probabilities are too high).
- iv) Histogram shows sharpness or how often certain probabilities are issued (distribution of forecast probability values).

Therefore, well-calibrated forecasts stay close to the diagonal 45° with frequent use of intermediate probability levels whereas deviations from the diagonal indicate bias, requiring recalibration of forecast models.

The purpose of ROC curves is to evaluate how well forecasts distinguish between occurrences and non-occurrences of events. The further above the diagonal line, the better the forecast's discrimination skill. The key elements to take in consideration while interpreting ROC curves are:

- i) X-axis corresponds to False Alarm Rate (FAR)

- ii) Y-axis represents Hit Rate (HR) axis
- iii) Diagonal line indicates no skill (random forecasts)
- iv) Closer to the upper-left corner indicates higher discrimination skill.

The Area Under the Curve (AUC) is interpreted as follow:

AUC = 1 indicates perfect discrimination.

AUC > 0.7 indicates useful forecast.

AUC \approx 0.5 indicates no discrimination (random).

Overall, high AUC scores indicate better forecast discrimination skill for key seasonal events.

Forecast quality assessment

It comes out from the analysis of the reliability diagrams displayed in subfigures a) of Figures 4.19 to 4.26, that most forecasts showed reasonable calibration, though some were overconfident (forecast probabilities too high) as shown in subfigures a) of Figures 4.20, 4.21, and 4.23 or underconfident (too low) (Figures 4.19a and 4.24a), especially at the extremes. The sharpness (the ability to issue confident forecasts) was moderate with some systems tending to issue probabilities clustered around climatology. For cessation forecast CMC1 SST hindcast (Figure 4.22a) and late season dry spells (Figures 4.25a and 4.26a), reliability diagrams displayed no resolution. The analysis of ROC curves (subfigures b in Figures 4.19 to 4.26) shows that most forecasts had AUC (Area Under the Curve) values around 0.5 (Figures 4.25b and 4.26b) or lower than 0.5, indicating no discrimination skill (forecasts performing on random guessing). Forecasts of onset and early dry spells typically had better ROC scores than cessation and late dry spells specially in the category normal.

The evaluation of the predictor's performances shows that the NASA SST anomaly hindcast (Figure 4.19) gives the best calibration and discrimination for predicting onset while CFSv2 precipitation hindcast (Figure 4.20) shows moderate performance with some calibration bias. Cessation forecasts show lower skill, hence need recalibration. Indeed, cessation forecasts using NASA precipitation hindcast (Figure 4.21) shows bias in reliability diagrams while the use of CMC1 SST anomaly hindcast (Figure 4.22) leads to slightly better calibration but lower ROC scores. For the prediction of early season dry spell durations, NASA SST anomaly initialized in April for July lead time is the best predictor compared to others as it leads to better discrimination (higher ROC scores in Figure 4.24) while CMC1 SST anomaly hindcast (Figure 4.22) gives moderate calibration. For the end season dry spell forecasts, GFDL SST anomaly initialized in April for JAS lead time performed better than GFDL SST anomaly which leads to a moderate performant forecast.

Findings from the forecast quality evaluation across the 4 predictands is summarized as follow:

Onset Forecasts showed the best overall performance, with good calibration and discrimination. Forecasts using SST anomalies as predictors generally performed better than those based on precipitation hindcasts.

Cessation Forecasts displayed less consistent skill. Reliability diagrams often showed bias, and ROC curves had lower AUCs compared to onset forecasts. Further model refinement may be required.

Dry Spell Forecasts Showed generally higher reliability and discrimination for early-season dry spells than for late-season ones. Forecasts for longer dry spells later in the season tended to be less reliable.

Conclusions on the evaluation of statistical forecasts in the PRESASS process

From the results, it can be concluded that the CPT-based forecasting system used for the statistical forecasts in the PRESASS shows strong potential for supporting climate-sensitive decision-making, particularly in onset and early dry spell duration prediction. However, forecasts for cessation date and late-season dry spells require additional refinement. The weak performance of predictors revealed for forecasts at regional level suggests to consider region-specific performance in future analyses to refine locally actionable insights.

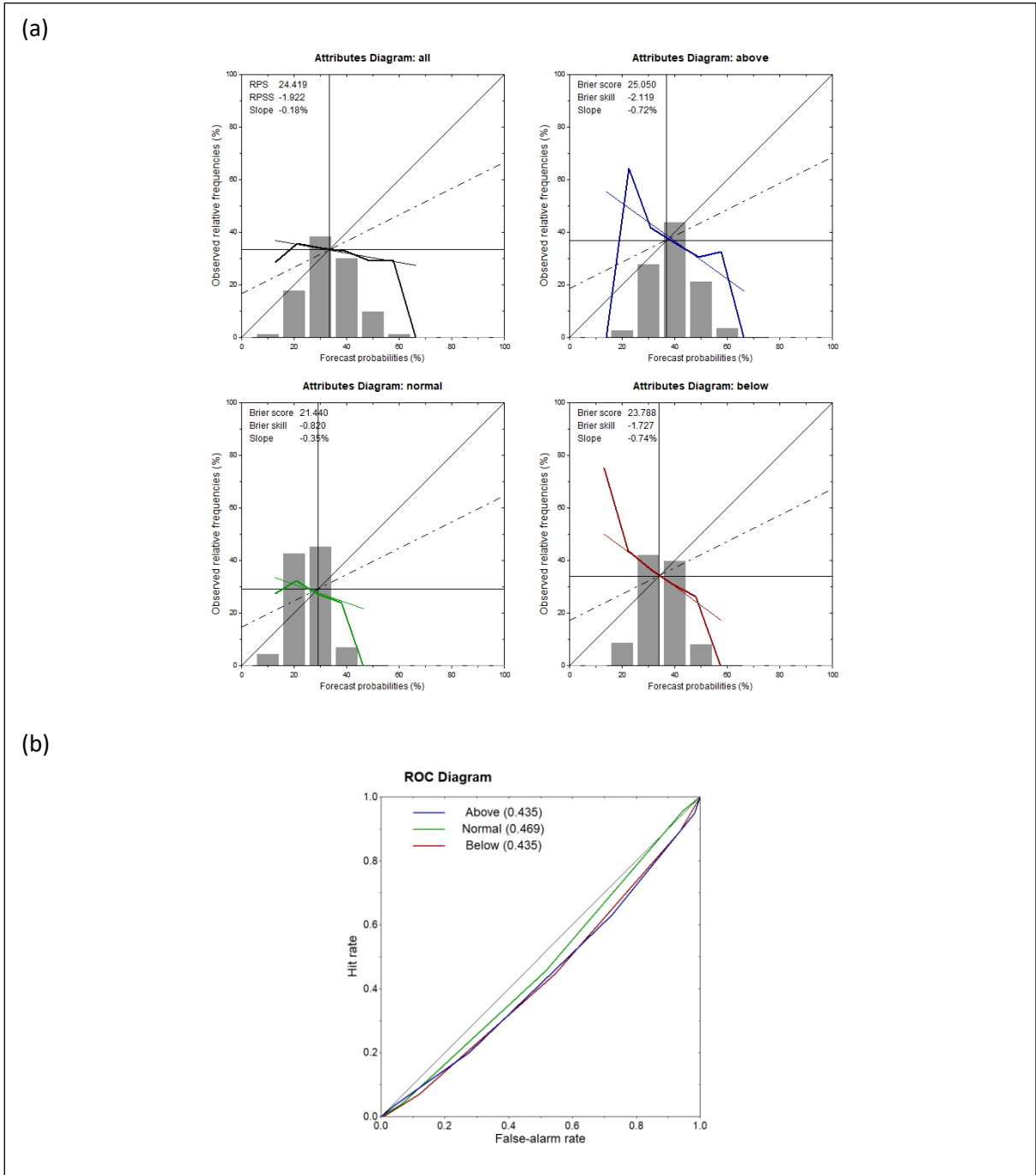


Figure 4.19. Reliability diagrams (a) and ROC curves (b) for onset forecast using SST anomaly hindcast from the NASA model initialized in April for July lead time. In subfigure b), the thick colored lines show the reliability curves, and the thick black line is the least squares weighted regression fit to the reliability curve. The weights are shown by the grey bars, which indicate the relative frequency of forecasts in each 10% bin. The thin horizontal and vertical lines indicate the relative frequency of occurrence of the predictand in the respective category, while the thin diagonal represents the line of perfect reliability.

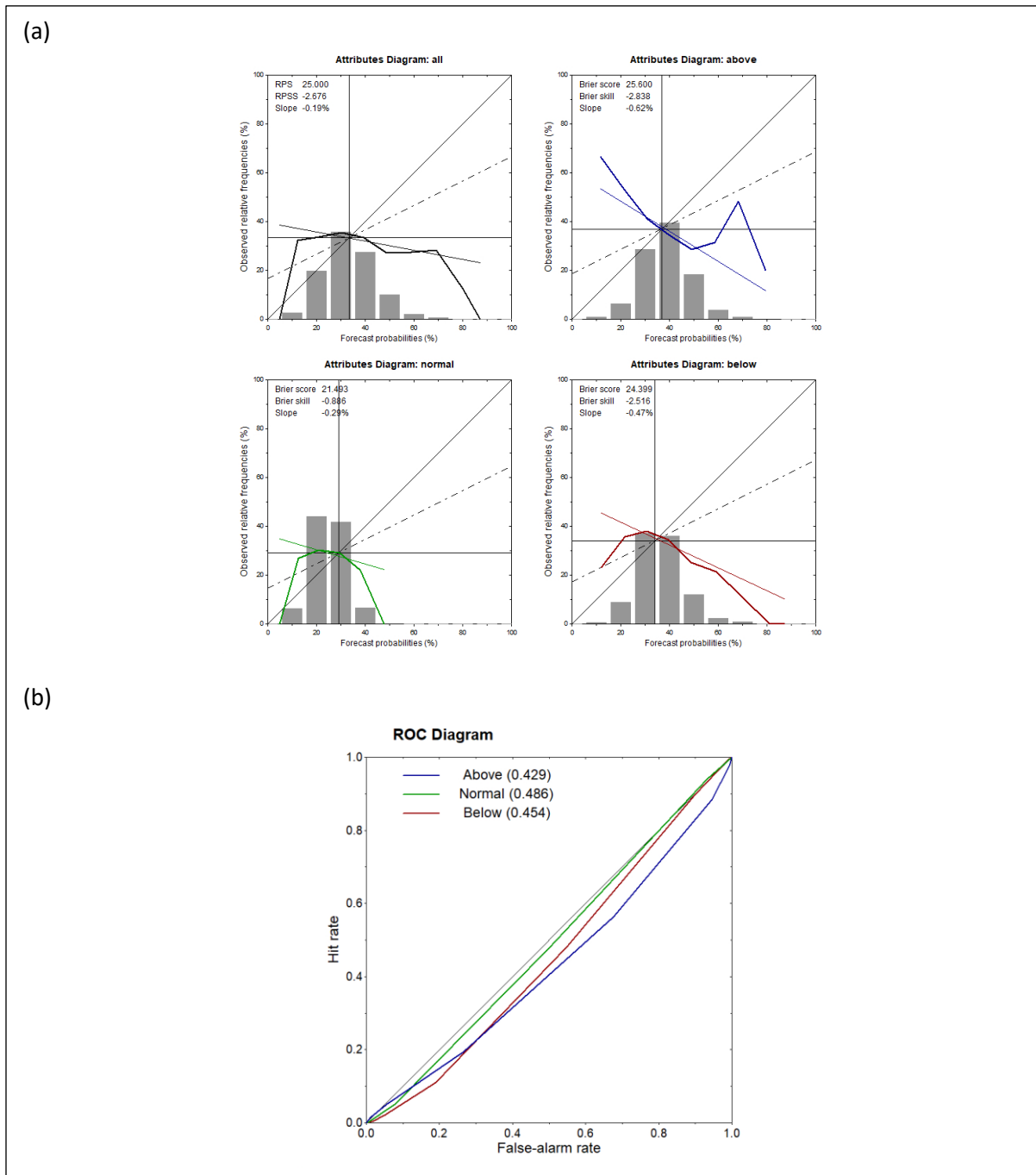


Figure 4.20. Reliability diagrams (a) and ROC curves (b) for onset forecast using precipitation hindcast from the CFSv2 model initialized in April for July lead time. In subfigure b), the thick colored lines show the reliability curves, and the thick black line is the least squares weighted regression fit to the reliability curve. The weights are shown by the grey bars, which indicate the relative frequency of forecasts in each 10% bin. The thin horizontal and vertical lines indicate the relative frequency of occurrence of predictand in the respective category, while the thin diagonal represents the line of perfect reliability.

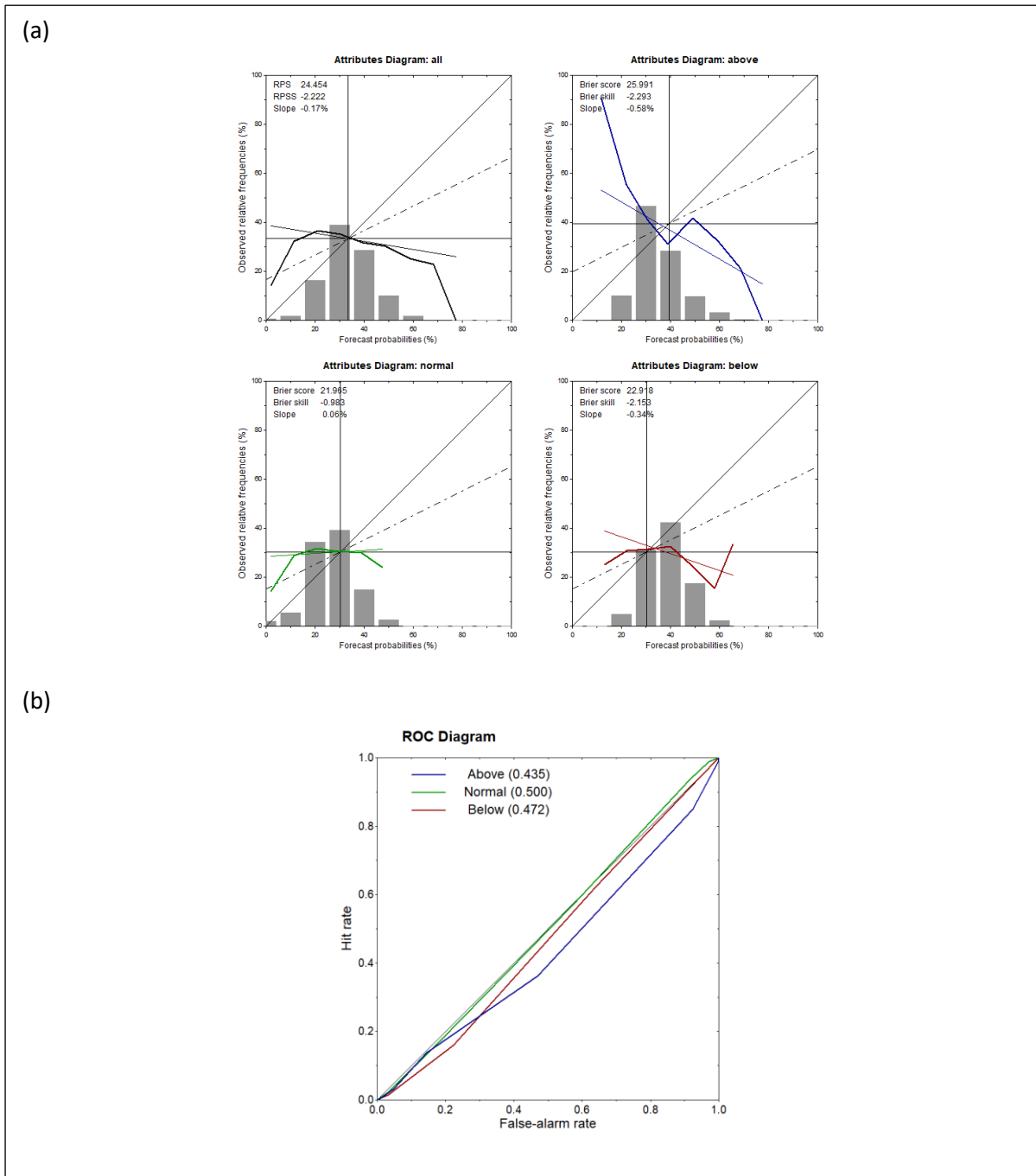


Figure 4.21. Reliability diagrams (a) and ROC curves (b) for cessation date forecast using precipitation hindcast from the NASA model initialized in April for SON lead time. In subfigure b), the thick colored lines show the reliability curves, and the thick black line is the least squares weighted regression fit to the reliability curve. The weights are shown by the grey bars, which indicate the relative frequency of forecasts in each 10% bin. The thin horizontal and vertical lines indicate the relative frequency of occurrence of predictand in the respective category, while the thin diagonal represents the line of perfect reliability.

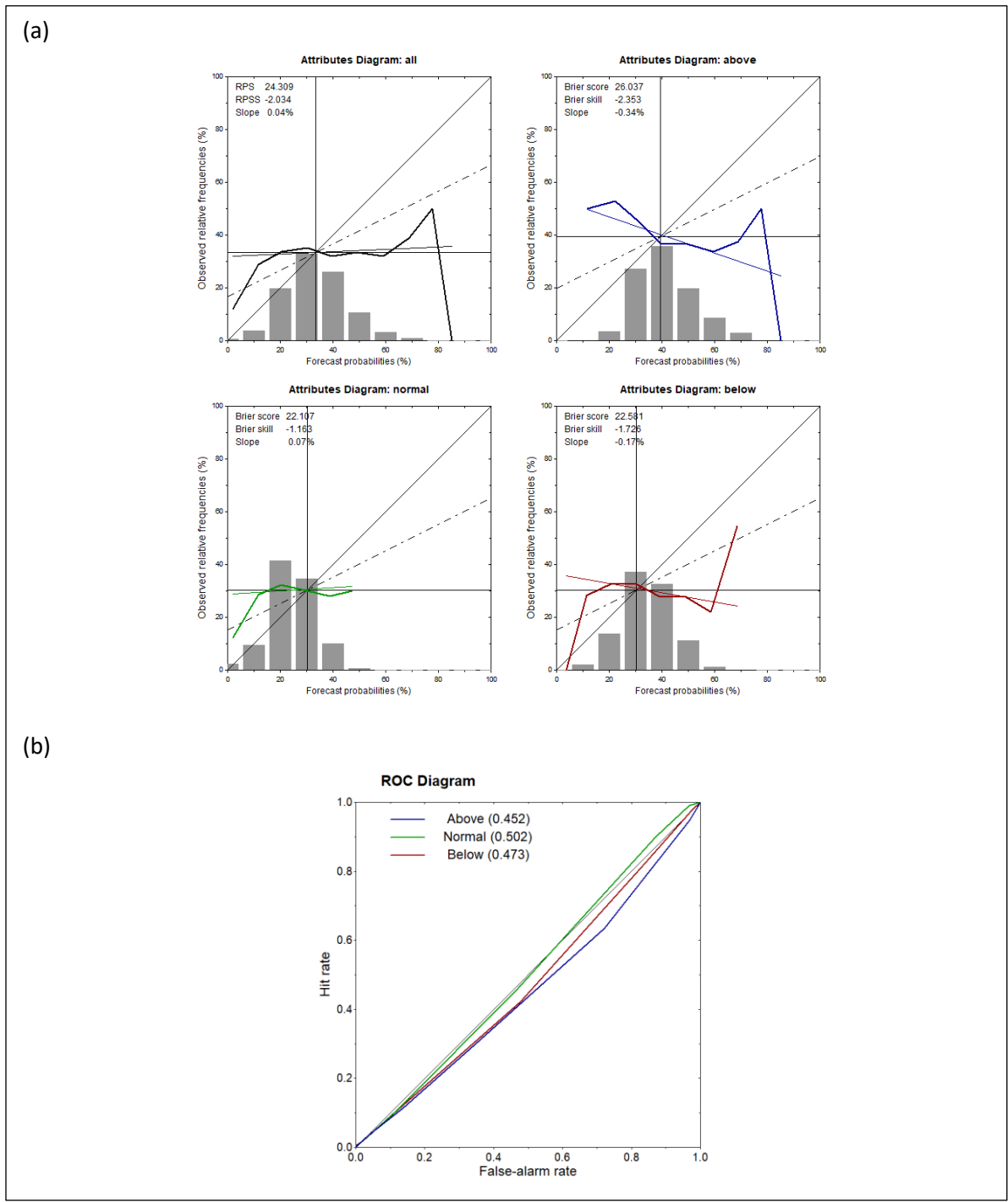


Figure 4.22. Reliability diagrams (a) and ROC curves (b) for cessation date forecast using SST anomaly hindcast from the CMC1 model initialized in April for August lead time. In subfigure b), the thick colored lines show the reliability curves, and the thick black line is the least squares weighted regression fit to the reliability curve. The weights are shown by the grey bars, which indicate the relative frequency of forecasts in each 10% bin. The thin horizontal and vertical lines indicate the relative frequency of occurrence of the predictand in the respective category, while the thin diagonal represents the line of perfect reliability.

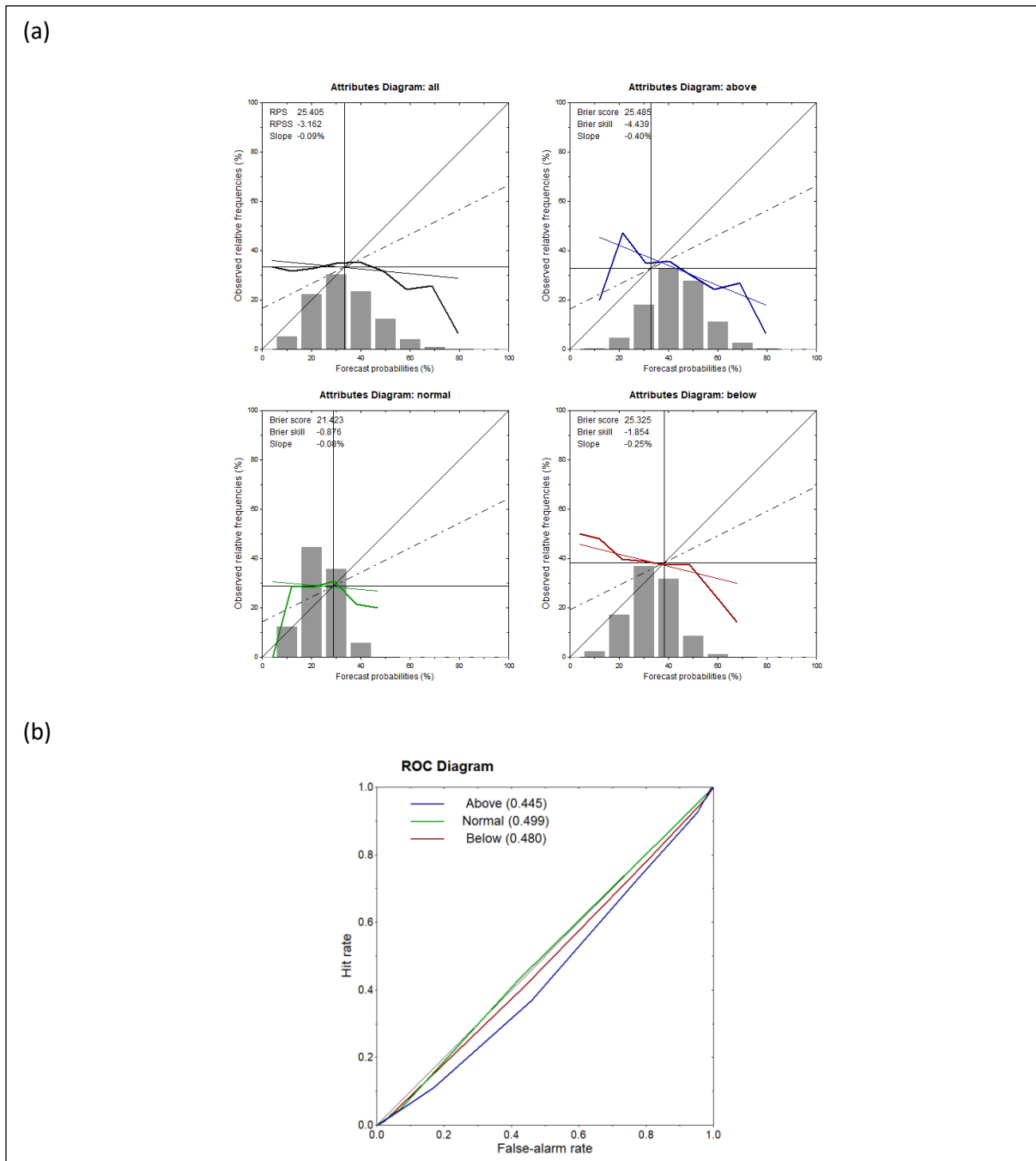


Figure 4.23. Reliability diagrams (a) and ROC curves (b) for early season dry spell duration forecast using SST anomaly hindcast from the CMC1 model initialized in April for JJA lead time. In subfigure b), the thick colored lines show the reliability curves, and the thick black line is the least squares weighted regression fit to the reliability curve. The weights are shown by the grey bars, which indicate the relative frequency of forecasts in each 10% bin. The thin horizontal and vertical lines indicate the relative frequency of occurrence of the predictand in the respective category, while the thin diagonal represents the line of perfect reliability.

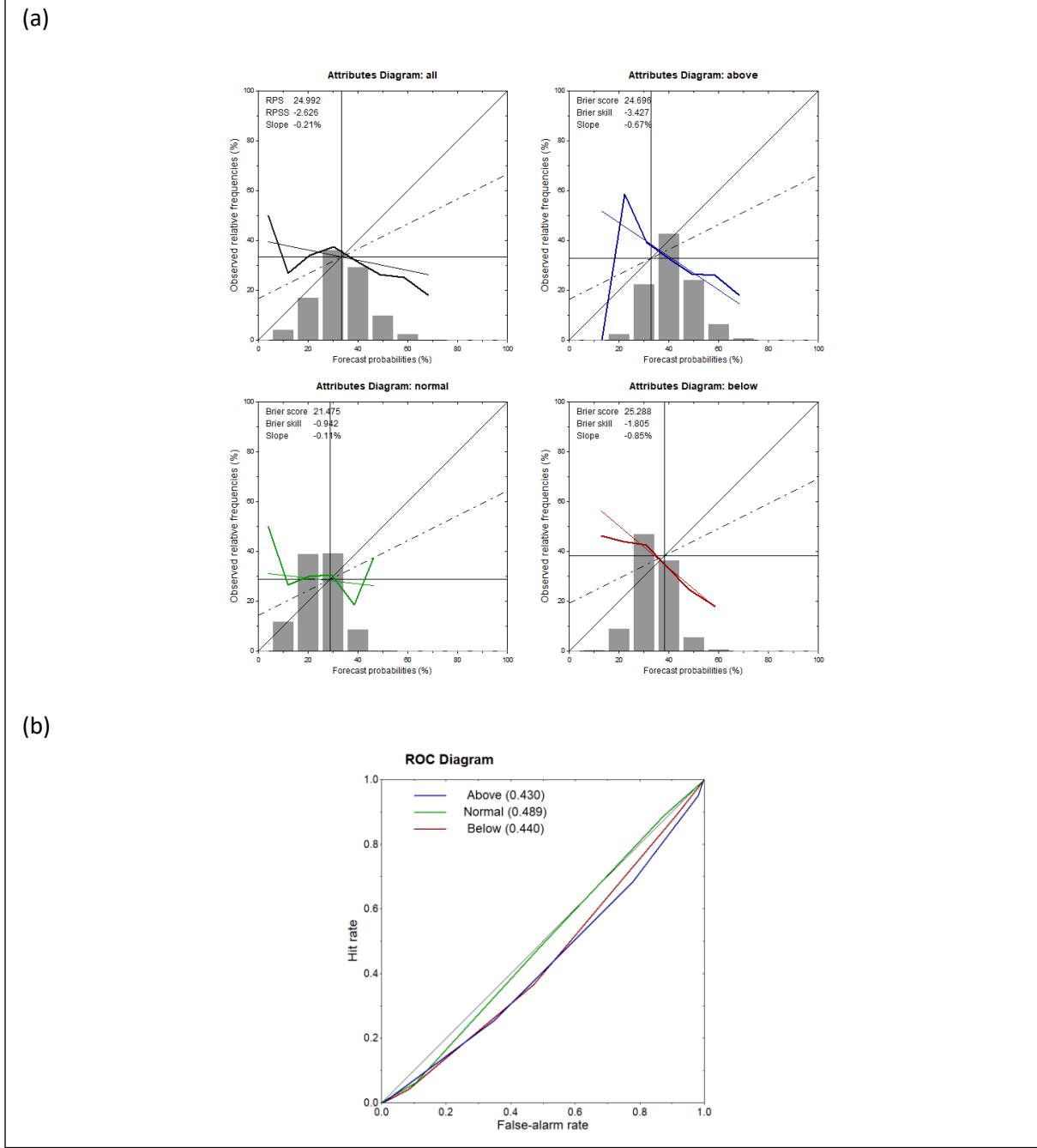


Figure 4.24. Reliability diagrams (a) and ROC curves (b) for early season dry spell duration forecast using SST anomaly hindcast from the NASA model initialized in April for July lead time. In subfigure b), the thick colored lines show the reliability curves, and the thick black line is the least squares weighted regression fit to the reliability curve. The weights are shown by the grey bars, which indicate the relative frequency of forecasts in each 10% bin. The thin horizontal and vertical lines indicate the relative frequency of occurrence of the predictand in the respective category, while the thin diagonal represents the line of perfect reliability.

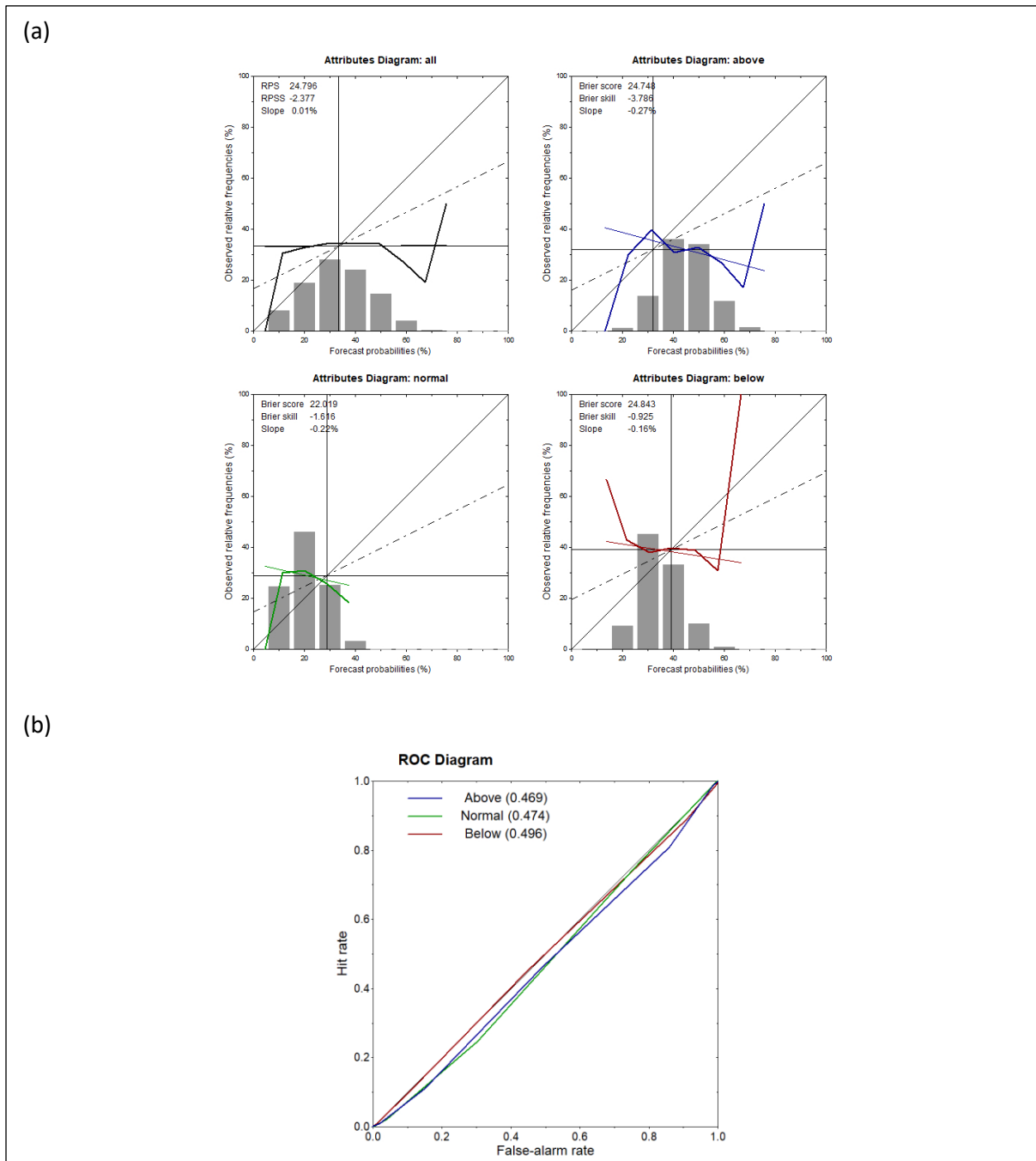
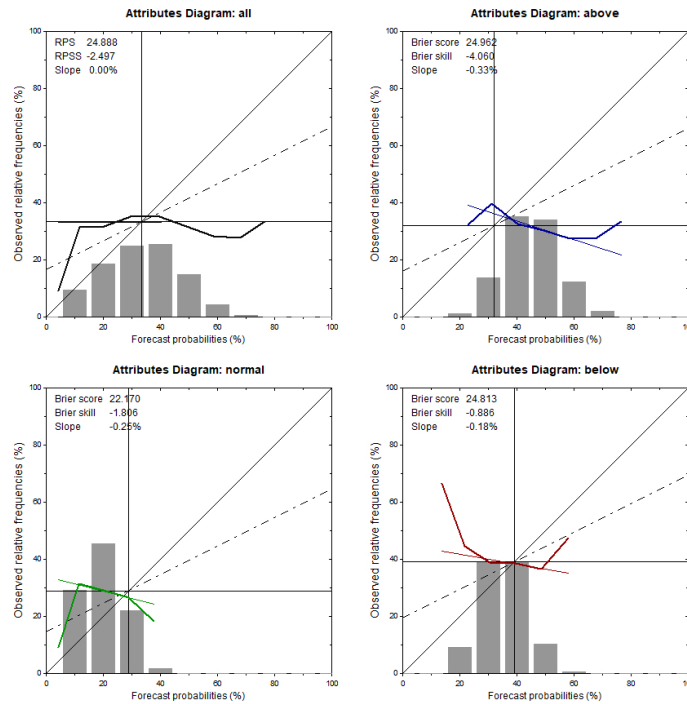


Figure 4.25. Reliability diagrams (a) and ROC curves (b) for late season dry spell duration forecast using SST anomaly hindcast from the GFDL model initialized in April for JAS lead time. In subfigure b), the thick colored lines show the reliability curves, and the thick black line is the least squares weighted regression fit to the reliability curve. The weights are shown by the grey bars, which indicate the relative frequency of forecasts in each 10% bin. The thin horizontal and vertical lines indicate the relative frequency of occurrence of the predictand in the respective category, while the thin diagonal represents the line of perfect reliability.

(a)



(b)

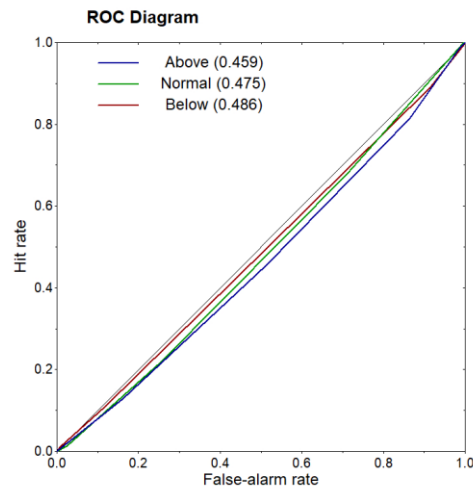


Figure 4.26. Reliability diagrams (a) and ROC curves (b) for late season dry spells duration forecast using SST anomaly hindcast from the NMME model initialized in April for JAS lead time. In subfigure b), the thick colored lines show the reliability curves, and the thick black line is the least squares weighted regression fit to the reliability curve. The weights are shown by the grey bars, which indicate the relative frequency of forecasts in each 10% bin. The thin horizontal and vertical lines indicate the relative frequency of occurrence of the predictand in the respective category, while the thin diagonal represents the line of perfect reliability.

4.1.2. Assessment of the PRESASS overall approach in forecasting season characteristics

In order to achieve this assessment, the PRESASS regional forecast maps (e.g., Figure 2.6) issued each year after the consensual experts meeting from 2013 to 2023 were digitalized to extract the probabilities for each of the categories (below-normal, normal and above normal) and for season onset date, cessation date and dry spells duration at the early and late stages of the season. Then the forecast probabilities were compared to the observed season parameters data over the same period using probabilities forecast verification methods recommended in the WMO guidelines. (Mason, 2018). The metrics calculated include Brier score, reliability score, resolution score, uncertainty and ROC presented in Table 4.7. The analysis will focus on the Brier score, reliability, resolution and ROC metrics. Figures 4.27 to 4.30 present the verification diagrams for season onset date forecast, season cessation date forecast, early season dry spells forecast and late season dry spells forecast.

Table 4.7 : Forecast verification metrics for (a) Onset date, (b) Cessation date, (c) Early season dry spells duration, (d) End of season dry spells duration

(a) Onset

Category	Brier Score	Reliability	Resolution	Uncertainty	AUC (ROC)
Above Normal	0.24552	0.02216	0.00443	0.22799	0.53328
Normal	0.21562	0.01024	0.00010	0.20484	0.48974
Below Normal	0.24269	0.01482	0.00160	0.23064	0.51795

(b) Cessation

Category	Brier Score	Reliability	Resolution	Uncertainty	AUC (ROC)
Above Normal	0.26265	0.01400	0.00081	0.24985	0.47977
Normal	0.21678	0.01062	0.00029	0.20564	0.48951
Below Normal	0.17972	0.00639	0.00036	0.17312	0.47305

(c) Early season dry spells

Category	Brier Score	Reliability	Resolution	Uncertainty	AUC (ROC)
Above Normal	0.24026	0.01450	0.00127	0.22633	0.50628
Normal	0.23537	0.00104	0.00020	0.23424	0.51265
Below Normal	0.21792	0.01636	0.00067	0.20134	0.50929

(d) End of season dry spells

Category	Brier Score	Reliability	Resolution	Uncertainty	AUC (ROC)
Above Normal	0.22589	0.00732	0.00023	0.21789	0.48737
Normal	0.23647	0.00331	0.00008	0.23364	0.51110
Below Normal	0.22618	0.01345	0.00051	0.21278	0.49906

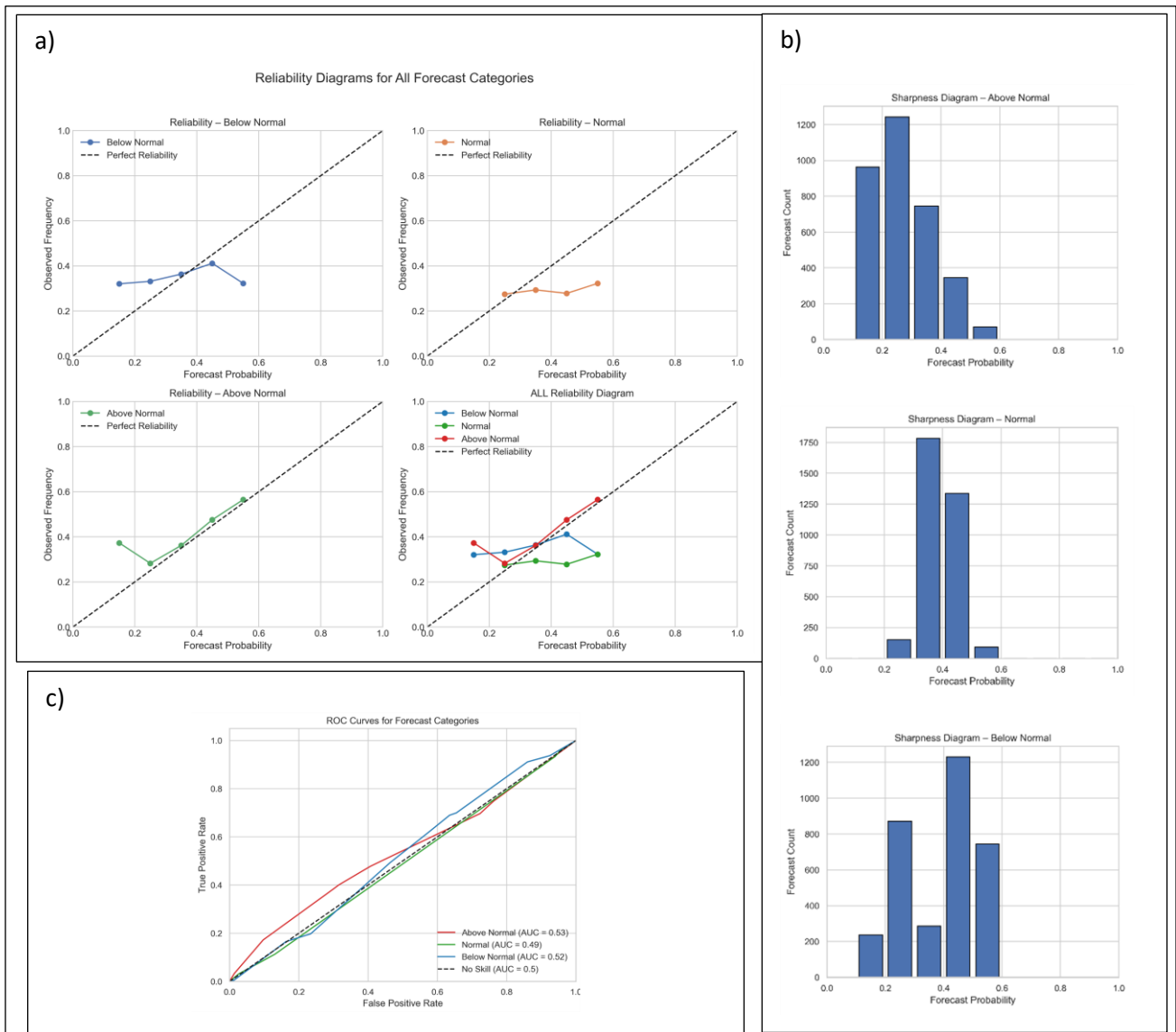


Figure 4.27. Reliability diagrams (a), Sharpness histograms (b) and ROC curves (c) for onset date forecast. In subfigure a), the thick colored lines show the reliability curves of the 3 forecast categories, the dash thin diagonal represents the line of perfect reliability

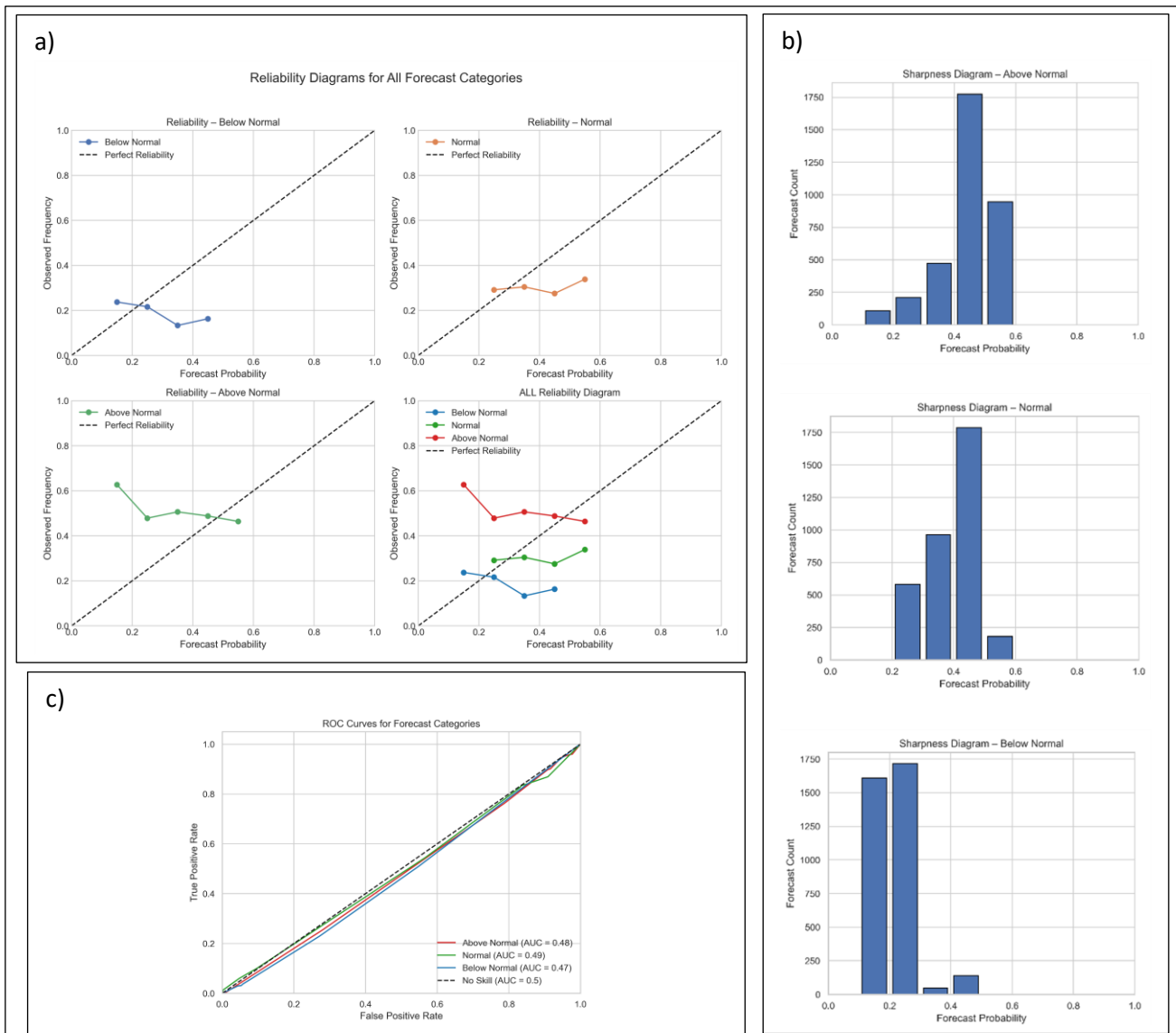


Figure 4.28. Reliability diagrams (a), Sharpness histograms (b) and ROC curves (c) for cessation date forecast. In subfigure a), the thick colored lines show the reliability curves of the 3 forecast categories, the dash thin diagonal represents the line of perfect reliability

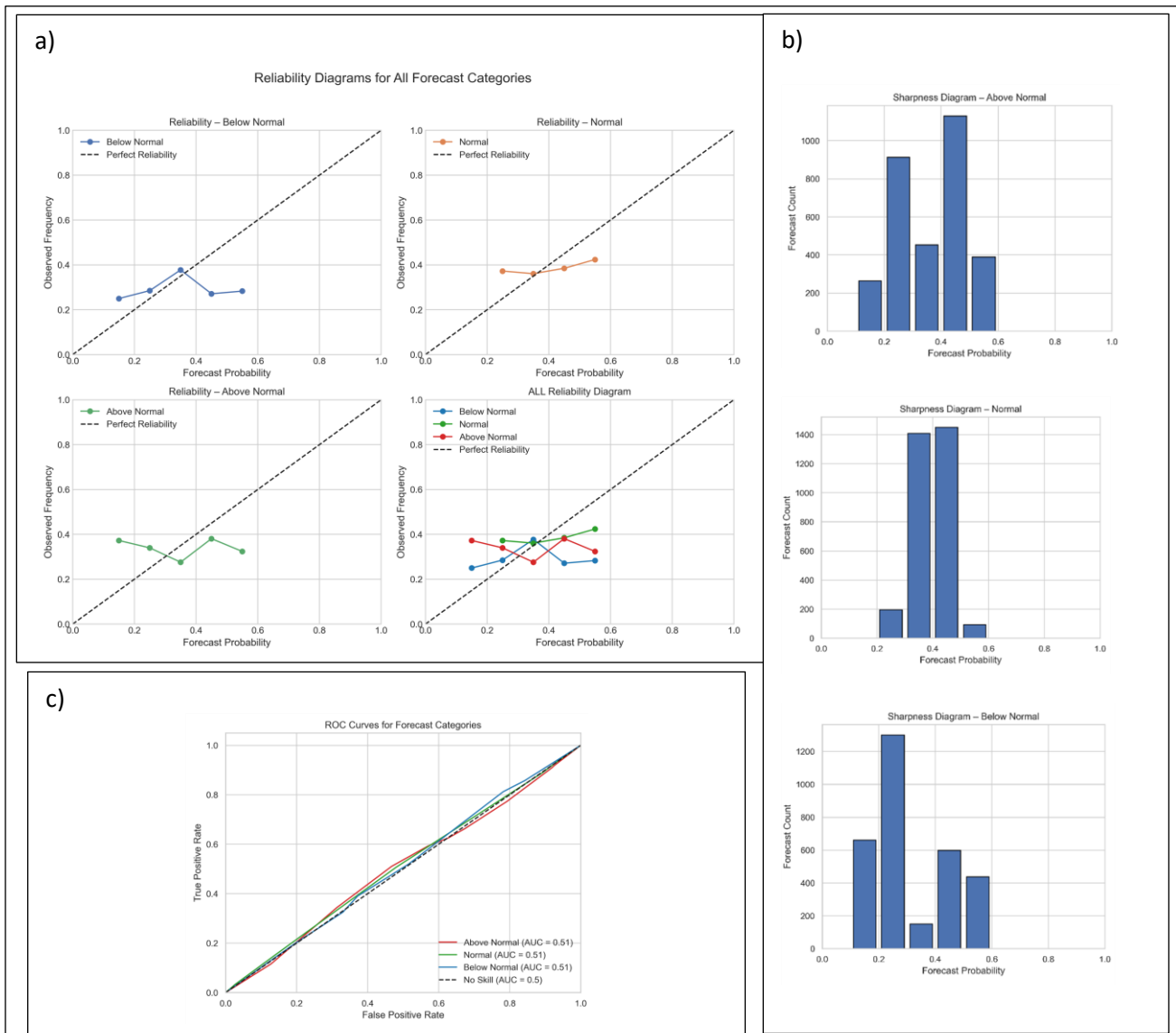


Figure 4.29. Reliability diagrams (a), Sharpness histograms (b) and ROC curves (c) for early season dry spell duration forecast. In subfigure a), the thick colored lines show the reliability curves of the 3 forecast categories, the dash thin diagonal represents the line of perfect reliability

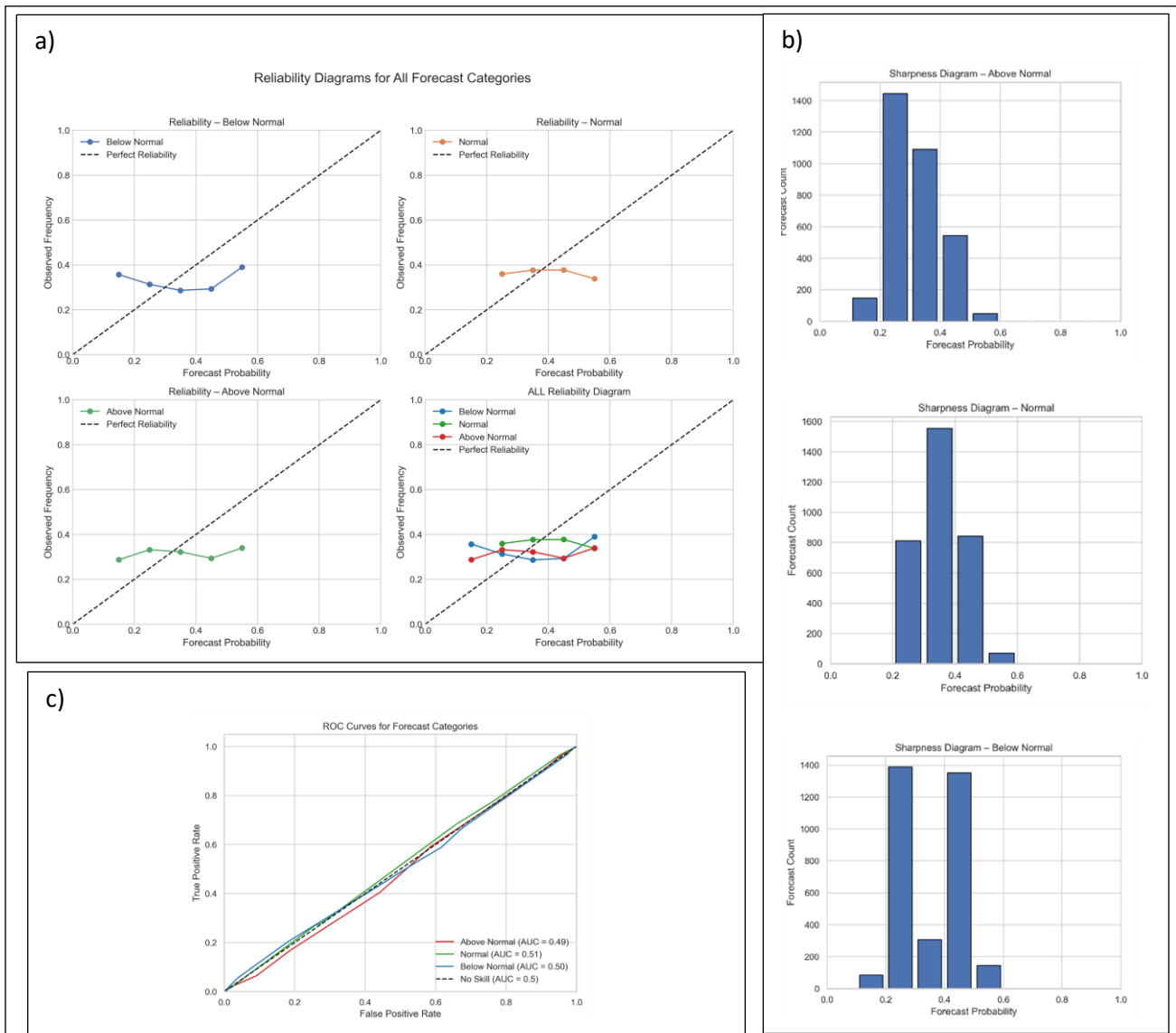


Figure 4.30. Reliability diagrams (a), Sharpness histograms (b) and ROC curves (c) for End season dry spell duration forecast. In subfigure a), the thick colored lines show the reliability curves of the 3 forecast categories, the dash thin diagonal represents the line of perfect reliability

Onset date forecast verification

Brier Score (lower values corresponds to better forecast accuracy) for onset date forecast (Table 4.7 a) suggests moderate forecast performance especially in the near-normal category (0.216). AUC values (~0.50–0.53) displayed in Figure 4.27c indicates that the forecasts are marginally better than random chance, but not highly discriminative. However, resolution values are low, suggesting onset date forecasts struggle to differentiate between categories. The reliability diagram and sharpness histograms (Figures 4.27a and 4.27b) highlight limited forecast sharpness and skill

Cessation date forecast verification

Brier Score for below-normal cessation dates (0.180) in Table 4.7 b suggests slightly better forecast accuracy. The AUC values below 0.50 (Figure 4.28) indicates forecast do not discriminate between cessation timing. The resolution is very low, especially in Above Normal, showing minimal forecast distinction from climatology. Therefore, improvement is needed in prediction skill for cessation date forecasting.

Early season dry spell forecast verification

Verification metrics in Table 4.7 c and Figure 4.29 show that forecast discrimination is slightly better (AUC = 0.50–0.51), but still indicating low discriminatory power and functional predictive skill. However, the low resolution values suggest difficulty in distinguishing dry spells severity.

Late season dry spell forecast verification

Table 4.7 d and Figure 4.30 show that scores and patterns are similar to early-season forecast. The best Brier Score is observed in the Above Normal category (0.226). AUC values are again near 0.5, denoting poor discriminatory skill.

Based on the findings it can be concluded that:

Low AUC scores (~ 0.47 – 0.53) and small resolution values across all forecasts indicate that the system struggles to distinguish between different outcomes and adds limited value over climatology. The onset date forecasts show slightly better skill than cessation forecasts, but still need improvement in resolution. The forecasts are generally unreliable, with a tendency toward over- or under-confidence. The "Normal" category often shows slightly better performance. The onset forecasts show slightly better skill than cessation forecasts, but still need improvement in resolution.

4.2. Possible ways to improve the dynamical aspects of the forecasting system

In order to reduce some of the shortcomings related to the PRESASS current forecasting system, we have looked for potential new predictors that may improve the season onset, cessation and dry spell forecast. Wet days frequency throughout the season and cumulative rainfall over different periods of the season were tested as predictors for the season parameters forecasts. The motivation to investigate on those potential predictors is based on recommendations in WMO-No. 1246 (WMO, 2020; Kumar et al., 2020) and findings from previous studies (Waongo et al., 2014; Moron et al., 2007, 2009) which showed that wet days' frequency within a season might have potential greater predictive skill that should be explored for development of tailored forecast products such as season onset in the WARCOF forecasting system. Additionally, the outperformance of precipitation predictors already used in the PRESASS over the SST predictors resulting from the predictors evaluation performed within the present research leads us to investigate further on the performance of cumulative rainfall over several time windows within the wet season. The findings from this investigation are presented in this section.

4.2.1. Using wet days as predictors to forecast season onset dates, cessation dates and dry spell duration

This section assesses the use of wet day frequency in different time windows as a predictor for key seasonal characteristics: onset date, early-season dry spells, cessation date, and end-of-season dry spells. Wet days, defined as days exceeding a threshold rainfall amount, can reflect the atmospheric and soil moisture conditions favorable to seasonal transitions. Their distribution and frequency over specific periods provide insights into the evolution of the rainy season and thus offer a potential tool for early forecasting.

4.2.1.1. Assessment of the correlation between wet days and season parameters forecast over Sahel

The potential of wet days frequency as predictor for season parameters forecast was investigated through regression. Tables 4.8 and 4.9 show the frequency of wet days over various periods of the season with season onset dates, early season dry spell duration, end of season date, and end of season dry spell duration, respectively.

Wet days frequency over the periods July, June-July-August, and June present relatively good correlation with onset dates compared to the other periods. For the early season dry spells, wet days frequency over the periods April-May-June, May and June periods show better correlation.

There is weak correlation between wet days frequency and season cessation dates. The highest positive correlation ($r = 0, 042$) is observed over the period September-October – November. Unlikely, dry spells duration towards the end of the season has better negative correlation with wet days frequency with r value extending from -0.417 to -0.364.

Table 4.8 : Pearson correlation coefficient (r) between wet days monthly / seasonal frequency and onset dates / early season dry spells duration (ESDS) duration

Wet days observation period	Correlation coefficient with onset dates (r)	Correlation coefficient with ESDS duration (r)
May	-0.213	-0.423
June	-0.365	-0.402
July	-0.385	-0.358
AMJ	-0.248	-0.424
MJJ	-0.351	-0.367
JJA	-0.371	-0.303
JAS	-0.343	-0.300

Table 4.9: Pearson correlation coefficient (r) between wet days monthly / seasonal frequency and cessation date / late season dry spells duration (LSDS) duration

Wet days observation period	Correlation coefficient with cessation dates (r)	Correlation coefficient with LSDS duration (r)
August	-0.087	-0.417
September	-0.145	-0.415
October	-0.040	-0.364
JAS	-0.051	-0.408
ASO	0.036	-0.408
SON	0.042	-0.379

4.2.1.2. Verification of forecasts made based on wet days frequency as predictors

Different monthly or seasonal aggregations of wet days (e.g., June, July, AMJ, SON) are analyzed in terms of their ability to produce probabilistic forecasts for the above-mentioned events. Each forecast is evaluated using reliability diagrams to assess calibration, ROC curves to determine discrimination ability, and sharpness diagrams to understand the distribution of forecast probabilities (see Figure 4.31 – 4.42).

Quality of onset date forecast

Wet days frequency observed in June and July showed moderate discrimination with ROC curves suggesting some ability to distinguish early from late onset. Reliability plots generally revealed some overconfidence, especially at high forecast probabilities, suggesting that the model may predict onset too confidently when it is not consistently observed. Sharpness was likely limited (narrow probability use), especially for July (Figures 4.31–4.33).

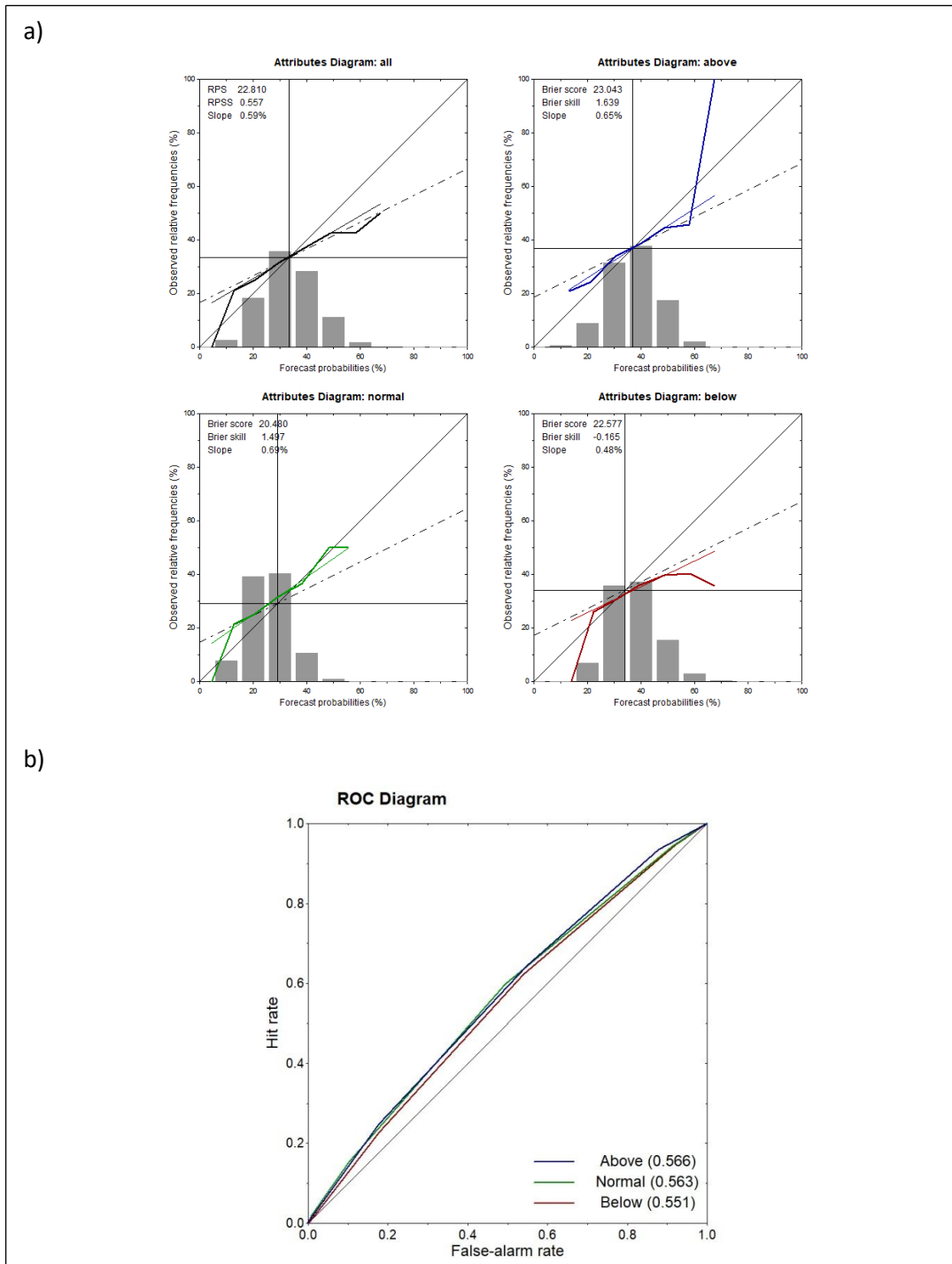


Figure 4.31. Reliability diagrams (a) and ROC curves (b) for onset forecast using wet days frequency during June as predictor. In subfigure b), the thick colored lines show the reliability curves, and the thick black line is the least squares weighted regression fit to the reliability curve. The weights are shown by the grey bars, which indicate the relative frequency of forecasts in each 10% bin. The thin horizontal and vertical lines indicate the relative frequency of occurrence of the predictand in the respective category, while the thin diagonal represents the line of perfect reliability.

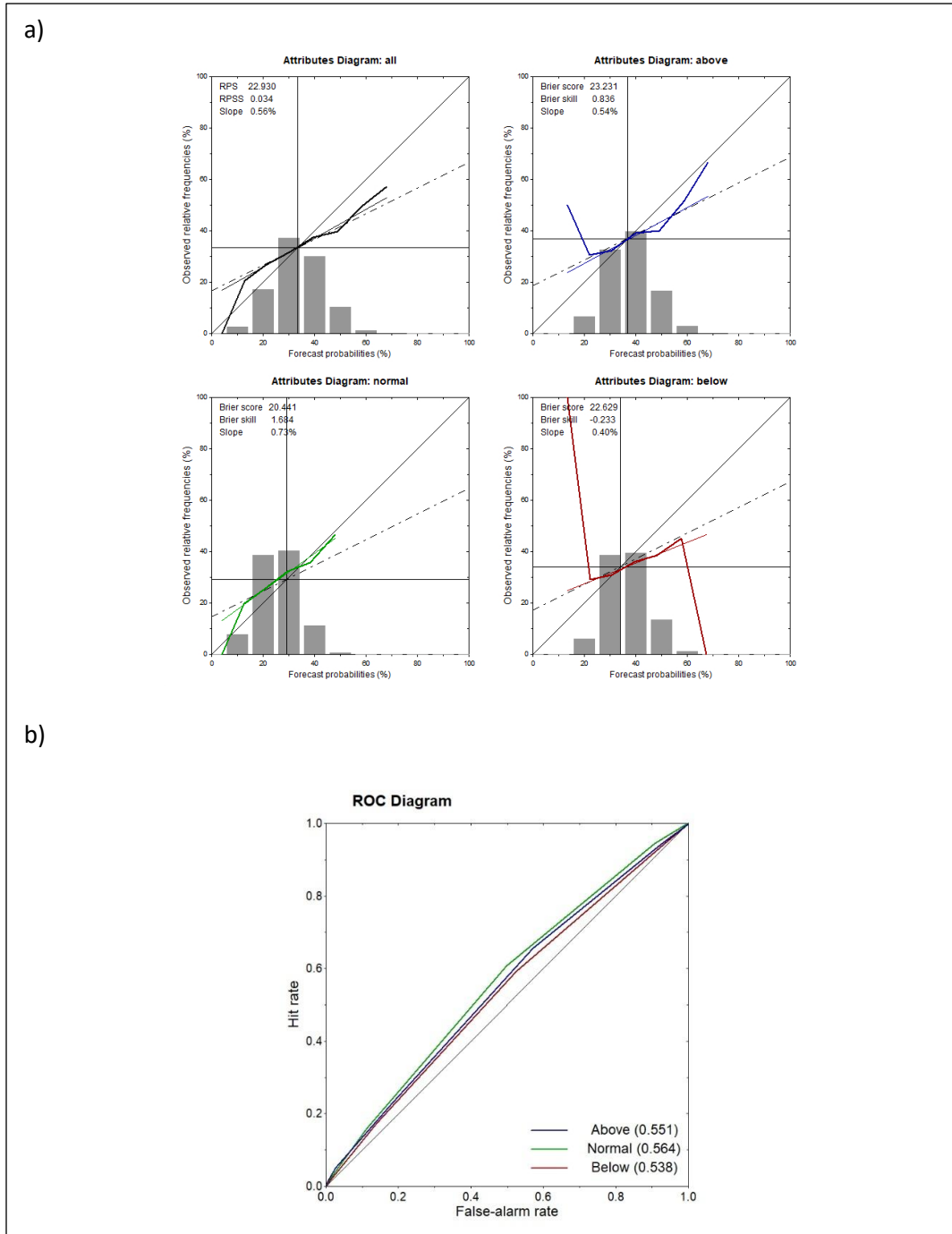


Figure 4.32. Reliability diagrams (a) and ROC curves (b) for onset forecast using wet days frequency during July as predictor. In subfigure b), the thick colored lines show the reliability curves, and the thick black line is the least squares weighted regression fit to the reliability curve. The weights are shown by the grey bars, which indicate the relative frequency of forecasts in each 10% bin. The thin horizontal and vertical lines indicate the relative frequency of occurrence of the predictand in the respective category, while the thin diagonal represents the line of perfect reliability.

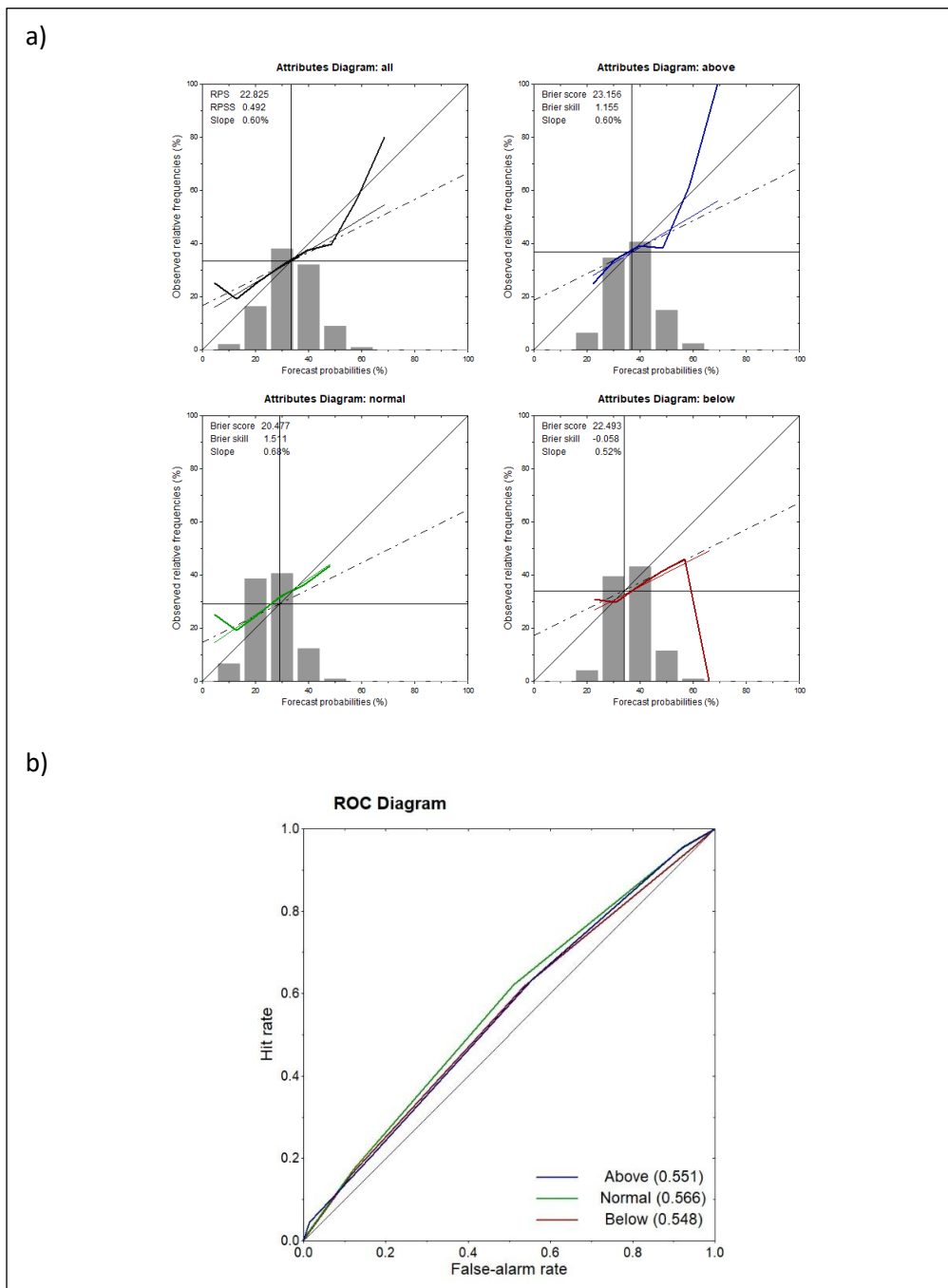


Figure 4.33. Reliability diagrams (a) and ROC curves (b) for onset forecast using wet days frequency during JJA as predictor. In subfigure b), the thick colored lines show the reliability curves, and the thick black line is the least squares weighted regression fit to the reliability curve. The weights are shown by the grey bars, which indicate the relative frequency of forecasts in each 10% bin. The thin horizontal and vertical lines indicate the relative frequency of occurrence of the predictand in the respective category, while the thin diagonal represents the line of perfect reliability.

Quality of early season dry spell forecast

Early season dry spell forecast based on wet days frequency observed in May and June had limited discrimination skill as the ROC curves are closer to the diagonal. The reliability was modest with signs of underconfidence in lower forecast ranges. AMJ (April–June) season predictors performed slightly better, possibly due to smoother accumulation of the signal (Figures 4.34–4.36).

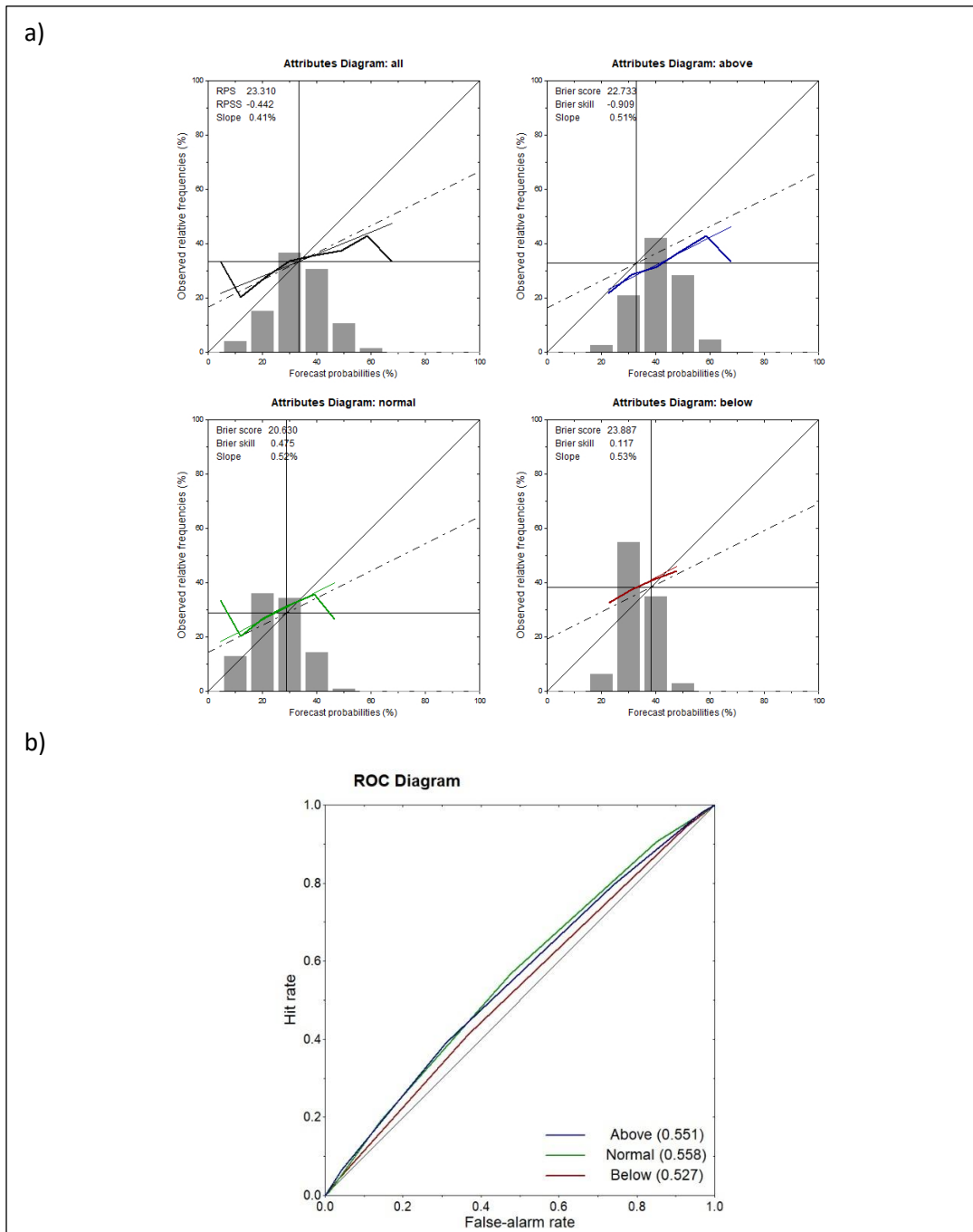


Figure 4.34. Reliability diagrams (a) and ROC curves (b) for early season dry spells duration forecast using wet days frequency during May as predictor. In subfigure b), the thick colored lines show the reliability curves, and the thick black line is the least squares weighted regression fit to the reliability curve. The weights are shown by the grey bars, which indicate the relative frequency of forecasts in each 10% bin. The thin horizontal and vertical lines indicate the relative frequency of occurrence of the predictand in the respective category, while the thin diagonal represents the line of perfect reliability.

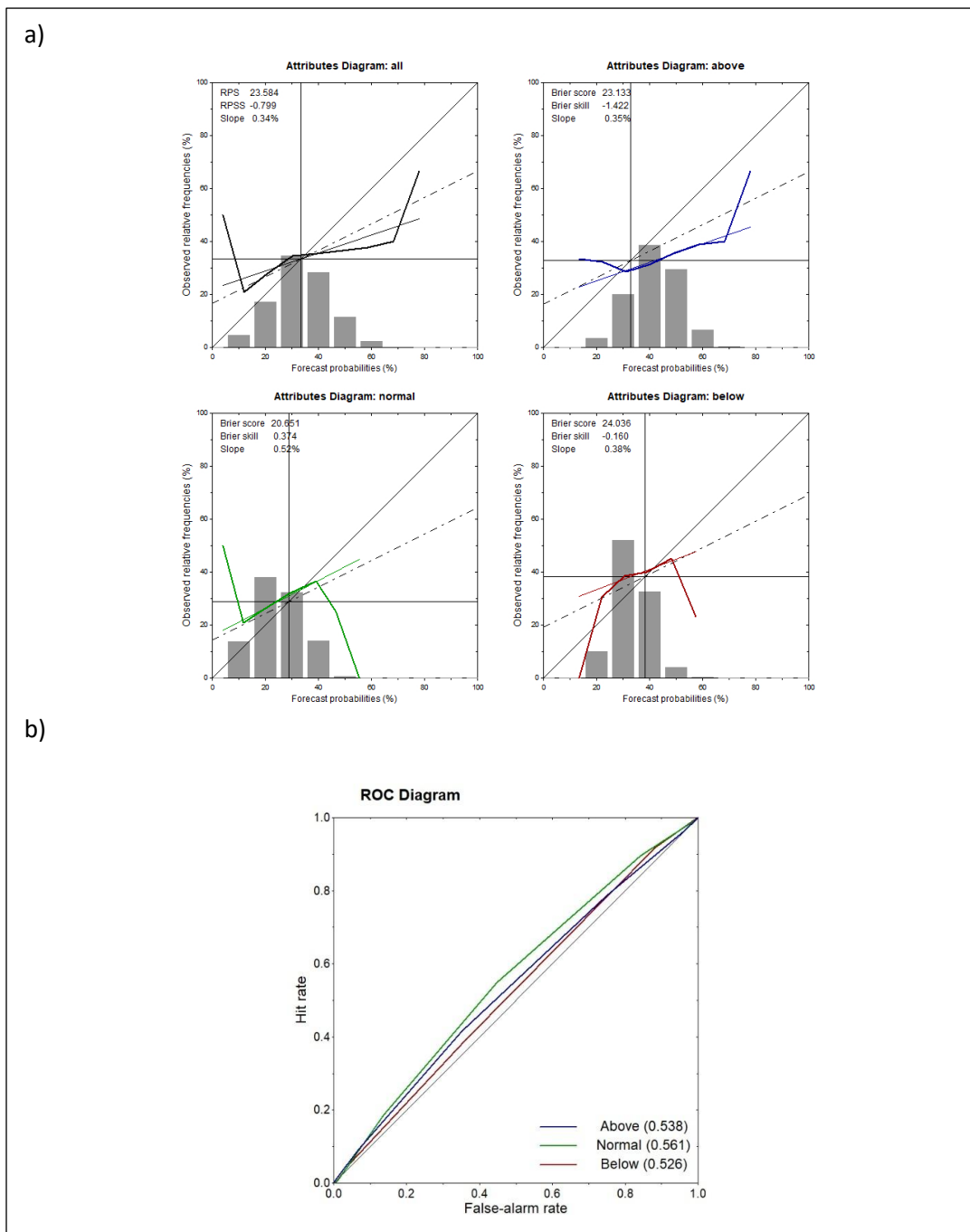


Figure 4.35. Reliability diagrams (a) and ROC curves (b) for early season dry spells duration forecast using wet days frequency during June as predictor. In subfigure b), the thick colored lines show the reliability curves, and the thick black line is the least squares weighted regression fit to the reliability curve. The weights are shown by the grey bars, which indicate the relative frequency of forecasts in each 10% bin. The thin horizontal and vertical lines indicate the relative frequency of occurrence of the predictand in the respective category, while the thin diagonal represents the line of perfect reliability.

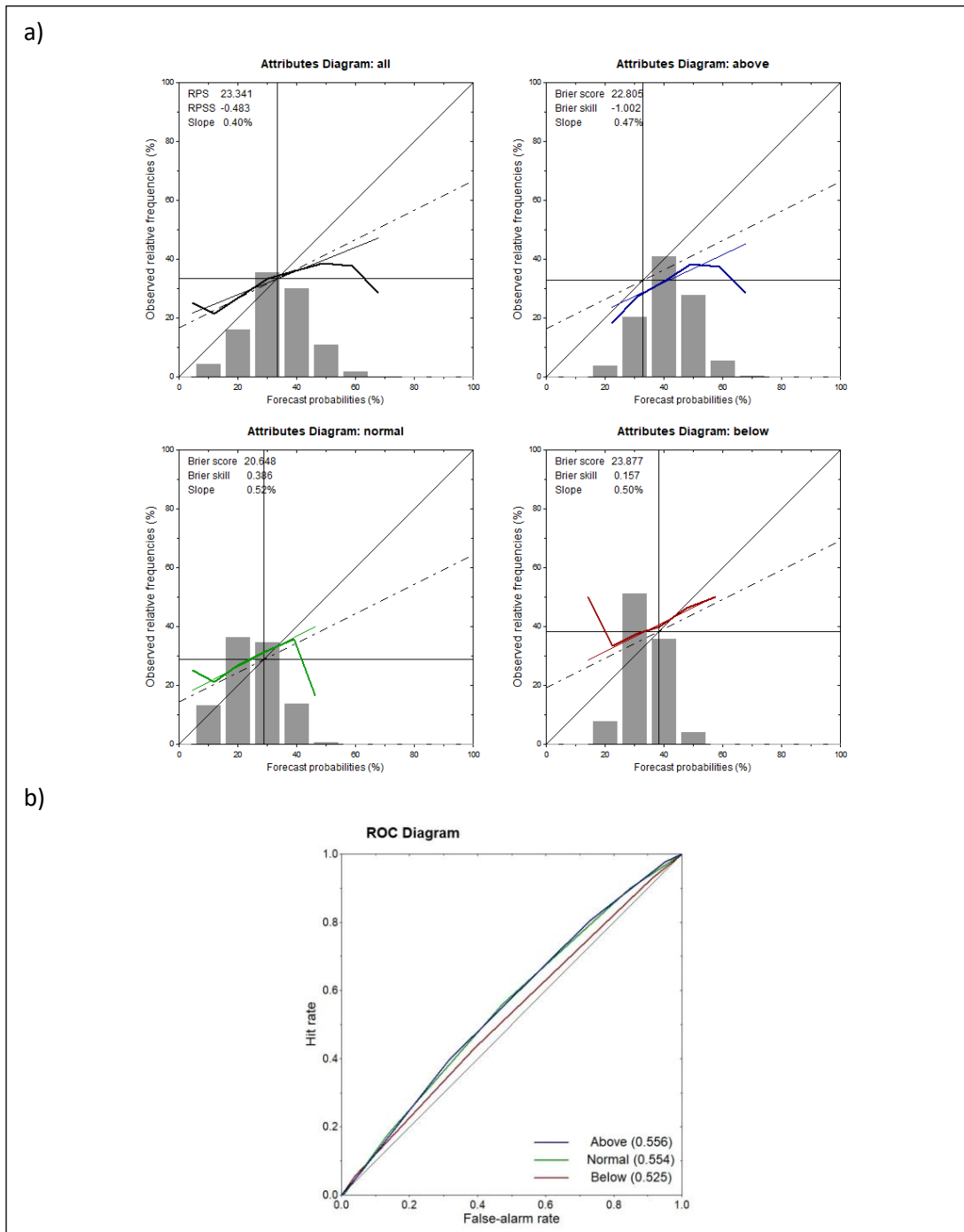


Figure 4.36. Reliability diagrams (a) and ROC curves (b) for early season dry spells duration forecast using wet days frequency during AMJ season as predictor. In subfigure b), the thick colored lines show the reliability curves, and the thick black line is the least squares weighted regression fit to the reliability curve. The weights are shown by the grey bars, which indicate the relative frequency of forecasts in each 10% bin. The thin horizontal and vertical lines indicate the relative frequency of occurrence of the predictand in the respective category, while the thin diagonal represents the line of perfect reliability.

Quality of cessation date forecast

ASO and SON wet days frequency provided useful skill for cessation date forecasting, especially frequencies observed in SON time window. ROC curves revealed better discrimination skills compared to the forecast of onset or dry spells. Reliability was mixed but improved in the October-based forecasts where forecast probabilities showed good alignment with observed frequencies, i.e. stronger signal in late season wet patterns. This indicates improved calibration and suggests that wet day frequency during SON may be a valuable predictor for identifying the cessation period with greater confidence (Figures 4.37–4.39).

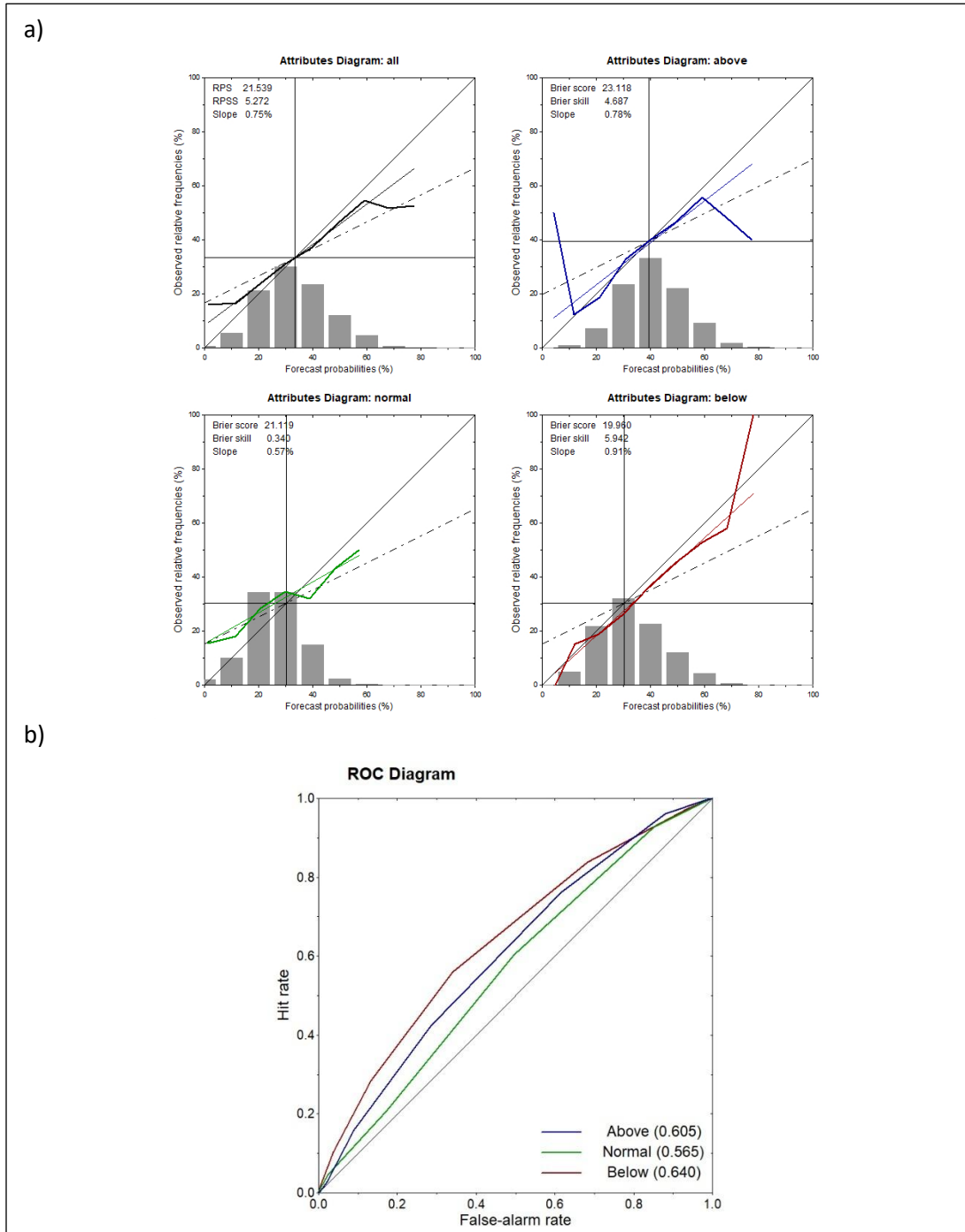


Figure 4.37. Reliability diagrams (a) and ROC curves (b) for cessation forecast using wet days frequency during ASO as predictor. In subfigure b), the thick colored lines show the reliability curves, and the thick black line is the least squares weighted regression fit to the reliability curve. The weights are shown by the grey bars, which indicate the relative frequency of forecasts in each 10% bin. The thin horizontal and vertical lines indicate the relative frequency of occurrence of the predictand in the respective category, while the thin diagonal represents the line of perfect reliability.

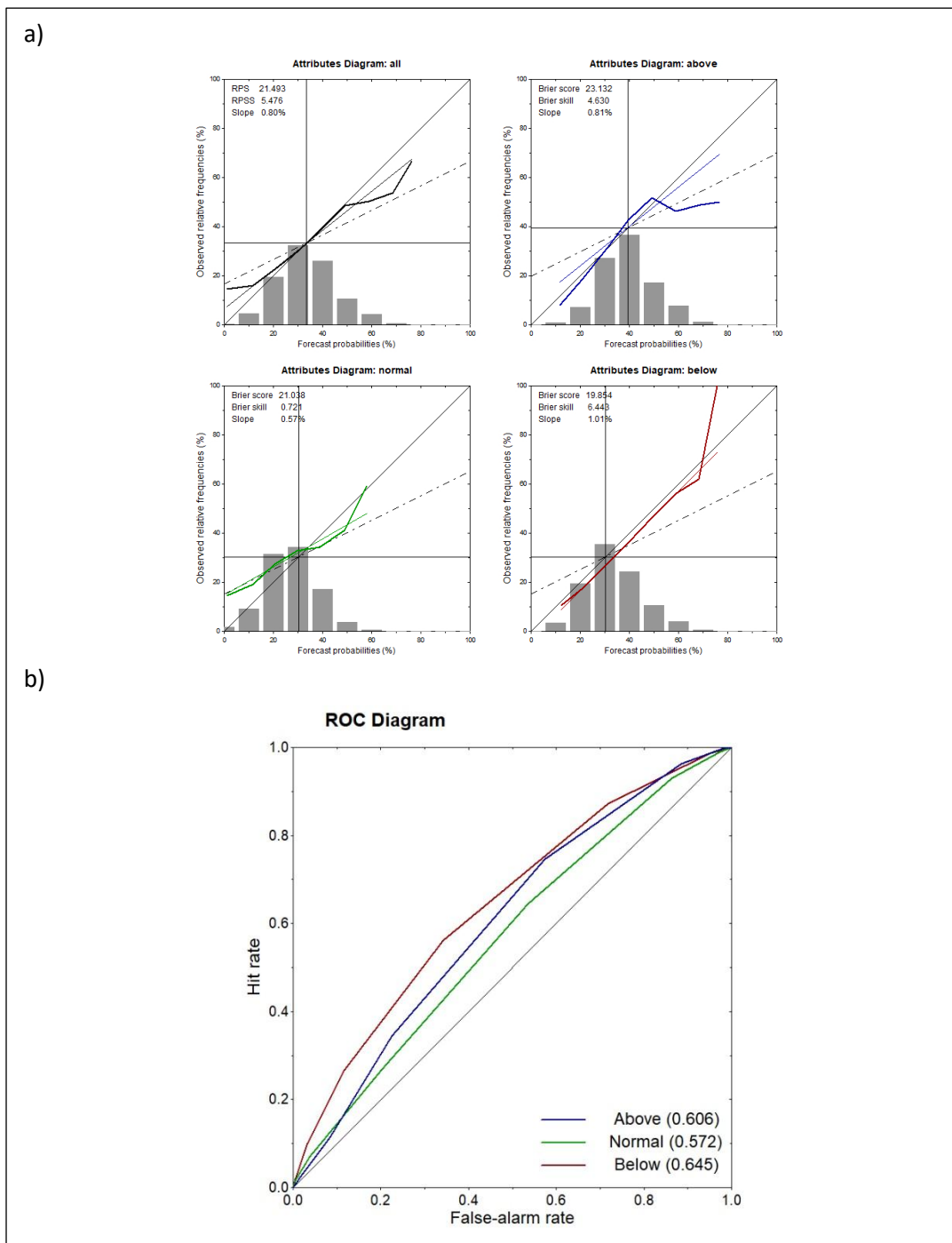


Figure 4.38. Reliability diagrams (a) and ROC curves (b) for cessation forecast using wet days frequency during SON period as predictor. In subfigure b), the thick colored lines show the reliability curves, and the thick black line is the least squares weighted regression fit to the reliability curve. The weights are shown by the grey bars, which indicate the relative frequency of forecasts in each 10% bin. The thin horizontal and vertical lines indicate the relative frequency of occurrence of the predictand in the respective category, while the thin diagonal represents the line of perfect reliability.

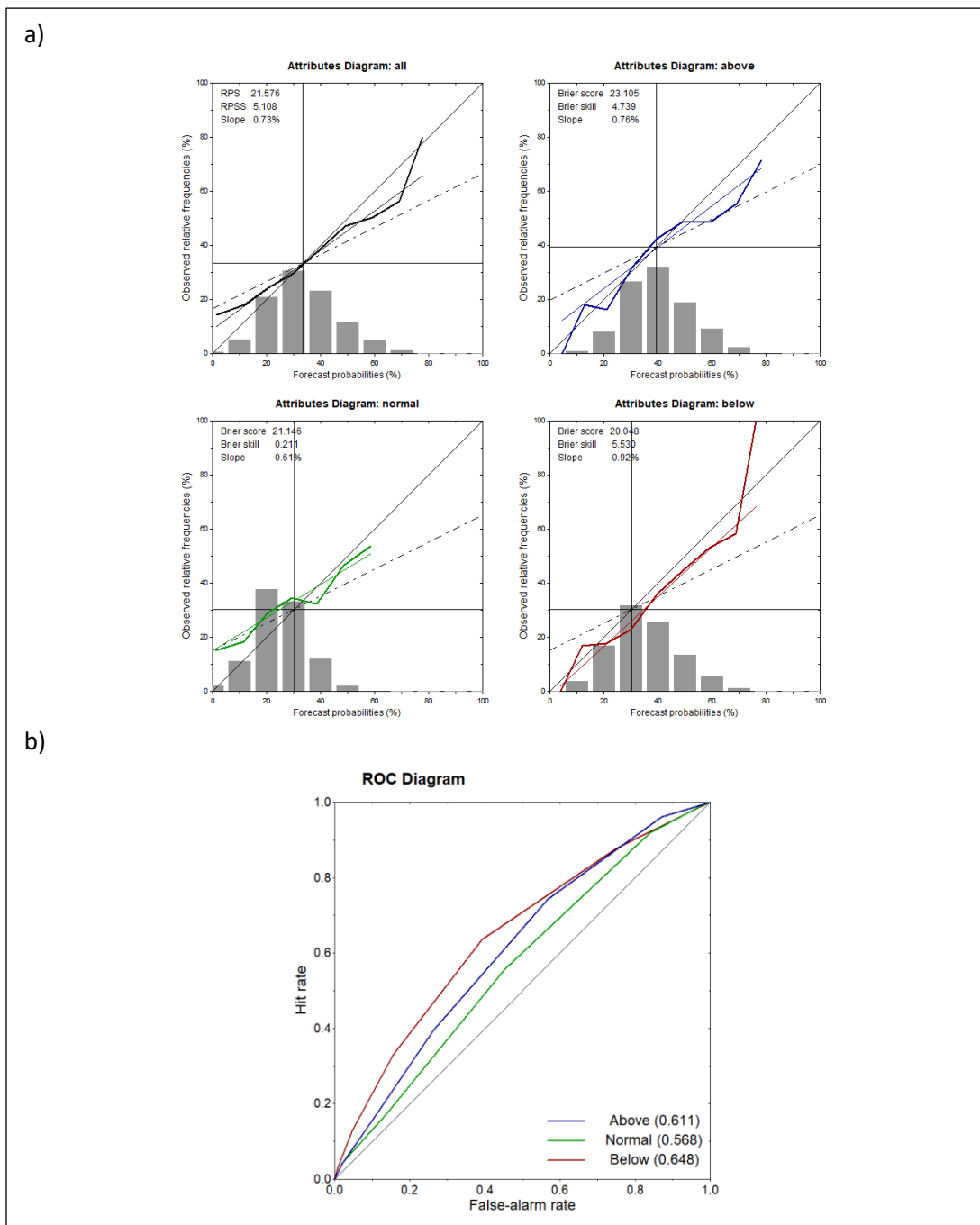


Figure 4.39. Reliability diagrams (a) and ROC curves (b) for cessation forecast using wet days frequency during October as predictor. In subfigure b), the thick colored lines show the reliability curves, and the thick black line is the least squares weighted regression fit to the reliability curve. The weights are shown by the grey bars, which indicate the relative frequency of forecasts in each 10% bin. The thin horizontal and vertical lines indicate the relative frequency of occurrence of the predictand in the respective category, while the thin diagonal represents the line of perfect reliability.

Quality of end-of-Season dry spells forecast

End of season dry spells forecast using August and September wet days frequencies as predictors had relatively poor skill. Reliability plots again showed overconfidence, particularly for extreme forecasts. Best performance was in ASO time window likely due to a more direct relation to season end (Figures 4.40–4.42).

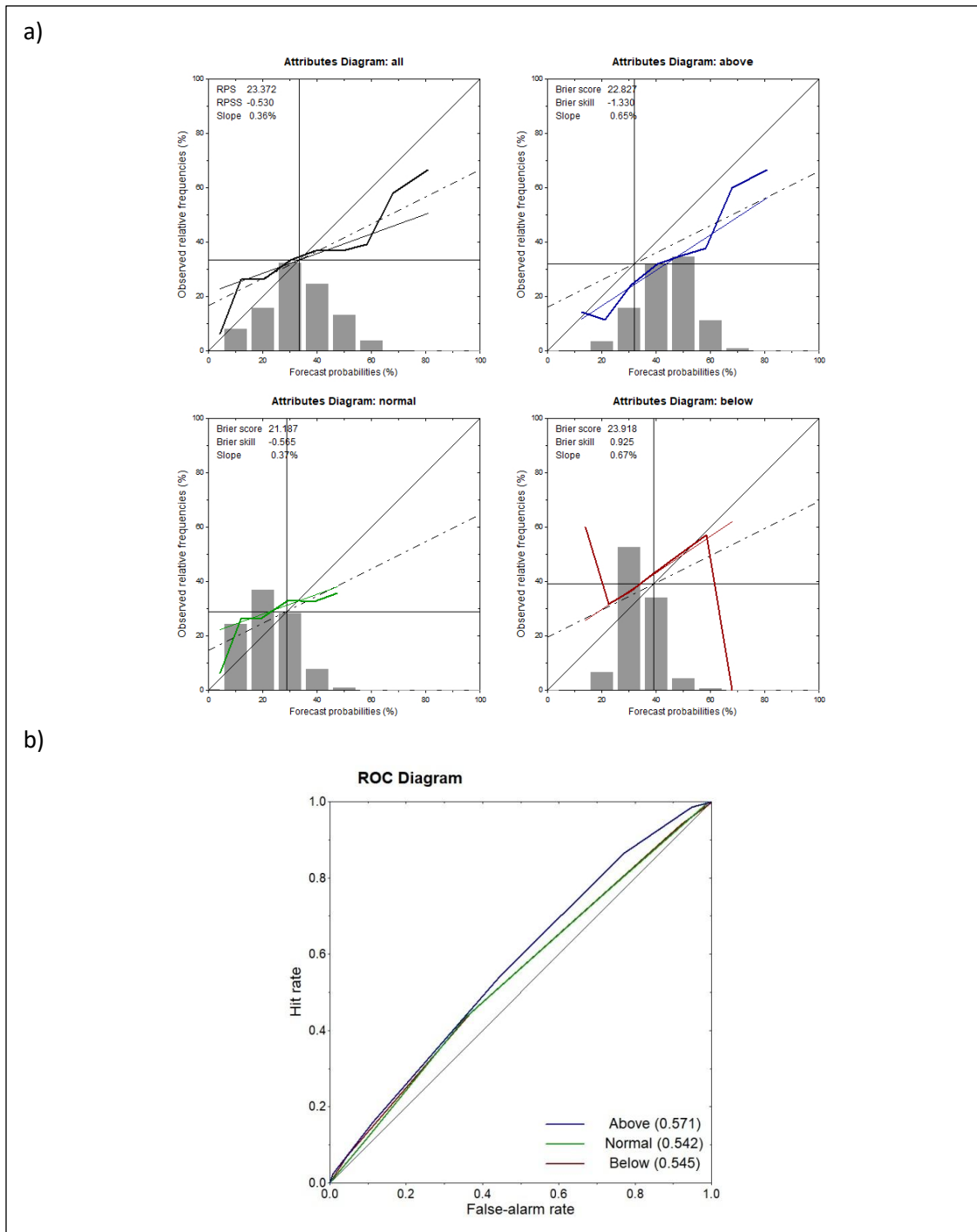


Figure 4.40. Reliability diagrams (a) and ROC curves (b) for end season dry spells duration forecast using wet days frequency during August as predictor. In subfigure b), the thick colored lines show the reliability curves, and the thick black line is the least squares weighted regression fit to the reliability curve. The weights are shown by the grey bars, which indicate the relative frequency of forecasts in each 10% bin. The thin horizontal and vertical lines indicate the relative frequency of occurrence of the predictand in the respective category, while the thin diagonal represents the line of perfect reliability.

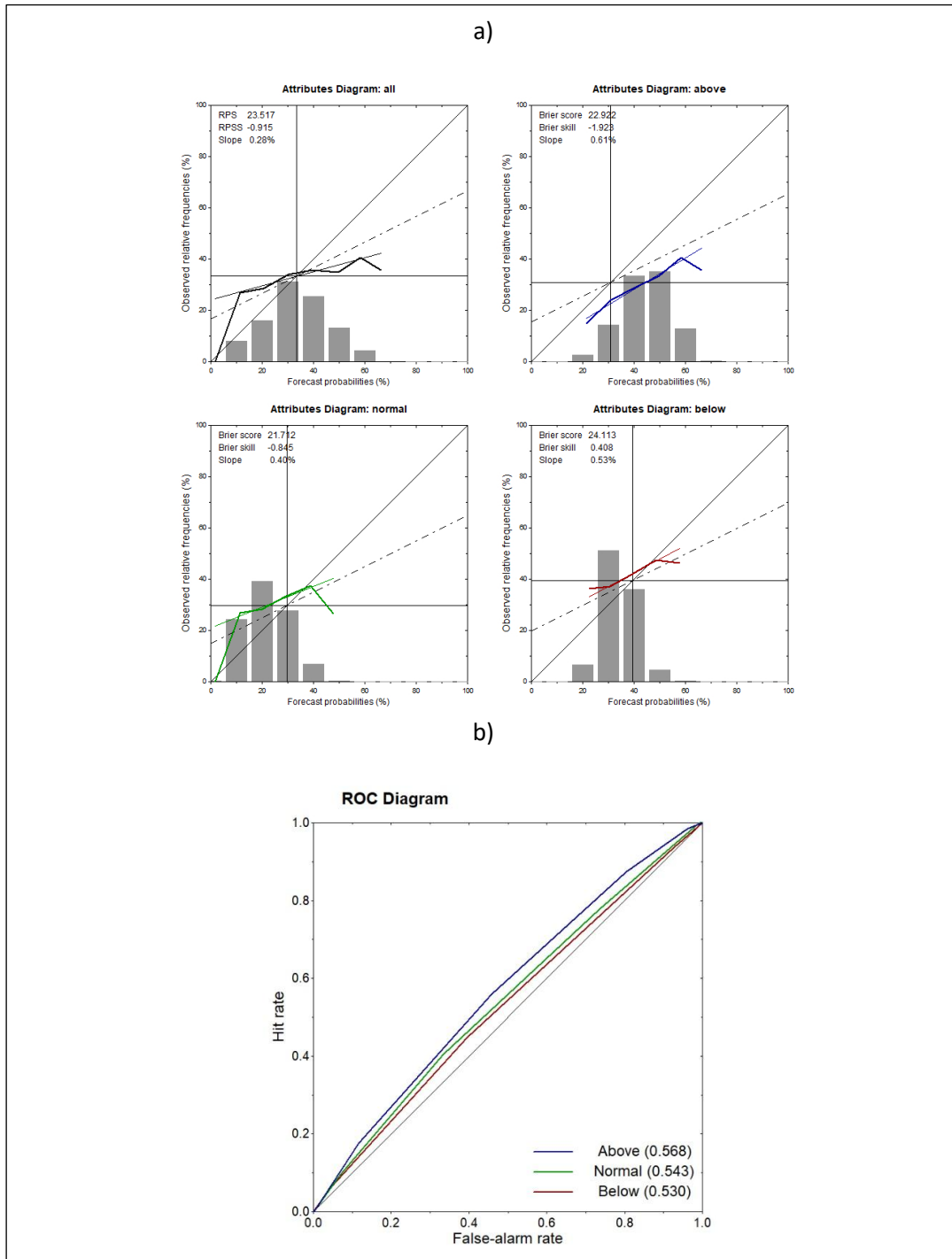


Figure 4.41. Reliability diagrams (a) and ROC curves (b) for end season dry spells duration forecast using wet days frequency during September as predictor. In subfigure b), the thick colored lines show the reliability curves, and the thick black line is the least squares weighted regression fit to the reliability curve. The weights are shown by the grey bars, which indicate the relative frequency of forecasts in each 10% bin. The thin horizontal and vertical lines indicate the relative frequency of occurrence of the predictand in the respective category, while the thin diagonal represents the line of perfect reliability.

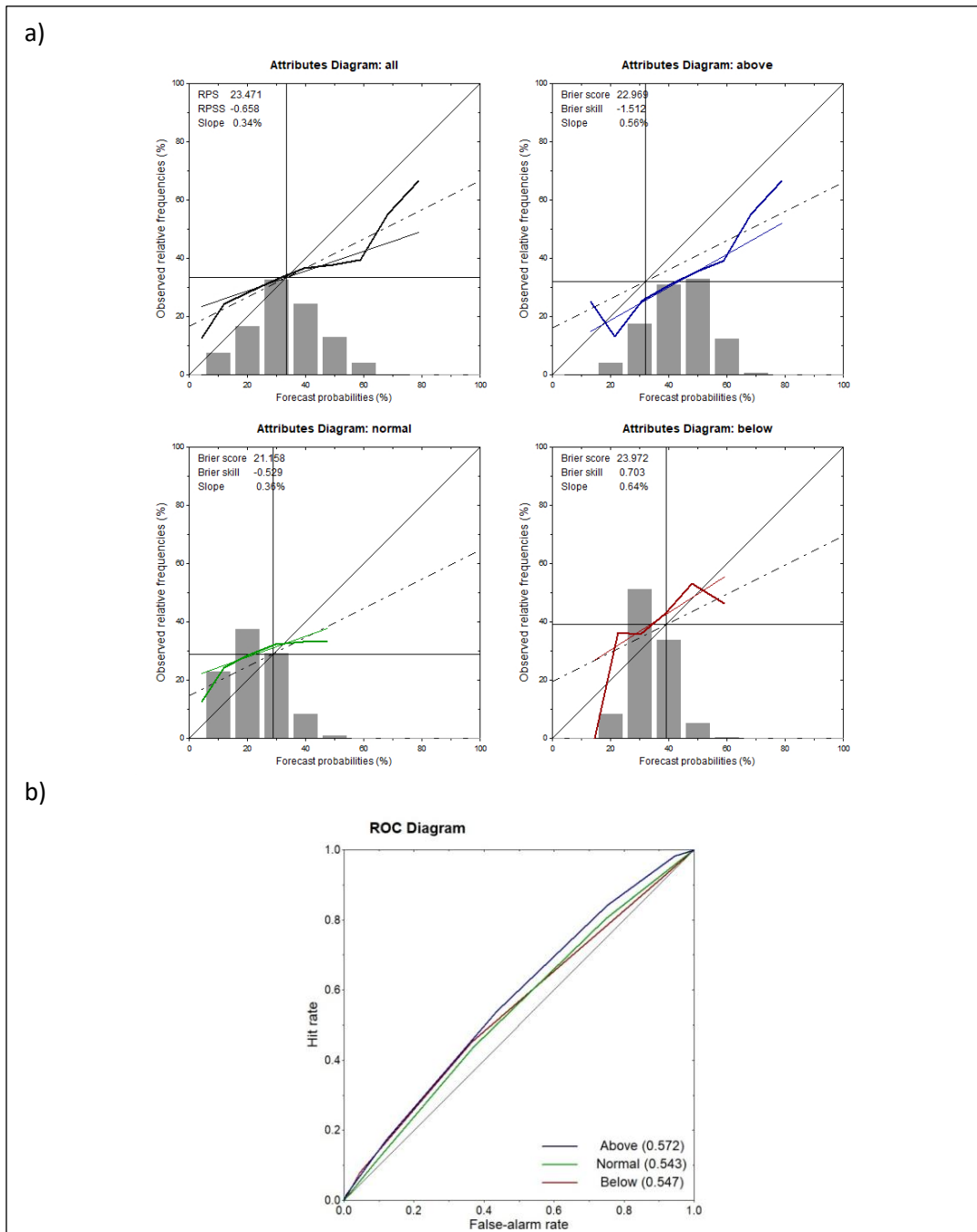


Figure 4.42. Reliability diagrams (a) and ROC curves (b) for end season dry spells duration forecast using wet days frequency during ASO period as predictor. In subfigure b), the thick colored lines show the reliability curves, and the thick black line is the least squares weighted regression fit to the reliability curve. The weights are shown by the grey bars, which indicate the relative frequency of forecasts in each 10% bin. The thin horizontal and vertical lines indicate the relative frequency of occurrence of the predictand in the respective category, while the thin diagonal represents the line of perfect reliability.

4.2.2. Using cumulative rainfall to forecast season onset dates over Niger

In this investigation, as described in section 3.4.2. in chapter 3, rainfall monthly totals and rolling seasonal totals were tested as predictors for season onset and cessation using rain gauges data from 50 stations in Niger over the period 1982-2021. Correlations between rainfall totals and actually observed onset data were checked first using linear regression. Then rainfall hindcasts (CFSV2) and historical observation data (station and satellite estimates) over the period of the season showing good correlation were used as predictors to forecast season onset. Then those forecasts were verified using CPT.

4.2.2.1. Assessment of the correlation between cumulative rainfall and season onset dates

The correlation coefficients resulting from the regression between the historical observed onset dates and the rainfall totals over various periods over the season are listed in Appendix D. It comes out from those results that the annual cumulative rainfall and the rainfall total over the JAS season have low correlation with the onset date, with r^2 values varying from 0 to 0.29 and from 0 to 0.11, respectively over the 50 records.

Regression analyses based on monthly rainfall totals (May, June, July, and August) and 2- to 3-months rolling totals (MJ, JJ, JA, AMJ, MJJ, JJA) yielded r^2 values ranging from 0.40 to a peak of 0.55. Among the records within this range, 49% of the strongest correlations were observed with AMJ rainfall totals, 37% with MJ totals, 10% with May totals, and 5% with June cumulative rainfall. Therefore, AMJ total rainfall was used as predictor in the following step.

4.2.2.2. Verification of forecast made using AMJ cumulative rainfall as predictors

A linear regression model using AMJ cumulative rainfall as predictor and season onset date as predictand was built using AMJ hindcasts from CFSv2 (raw model output and bias corrected hindcast). The model was trained over the first 20 years of the period 1991-2020, then it was used to perform retroactive forecast of the season onset over the remaining period (2011-2020). Reliability and ROC diagrams were plotted to assess the reliability and the discrimination of the forecasts resulting from this process.

Figures 4.43 to 4.47 show the reliability diagrams and ROC curves for the verification of onset forecasts using respectively CFSv2 hindcast (raw model output and bias corrected hindcast), Station gauge data, GPCC and CHRIPS observation data.

Quality of onset date forecast using CFSv2 non-corrected hindcast

The forecast using non-corrected CFSv2 as predictor had moderate reliability in near-normal category but for above and below normal categories, forecasts showed deviations from perfect reliability, with certain probability bins displaying mismatches between forecast probabilities and observed frequencies. The ROC curve for the near-normal show better discrimination compared to the other categories but the AUC remains fair (~0.6) (Figure 4.43).

Quality of onset date forecast using CFSv2 bias corrected hindcast

The bias corrected CFSv2 hind cast showed similar reliability than the non-corrected predictor and slight AUC improvement for above and below normal categories. This suggests that the bias correction applied on the predictor moderately improves the forecast discriminatory skill (Figure 4.44).

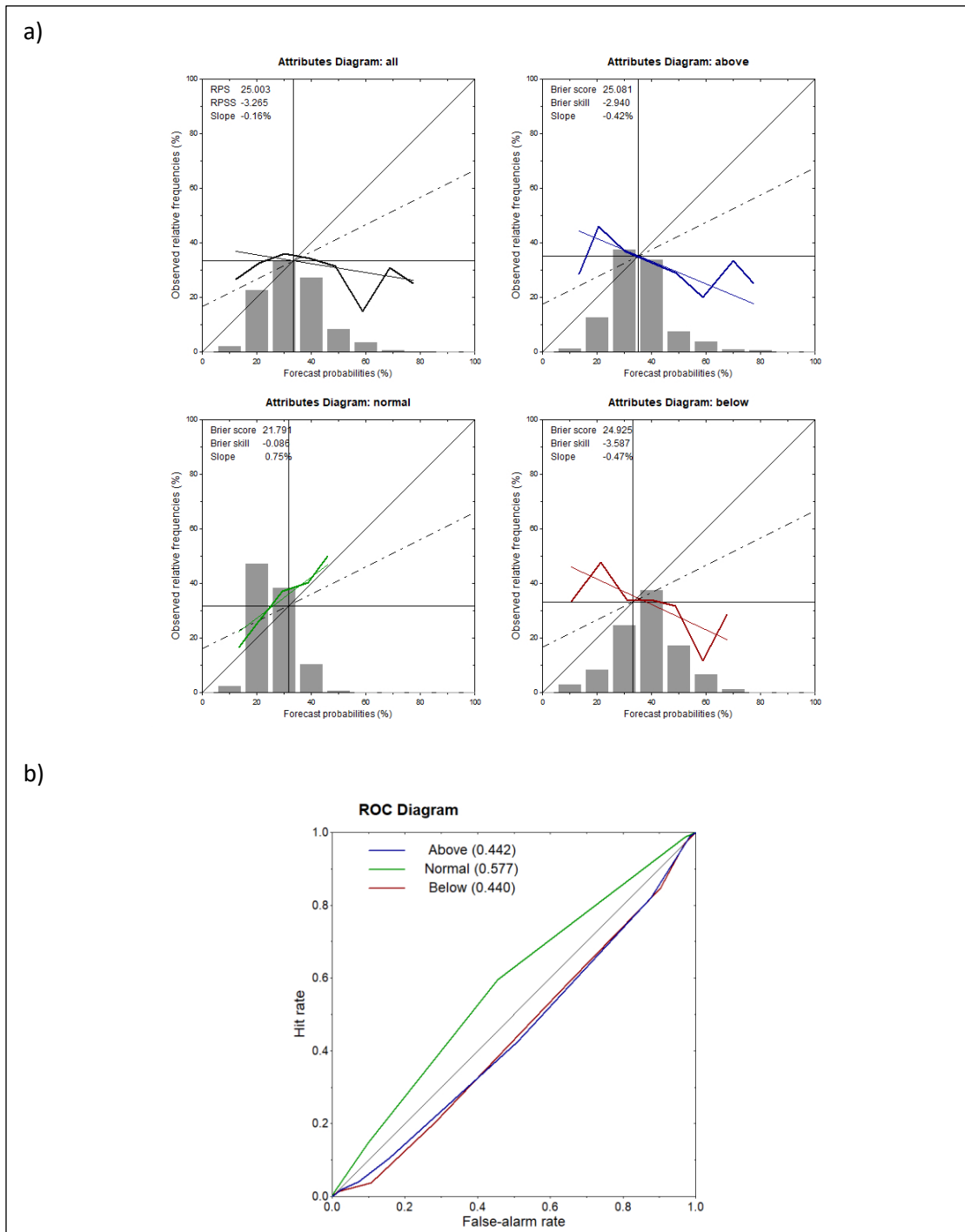


Figure 4.43. Reliability diagrams (a) and ROC curves (b) for onset forecast made by using AMJ rainfall hindcast from CFSv2 as predictor. In subfigure b), the thick colored lines show the reliability curves, and the thick black line is the least squares weighted regression fit to the reliability curve. The weights are shown by the grey bars, which indicate the relative frequency of forecasts in each 10% bin. The thin horizontal and vertical lines indicate the relative frequency of occurrence of the predictand in the respective category, while the thin diagonal represents the line of perfect reliability.

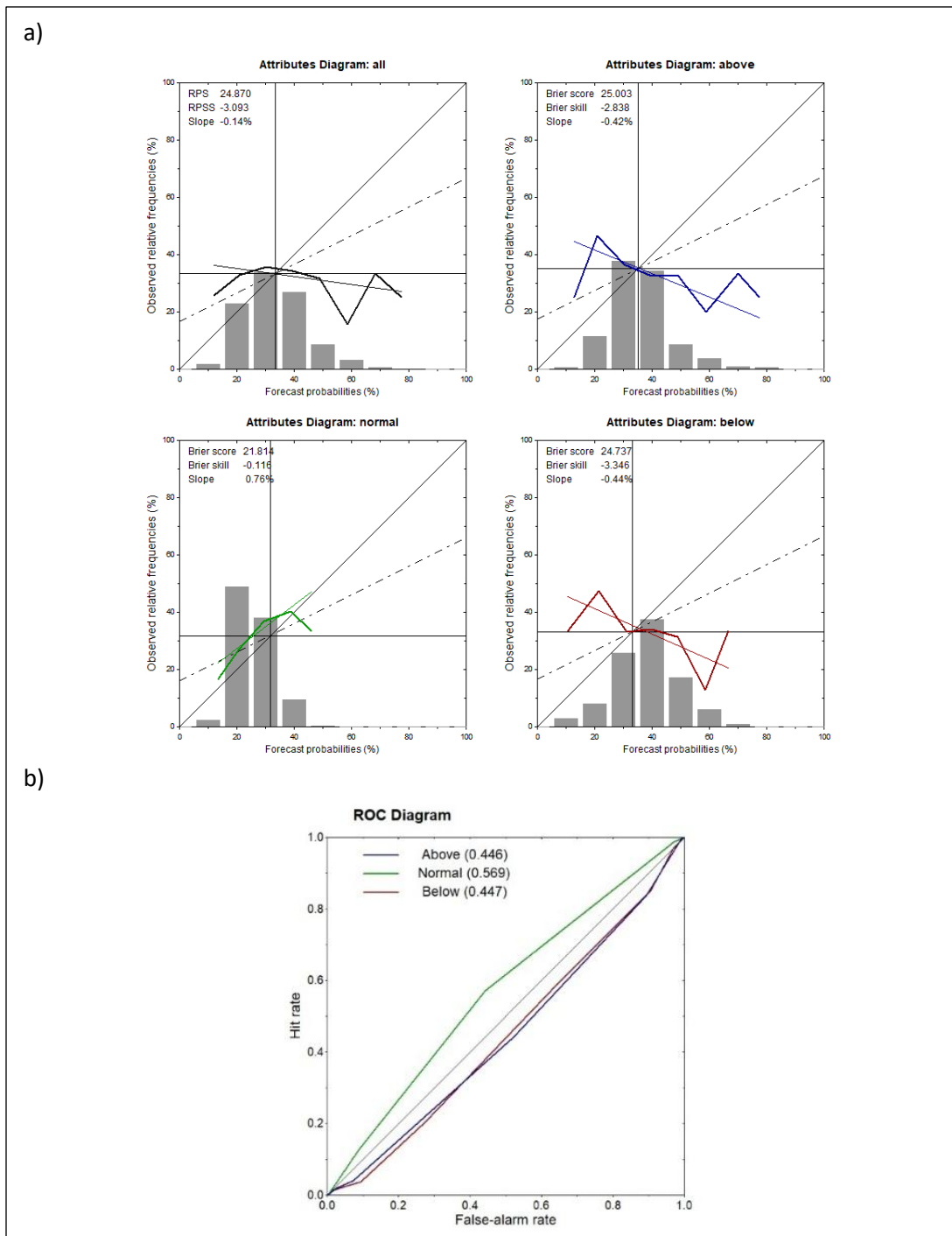


Figure 4.44. Reliability diagrams (a) and ROC curves (b) for onset forecast made by using AMJ rainfall bias corrected hindcast from CFSv2 as predictor. In subfigure b), the thick colored lines show the reliability curves, and the thick black line is the least squares weighted regression fit to the reliability curve. The weights are shown by the grey bars, which indicate the relative frequency of forecasts in each 10% bin. The thin horizontal and vertical lines indicate the relative frequency of occurrence of the predictand in the respective category, while the thin diagonal represents the line of perfect reliability.

Quality of onset date forecast using observation-based predictors

Figure 4.45, Figure 4.46, and Figure 4.47 show the verification metrics of forecasts using respectively GPCC, CHIRPS and Station data as predictors. It comes out from those Figures that all the observation dataset used as predictors allow forecast with high reliability and discrimination skills. Station and CHIRPS data offer the best performance.

In conclusions, testing the ability of wet days and cumulative rainfall to predict season characteristics revealed that wet days frequency can provide useful early indicators for onset and cessation, though less effective for dry spells duration forecast. Cumulative rainfall, especially AMJ, offers stronger predictive skill for season onset date prediction. This predictor performs better when using observed datasets instead of hindcasts from GCM runs.

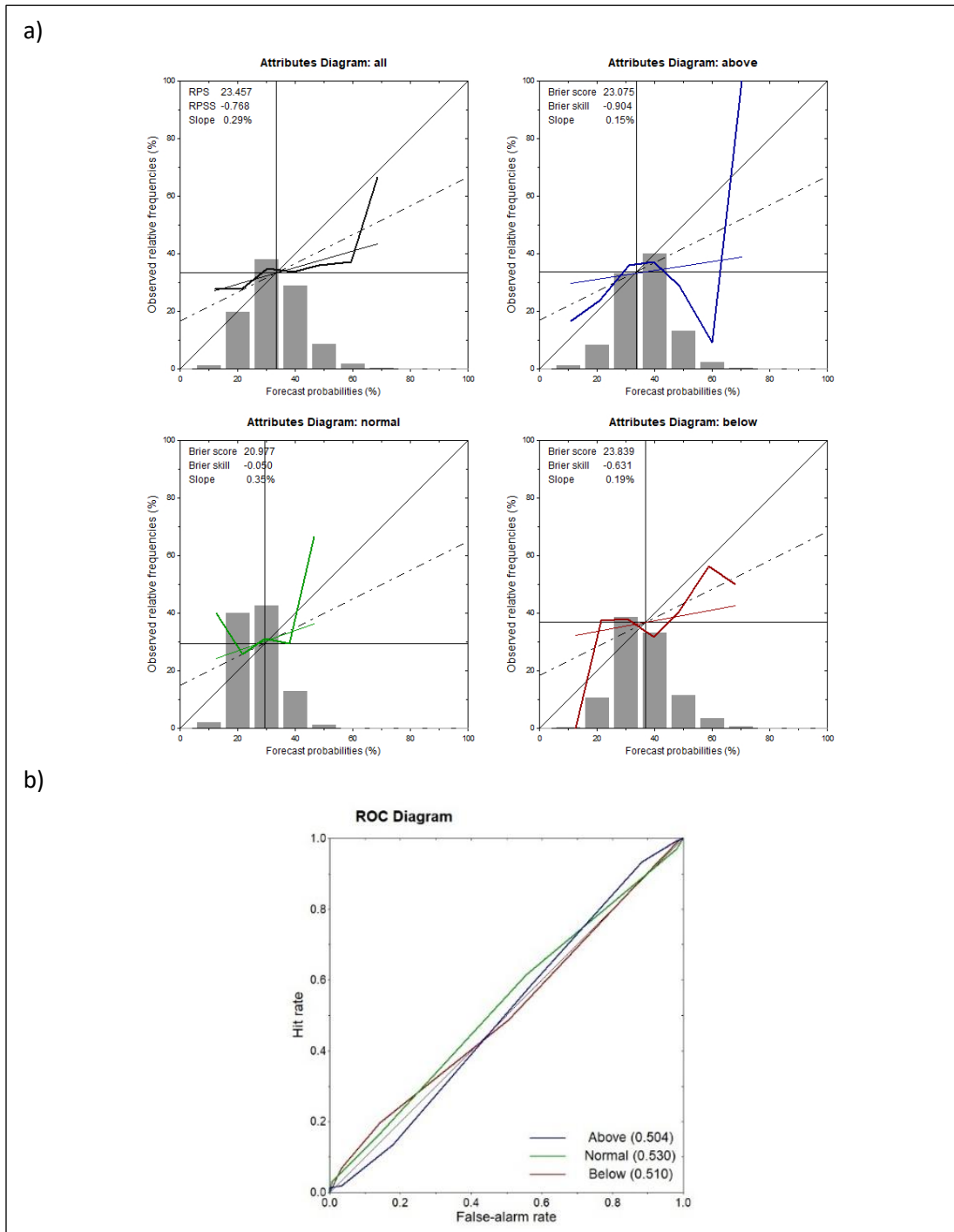


Figure 4.45. Reliability diagrams (a) and ROC curves (b) for onset forecast made by using GPCP rainfall observation data cumulated over AMJ period as predictor. In subfigure b), the thick colored lines show the reliability curves, and the thick black line is the least squares weighted regression fit to the reliability curve. The weights are shown by the grey bars, which indicate the relative frequency of forecasts in each 10% bin. The thin horizontal and vertical lines indicate the relative frequency of occurrence of the predictand in the respective category, while the thin diagonal represents the line of perfect reliability.

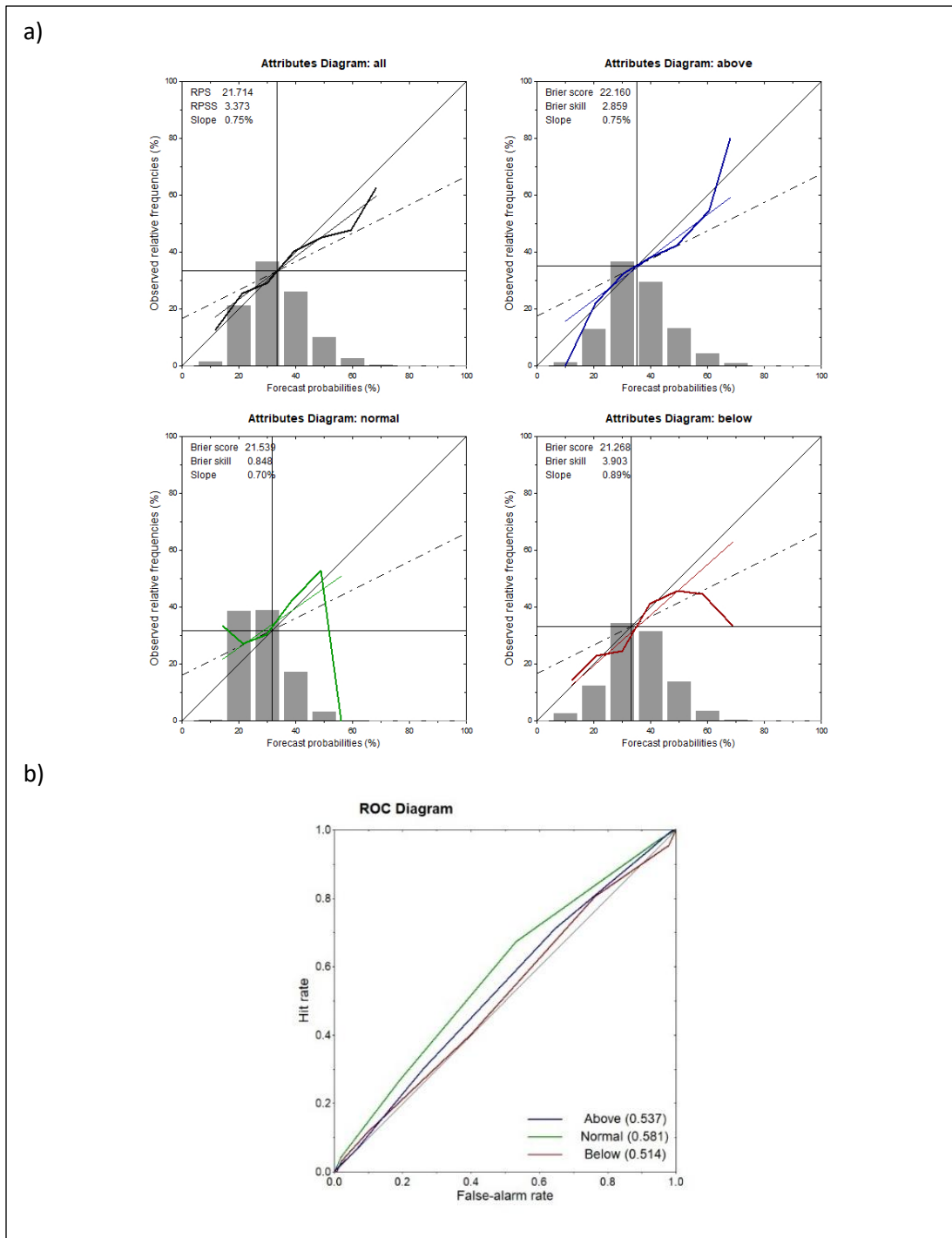


Figure 4. 46. Reliability diagrams (a) and ROC curves (b) for onset forecast made by using CHRIPS rainfall observation data cumulated over AMJ period as predictor. In subfigure b), the thick colored lines show the reliability curves, and the thick black line is the least squares weighted regression fit to the reliability curve. The weights are shown by the grey bars, which indicate the relative frequency of forecasts in each 10% bin. The thin horizontal and vertical lines indicate the relative frequency of occurrence of the predictand in the respective category, while the thin diagonal represents the line of perfect reliability.

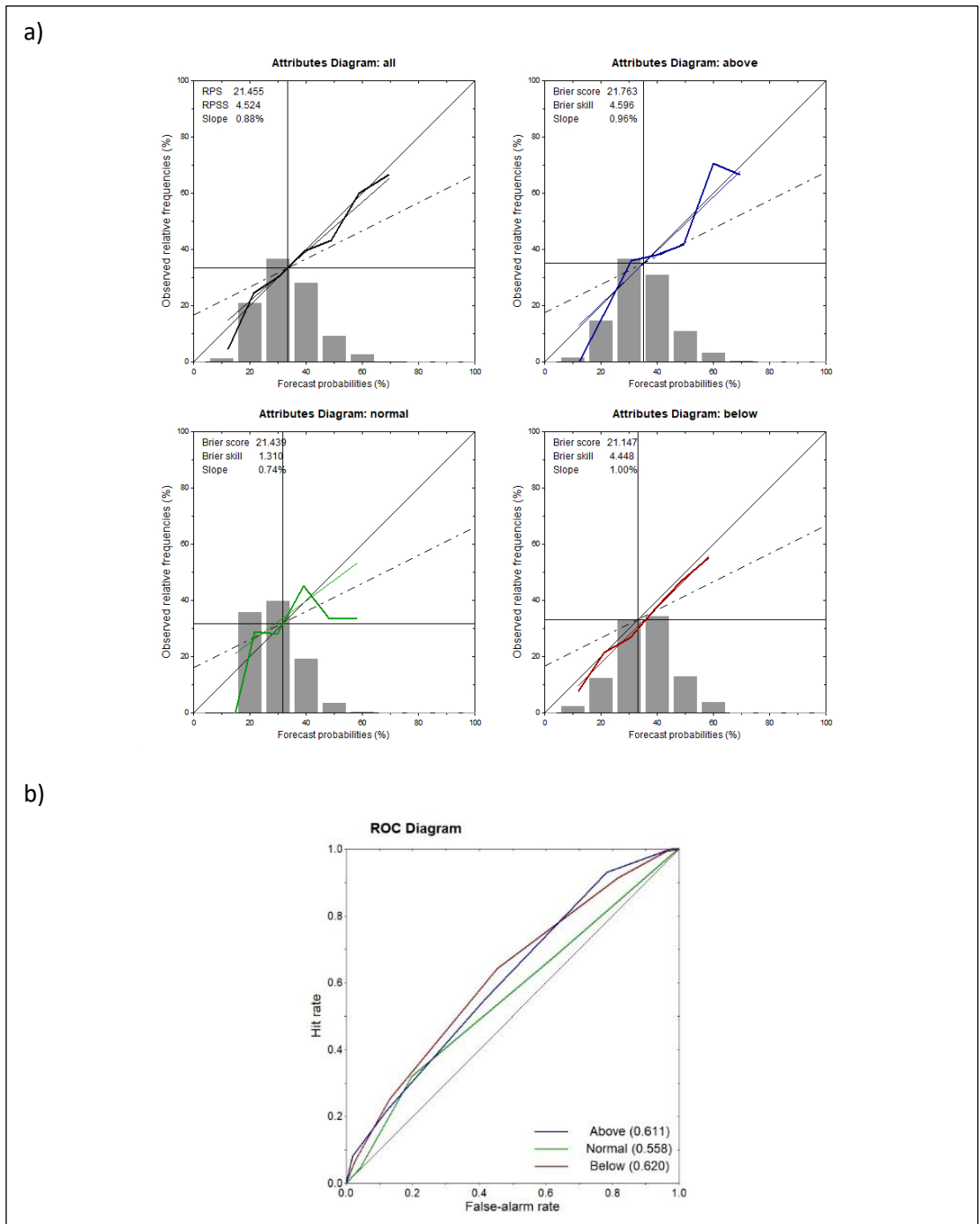


Figure 4.47. Reliability diagrams (a) and ROC curves (b) for onset forecast using station rainfall data cumulated over AMJ period as predictor. In subfigure b), the thick colored lines show the reliability curves, and the thick black line is the least squares weighted regression fit to the reliability curve. The weights are shown by the grey bars, which indicate the relative frequency of forecasts in each 10% bin. The thin horizontal and vertical lines indicate the relative frequency of occurrence of the predictand in the respective category, while the thin diagonal represents the line of perfect reliability.

4.3. Forecast information dissemination and on-farm use: Current state and perspectives

This section assesses the forecast information dissemination and use within rural agricultural communities in the Southwest of Niger. Data to achieve the evaluation were collected through a survey and a 2-years (2023 and 2024) on-farm experiments implemented in this area involving a sample of 619 farmers for the survey and 60 farmers for the on-farm demonstration trials (Sitta, 2025).

4.3.1. Current state of the forecast information use from survey outcomes in Southwest Niger

This study assesses the current use of seasonal forecast products at the farm level, the farmers' perception of the seasonal forecast products, and how those products are disseminated to identify strategies to increase farmers' use of climate services in general and forecast information in particular. A sample of 619 farmers was interviewed through a survey conducted in November - December 2022 in 16 villages located within 4 municipalities (Guéchémé, Tounouga, Kiota, and N'Dounga) in the Southwest of Niger. Information about the proportion of farmers receiving and using forecast information, farmers' perception of the forecast products, and information dissemination channels, were collected and analyzed. The perspectives for conducting further research through the on-farm demonstration trials with a view of assessing the possible gains in using the forecast information were explored as well during the survey.

4.3.1.1. Forecast information dissemination

Findings from the survey data analysis showed a low proportion (42.3%) of farmers receiving agroclimatic information released by the meteorological service and other climate services suppliers. This agrees with Roncoli et al. (2009) who found inequitable dissemination of information across the communities due to social tensions related to political power, leadership, or land ownership.

It comes out from the survey results that the forecast dissemination through roving seminars/workshops does not make the information to be widely diffused as expected. Eighty-one percent (81%) of farmers receiving the information declared getting that through radio broadcasts while only 5% of farmers declared receiving the information through roving seminars way (Table 4.10). From the discussion with survey respondents, one of the reasons behind the message not being well transmitted through the workshops' participants who were supposed to do so throughout their neighborhoods is their education level. Most of the time, the village chief sends a family member to the workshops without considering if the person can assimilate or not the training/information to be delivered at the workshops. Another important observation is the lack of interest from the farmers who did not participate in the workshop having believed that it is a waste of time to listen to information that they may not be able to use as a result of resource limitations or religious belief. Survey records in Table 4.11 show that 49% of the whole sample suggests radio broadcasts as the fastest and most adapted way to get the information to the farmers while 27% prefer to pass the information through the village chief for timely dissemination. Therefore, future strategies to enhance climate information dissemination across rural communities should engage mixed methods such as combining radios, community leaders, and ITC technologies for efficiency.

Table 4.10 : Information reception status through the various dissemination channels

Dissemination Channels	Number of respondents	Proportion (%) out of the total number of respondents who received the information	Proportion (%) out of the total sample
TV	26	10	4
Radio	212	81	34
Village Chief	23	9	4
Local Agricultural Extension Agent	15	6	2
Roving Seminars / Workshops	14	5	2
Others (Community relay at the mosque, local rainfall data observer, WhatsApp, Facebook Personal communication)	58	22	9

Table 4. 11 : Preferred information dissemination channels by farmers

Dissemination Channels	Number of respondents	Proportion (%) out of the total sample
TV	26	4
Radio	212	34
Village Chief	23	4
Local Agricultural Extension Agent	15	2
Roving Seminars / Workshops	14	2
Other (Community relay at the mosque, local rainfall data observer, WhatsApp, Facebook, Personal communication)	58	9

4.3.1.2. Perception and use of the forecast products and other climate services

Seasonal forecast information seems to be the most appreciated information among the package of climate services provided by the Meteorological Service to farmers during the implementation of ANADIA and PASEC initiatives. 63% of the respondents receiving the agroclimatic information affirmed that seasonal forecast is the most relevant information to them. This is followed by information about the crops' evolution throughout the season (13% of respondents) and the daily weather forecast information (11%) (Figure 4.48).

Figure 4.49 shows farmers' appreciation of the various seasonal forecast information provided to them. The results show that 62% of the respondents receiving the information found the forecast information useful to very useful for application to their agricultural activities. Most of those receiving the information (93%) declared that they have effectively used at least one of the seasonal forecast products and 96% of those users affirmed that it has been beneficial to apply the information in their decision-making process. However, out of the total survey sample (i.e. sample including farmers not receiving the information), only 39% of respondents use the forecast information for their agricultural activities.

A large proportion (78%) of farmers among survey respondents who have declared no use or a very low to fairly use of the information are either illiterate, or having primary school level or only qur'anic education. Those outcomes show that despite the efforts to reduce the communication gap of climate services, the rate of utilization of seasonal forecast information in farming systems is still low as was revealed by Tarhule and Lamb (2003), and Tarchiani et al. (2017), and Wood et al. (2014) who found evidence that households reported making farming changes in recent years in west Africa are associated with access to weather information, assets, and participation in social

institutions such as saving/credits and loan groups and/or agricultural or natural resources management-related group.

For the proportion of farmers using the forecast information, the application of seasonal forecasts depends on the type of activities and the opportunities available to them. Field preparation (85% of respondents), variety choice (45% of respondents), and choice of the planting date (47%) were the three main activities for which they declared they had made their decision based on forecast information (Figure 4.50). This is in agreement with Roudier et al. (2014) who simulated crop management based on seasonal and 10-day forecasts with farmers in Senegal and found that change in sowing date and crop variety choice, if applicable, were the most prevalent use of forecast information.

To differentiate the relevance of each of the forecast products for on-farm decision-making, respondents were asked which of them, they consider to be the most important for their agricultural activities. The results showed that season onset and season cumulative rainfall forecast are respectively considered by 45% and 34% of the farmers as the most important information for their activities while early season dry spells, end of season dry spells, and cessation dates forecast information are considered to be the most important information by 9%, 8%, and 4% respectively of farmers receiving forecast information (Figure 4.51).

4.3.1.3. Major constraints to agriculture productivity and crop yield

Major constraints faced in the farming system were discussed during the survey. Figure 4.52 shows that most of the respondents consider Drought (62%), followed by floods (59%), sowing failure (59%), extreme winds (56%), and crop pest attacks (54%) as major risks to Agricultural productivity. Early cessation of the rainy season and crop diseases were also identified as major

risks by 38% and 23% of the respondents respectively. Other limitations have been mentioned by 28% of the respondents. Those include the farmer's inaccessibility to fertilizers, improved seeds, late season onset, extreme rainfall events, and extreme winds. It comes from those results that most farmers are aware of the area's major climatic risks for agriculture and food production.

4.3.1.4. Needs Assessment for Further Climate Services

Besides the information already available to them, survey participants were asked about their needs for further climate services for their daily activities. Figure 4.53 indicates that the largest number of responses came for weather information for pest management (37%), followed by information on crop insurance (22%) and Temperature forecast (19%). The proportions of respondents declaring the need for dust storm forecast, dry haze forecast, dust concentration information, and some other information, including extreme rainfall alert and extreme wind event forecast, were lower than for the previous categories.

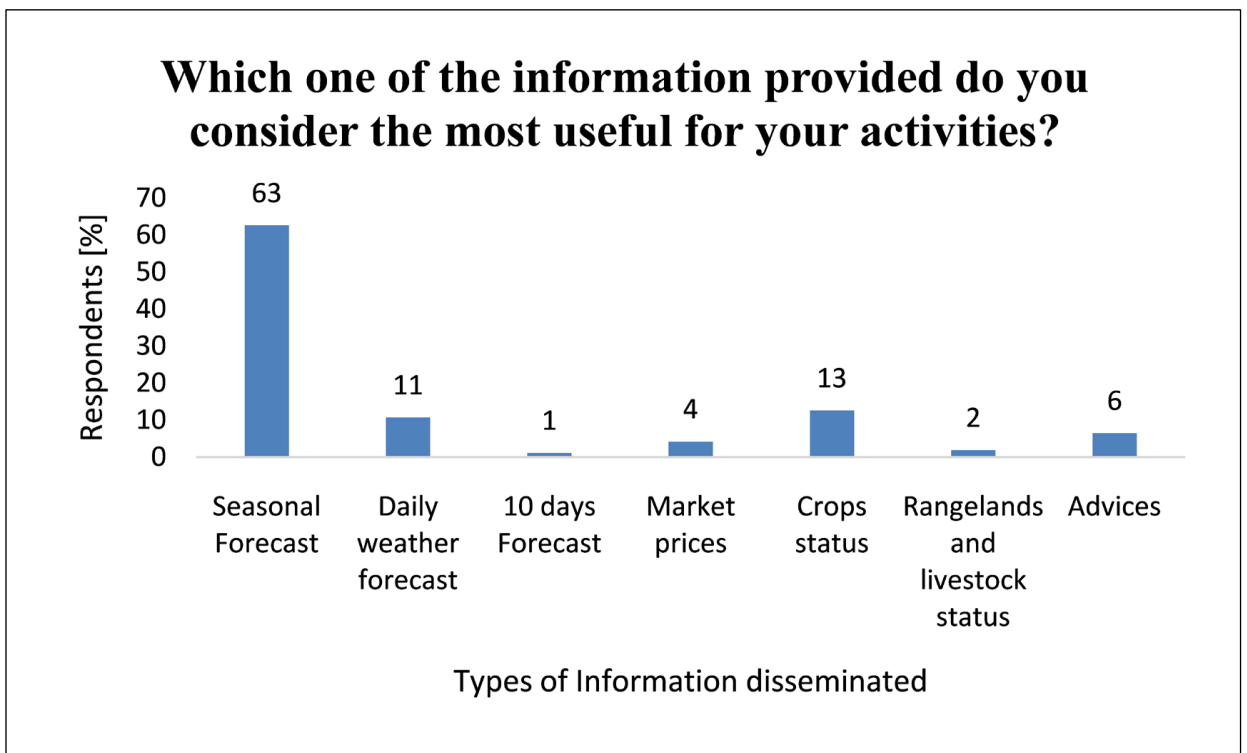


Figure 4.48. Farmer's perception of the different types of climate information provided to them

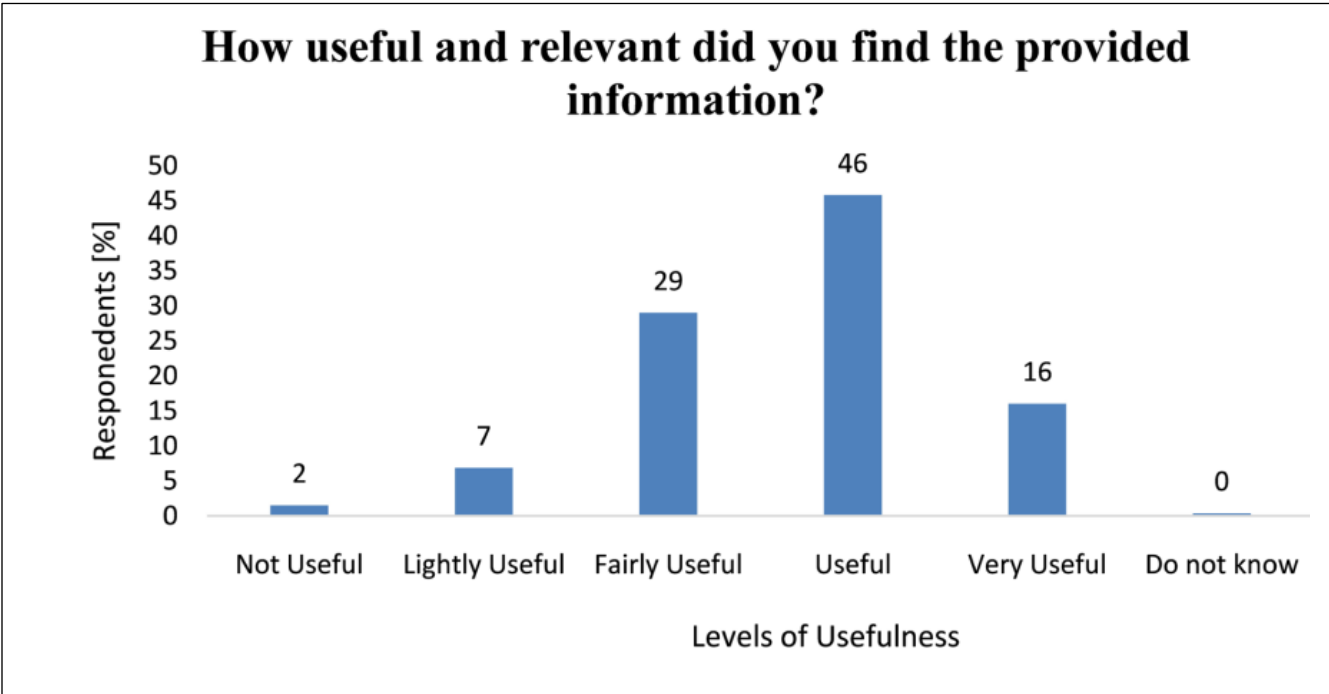


Figure 4.49. Farmer’s appreciation of the different types of seasonal forecast products.

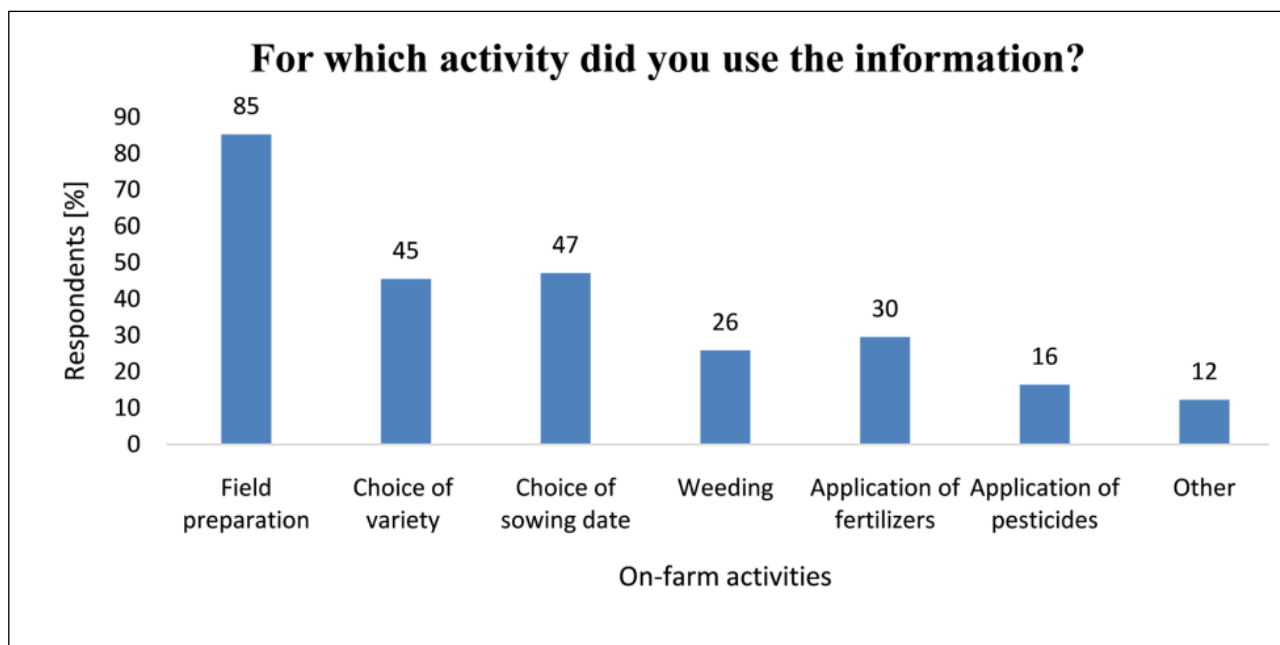


Figure 4.50. Application of climate information to on-farm activities.

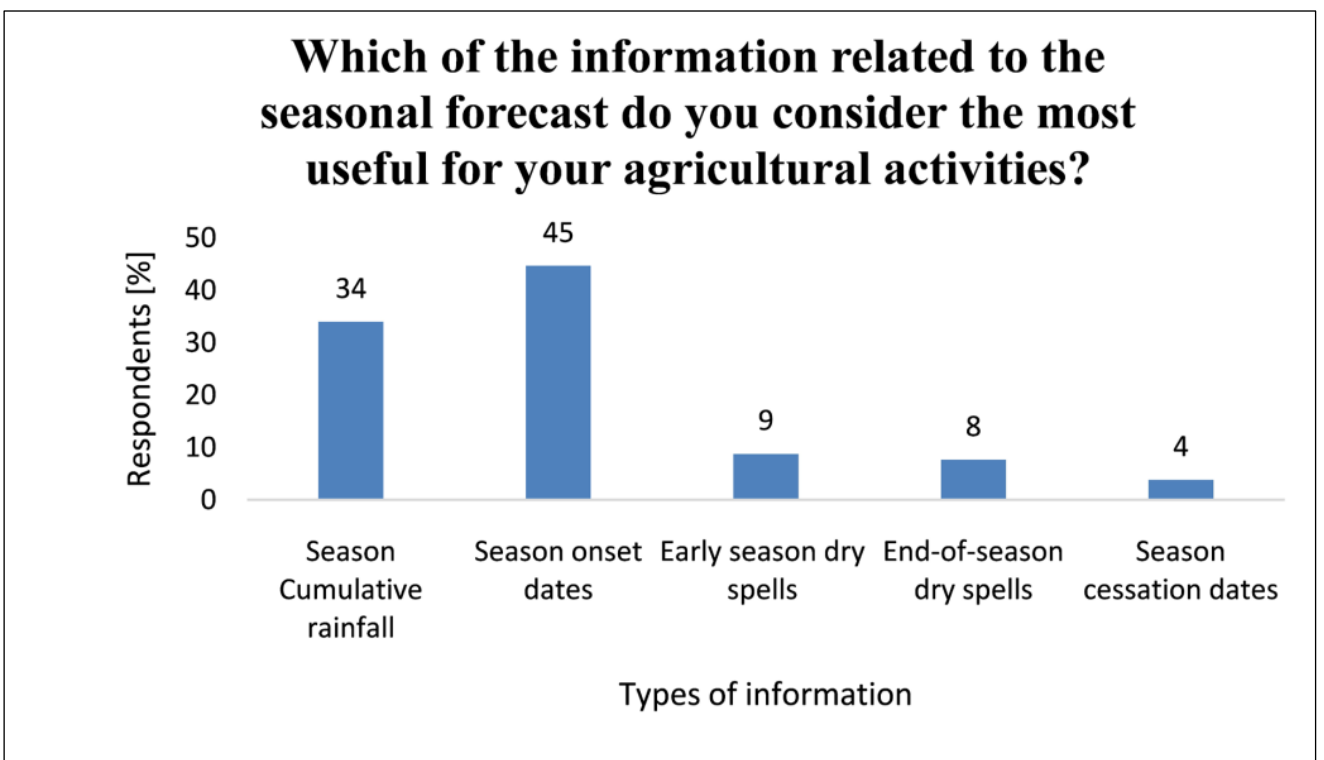


Figure 4.51. Farmers' appreciation of seasonal forecast products.

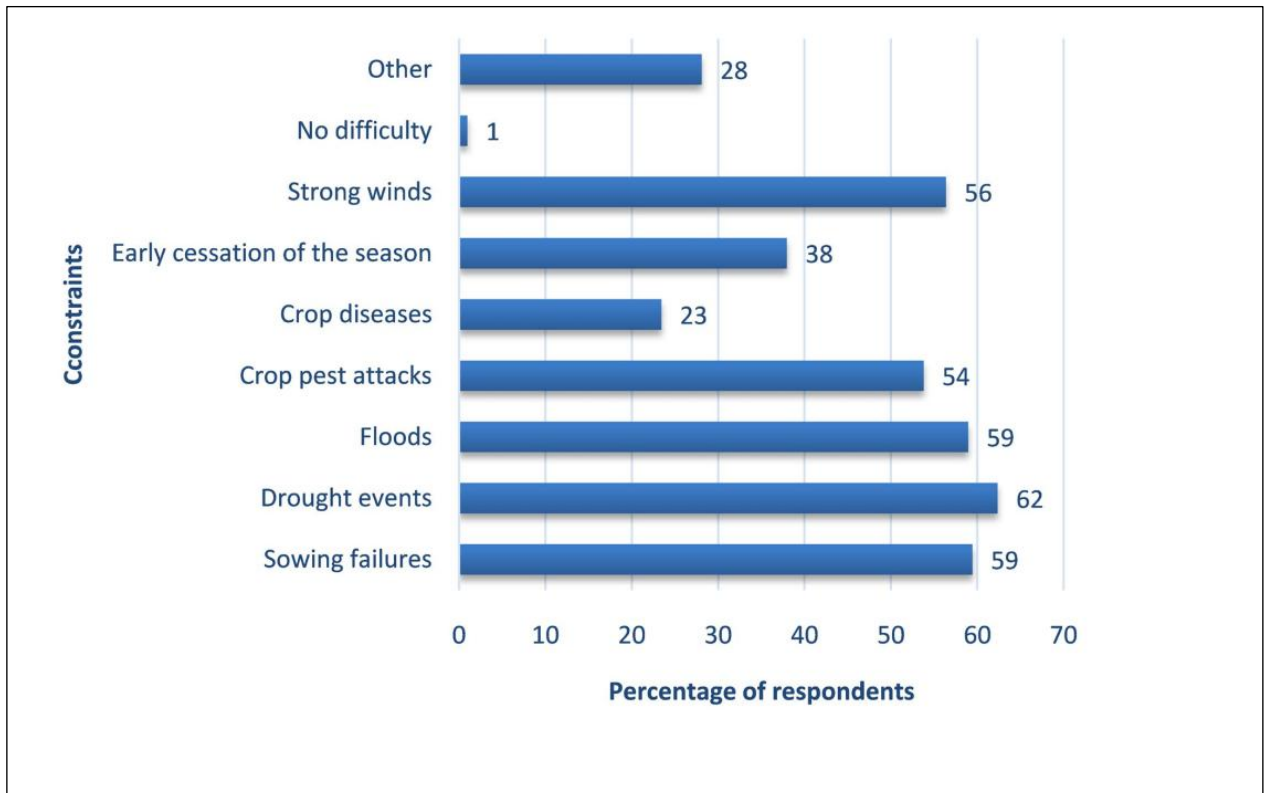


Figure 4.52. Major constraints encountered during the growing season.

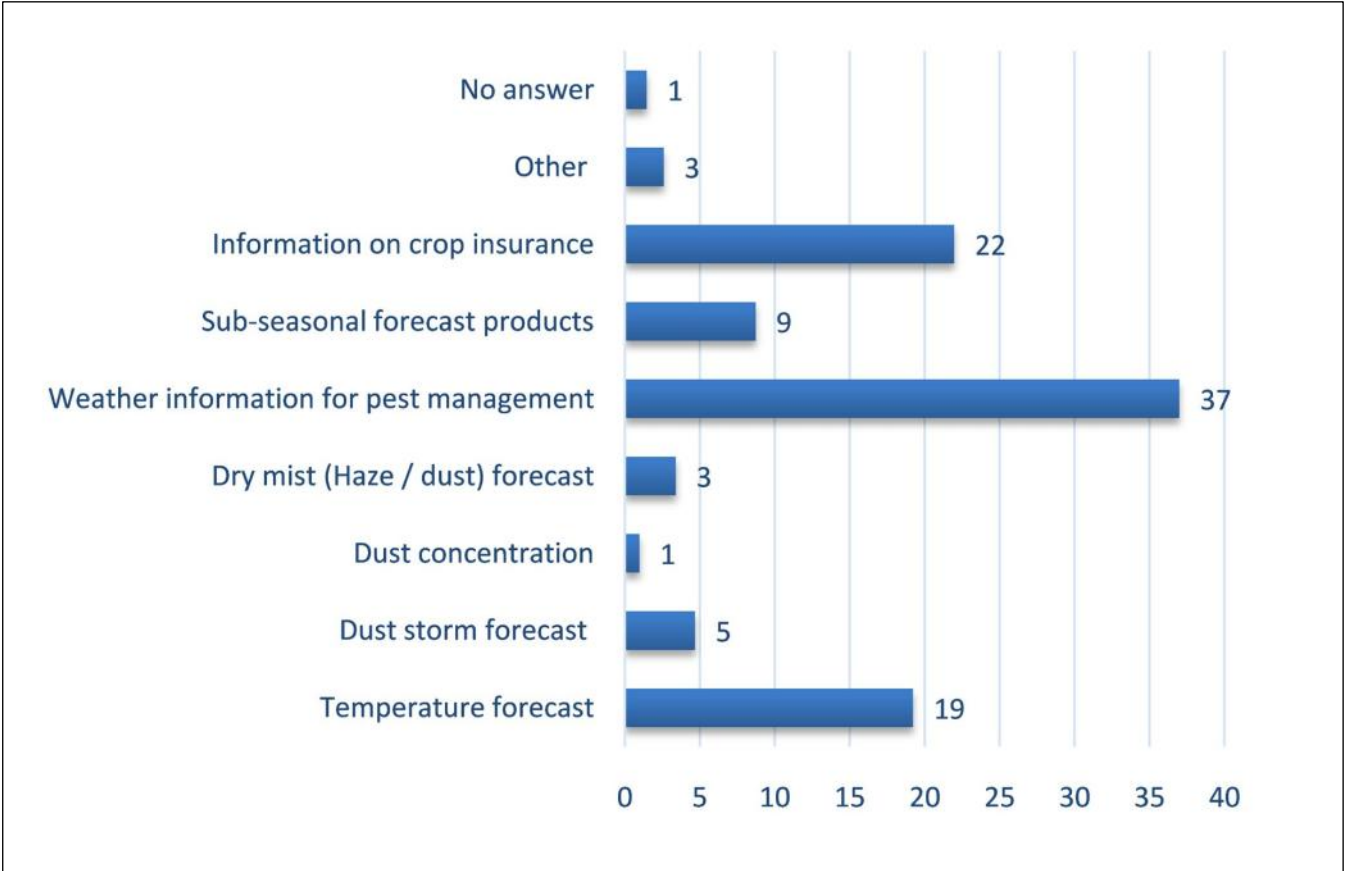


Figure 4.53. Additional climate services needed by farmers

4.3.2. Assessing the impacts of forecast information use on crop yield through on-farm demonstration trials

On-farm demonstration experiments were carried out in 12 villages located within three municipalities in Southwest Niger during the 2023 and 2024 growing seasons to evaluate the benefits related to the use of forecast information and recommendations in farmers' decision-making scheme. Five farmers in each of the villages were involved in the experiments. Three treatments (full application of forecast information and recommendations T_1 , application of seasonal forecast recommendations combined to farmers practices T_2 , and control treatment T_0 where only farmers practices were applied) were set up within each of the 60 experimental plots. Plate 4.1. shows the aspects of millet crops from the demonstration treatment (T_1) plot and the control treatment (T_0) plot at

Figure 4.54 shows the average millet grain yield over the three municipalities resulting from the 2023 and 2024 cropping season. Overall, from Figure 4.54a, we notice that the higher average yields were observed at Tounouga and there is a difference of millet yield across the treatments with higher average yield associated with T_1 . The higher yield average at Tounouga compared to the two other locations may be related to their localization. Indeed, Tounouga is located in the sudanian zone where the annual rainfall is greater than 800 mm whereas Guecheme and N'Dounga are in the Sahelian zone with annual rainfall varying between 500 to 600 mm. The better adaptability to the sudanian zone of the millet variety used can be one of the factors of this fact.

Figure 4.54b shows interannual variation of Yield at Guecheme and Tounouga. The decrease of yields observed at Guecheme in 2023 is related to an extended drought period that occurred in August that affected crops during the fructification phase, i.e. the crop high water-sensitive period. At Tounouga where the interannual variability of millet yield was high (Figure 4.55), persistent

flash flood events during the growing season were the primary factor contributing to the yield reduction in 2024. Many experimental plots experienced partial or complete flooding, resulting in low harvests in the affected areas of the fields. Figure 4.54b shows also that the difference of the average yields resulting from T_1 compared to T_2 and the two other treatments are more noticeable for Guecheme and N'Dounga than Tounouga leading to the suggestion that the forecast recommendations show more benefits in dryer conditions.

Analysis of variance was performed to test the statistical significance of the difference in mean yield across the three treatments. Table 4.12 shows the results of the ANOVA test performed after setting up the null hypothesis (H_0) as there is no difference in yield among treatments and the alternative hypothesis (H_1) set as at least one treatment leads to a statistically significant different yield. The ANOVA Table contains the Sum of Squares (SS) measuring the variability, the Degrees of Freedom (DF) giving the Number of independent values, the F-statistic showing the ratio of variance explained by treatment vs. unexplained variance and the p-value indicating the statistical significance between the yields from the 3 treatments. The F-statistic = 8,3478 indicating the ratio of variation between the treatment groups (T_0, T_1, T_2) compared to the variation within each group suggests that the differences between treatments are substantial, therefore the treatment effects on yield are strong. The p-value = 0.0003, less than 0.05, suggests also that the null hypothesis is rejected, meaning that at least one treatment leads to a statistically significant difference in yield.



Oumarou Harouna,
Daney Village, T₁
(demonstration plot)



Oumarou Harouna,
Daney Village, T₀
(control plot)

Plate 4. 1: Millet crops in experiment plot (left) and control plot (right) during *the* cropping cycle at Tounouga

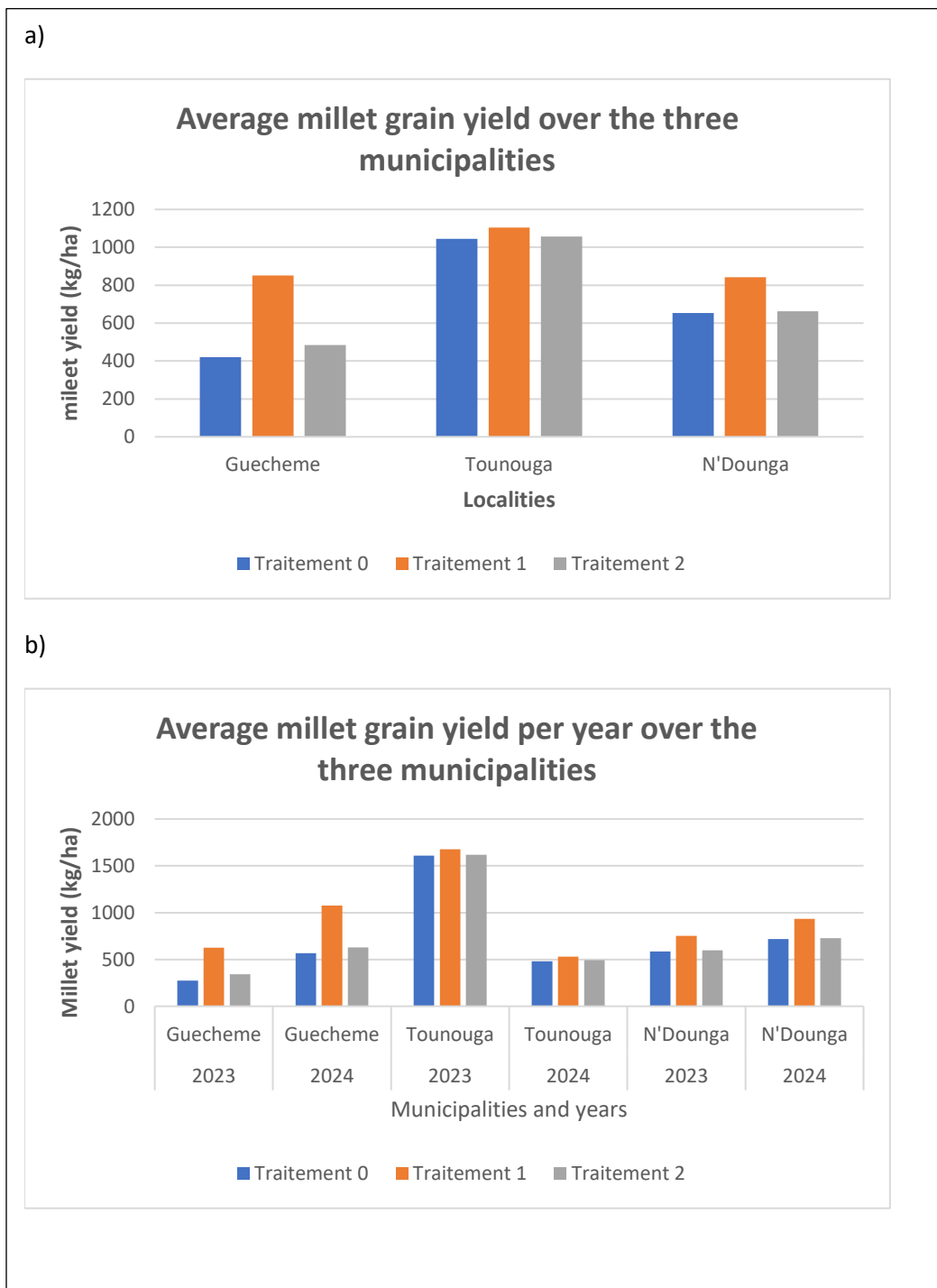


Figure 4.54. Average millet grain yield (kg/ha) a) per treatment and per municipality over the 2 years of experiments; b) per treatment, per year and per municipality

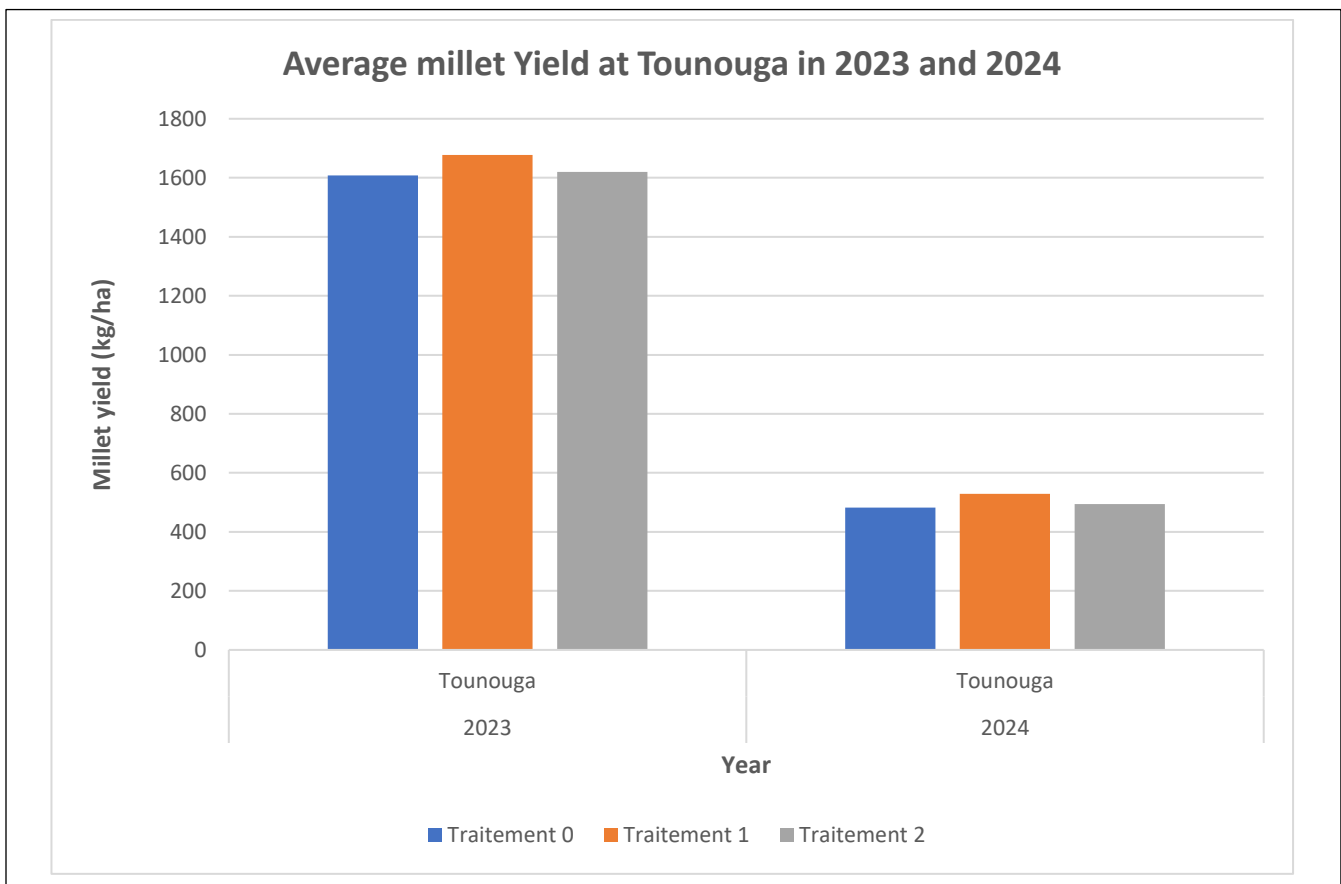


Figure 4. 55. Average millet yield (kg/ha) per treatment and per year at Tounouga

Table 4.12: ANOVA Table comparing the 3 treatments

	sum_sq (SS)	df	F ratio	Prob > F (p-value)
C(Treatment)	3734695	2	8,3478	0,0003
Residual	75831761	339		

To determine which specific treatments are significantly different from each other, the treatments were compared pairwise (i.e. T_1 vs T_0 , T_1 vs T_2 , and T_2 vs T_0) through Tukey's Honestly Significant Difference (HSD) test. The results of the Turkey HSD test are given in Table 4.13. It comes out from those results that T_1 comparison to T_0 , then to T_2 shows a significant increase in grain yield of 234 kg/ha (p-value = 0.0007) and of 205 kg/ha, respectively, compared to T_2 (p-value = 0.0032). However, the difference of average grain yield between T_2 and T_0 (+29 Kg/ha) is not significant as p-value = 0.89. Based on that, we can affirm that only the full adoption of forecast-based practices (T_1) leads to significantly better yields.

The interaction between treatment and location effects was analyzed using a multiple linear regression model including site effects as additional variable to the treatment. Figure 4.56, the boxplot comparing yield distributions across treatments and municipalities (Guecheme, Tounouga, N'Dounga) shows noticeable improvement in median yield under T_1 , with less variability than T_0 or T_2 at Guecheme. It shows also consistent yields across treatments; only minor benefit from T_1 at Tounouga. Additionally, the figure indicates high variability in all treatments, but highest median under T_1 at N'Dounga.

Based on that, it can be concluded that the impact of forecast use varies by location, with T_1 consistently providing higher or more stable yields, especially in Guecheme and N'Dounga.

Table 4. 13: Tukey HSD test results

Multiple Comparison of Means - Tukey HSD, FWER=0.05

```

=====
group1 group2  meandiff p-adj    lower    upper    reject
-----
      0      1   233.7817 0.0007    86.2886 381.2747   True
      0      2    28.5925 0.8925  -119.5348 176.7198  False
      1      2  -205.1891 0.0032  -352.0225 -58.3558   True
-----

```

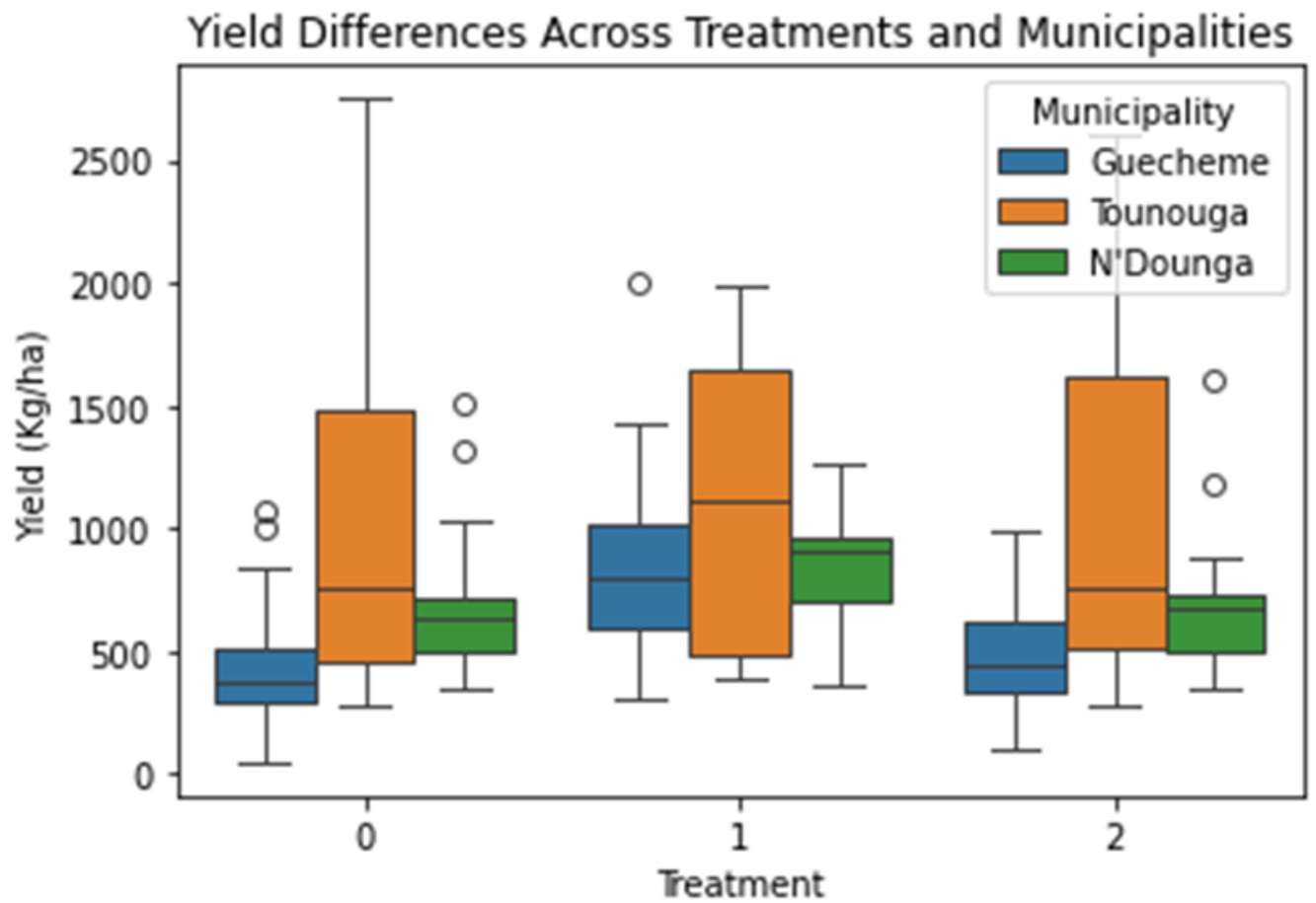


Figure 4.56. Yield Differences across treatments and municipalities, Guecheme (blue), Tounouga (orange) and N'Dounga (Green)

In summary, using seasonal forecast information significantly improves millet yield, especially when farmers fully adopt the recommended practices (T₁). Partial application of forecast recommendations or combination with traditional practices (T₂) does not yield significant improvement over the control treatment. The benefit of forecast use is location-dependent and is more obvious in dryer areas, confirming the importance and ability of seasonal forecast in helping farmers to adapt to constraining semi-arid climate. The location effects highlight the necessity of adapting forecast dissemination and support to local contexts.

4.4. General Discussion

This research aims to assess and improve the operational seasonal forecast production and use over Sahelian West Africa regarding key rainfall seasonal parameters which are onset date, cessation date and dry spell duration. Specifically, it focused on the assessment of the on-going forecasting system skills and performance, the investigation of eventual ways for improvements of the method, and the evaluation of the on-farm use of the forecast products. The evaluation built on a broader context of limited but growing research on intra-seasonal predictability over West Africa (Sultan et al., 2020; Rauch et al., 2019), and addresses critical gaps identified in WARCOF's verification processes (Mason and Chidzambwa, 2011; Bliefernicht et al., 2019; Pirret et al., 2020). The evaluation utilized a range of skill metrics and diagnostic tools, including Pearson correlation coefficients, Brier Scores, Hit Skill Scores (HSS), Reliability Diagrams, and ROC curves. The results provide valuable insights into the strengths and limitations of different predictor types and seasonal windows in forecasting key seasonal events. The performance of forecast products on the farm were assessed as well through field surveys and field experiments. The main findings from those various assessments are discussed in this section.

4.4.1. Forecast performance and predictability of season parameters

4.4.1.1. Current predictor and model performance

The evaluation of the statistical relationships between the current predictors used in the PRESASS forecasting system with the season parameters revealed overall moderate to weak correlation across the predictors based on the Pearson's correlation coefficients obtained from the cross validation as well as the retroactive validation.

The findings indicate that precipitation hindcasts generally yield better localized forecast skills than sea surface temperature (SST) anomalies, particularly for early-season variables like onset and early dry spells. Precipitation-based predictors, particularly from models such as NASA and CFSv2, demonstrated stronger skills for early season events like onset dates and early dry spells. This is likely due to their closer alignment with land-atmosphere processes as was reported by N'diaye (2010) for CFS coupled model which he found to have some skill for onset prediction for the southern Senegal; and mesoscale convective activity, which are not as well captured by broader SST patterns. These results align with those of Tarhule et al. (2009), N'Diaye (2010), Dunning et al. (2017), and Liu et al. (2021), who emphasized the importance of local and regional factors, land-atmosphere variables in driving local rainfall processes, especially in the Sahel, and in the onset of the West African monsoon.

In contrast, SST predictors, especially those from multi-model ensemble such as NMME, and high performing model like GFDL provided more consistent skill for later-season variables (cessation dates and dry spells) at broader spatial scales, echoing results from Barnston et al. (2010) and Rodrigues et al. (2014). This is also in line with literature highlighting the role of tropical Atlantic and Pacific SSTs in modulating late-season rainfall over West Africa (Fontaine et al., 2011; Rowell et al., 2001).

The use of multi-model ensembles also proved beneficial, often outperforming single-model forecasts by reducing biases and improving reliability. This finding supports the conclusions of Robertson et al. (2015) and Liu et al. (2021), who showed the advantages of ensemble systems in seasonal forecast calibration and skill enhancement.

4.4.1.2. Reliability and discrimination of forecasts

Reliability diagrams revealed that while some forecasts were well-calibrated, particularly for onset dates using SST anomalies from NASA, others exhibited overconfidence or underconfidence. Overconfident forecasts tend to overstate the likelihood of an event occurring, while underconfident forecasts are too conservative. In several cases, forecast sharpness (i.e., how confidently probabilities are issued) was limited, particularly for late season dry spells. These patterns reflect common challenges in seasonal climate forecasting, where trade-offs between sharpness and reliability often emerge (Wilks, 2011).

ROC curve analysis confirmed that onset forecasts had the best discrimination skill. However, forecasts for cessation dates and late-season dry spells showed weaker skills, with AUC values often close to 0.5, indicating performance near random chance. This finding suggests a need for refinement of late-season forecasting strategies, potentially through new predictors or enhanced regional calibration.

The study also reinforces Hansen et al. (2011) and Rauch et al. (2019) findings, who observed that WARCOF forecasts suffer from overgeneralization and lack of skill in probabilistically predicting near-normal outcomes.

4.4.2. Added value of potential new predictors: wet days frequency and cumulative rainfall

We also explored potential new predictor variables, such as wet-days frequency and cumulative rainfall over various time windows, which showed promising results, especially for onset forecasting. Wet-day frequencies in June and July were moderately correlated with onset dates, and their use as predictors led to more skillful and reliable forecasts than SST-based predictors in some cases. The ROC curve analysis confirmed that onset forecasts had the best discrimination skill ($AUC > 0.6$) when based on rainfall predictors or wet-day frequencies in June and July. This supports arguments by Laux et al. (2010) and Fall et al. (2021) advocating for the use of high-resolution and intra-seasonal indicators in forecast systems for rainfed agriculture. Similarly, cumulative rainfall totals for the AMJ (April–June) period showed strong correlation with observed onset dates, especially when derived from high-quality observational datasets like CHIRPS and GPCC. These findings resonate also with previous studies that highlight the usefulness of intra-seasonal indicators and antecedent conditions for sub-seasonal to seasonal forecasts (Nicholson, 2013; Marteau et al., 2009).

4.4.3. Forecast dissemination and user engagement for forecast information use

The third part of this research investigated how forecast information is disseminated, perceived, and used by farmers in Southwest Niger. This component provides valuable insights into the "last-mile" challenges of climate services in semi-arid agricultural systems in the context of climate change.

Consistent with previous studies (Roncoli et al., 2009; Tarhule & Lamb, 2003), survey findings show that only 42.3% of farmers received seasonal forecast information, with access disproportionately limited by education and other socio-economical impediments. The discussion

with farmers during the survey revealed that they could not access or use seasonal forecast information appropriately because of socio-economic impediments and inappropriate information dissemination ways as found by Roncoli et al. (2009) in Burkina Faso, Masesi et al. (2018) in semi-arid eastern Kenya, Alexander and Block (2022) highlighting the inability of limited resources farmers to invest in an ex-ante option integrating forecast information in decision-making, and Zagre et al. (2024) who found a statistically significant impact of socioeconomic and institutional factors on farmers' decisions to adopt Climate-Smart Technology (CST) in Senegal.

Our findings agree also with Nyoni et al. (2024), who highlighted the key role farmers' education play in awareness, access, use, value, and uptake characterizing the process of adoption of a climate information service. The low level of education of farmers is thus a major limiting factor to the use of the information as the probabilistic and complex aspect (Tall et al., 2014) and the dissemination format of the forecast, that remain inaccessible even for those who have a certain level of education. Based on that and as previously recommended by Sultan et al. (2020), our findings infer the need for more face-to-face information dissemination workshops and other capacity-building activities in advance before deploying a hybrid dissemination scheme to make the users understand the information provided and allow extensive use of forecast information.

Regarding the forecast dissemination means, the survey revealed that most farmers rely on radio (81%) for climate information, while roving seminars have limited diffusion due to ineffective information dissemination at larger scale and workshop participant selection, confirming challenges noted in Blench (1999), Roudier et al. (2014), Tarchiani et al. (2017), Seydou et al. (2023). However, Tall et al. (2014) reported that face-to face dialogue between farmers and experts is the comprehensive way to communicate complex seasonal climate information rather than media-based dissemination. An adequate information system involving climate services providers,

community radios and leaders, farmers, and relaying on new ITC would allow a timely diffusion of forecast information.

Despite these constraints, there is a high latent demand for climate services. Among those who received information, 93% used forecasts at least once, and 96% found it beneficial. These results support the findings of Hansen et al. (2011) and Roudier et al. (2014), who noted that farmers are more likely to use forecast information when it is timely, relevant, and linked to practical decisions.

Survey outcomes show that farmers are aware of choosing the optimum planting dates and the adequate crop and varieties based on the forecast of season onset and the cumulative rainfall. Those are important on-farm good practices to cope with the variability reported as well by Bojang et al. (2020) and Sivakumar et al. (1992). The farmers' preference for onset and seasonal total rainfall forecasts over cessation and dry spell forecasts reflects both the perceived immediacy of planting decisions and the limited capacity to respond to forecasts with longer lead times or uncertain outcomes. This prioritization aligns with Marteau et al. (2009) and Sivakumar (1988).

The disconnect between forecast availability and use is not merely technical, it is institutional and socio-economical. Recommendations by Hansen et al. (2019) and Rauch et al. (2019) to improve the downscaling, visualization, and framing of forecasts remain highly relevant. Participatory communication, simplified probabilistic framing, and integration into local knowledge systems are essential to enhance legitimacy and use.

Our study suggests that, improving farmers' access to credits and to adapted technologies such as improved varieties, fertilizers, mechanization and capacity building of all stakeholders may be good strategies to increase the adoption and application of seasonal forecasts in the on-farm decision-making process.

The two-year on-farm demonstration trials offer robust quantitative evidence that full adoption of forecast recommendations (T_1) leads to statistically significant yield gains (up to 234 kg/ha over traditional practice). Interestingly, yield gains were more pronounced in drier municipalities (Guéchémé and N'Dounga) than in Tounouga, a more humid zone. This suggests that forecast use may have greater marginal benefits under higher climate stress, emphasizing its potential in the context of climate adaptation. These results are consistent with studies such as Traore et al. (2017) and Ingram et al. (2002), which demonstrate that actionable climate information can improve productivity when farmers have the means and support to act on it.

Conversely, partial adoption (T_2) had no significant benefit over control, highlighting the importance of complete and confident application of forecast guidance for impact realization. This limited difference between T_0 and T_2 treatments also indicates that partial adoption or mixing traditional practices with forecast advice may dilute benefits, a pattern also noted by Roudier et al. (2012).

CHAPTER FIVE

CONCLUSIONS AND RECOMMENDATIONS

5.1. Conclusions

This dissertation explored three critical dimensions of seasonal climate forecasting in the West African Sahel: the scientific performance assessment of the PRESASS statistical forecasting system for predicting onset, cessation, and dry spells; the system calibration with potentials new predictors; and the real-world dissemination and application of this forecast information among smallholder farmers in Southwest Niger.

The technical analysis demonstrated that forecast resolution and skill remain uneven across regions, predictors, and lead times. The findings highlight that the PRESASS approach, while innovative in combining statistical and expert-based methods, still relies heavily on Sea Surface Temperature (SST) predictors, which are better suited for large-scale anomalies than local convective dynamics. Precipitation hindcasts, particularly those from the NASA and CFSv2 models, emerged as the most reliable predictors for onset dates and early-season dry spells, outperforming SST anomalies for localized forecasts. However, multi-model SST ensembles still showed relevance for broader-scale, late-season events such as cessation.

The study also identified wet-days frequency and April-May_June (AMJ) cumulative rainfall as promising alternative predictors that improved skill in onset forecasting when incorporated into statistical models. Improved performance may require other new predictors (e.g., soil moisture, vegetation indices) or enhanced downscaling approaches.

Forecast reliability and discrimination were highest for onset forecasts and generally weakest for late-season parameters, confirming the need for season-specific and location-specific forecast

optimization. Furthermore, the evaluation showed that post-processing and recalibration are needed for forecast elements with low discrimination skill, particularly cessation and late dry spells.

Parallel findings from the farmer survey and on-farm experiments revealed that forecast access and use remain limited despite high demand and perceived utility. Only 42.3% of surveyed farmers had access to forecast information, and usage depended strongly on education level and dissemination channel. Nonetheless, when forecast information was accessed and fully applied, it led to statistically significant increases in millet yields, particularly in drier municipalities such as Guéchémé and N'Dounga. This validates the practical value of forecasts for climate adaptation in vulnerable regions.

In summary, the findings illustrate that while the technical performance of seasonal forecasts is advancing, the value chain from prediction to use still faces gaps, particularly in communication, interpretation, and adoption. Bridging these gaps requires not only scientific improvements but also institutional and social innovation.

5.2. Recommendations

Based on the findings of this study, the following recommendations are proposed for enhancing both the performance and the impact of seasonal forecasts to the Sahelian Agriculture:

For Forecast system development and technical institutions (e.g., ACMAD, AGRHYMET):

- i) Prioritize precipitation-based predictors for onset and dry spell forecasting at national and subnational scales.
- ii) Integrate multi-model SST ensembles (e.g., NMME) for regional-scale cessation forecasts to increase robustness.

- iii) Incorporate new predictors such as wet-days frequency and AMJ rainfall totals into operational statistical forecasting tools (e.g., CPT).
- iv) Optimize forecast lead times by focusing on seasonal windows (June-July-August - JJA for early season; August-September-October - ASO for late season) with historically higher skill.
- v) Implement recalibration and post-processing protocols for low-skill forecasts, particularly cessation and late-season dry spells.

For Climate service providers and extension services:

- i) Scale up the use of integrated dissemination channels (radio, trusted local intermediaries, and mobile technologies and other ICT tools) to reach wider and more diverse farming populations at the last-miles.
- ii) Tailor communication strategies to literacy levels, cultural contexts, and local decision-making timelines to improve forecast comprehension and trust.
- iii) Invest in participatory training and demonstrations, especially in drier regions, to promote full adoption of forecast-based recommendations.
- iv) As the on-farm demonstration trials were implemented in limited area, further studies may consider extending this research to other agroclimatic zones of West Africa

For policymakers and agricultural development agencies:

- i) Institutionalize on-farm forecast impact monitoring, such as demonstration trials, to continuously refine forecast products and recommendations.
- ii) Prioritize investment in forecast-based agricultural planning tools, especially in semi-arid regions where climate risk is highest and forecast benefits are most pronounced.

- iii) Promote inclusive climate services that actively engage women, youth, and marginalized groups to ensure equitable access and benefit-sharing.

5.3. Contributions to Knowledge

This dissertation makes several original contributions to the interdisciplinary field of climate services and agricultural adaptation in West Africa:

Empirical evaluation of PRESASS forecast skill for onset, cessation, and dry spells

This study presents one of the first comprehensive empirical evaluations of PRESASS forecast performance using statistical verification metrics (Brier Score, ROC curves, Reliability Diagrams) for rainfall onset, cessation, and intra-seasonal dry spells across the Sahel. By disaggregating skill by predictor type, forecast window, and season parameter, the study provides granular evidence that precipitation-based predictors significantly outperform SST anomalies for early-season forecasts. This refines the current understanding of predictor-performance relationships in WARCOF systems and validates calls for recalibrated and parameter-specific forecast development.

Integration of new predictors into statistical forecasting workflows

The research introduces and tests wet-day frequency and cumulative rainfall totals as alternative predictors within CPT-based statistical forecasts—variables rarely used in operational settings. These predictors were shown to improve onset forecast skill and offer practical, observation-based solutions to the persistent issues of poor resolution and local relevance in WARCOF products. This offers a practical methodological innovation that can be adopted by national meteorological services and regional climate centers.

Quantitative evidence of forecast impact on Crop yield through on-farm experiments

Through a two-year on-farm trial, the study provides robust field-based evidence that the full adoption of seasonal forecast guidance significantly improves millet yield, particularly in drier municipalities. This is one of the few studies to move beyond simulation or perception-based assessments, offering quantified, statistically tested results on the real-world impact of forecast use. This strengthens the case for integrating climate services into agricultural decision-making frameworks and investment priorities.

Diagnosis of “Last-Mile” gaps in forecast dissemination and use

Building on primary survey data from over 600 farmers, this work documents the social, educational, and institutional barriers limiting forecast uptake in rural Niger. It confirms previous findings but advances the discourse by linking access and use rates with specific dissemination channels (radio vs. workshops), education levels, and forecast types preferred by farmers. These insights provide actionable evidence for designing more inclusive, equitable, and farmer-centered communication strategies.

Bridging technical forecast design and farmer decision-making needs

By combining forecast skill evaluation with user-level impact assessment, this study bridges the long-standing gap between forecast production and application. It demonstrates that forecast value is not simply a function of scientific accuracy, but also of accessibility, relevance, and context. This work therefore contributes to the co-evolution of climate science and local adaptation strategies, offering a blueprint for future transdisciplinary research on climate information services in developing regions.

5.4. Limitations, suggestions and implications for Further Studies

Forecast skill and predictors assessment

Despite the encouraging results for certain predictors and lead times, the overall forecast resolution and discrimination remained low, especially for cessation and late-season dry spells. The weak performance of these forecasts indicates limited added value over climatology and suggests that the current forecasting system would benefit from further improvements in predictor selection, spatial calibration, and lead-time optimization.

Future research could focus on:

- i) Incorporating land surface indicators (e.g., soil moisture, vegetation indices)
- ii) Testing the cumulative rainfall over some time windows as predictor for prediction of other season parameters (cessation and late season dry spells)
- iii) Applying advanced post-processing techniques (e.g., machine learning or Bayesian recalibration)
- iv) Increasing spatial patchiness to account for localized forecast variations

Additionally, collaboration with forecast users, such as farmers, planners, and disaster managers, may help align forecast design with practical decision-making needs, improving both relevance and uptake as recommended in WMO (2020) guidance on operational practices for objective seasonal forecasting.

Implications for Scaling forecast use

These findings have clear implications for scaling forecast use. The implications are:

- i) Effective dissemination must go beyond information access to include trust-building, training, and locally relevant framing.
- ii) Forecast services should be co-designed with farmers, incorporating their preferences while also communicating the benefits of less familiar forecast products (e.g., dry spells).

Differentiated strategies are required by location and user profile, recognizing that the same message may yield different outcomes depending on context and constraints.

REFERENCES

Adamou, R., Ibrahim, B., Bonkaney, A. L., Seyni, A. A., & Idrissa, M. (2021). Niger-Land, climate, energy, agriculture and development: A study in the Sudano-Sahel Initiative for Regional Development, Jobs, and Food Security.

AGRHYMET (2011). Prevision saisonniere des pluies et des debits des cours d'eau en Afrique de l'Ouest pour la saison des pluies 2011. Bulletin N° M01/2011.

<https://bibliocilss.pariis.net/files/original/13c5fb23d184644d382c8f1a05c17b064af39e74.pdf>

Alexander, S., & Block, P. (2022). Integration of seasonal precipitation forecast information into local-level agricultural decision-making using an agent-based model to support community adaptation. *Climate Risk Management*, 36, 100417.

<https://doi.org/10.1016/j.crm.2022.100417>

Bacci, M., Ousman Baoua, Y., & Tarchiani, V. (2020). Agrometeorological forecast for smallholder farmers: A powerful tool for weather-informed crops management in the Sahel. *Sustainability*, 12(8), 3246

Barnston, A. G., Li, S., Mason, S. J., DeWitt, D. G., Goddard, L., & Gong, X. (2010). Verification of the first 11 years of IRI's seasonal climate forecasts. *Journal of Applied Meteorology and Climatology*, 49(3), 493-520.

Bello, N. J. (1996). An investigation of the characteristics of the onset and cessation of the rains in Nigeria. *Theoretical and applied climatology*, 54, 161-173.

Blench, R. (1999). Seasonal climatic forecasting: who can use it and how should it be disseminated. *Natural resource perspectives*, 47(001). <https://hdl.handle.net/10535/3754>

Bliefernicht, J., Waongo, M., Salack, S., Seidel, J., Laux, P., & Kunstmann, H. (2019). Quality and value of seasonal precipitation forecasts issued by the West African regional climate outlook forum. *Journal of Applied Meteorology and Climatology*, 58(3), 621-642. <https://doi.org/10.1175/JAMC-D-18-0066.1>

Bojang, F., Traore, S., Togola, A., & Diallo, Y. (2020). Farmers perceptions about climate change, management practice and their on-farm adoption strategies at rice fields in Sapu and Kuntaur of the Gambia, West Africa. *American Journal of Climate Change*, 9(01), 1. <https://doi.org/10.4236/ajcc.2020.91001>

Cane, M. A., & Eshel, G. (1994). Forecasting Zimbabwean maize yield using eastern equatorial Pacific sea surface temperature. *Nature*, 370(6486).

Chiputwa, B., Blundo-Canto, G., Steward, P., Andrieu, N., & Ndiaye, O. (2022). Co-production, uptake of weather and climate services, and welfare impacts on farmers in Senegal: A panel data approach. *Agricultural Systems*, 195, 103309.

<https://doi.org/10.1016/j.agsy.2021.103309>

Daron, J., Allen, M., Bailey, M., Ciampi, L., Cornforth, R., Costella, C., ... & Ticehurst, H. (2021). Integrating seasonal climate forecasts into adaptive social protection in the Sahel. *Climate and Development*, 13(6), 543-550.

Delworth, T. L., Broccoli, A. J., Rosati, A., Stouffer, R. J., Balaji, V., Beesley, J. A., ... & Zhang, R. (2006). GFDL's CM2 global coupled climate models. Part I: Formulation and simulation characteristics. *Journal of Climate*, 19(5), 643-674.

Diallo, I., C. L. Bain, A. T. Gaye, W. Moufouma-Okia, C. Niang, M. D. B. Dieng, and R. Graham, 2014: Simulation of the West African monsoon onset using the HADGEM3-RA regional climate model. *J. Climate Dyn.*, 43, 575–594, doi:10.1007/s00382-014-2219-0

Diallo, I., Sylla, M. B., Camara, M., & Gaye, A. T. (2013). Interannual variability of rainfall over the Sahel based on multiple regional climate models simulations. *Theoretical and Applied Climatology*, 113, 351-362.

Dunning, C. M., Black, E. C., & Allan, R. P. (2016). The onset and cessation of seasonal rainfall over Africa. *Journal of Geophysical Research: Atmospheres*, 121(19), 11-405.

Fall, C. M. N., Lavaysse, C., Drame, M. S., Panthou, G., & Gaye, A. T. (2021). Wet and dry spells in Senegal: comparison of detection based on satellite products, reanalysis, and in situ estimates. *Natural Hazards and Earth System Sciences*, 21(3), 1051-1069.

Fitzpatrick, R. G., Bain, C. L., Knippertz, P., Marsham, J. H., & Parker, D. J. (2015). The West African monsoon onset: A concise comparison of definitions. *Journal of Climate*, 28(22), 8673-8694.

Fontaine, B., Gaetani, M., Ullmann, A., & Roucou, P. (2011). Time evolution of observed July–September Sea Surface Temperature-Sahel climate teleconnection with removed quasi-global effect (1900–2008). *Journal of Geophysical Research: Atmospheres*, 116(D4).

Gent, P. R., Danabasoglu, G., Donner, L. J., Holland, M. M., Hunke, E. C., Jayne, S. R., ... & Zhang, M. (2011). The community climate system model version 4. *Journal of climate*, 24(19), 4973-4991.

Glantz, M. (1977). The value of a long-range weather forecast for the West African Sahel. *Bulletin of the American Meteorological Society*, 58(2), 150-158. [https://doi.org/10.1175/1520-0477\(1977\)058<0150:TVOALR>2.0.CO;2](https://doi.org/10.1175/1520-0477(1977)058<0150:TVOALR>2.0.CO;2)

- Graef, F., & Stahr, K. (2000). Incidence of soil surface crust types in semi-arid Niger. *Soil and Tillage Research*, 55(3-4), 213-218.
- Graham, R., Colman, A., Vellinga, M., & Wallace, E. (2012). Use of dynamical seasonal forecasts in the consensus outlooks of African Regional Climate Outlook Forums (RCOFs). In *Proceedings of ECMWF Seminar on Seasonal Prediction* (pp. 237-256).
- Hansen, J. W., Mason, S. J., Sun, L., & Tall, A. (2011). Review of seasonal climate forecasting for agriculture in sub-Saharan Africa. *Experimental Agriculture*, 47(2), 205-240. <https://doi.org/10.1017/S0014479710000876>
- Hansen, J. (2015). Training workshop on communicating weather and climate information with farmers, Same, Tanzania, September 2013. In *CCAFS Workshop Report*.
- Hansen, J. W., Vaughan, C., Kagabo, D. M., Dinku, T., Carr, E. R., Körner, J., & Zougmore, R. B. (2019). Climate services can support African farmers' context-specific adaptation needs at scale. *Frontiers in Sustainable Food Systems*, 3, 21. <https://doi.org/10.3389/fsufs.2019.00021>
- Hansen J, Grossi A, Trzaska S, Dinku T, Baethgen W. 2022. Scaling Out the Next Generation of Seasonal Climate Forecasts in Africa. *AICCRA Info Note. Accelerating Impacts of CGIAR Climate Research for Africa (AICCRA)*. <https://hdl.handle.net/10568/125770>
- Hellmuth ME, Moorhead A, Thomson MC and Williams J (eds). 2007. *Climate Risk Management in Africa: Learning from Practice*. New York: International Research Institute for Climate and Society (IRI), Columbia University
- Hess, T.M., Stephens, W., & Mayrah, U.M. (1995). Rainfall trends in the north east arid zone of Nigeria. *Agricultural and Forest meteorology*, 74, 87-97
- Hurrell, J. W., Holland, M. M., Gent, P. R., Ghan, S., Kay, J. E., Kushner, P. J., ... & Marshall, S. (2013). The community earth system model: a framework for collaborative research. *Bulletin of the American Meteorological Society*, 94(9), 1339-1360.
- Ingram, K. T., Roncoli, M. C., & Kirshen, P. H. (2002). Opportunities and constraints for farmers of West Africa to use seasonal precipitation forecasts with Burkina Faso as a case study. *Agricultural systems*, 74(3), 331-349. [https://doi.org/10.1016/S0308-521X\(02\)00044-6](https://doi.org/10.1016/S0308-521X(02)00044-6)
- Institut National de la Statistique (INS). (2014). *Niger / répertoire national des localités (RENALOC)*. Niamey, Niger, 2014. <http://arks.princeton.edu/ark:/88435/dsp012227ms07n>
- Issoufou, W. S., Mahamane, A., & Ousseini, I. (2012). La Surveillance Ecologique et Environnementale au Niger: Un instrument d'aide à la décision. *Options Méditerranéennes. Sér. B. Etudes Rech*, 68, 219-230.

- Kharin, V. V., Boer, G. J., Merryfield, W. J., Scinocca, J. F., & Lee, W. S. (2012). Statistical adjustment of decadal predictions in a changing climate. *Geophysical Research Letters*, 39(19).
- Kumar, A., Ceron, J., Coelho, C., Ferranti, L., Graham, R., Jones, D., ... & Rodriguez, E. (2020). Guidance on operational practices for objective seasonal forecasting. World Meteorological Organization, WMO, (1246).
- Laux, P., Kunstmann, H., & Bárdossy, A. (2008). Predicting the regional onset of the rainy season in West Africa. *International Journal of Climatology: A Journal of the Royal Meteorological Society*, 28(3), 329-342. <https://doi.org/10.1002/joc.1542>
- Laux, P., Wagner, S., Wagner, A., Jacobeit, J., Bárdossy, A., & Kunstmann, H. (2009). Modelling daily precipitation features in the Volta Basin of West Africa. <https://doi.org/10.1002/joc.1852>
- Lu, J., & Delworth, T. L. (2005). Oceanic forcing of the late 20th century Sahel drought. *Geophysical Research Letters*, 32(22).
- Marteau, R., Moron, V., & Philippon, N. (2009). Spatial coherence of monsoon onset over western and central Sahel (1950–2000). *Journal of Climate*, 22(5), 1313-1324.
- Masesi, G. K., Wambugu, S. K., & Recha, C. W. (2018). Socio-economic factors influencing utilization of seasonal climate forecast among smallholder farmers in SemiArid Lower Eastern Kenya: A Case of Masinga Sub-County. *Journal of Environment and Earth Scienc*, 8.
- Mason, S. J. (2018). Guidance on verification of operational seasonal climate forecasts. WMO 1220, 81 pp.
- Mason, S., & Chidzambwa, S. (2009). Position paper: Verification of RCOF forecasts. IRI Tech. Rep. 09-02, 26 pp., <https://doi.org/10.7916/D85T3SB0>.
- Merryfield, W. J., Lee, W. S., Boer, G. J., Kharin, V. V., Scinocca, J. F., Flato, G. M., ... & Polavarapu, S. (2013). The Canadian seasonal to interannual prediction system. Part I: Models and initialization. *Monthly weather review*, 141(8), 2910-2945.
- Mertz, O., Mbow, C., Reenberg, A., & Diouf, A. (2009). Farmers' perceptions of climate change and agricultural adaptation strategies in rural Sahel. *Environmental management*, 43, 804-816.
- Moron, V., Robertson, A. W., Ward, M. N., & Camberlin, P. (2007). Spatial coherence of tropical rainfall at the regional scale. *Journal of Climate*, 20(21), 5244-5263.
- Moron, V., Lucero, A., Hilario, F., Lyon, B., Robertson, A. W., & DeWitt, D. (2009). Spatio-temporal variability and predictability of summer monsoon onset over the Philippines. *Climate dynamics*, 33, 1159-1177.

Mouhamed, L., Traore, S. B., Alhassane, A., & Sarr, B. (2013). Evolution of some observed climate extremes in the West African Sahel. *Weather and Climate Extremes*, 1, 19-25.

Ndiaye, O. (2010). The predictability of the Sahelian climate: seasonal Sahel rainfall and onset over Senegal. Columbia University.

Nicholson SE, Grist JP (2001) A conceptual model for understanding rainfall variability in the West African Sahel on interannual and interdecadal timescales. *Int J Climatol*. doi:10.1002/joc.648

Nicholson, S. E. (2013). The West African Sahel: A review of recent studies on the rainfall regime and its interannual variability. *International Scholarly Research Notices*, 2013(1), 453521

Nicholson, S. E. (2018). Climate of the Sahel and West Africa. In *Oxford research encyclopedia of climate science*.

Nyong, A., Adesina, F., & Osman Elasha, B. (2007). The value of indigenous knowledge in climate change mitigation and adaptation strategies in the African Sahel. *Mitigation and Adaptation Strategies for Global Change*, 12, 787-797.

Nyoni, R. S., Bruelle, G., Chikowo, R., & Andrieu, N. (2024). Targeting smallholder farmers for climate information services adoption in Africa: a systematic literature review. *Climate Services*, 34, 100450. <https://doi.org/10.1016/j.cliser.2024.100450>

Ogallo, L., Bessemoulin, P., Ceron, J. P., Mason, S. J., & Connor, S. J. (2008). Adapting to climate variability and change: the Climate Outlook Forum process.

Pirret, J. S., Daron, J. D., Bett, P. E., Fournier, N., & Foamouhoue, A. K. (2020). Assessing the skill and reliability of seasonal climate forecasts in Sahelian West Africa. *Weather and Forecasting*, 35(3), 1035-1050.

Rauch, M., Bliefernicht, J., Laux, P., Salack, S., Waongo, M., & Kunstmann, H. (2019). Seasonal forecasting of the onset of the rainy season in West Africa. *Atmosphere*, 10(9), 528.

Rienecker, M., Lim, Y. K., Infanti, J. M., Wood, E. F., Schubert, S. D., Merryfield, W. J., ... & Denis, B. (2013). The North American Multi-Model Ensemble (NMME): Phase-1 Seasonal to Interannual Prediction, Phase-2 Toward Developing Intra-Seasonal Prediction.

Roncoli, C., Jost, C., Kirshen, P., Sanon, M., Ingram, K. T., Woodin, M., ... & Hoogenboom, G. (2009). From accessing to assessing forecasts: an end-to-end study of participatory climate forecast dissemination in Burkina Faso (West Africa). *Climatic Change*, 92, 433-460. <https://doi.org/10.1007/s10584-008-9445-6>

Roudier, P., Sultan, B., Quirion, P., Baron, C., Alhassane, A., Traoré, S. B., & Muller, B. (2012). An ex-ante evaluation of the use of seasonal climate forecasts for millet growers in SW Ni-ger. *International Journal of Climatology*, 32, 759-771. <https://doi.org/10.1002/joc.2308>

- Roudier, P., Muller, B., d'Aquino, P., Roncoli, C., Soumaré, M. A., Batté, L., & Sultan, B. (2014). The role of climate forecasts in smallholder agriculture: Lessons from participatory re-research in two communities in Senegal. *Climate Risk Management*, 2, 42-55. <https://doi.org/10.1016/j.crm.2014.02.001>
- Rowell, D. P. (2001). Teleconnections between the tropical Pacific and the Sahel. *Quarterly Journal of the Royal Meteorological Society*, 127(575), 1683-1706
- Rowell, D. P. (2013). Simulating SST teleconnections to Africa: What is the state of the art?. *Journal of Climate*, 26(15), 5397-5418.
- Saha, S., Moorthi, S., Wu, X., Wang, J., Nadiga, S., Tripp, P., ... & Becker, E. (2014). The NCEP climate forecast system version 2. *Journal of climate*, 27(6), 2185-2208.
- Seydou, T. H., Agali, A., Aissatou, S., Seydou, T. B., Issaka, L., & Ibrahim, B. M. (2023). Evaluation of the impact of seasonal Agroclimatic information used for early warning and farmer communities' vulnerability reduction in southwestern Niger. *Climate*, 11(2), 31. <https://doi.org/10.3390/cli11020031>
- Siegmund, J., Bliedernicht, J., Laux, P., & Kunstmann, H. (2015). Toward a seasonal precipitation prediction system for West Africa: Performance of CFSv2 and high-resolution dynamical downscaling. *Journal of Geophysical Research: Atmospheres*, 120(15), 7316-7339.
- Sissoko, K., van Keulen, H., Verhagen, J., Tekken, V., & Battaglini, A. (2011). Agriculture, livelihoods and climate change in the West African Sahel. *Regional Environmental Change*, 11, 119-125.
- Sitta, A., Bré, S., Balogun, I. A., Laux, P., & Paeth, H. (2025). Dissemination and On-Farm Use of the Seasonal Forecast and Other Climate Services in Southwest Niger. *American Journal of Climate Change*, 14(2), 147-169.
- Sivakumar, M. V. K., 1988: Predicting rainy season potential from the onset of rains in southern Sahelian and Sudanian climatic zones of West Africa. *Agric. For. Meteorol.*, 42, 295–305.
- Sivakumar, M. V. K. (1992). Climate change and implications for agriculture in Niger. *Climatic change*, 20(4), 297-312. <https://doi.org/10.1007/BF00142424>
- Stern, R. D., Dennett, M. D., & Garbutt, D. J. (1981). The start of the rains in West Africa. *Journal of Climatology*, 1(1), 59-68.
- Sultan, B., Lejeune, Q., Menke, I., Maskell, G., Lee, K., Noblet, M., ... & Roudier, P. (2020). Current needs for climate services in West Africa: Results from two stakeholder surveys. *Climate Services*, 18, 100166. <https://doi.org/10.1016/j.cliser.2020.100166>

- Tall, A., Hansen, J., Jay, A., Campbell, B. M., Kinyangi, J., Aggarwal, P. K., & Zougmore, R. B. (2014). Scaling up climate services for farmers: Mission Possible. Learning from good practice in Africa and South Asia. CCAFS Report.
- Tarchiani, V., Camacho, J., Coulibaly, H., Rossi, F., & Stefanski, R. (2018). Agrometeorological services for smallholder farmers in West Africa. *Advances in Science and Research*, 15, 15-20. <https://doi.org/10.5194/asr-15-15-2018>
- Tarchiani, V., Rossi, F., Camacho, J., Stefanski, R., Mian, K. A., Pokperlaar, D. S., ... & Sitta Adamou, A. (2017). Smallholder Farmers Facing Climate Change in West Africa: Decision-Making between Innovation and Tradition 1. *Journal of Innovation Economics & Management*, (0), art13_I-art13_XXVI.Graef & Stahr., 2000. <https://doi.org/10.3917/jie.pr1.0013>
- Tarhule, A., & Lamb, P. J. (2003). Climate Research and Seasonal Forecasting for West Africans: Perceptions, Dissemination, and Use? Perceptions, Dissemination, and Use? *Bulletin of the American Meteorological Society*, 84(12), 1741-1760. <https://doi.org/10.1175/BAMS-84-12-1741>
- Tarhule, A., Saley-Bana, Z., & Lamb, P. J. (2009). Rainwatch: A prototype GIS for rainfall monitoring in West Africa. *Bulletin of the American Meteorological Society*, 90(11), 1607-1614.
- Tearfund (2008). A Review of Recent Trends and Projected Climate Change for Niger, West Africa. Tearfund, Teddington, UK.
- Tejada, J. J., & Punzalan, J. R. B. (2012). On the misuse of Slovin's formula. *The philippine statistician*, 61(1), 129-136.
- Traoré, P. C. S., Kouressy, M., Vaksmann, M., Tabo, R., Maikano, I., Traoré, S. B., & Cooper, P. (2007). Climate prediction and agriculture: What is different about Sudano-Sahelian West Africa?. In *Climate prediction and agriculture: Advances and challenges* (pp. 189-203). Berlin, Heidelberg: Springer Berlin Heidelberg. https://doi.org/10.1007/978-3-540-44650-7_19.
- Vecchi, G. A., Delworth, T., Gudgel, R., Kapnick, S., Rosati, A., Wittenberg, A. T., ... & Zhang, S. (2014). On the seasonal forecasting of regional tropical cyclone activity. *Journal of Climate*, 27(21), 7994-8016.
- Vellinga, M., Arribas, A., & Graham, R. (2013). Seasonal forecasts for regional onset of the West African monsoon. *Climate Dynamics*, 40, 3047-3070.
- Wanders, N., & Wood, E. F. (2018). Assessing seasonal climate forecasts over Africa to support decision-making. In *Bridging Science and Policy Implication for Managing Climate Extremes* (pp. 1-15).

Waongo, M., Laux, P., Traoré, S. B., Sanon, M., & Kunstmann, H. (2014). A crop model and fuzzy rule based approach for optimizing maize planting dates in Burkina Faso, West Africa. *Journal of Applied Meteorology and Climatology*, 53(3), 598-613.

Wezel, A., & Haigis, J. (2002). Fallow cultivation system and farmers' resource management in Niger, West Africa. *Land Degradation and Development*, 13(3), 221-231. <https://doi.org/10.1002/ldr.499>

Wilks, D. S. (2011). *Statistical methods in the atmospheric sciences* (Vol. 100). Academic press.

Wood, S. A., Jina, A. S., Jain, M., Kristjanson, P., & DeFries, R. S. (2014). Smallholder farmer cropping decisions related to climate variability across multiple regions. *Global Environmental Change*, 25, 163-172. <https://doi.org/10.1016/j.gloenvcha.2013.12.011>

World Meteorological Organization (WMO). (2020). *Guidance on operational practices for objective seasonal forecasting*.

Zagre, I., Akinseye, F. M., Worou, O. N., Kone, M., & Faye, A. (2024). Climate change adaptation strategies among smallholder farmers in Senegal's semi-arid zone: role of socio-economic factors and institutional supports. *Frontiers in Climate*, 6, 1332196. <https://doi.org/10.3389/fclim.2024.1332196>

APPENDICES

Appendix A: Field Survey questionnaire

Survey questionnaire: Collection of information to establish the baseline situation regarding the communication and use of the seasonal forecasts and other agrometeorological advices by farmers in the study area

Version: 3 – Date 25/10/2022

Identification

Q1 Questionnaire number

Q2 Country: ____

Q3 Region: ____

Q4 Commune: ____

Q5 Village: ____

Q6 Name and surname of respondent ____

Socio-demographic characteristics

Q7 Sex of respondent: ____

Q8 Age of respondent: ____

Q9 Respondent's level of education:

- 9.1. Quranic
- 9.2. Primary not completed
- 9.3. Primary completed
- 9.4. Secondary not completed
- 9.5. Secondary Completed
- 9.6. High School
- 9.7. Bachelor
- 9.8. Masters or higher
- 9.9. Other (specify)

Q10 Name of the investigator: ____

Q11 Main crop (1=millet 2=sorghum 3=maize 4=wheat 5=cowpea 6=groundnut 7=rice 8=sesame 9=voandzou 99=other (please specify): ____

Q12 Area under the main crop: ___

Q13 Date of first sowing: _____ Q13 Date of last sowing (successful): _____

Q14 Number of sowing events: ___

Q15 Did you use the data from the farmer's rain gauge provided by the National Meteorological Service?
Yes/No

15.1. = YES 15.2=NO

Q16 If yes for which activity(ies)?

- 16.1. Field preparation
- 16.2 Sowing
- 16.3. Weeding
- 16.4. Application of fertilizers
- 16.5. Application of pesticides
- 16.6. Other (specify):

Q17 Do you receive agrometeorological information provided by the Meteorological Service during the cropping season?

YES NO (if NO, please proceed to Q28)

Q18 If yes, which ones?

- 19.1. Seasonal forecast
- 19.2. 10 days agrometeorological forecast
- 19.3. Daily weather forecast broadcast
- 19.4. Advices
- 19.5. Dekadal bulletins
- 19.6. Other (specify)

Q19 If, YES, how did you receive the information? (Several choices possible)

- 20.1. Television
- 20.2. Radio
- 20.3. Village chief
- 20.4. local agricultural extension agent
- 20.5. Seasonal forecast restitution workshop/s
- Sms / whatsapp messages
- 20.6. Others, please specify....

Q20 Do you find the information provided useful and relevant? How useful are those information

YES NO

Yes, NO why? _____

(1) Not useful at all (2) Not useful (3) Fairly Useful (4) Useful

(5) Very useful

Justify: _____

Q21 Did you use the information you received for your activities implementation? At what level ?

YES NO

(1) Very low utilization (2) Low utilization (3) Fairly utilization (4) High Utilization

(5) Very high utilization

Q22 If YES, in which activity did you use the information?

- 23.1. Field preparation
- 23.2. Seeds Choice which seed?
- 23.3. Choice of sowing date
- 23.4. Weeding
- 23.5. Application of fertilizers
- 23.6. Pesticides
- 23.7. Other, _____

Q23. Do you think that the information received has been beneficial to your activities?

Yes / No

If yes:

- 23.1. It allowed me to produce more
- 23.2. It allowed me to reduce the risk
- 23.3. It has allowed me to reduce costs
- 23.4. It makes the farming business more encouraging
- 23.4. Other _____

Q24. What information do you consider most useful? Rank the information according to their importance in your point of view

- 24.1. Seasonal forecast
- 24.2. Daily weather forecast
- 24.3. 10 days Forecast

- 24.4. Market prices
- 24.5. crops status
- 24.6. rangelands and livestock status
- 24.7. Advices
- 24.8. Other, specify....

Q25. Which of the information related to the seasonal forecast do you consider most useful for your agricultural activities? Rank them by importance

- 25.1. Cumulative rainfall
- 25.2. Season onset dates
- 25.2. Early season dry spells
- 25.3. End-of-season dry spells
- 25.4. Season cessation dates

Q26 What other types of weather forecasts or information do you want to get in addition? Give multiple choice answers (temperature forecast for instance, sub-seasonal forecast products (explain what are those products in local language), add other (specify)

- 26.1. Temperature forecast
- 26.2. Dust storm forecast
- 26.3. Dust concentration
- 26.4. Mist forecast (dust mist, dry mist)
- 26.5. Weather information for pest management
- 26.6. Sub-seasonal to seasonal forecast products
- 26.7. Information on climate insurance
- 26.8. Other (please spicify) _____

Q27 According to your perception, how was the onset of the rainy season in your village this year?

- 27.1. Normal
- 27.2. Early
- 27.3. Delayed
- 27.4. Do not know

Q28 According to your perception, how was the end of the rainy season in your village this year?

- 28.1. Normal
- 28.2. Early
- 28.3. Delayed
- 28.4. Do not know

Q29 Did you observe dry spells in your area at the beginning of this season?

YES NO Do not know

If yes, were they for duration:

29.1. Normal

29.2. Short

29.3. Long

29.4. Do not know

Q30 Did you observe dry spells in your area in the middle of this season?

YES NO Do not know

If yes, were they for duration:

30.1. Normal?

30.2. Short?

30.3. Long?

30.4. Do not know

Q31 Did you observe dry spells in your area at the end of this season (before the maturity of crops)?

YES NO

If yes, were they for duration:

31.1. Normal?

31.2. Short?

31.3. Long?

31.4. Do not know

Q32 Among the agrometeorological/climate information produced and disseminated, which one (s) would you like to receive before and during the cropping season for your activities (in order of preference)?

Q33 What is the fastest and best adapted way to get the information to you?

- 33.1. Television
 - 33.2. Radio preferred transmission times.....
 - 33.3. Village chief
 - 33.4. local agricultural extension agent
 - 33.5. Workshop/seminar to report on the results of the seasonal forecast
 - 33.6. SMS or WhatsApp messages
 - 33.7. Other ... specify....
-

Q34 What are the major difficulties you have encountered during this cropping season?

- 34.1. Sowing failures
- 34.2. Drought events
- 34.3. Flooding
- 34.4. Crop pest attacks
- 34.5. Crop diseases
- 34.6. Early cessation of rainfall
- 34.7. Strong winds
- 34.8. No difficulty
- 34.9. Other:

Q35 How was your crop yield for this campaign?

- 35.1. Exceptional
- 35.2. Satisfactory
- 35.3. Normal
- 35.4. Low
- 35.5. Very low

Q36 Explain the reasons for success or failure

Q37 Do you know the yield and surface area of your fields?

1=YES 2=NO

Q38 If, YES, approximatively, what is the size of your cropped area this year? __ HA

Q39 If, YES, how many Kg do you estimate your production this year? _____ KG /Bundles (to be converted in KG/HA)

Appendix B: Experiments data collection forms

Appendix B1: Farmers and plots identification form

ESSAI DE DEMONSTRATION DE L'UTILISATION DES PREVISIONS SAISONNIERES EN MILIEU PAYSAN

FICHE D'IDENTIFICATION DES PARCELLES SUIVIES EN MILIEU PAYSAN

(A remplir pour chaque parcelle)

(Choisissez de préférence une parcelle individuelle gérée par le paysan pilote)

Commune : _____ Site/Village : _____		Année : __2023__	
Parcelle N°: _____		Superficie parcelle : _____ Nom du Paysan : _____	
Age Paysan : _____		Genre Paysan : _____ Nombre de personnes dans le ménage du Paysan _____	
Traitement 1: ___ Prévisions saisonnières et application du paquet technologique complet			
Culture principale : _____		Culture associée : _____	
Nom de la variété : _____		_____	
Source de la variété : _____		_____	
Durée de cycle : <input type="checkbox"/> Précoce (<90 jours)		<input type="checkbox"/> Précoce (<90 jours)	
<input type="checkbox"/> Intermédiaire (90-120 jours)		<input type="checkbox"/> Intermédiaire (90-120 jours)	
<input type="checkbox"/> Tardive (> 120 jours)		<input type="checkbox"/> Tardive (> 120 jours)	
<input type="checkbox"/> Photopériodique		<input type="checkbox"/> Photopériodique	
Type de Sol:			
Profondeur : <input type="checkbox"/> Profond		<input type="checkbox"/> peu profond	
Texture :			
<input type="checkbox"/> rocailleuse;			
<input type="checkbox"/> sableuse ;			
<input type="checkbox"/> sablo-argileuse ;			
<input type="checkbox"/> argileuse;			
Topographie :		Travail du sol	
<input type="checkbox"/> terrain plat		<input type="checkbox"/> Aucun	
<input type="checkbox"/> haut de pente		<input type="checkbox"/> Grattage simple	
<input type="checkbox"/> milieu de pente		<input type="checkbox"/> Labour à plat	
<input type="checkbox"/> bas de pente		<input type="checkbox"/> Billonnage	
Fumure		Dose (kg/ha)	
<input type="checkbox"/> Aucune		_____	
<input type="checkbox"/> Parcage		_____	
<input type="checkbox"/> Fumier		_____	
<input type="checkbox"/> Compost		_____	
<input type="checkbox"/> NPK		_____	
<input type="checkbox"/> Phosphate naturel		_____	
<input type="checkbox"/> Urée		_____	
<input type="checkbox"/> Autre		_____	
		Date d'apport	
		____/____/____	
		____/____/____	
		____/____/____	
		____/____/____	
		____/____/____	
		____/____/____	
Semis			
Culture principale		Date	
Type		Densité : 1 2 3	
<input type="checkbox"/> En humide		____/____/____	
<input type="checkbox"/> Ressemis		____/____/____	
		Distance 11 poquets _____/_____/_____	
		Nbre plants 10 poquets _____/_____/_____	
Culture secondaire		1 2 3	
<input type="checkbox"/> A sec		____/____/____	
<input type="checkbox"/> En humide		____/____/____	
<input type="checkbox"/> Ressemis		____/____/____	
		Distance 6 lignes _____/_____/_____	
		Distance 6 poquets _____/_____/_____	
		Nbre plants 5 poquets _____/_____/_____	

Commune : _____ Site/Village : _____ Année : 2023

Parcelle N°: _____ Superficie parcelle : _____ Nom Paysan : _____

Age Paysan : _____ Genre Paysan : _____ Nombre de personnes dans le ménage du Paysan _____

Traitement 2: Prévisions saisonnières combinées avec pratiques paysannes

Culture principale : _____ Culture associée : _____

Nom de la variété : _____

Source de la variété : _____

Durée de cycle : Précoce (<90 jours) Intermédiaire (90-120 jours) Tardive (> 120 jours) Photopériodique

Précoce (<90 jours) Intermédiaire (90-120 jours) Tardive (> 120 jours) Photopériodique

Type de Sol:

Profondeur : Profond peu profond

Texture : rocailleuse; sableuse ; sablo-argileuse ; argileuse;

Topographie : terrain plat haut de pente milieu de pente bas de pente

Travail du sol
 Aucun Grattage simple Labour à plat Billonnage

Fumure	Dose (kg/ha)	Date d'apport
<input type="checkbox"/> Aucune	_____	____/____/____
<input type="checkbox"/> Parcage	_____	____/____/____
<input type="checkbox"/> Fumier	_____	____/____/____
<input type="checkbox"/> Compost	_____	____/____/____
<input type="checkbox"/> NPK	_____	____/____/____
<input type="checkbox"/> Phosphate naturel	_____	____/____/____
<input type="checkbox"/> Urée	_____	____/____/____
<input type="checkbox"/> Autre	_____	____/____/____

Semis

Culture principale	Date	Densité :	1	2	3
<input type="checkbox"/> A sec	____/____/____	Distance 11 lignes	____/____/____		
<input type="checkbox"/> En humide	____/____/____	Distance 11 poquets	____/____/____		
<input type="checkbox"/> Ressemis	____/____/____	Nbre plants 10 poquets	____/____/____		
Culture secondaire			1	2	3
<input type="checkbox"/> A sec	____/____/____	Distance 6 lignes	____/____/____		
<input type="checkbox"/> En humide	____/____/____	Distance 6 poquets	____/____/____		
<input type="checkbox"/> Ressemis	____/____/____	Nbre plants 5 poquets	____/____/____		

Commune : _____ Site/Village : _____ Année : 2023

Parcelle N°: _____ Superficie parcelle : _____ Nom Paysan : _____

Age Paysan : _____ Genre Paysan : _____ Nombre de personnes dans le ménage du Paysan _____

Traitement 0: Pratiques paysannes

Culture principale : _____ Culture associée : _____

Nom de la variété : _____

Source de la variété : _____

Durée de cycle : Précoce (<90 jours) Intermédiaire (90-120 jours) Tardive (> 120 jours) Photopériodique

Précoce (<90 jours) Intermédiaire (90-120 jours) Tardive (> 120 jours) Photopériodique

Type de Sol:

Profondeur : Profond peu profond

Texture : rocailleuse; sableuse ; sablo-argileuse ; argileuse;

Topographie : terrain plat haut de pente milieu de pente bas de pente

Travail du sol Aucun Grattage simple Labour à plat Billonnage

Fumure	Dose (kg/ha)	Date d'apport
<input type="checkbox"/> Aucune	_____	____/____/____
<input type="checkbox"/> Parcage	_____	____/____/____
<input type="checkbox"/> Fumier	_____	____/____/____
<input type="checkbox"/> Compost	_____	____/____/____
<input type="checkbox"/> NPK	_____	____/____/____
<input type="checkbox"/> Phosphate naturel	_____	____/____/____
<input type="checkbox"/> Urée	_____	____/____/____
<input type="checkbox"/> Autre	_____	____/____/____

Semis

Culture principale	Date	Densité :	1	2	3
Type					
<input type="checkbox"/> A sec	____/____/____	Distance 11 lignes	____/____/____		
<input type="checkbox"/> En humide	____/____/____	Distance 11 poquets	____/____/____		
<input type="checkbox"/> Ressemis	____/____/____	Nbre plants 10 poquets	____/____/____		
Culture secondaire			1	2	3
<input type="checkbox"/> A sec	____/____/____	Distance 6 lignes	____/____/____		
<input type="checkbox"/> En humide	____/____/____	Distance 6 poquets	____/____/____		
<input type="checkbox"/> Ressemis	____/____/____	Nbre plants 5 poquets	____/____/____		



Appendix B3: Cropping activities monitoring form

ESSAI DE DEMONSTRATION DE L'UTILISATION DES PREVISIONS SAISONNIERES EN MILIEU PAYSAN

Fiche de suivi des opérations culturales

Année _____ N° Parcelle _____ Commune _____ Site/Village _____

Nom paysan _____ Nom Observateur _____

Traitement	Activité	Nombre	Date	Méthode / produits utilisés
	Préparation des sols	1		
	Semis	1		
	Traitement des semences au fongicide	1		
	Ressemis	1er		
		2eme		
		3eme		
	Démariage	1		
	Sarclage	1er		
		2eme		
	Fertilisation	1er		
		2eme		
		3eme		
	Traitement phytosanitaire	1er		
		2eme		
		3eme		
	Autres opérations	1er		
		2eme		
		3eme		

Autres observtaions _____

Appendix B4: Yield data collection form

ESSAI DE DEMONSTRATION DE L'UTILISATION DES PREVISIONS SAISONNIERES EN MILIEU PAYSAN																						
ANNEE 2023																						
Fiche d'évaluation des rendements des cultures																						
Pays:										Village: Nom observateur:												
Commune:										N° Parcelle												
Culture principale : (Mil)										Culture associée :												
N° Traitement	Date de récolte	N° Carré	Nombre de poquets	Nombre d'épis	Poids frais épis (kg)	Poids frais pailles (kg)	Poids sec épis (kg)	Poids sec pailles (kg)	Poids sec grains (kg)	Poids 1000 grains (kg)	N° Traitement	Date de récolte	N° Carré	Nombre de poquets	Nombre d'épis de sorgho / de gousses de niébé ou	Poids frais épis / gousses (kg)	Poids frais pailles / fanes (kg)	Poids sec épis / gousses (kg)	Poids sec pailles / fanes (kg)	Poids sec grains	Poids 1000 grains (kg)	
		1											1									
		2											2									
		3											3									
		1											1									
		2											2									
		3											3									
		1											1									
		2											2									
		3											3									

Appendix C: Goodness indices from the cross-validation regressions runs using CPT

Modele April initialized	GCM output Achronyme (hindcast)	Predictor X	GCM output lead time	Domain used for prediction	Predictand Y	Goodness index
nasa	nasa_sst_hcst_Apric_7_1991	SST	July	4	Onset date	-0,432
cfsv2	cfsv2_precip_hcst_Apric_7_1991	precip	July	7	Onset date	-0,432
nasa	nasa_sst_hcst_Apric_6-8_1991-2020	SST	JJA	4	Onset date	-0,431
cfsv2	cfsv2_sst_hcst_Apric_5_1991	SST	May	5	Onset date	-0,430
cmc1	cmc1_sst_hcst_Apric_6-8_1991-2020	SST	JJA	6	Onset date	-0,429
nasa	nasa_sst_hcst_Apric_5_1991	SST	May	5	Onset date	-0,427
cfsv2	cfsv2_sst_hcst_Apric_5_1991	SST	May	6	Onset date	-0,425
cfsv2	cfsv2_sst_hcst_Apric_6_1991	SST	June	6	Onset date	-0,425
nasa	nasa_sst_hcst_Apric_6_1991	SST	June	5	Onset date	-0,425
cfsv2	cfsv2_sst_hcst_Apric_5-7_1991-2020	SST	MJJ	6	Onset date	-0,424
nasa	nasa_sst_hcst_Apric_5-7_1991-2020	SST	MJJ	5	Onset date	-0,424
ncar_ccsm4	ncar_ccsm4_precip_hcst_Apric_7_1991	precip	July	7	Onset date	-0,424
nasa	nasa_sst_hcst_Apric_6_1991	SST	June	3	ESDS	-0,489
cmc1	cmc1_sst_hcst_Apric_6-8_1991-2020	SST	JJA	6	ESDS	-0,441
nasa	nasa_precip_hcst_Apric_7_1991	precip	July	7	ESDS	-0,439
nasa	nasa_sst_hcst_Apric_6-8_1991-2020	SST	JJA	6	ESDS	-0,438
cmc2	cmc2_precip_hcst_Apric_5_1991	precip	May	7	ESDS	-0,438
gfdl	gfdl_sst_hcst_Apric_7_1991	SST	July	4	ESDS	-0,437
cmc1	cmc1_sst_hcst_Apric_6-8_1991-2020	SST	JJA	4	ESDS	-0,436
gfdl	gfdl_sst_hcst_Apric_6-8_1991-2020	SST	JJA	4	ESDS	-0,436
cmc1	cmc1_sst_hcst_Apric_5-7_1991-2020	SST	MJJ	6	ESDS	-0,435
nasa	nasa_sst_hcst_Apric_5-7_1991-2020	SST	MJJ	6	ESDS	-0,435
nasa	nasa_sst_hcst_Apric_6-8_1991-2020	SST	JJA	3	ESDS	-0,435
nasa	nasa_sst_hcst_Apric_6_1991	SST	June	5	ESDS	-0,435
nasa	nasa_precip_hcst_Apric_9-11_1991-2020	precip	SON	7	Cessation date	-0,473
cmc1	cmc1_sst_hcst_Apric_8_1991	SST	Aug	3	Cessation date	-0,469

nmme	nmme_sst_hcst_Apric_8-10_1991-2020	SST	ASO	4	Cessation date	-0,465
cmc2	cmc2_sst_hcst_Apric_8_1991	SST	Aug	3	Cessation date	-0,465
cmc1	cmc1_sst_hcst_Apric_7-9_1991-2020	SST	JAS	3	Cessation date	-0,464
nmme	nmme_sst_hcst_Apric_9-11_1991-2020	SST	SON	5	Cessation date	-0,464
cmc1	cmc1_sst_hcst_Apric_9_1991	SST	Sept	3	Cessation date	-0,463
cmc2	cmc2_sst_hcst_Apric_7-9_1991-2020	SST	JAS	3	Cessation date	-0,462
nmme	nmme_sst_hcst_Apric_9_1991	SST	Sept	4	Cessation date	-0,460
cmc2	cmc2_precip_hcst_Apric_8_1991	precip	Aug	7	Cessation date	-0,459
cfsv2	cfsv2_sst_hcst_Apric_9-11_1991-2020	SST	SON	4	Cessation date	-0,457
cmc2	cmc2_sst_hcst_Apric_9_1991	SST	Sept	3	Cessation date	-0,457
nmme	nmme_sst_hcst_Apric_9_1991	SST	Sept	5	Cessation date	-0,455
nmme	nmme_sst_hcst_Apric_10_1991	SST	Oct	5	Cessation date	-0,455
nmme	nmme_sst_hcst_Apric_7-9_1991-2020	SST	JAS	4	Cessation date	-0,453
nmme	nmme_sst_hcst_Apric_7-9_1991-2020	SST	JAS	5	Cessation date	-0,453
nmme	nmme_sst_hcst_Apric_8-10_1991-2020	SST	ASO	5	Cessation date	-0,453
gfdl	gfdl_sst_hcst_Apric_8_1991	SST	Aug	5	Cessation date	-0,451
gfdl	gfdl_sst_hcst_Apric_7-9_1991-2020	SST	JAS	5	LSDS	-0,446
nmme	nmme_sst_hcst_Apric_7-9_1991-2020	SST	JAS	3	LSDS	-0,444
cfsv2	cfsv2_sst_hcst_Apric_9_1991	SST	Sept	5	LSDS	-0,442
cfsv2	cfsv2_sst_hcst_Apric_8_1991	SST	Aug	1	LSDS	-0,428
ncar_ccsm4	ncar_ccsm4_sst_hcst_Apric_8_1991	SST	Aug	3	LSDS	-0,427
nasa	nasa_precip_hcst_Apric_10_1991	precip	Oct	7	LSDS	-0,427
cfsv2	cfsv2_sst_hcst_Apric_8-10_1991-2020	SST	ASO	3	LSDS	-0,426
cmc1	cmc1_sst_hcst_Apric_7-9_1991-2020	SST	JAS	3	LSDS	-0,426
cfsv2	cfsv2_sst_hcst_Apric_10_1991	SST	Oct	3	LSDS	-0,426
cmc1	cmc1_sst_hcst_Apric_8_1991	SST	Aug	3	LSDS	-0,426
nasa	nasa_sst_hcst_Apric_9_1991	SST	Sept	4	LSDS	-0,426
nasa	nasa_sst_hcst_Apric_10_1991	SST	Oct	3	LSDS	-0,426
nasa	nasa_precip_hcst_Apric_7-9_1991-2020	precip	JAS	7	LSDS	-0,426
cfsv2	cfsv2_sst_hcst_Apric_8_1991	SST	Aug	2	LSDS	-0,425
cmc1	cmc1_sst_hcst_Apric_9_1991	SST	Sept	3	LSDS	-0,425

nasa	nasa_sst_hcst_Apric_8_1991	SST	Aug	5	LSDS	-0,425
ncar_ccsm4	ncar_ccsm4_sst_hcst_Apric_9_1991	SST	Sept	3	LSDS	-0,425
nasa	nasa_precip_hcst_Apric_9_1991	precip	Sept	7	LSDS	-0,425
gfdl	gfdl_sst_hcst_Apric_6_1991	SST	June	6	Onset date	-0,423
ncar_ccsm4	ncar_ccsm4_precip_hcst_Apric_6_1991	precip	June	7	Onset date	-0,423
nasa	nasa_sst_hcst_Apric_6-8_1991-2020	SST	JJA	6	Onset date	-0,422
nmme	nmme_sst_hcst_Apric_6-8_1991-2020	SST	JJA	6	Onset date	-0,422
cfsv2	cfsv2_sst_hcst_Apric_7_1991	SST	July	6	Onset date	-0,422
cfsv2	cfsv2_precip_hcst_Apric_5-7_1991-2020	precip	MJJ	7	Onset date	-0,422
gfdl	gfdl_sst_hcst_Apric_6-8_1991-2020	SST	JJA	1	Onset date	-0,421
ncar_ccsm4	ncar_ccsm4_sst_hcst_Apric_5-7_1991-2020	SST	MJJ	4	Onset date	-0,421
nmme	nmme_sst_hcst_Apric_5-7_1991-2020	SST	MJJ	6	Onset date	-0,421
cmc1	cmc1_precip_hcst_Apric_5_1991	precip	May	7	Onset date	-0,421
cfsv2	cfsv2_sst_hcst_Apric_6-8_1991-2020	SST	JJA	6	Onset date	-0,420
cmc1	cmc1_sst_hcst_Apric_5-7_1991-2020	SST	MJJ	6	Onset date	-0,420
nasa	nasa_sst_hcst_Apric_7_1991	SST	July	4	ESDS	-0,434
cmc2	cmc2_sst_hcst_Apric_6-8_1991-2020	SST	JJA	6	ESDS	-0,433
nmme	nmme_sst_hcst_Apric_7_1991	SST	July	5	ESDS	-0,433
nasa	nasa_precip_hcst_Apric_5-7_1991-2020	precip	MJJ	7	ESDS	-0,433
nmme	nmme_precip_hcst_Apric_5-7_1991-2020	precip	MJJ	7	ESDS	-0,433
nasa	nasa_sst_hcst_Apric_7_1991	SST	July	3	ESDS	-0,432
nasa	nasa_sst_hcst_Apric_7_1991	SST	July	5	ESDS	-0,432
nasa	nasa_sst_hcst_Apric_7_1991	SST	July	6	ESDS	-0,432
gfdl	gfdl_sst_hcst_Apric_5-7_1991-2020	SST	MJJ	4	ESDS	-0,431
cmc1	cmc1_precip_hcst_Apric_6_1991	precip	June	7	ESDS	-0,431
nasa	nasa_sst_hcst_Apric_5-7_1991-2020	SST	MJJ	5	ESDS	-0,430
nmme	nmme_sst_hcst_Apric_5-7_1991-2020	SST	MJJ	5	ESDS	-0,430
cfsv2	cfsv2_sst_hcst_Apric_10_1991	SST	Oct	4	Cessation date	-0,450
cmc1	cmc1_sst_hcst_Apric_8-10_1991-2020	SST	ASO	3	Cessation date	-0,447
cfsv2	cfsv2_sst_hcst_Apric_8-10_1991-2020	SST	ASO	5	Cessation date	-0,446
cmc1	cmc1_sst_hcst_Apric_10_1991	SST	Oct	3	Cessation date	-0,445

cmc1	cmc1_sst_hcst_Apric_9_1991	SST	Sept	4	Cessation date	-0,444
cfsv2	cfsv2_sst_hcst_Apric_8-10_1991-2020	SST	ASO	4	Cessation date	-0,443
gfdl	gfdl_sst_hcst_Apric_7-9_1991-2020	SST	JAS	4	Cessation date	-0,442
nmme	nmme_sst_hcst_Apric_9-11_1991-2020	SST	SON	4	Cessation date	-0,442
cfsv2	cfsv2_sst_hcst_Apric_9_1991	SST	Sept	5	Cessation date	-0,442
cmc1	cmc1_sst_hcst_Apric_7-9_1991-2020	SST	JAS	1	Cessation date	-0,441
cmc2	cmc2_sst_hcst_Apric_8-10_1991-2020	SST	ASO	3	Cessation date	-0,441
gfdl	gfdl_sst_hcst_Apric_8_1991	SST	Aug	4	Cessation date	-0,440
gfdl	gfdl_sst_hcst_Apric_9_1991	SST	Sept	4	Cessation date	-0,440
nmme	nmme_sst_hcst_Apric_8_1991	SST	Aug	3	Cessation date	-0,440
nmme	nmme_sst_hcst_Apric_8_1991	SST	Aug	5	Cessation date	-0,440
cmc1	cmc1_sst_hcst_Apric_8_1991	SST	Aug	4	Cessation date	-0,439
cmc1	cmc1_precip_hcst_Apric_9-11_1991-2020	precip	SON	7	Cessation date	-0,438
cfsv2	cfsv2_sst_hcst_Apric_7-9_1991-2020	SST	JAS	5	Cessation date	-0,435
cfsv2	cfsv2_sst_hcst_Apric_7-9_1991-2020	SST	JAS	2	LSDS	-0,424
cfsv2	cfsv2_sst_hcst_Apric_9-11_1991-2020	SST	SON	6	LSDS	-0,424
cmc1	cmc1_sst_hcst_Apric_8-10_1991-2020	SST	ASO	3	LSDS	-0,424
ncar_ccsm4	ncar_ccsm4_sst_hcst_Apric_7-9_1991-2020	SST	JAS	3	LSDS	-0,424
cmc1	cmc1_sst_hcst_Apric_10_1991	SST	Oct	3	LSDS	-0,424
nasa	nasa_sst_hcst_Apric_8_1991	SST	Aug	4	LSDS	-0,424
nasa	nasa_sst_hcst_Apric_8-10_1991-2020	SST	ASO	3	LSDS	-0,423
ncar_ccsm4	ncar_ccsm4_sst_hcst_Apric_10_1991	SST	Oct	3	LSDS	-0,423
cfsv2	cfsv2_sst_hcst_Apric_9-11_1991-2020	SST	SON	3	LSDS	-0,422
cmc1	cmc1_sst_hcst_Apric_7-9_1991-2020	SST	JAS	4	LSDS	-0,422
nasa	nasa_sst_hcst_Apric_7-9_1991-2020	SST	JAS	3	LSDS	-0,422
nasa	nasa_sst_hcst_Apric_7-9_1991-2020	SST	JAS	5	LSDS	-0,422
nmme	nmme_sst_hcst_Apric_9-11_1991-2020	SST	SON	3	LSDS	-0,422
cfsv2	cfsv2_sst_hcst_Apric_9_1991	SST	Sept	2	LSDS	-0,422
cmc1	cmc1_sst_hcst_Apric_8_1991	SST	Aug	4	LSDS	-0,422
gfdl	gfdl_sst_hcst_Apric_8_1991	SST	Aug	2	LSDS	-0,422
nasa	nasa_sst_hcst_Apric_9_1991	SST	Sept	3	LSDS	-0,422

cmc1	cmc1_sst_hcst_Apric_9-11_1991-2020	SST	SON	3	LSDS	-0,421
nmme	nmme_sst_hcst_Apric_7_1991	SST	July	6	Onset date	-0,420
ncar_ccsm4	ncar_ccsm4_precip_hcst_Apric_5-7_1991-2020	precip	MJJ	7	Onset date	-0,420
nasa	nasa_precip_hcst_Apric_7_1991	precip	July	7	Onset date	-0,419
ncar_ccsm4	ncar_ccsm4_sst_hcst_Apric_6_1991	SST	June	5	Onset date	-0,418
gfdl	gfdl_precip_hcst_Apric_6-8_1991-2020	precip	JJA	7	Onset date	-0,418
gfdl	gfdl_sst_hcst_Apric_5_1991	SST	May	6	Onset date	-0,417
gfdl	gfdl_sst_hcst_Apric_5-7_1991-2020	SST	MJJ	6	Onset date	-0,416
nasa	nasa_sst_hcst_Apric_5-7_1991-2020	SST	MJJ	6	Onset date	-0,416
gfdl	gfdl_sst_hcst_Apric_7_1991	SST	July	6	Onset date	-0,414
gfdl	gfdl_sst_hcst_Apric_7_1991	SST	July	1	Onset date	-0,413
ncar_ccsm4	ncar_ccsm4_sst_hcst_Apric_7_1991	SST	July	4	Onset date	-0,413
cfsv2	cfsv2_precip_hcst_Apric_6-8_1991-2020	precip	JJA	7	Onset date	-0,411
cfsv2	cfsv2_sst_hcst_Apric_5_1991	SST	May	6	ESDS	-0,430
cfsv2	cfsv2_precip_hcst_Apric_6_1991	precip	June	7	ESDS	-0,430
gfdl	gfdl_precip_hcst_Apric_7_1991	precip	July	7	ESDS	-0,430
nasa	nasa_sst_hcst_Apric_6-8_1991-2020	SST	JJA	5	ESDS	-0,429
cmc2	cmc2_sst_hcst_Apric_5_1991	SST	May	6	ESDS	-0,429
nasa	nasa_sst_hcst_Apric_6-8_1991-2020	SST	JJA	4	ESDS	-0,428
cmc1	cmc1_sst_hcst_Apric_5_1991	SST	May	6	ESDS	-0,428
cmc2	cmc2_sst_hcst_Apric_6_1991	SST	June	6	ESDS	-0,428
nasa	nasa_sst_hcst_Apric_5_1991	SST	May	5	ESDS	-0,428
nmme	nmme_sst_hcst_Apric_6-8_1991-2020	SST	JJA	6	ESDS	-0,427
cmc1	cmc1_sst_hcst_Apric_5_1991	SST	May	2	ESDS	-0,427
nmme	nmme_precip_hcst_Apric_6-8_1991-2020	precip	JJA	7	ESDS	-0,427
cmc1	cmc1_sst_hcst_Apric_7-9_1991-2020	SST	JAS	4	Cessation date	-0,435
cmc1	cmc1_sst_hcst_Apric_9-11_1991-2020	SST	SON	3	Cessation date	-0,434
cfsv2	cfsv2_sst_hcst_Apric_10_1991	SST	Oct	5	Cessation date	-0,433
cmc1	cmc1_precip_hcst_Apric_7-9_1991-2020	precip	JAS	7	Cessation date	-0,430
cmc1	cmc1_sst_hcst_Apric_8-10_1991-2020	SST	ASO	4	Cessation date	-0,429
cmc1	cmc1_sst_hcst_Apric_8_1991	SST	Aug	1	Cessation date	-0,429

cmc1	cmc1_sst_hcst_Apric_8_1991	SST	Aug	2	Cessation date	-0,429
cfsv2	cfsv2_sst_hcst_Apric_9-11_1991-2020	SST	SON	5	Cessation date	-0,427
nasa	nasa_sst_hcst_Apric_9_1991	SST	Sept	5	Cessation date	-0,426
cmc1	cmc1_precip_hcst_Apric_8_1991	precip	Aug	7	Cessation date	-0,426
cmc1	cmc1_precip_hcst_Apric_10_1991	precip	Oct	7	Cessation date	-0,426
gfdl	gfdl_sst_hcst_Apric_9-11_1991-2020	SST	SON	5	Cessation date	-0,425
cmc2	cmc2_sst_hcst_Apric_9-11_1991-2020	SST	SON	3	Cessation date	-0,423
cmc1	cmc1_sst_hcst_Apric_10_1991	SST	Oct	4	Cessation date	-0,423
nmme	nmme_sst_hcst_Apric_10_1991	SST	Oct	4	Cessation date	-0,423
cmc1	cmc1_sst_hcst_Apric_9_1991	SST	Sept	2	Cessation date	-0,422
ncar_ccsm4	ncar_ccsm4_sst_hcst_Apric_10_1991	SST	Oct	2	Cessation date	-0,422
cmc1	cmc1_precip_hcst_Apric_9_1991	precip	Sept	7	Cessation date	-0,422
ncar_ccsm4	ncar_ccsm4_sst_hcst_Apric_8-10_1991-2020	SST	ASO	3	LSDS	-0,421
cmc1	cmc1_sst_hcst_Apric_9_1991	SST	Sept	4	LSDS	-0,421
cmc2	cmc2_sst_hcst_Apric_8_1991	SST	Aug	1	LSDS	-0,421
nasa	nasa_sst_hcst_Apric_10_1991	SST	Oct	4	LSDS	-0,421
nmme	nmme_sst_hcst_Apric_10_1991	SST	Oct	3	LSDS	-0,421
cfsv2	cfsv2_sst_hcst_Apric_7-9_1991-2020	SST	JAS	1	LSDS	-0,420
cmc2	cmc2_sst_hcst_Apric_7-9_1991-2020	SST	JAS	1	LSDS	-0,420
cmc2	cmc2_sst_hcst_Apric_9-11_1991-2020	SST	SON	2	LSDS	-0,420
nasa	nasa_sst_hcst_Apric_7-9_1991-2020	SST	JAS	4	LSDS	-0,420
nmme	nmme_sst_hcst_Apric_8-10_1991-2020	SST	ASO	3	LSDS	-0,420
cmc2	cmc2_sst_hcst_Apric_9_1991	SST	Sept	1	LSDS	-0,420
nasa	nasa_sst_hcst_Apric_8_1991	SST	Aug	3	LSDS	-0,420
cmc2	cmc2_sst_hcst_Apric_8-10_1991-2020	SST	ASO	1	LSDS	-0,419
cmc2	cmc2_sst_hcst_Apric_9-11_1991-2020	SST	SON	1	LSDS	-0,419
cmc1	cmc1_sst_hcst_Apric_10_1991	SST	Oct	4	LSDS	-0,419
cmc2	cmc2_sst_hcst_Apric_10_1991	SST	Oct	1	LSDS	-0,419
cfsv2	cfsv2_sst_hcst_Apric_8-10_1991-2020	SST	ASO	2	LSDS	-0,418
cmc1	cmc1_sst_hcst_Apric_8-10_1991-2020	SST	ASO	4	LSDS	-0,418
nasa	nasa_sst_hcst_Apric_6-8_1991-2020	SST	JJA	5	Onset date	-0,410

gfdl	gfdl_precip_hcst_Apric_7_1991	precip	July	7	Onset date	-0,410
gfdl	gfdl_sst_hcst_Apric_6-8_1991-2020	SST	JJA	6	Onset date	-0,409
ncar_ccsm4	ncar_ccsm4_sst_hcst_Apric_5-7_1991-2020	SST	MJJ	6	Onset date	-0,409
cmc2	cmc2_sst_hcst_Apric_6-8_1991-2020	SST	JJA	6	Onset date	-0,408
gfdl	gfdl_sst_hcst_Apric_5-7_1991-2020	SST	MJJ	1	Onset date	-0,408
nmme	nmme_sst_hcst_Apric_6_1991	SST	June	6	Onset date	-0,408
cmc2	cmc2_sst_hcst_Apric_6-8_1991-2020	SST	JJA	3	Onset date	-0,406
cmc1	cmc1_sst_hcst_Apric_7_1991	SST	July	6	Onset date	-0,406
gfdl	gfdl_sst_hcst_Apric_6-8_1991-2020	SST	JJA	2	Onset date	-0,405
ncar_ccsm4	ncar_ccsm4_sst_hcst_Apric_5_1991	SST	May	6	Onset date	-0,405
ncar_ccsm4	ncar_ccsm4_sst_hcst_Apric_7_1991	SST	July	6	Onset date	-0,403
cmc2	cmc2_sst_hcst_Apric_5_1991	SST	May	4	ESDS	-0,426
nmme	nmme_precip_hcst_Apric_7_1991	precip	July	7	ESDS	-0,426
cmc1	cmc1_sst_hcst_Apric_5_1991	SST	May	5	ESDS	-0,425
cmc1	cmc1_sst_hcst_Apric_7_1991	SST	July	6	ESDS	-0,425
cmc2	cmc2_sst_hcst_Apric_5_1991	SST	May	2	ESDS	-0,425
nmme	nmme_sst_hcst_Apric_5-7_1991-2020	SST	MJJ	6	ESDS	-0,424
cfsv2	cfsv2_sst_hcst_Apric_6_1991	SST	June	6	ESDS	-0,424
nmme	nmme_sst_hcst_Apric_5_1991	SST	May	6	ESDS	-0,424
nmme	nmme_sst_hcst_Apric_6_1991	SST	June	5	ESDS	-0,424
cmc2	cmc2_sst_hcst_Apric_5-7_1991-2020	SST	MJJ	6	ESDS	-0,423
nasa	nasa_sst_hcst_Apric_5-7_1991-2020	SST	MJJ	3	ESDS	-0,423
nmme	nmme_sst_hcst_Apric_6-8_1991-2020	SST	JJA	5	ESDS	-0,423
cmc2	cmc2_precip_hcst_Apric_9_1991	precip	Sept	7	Cessation date	-0,422
cmc1	cmc1_sst_hcst_Apric_9-11_1991-2020	SST	SON	4	Cessation date	-0,421
gfdl	gfdl_sst_hcst_Apric_8-10_1991-2020	SST	ASO	4	Cessation date	-0,421
ncar_ccsm4	ncar_ccsm4_sst_hcst_Apric_8-10_1991-2020	SST	ASO	2	Cessation date	-0,421
ncar_ccsm4	ncar_ccsm4_sst_hcst_Apric_9-11_1991-2020	SST	SON	2	Cessation date	-0,421
nasa	nasa_sst_hcst_Apric_8_1991	SST	Aug	3	Cessation date	-0,421
ncar_ccsm4	ncar_ccsm4_sst_hcst_Apric_9_1991	SST	Sept	2	Cessation date	-0,421
gfdl	gfdl_sst_hcst_Apric_8_1991	SST	Aug	1	Cessation date	-0,420

cmc2	cmc2_sst_hcst_Apric_10_1991	SST	Oct	1	Cessation date	-0,419
nmme	nmme_precip_hcst_Apric_9-11_1991-2020	precip	SON	7	Cessation date	-0,419
cmc1	cmc1_sst_hcst_Apric_7-9_1991-2020	SST	JAS	2	Cessation date	-0,418
gfdl	gfdl_sst_hcst_Apric_7-9_1991-2020	SST	JAS	1	Cessation date	-0,418
cmc2	cmc2_sst_hcst_Apric_10_1991	SST	Oct	2	Cessation date	-0,418
gfdl	gfdl_sst_hcst_Apric_10_1991	SST	Oct	5	Cessation date	-0,418
nasa	nasa_precip_hcst_Apric_8_1991	precip	Aug	7	Cessation date	-0,418
ncar_ccsm4	ncar_ccsm4_sst_hcst_Apric_7-9_1991-2020	SST	JAS	2	Cessation date	-0,417
gfdl	gfdl_sst_hcst_Apric_9_1991	SST	Sept	1	Cessation date	-0,417
gfdl	gfdl_sst_hcst_Apric_9-11_1991-2020	SST	SON	2	Cessation date	-0,416
cmc2	cmc2_sst_hcst_Apric_8-10_1991-2020	SST	ASO	2	LSDS	-0,418
cmc2	cmc2_sst_hcst_Apric_8-10_1991-2020	SST	ASO	4	LSDS	-0,418
nasa	nasa_sst_hcst_Apric_9-11_1991-2020	SST	SON	3	LSDS	-0,418
cfsv2	cfsv2_sst_hcst_Apric_10_1991	SST	Oct	2	LSDS	-0,418
cmc2	cmc2_sst_hcst_Apric_10_1991	SST	Oct	2	LSDS	-0,418
cmc2	cmc2_precip_hcst_Apric_9-11_1991-2020	precip	SON	7	LSDS	-0,418
cmc2	cmc2_sst_hcst_Apric_9-11_1991-2020	SST	SON	4	LSDS	-0,416
nmme	nmme_sst_hcst_Apric_9-11_1991-2020	SST	SON	6	LSDS	-0,416
cmc2	cmc2_sst_hcst_Apric_9_1991	SST	Sept	4	LSDS	-0,416
nmme	nmme_sst_hcst_Apric_9_1991	SST	Sept	3	LSDS	-0,416
cmc2	cmc2_precip_hcst_Apric_8-10_1991-2020	precip	ASO	7	LSDS	-0,416
cmc2	cmc2_sst_hcst_Apric_7-9_1991-2020	SST	JAS	2	LSDS	-0,415
cmc2	cmc2_sst_hcst_Apric_9_1991	SST	Sept	2	LSDS	-0,415
cmc2	cmc2_sst_hcst_Apric_10_1991	SST	Oct	6	LSDS	-0,415
cfsv2	cfsv2_sst_hcst_Apric_9-11_1991-2020	SST	SON	2	LSDS	-0,414
cmc2	cmc2_sst_hcst_Apric_7-9_1991-2020	SST	JAS	4	LSDS	-0,414
gfdl	gfdl_sst_hcst_Apric_7-9_1991-2020	SST	JAS	2	LSDS	-0,414
cfsv2	cfsv2_sst_hcst_Apric_10_1991	SST	Oct	6	LSDS	-0,414
nmme	nmme_sst_hcst_Apric_7_1991	SST	July	5	Onset date	-0,403
nasa	nasa_sst_hcst_Apric_6_1991	SST	June	4	Onset date	-0,402
gfdl	gfdl_sst_hcst_Apric_6-8_1991-2020	SST	JJA	5	Onset date	-0,401

cmc2	cmc2_sst_hcst_Apric_6_1991	SST	June	4	Onset date	-0,401
ncar_ccsm4	ncar_ccsm4_sst_hcst_Apric_6-8_1991-2020	SST	JJA	6	Onset date	-0,400
nmme	nmme_sst_hcst_Apric_6_1991	SST	June	4	Onset date	-0,400
cmc2	cmc2_sst_hcst_Apric_5-7_1991-2020	SST	MJJ	3	Onset date	-0,399
nmme	nmme_sst_hcst_Apric_5-7_1991-2020	SST	MJJ	5	Onset date	-0,399
ncar_ccsm4	ncar_ccsm4_sst_hcst_Apric_7_1991	SST	July	3	Onset date	-0,399
cmc2	cmc2_sst_hcst_Apric_5-7_1991-2020	SST	MJJ	4	Onset date	-0,398
cmc1	cmc1_sst_hcst_Apric_6_1991	SST	June	4	Onset date	-0,398
ncar_ccsm4	ncar_ccsm4_sst_hcst_Apric_5-7_1991-2020	SST	MJJ	3	Onset date	-0,397
cfsv2	cfsv2_sst_hcst_Apric_5_1991	SST	May	2	ESDS	-0,423
cmc1	cmc1_sst_hcst_Apric_6_1991	SST	June	6	ESDS	-0,423
cmc1	cmc1_sst_hcst_Apric_7_1991	SST	July	4	ESDS	-0,423
nmme	nmme_sst_hcst_Apric_7_1991	SST	July	6	ESDS	-0,423
cmc2	cmc2_sst_hcst_Apric_7_1991	SST	July	6	ESDS	-0,422
gfdl	gfdl_sst_hcst_Apric_6_1991	SST	June	6	ESDS	-0,421
nasa	nasa_sst_hcst_Apric_5_1991	SST	May	6	ESDS	-0,421
gfdl	gfdl_precip_hcst_Apric_5-7_1991-2020	precip	MJJ	7	ESDS	-0,421
cmc1	cmc1_sst_hcst_Apric_5_1991	SST	May	1	ESDS	-0,420
gfdl	gfdl_sst_hcst_Apric_5_1991	SST	May	6	ESDS	-0,420
nmme	nmme_sst_hcst_Apric_5_1991	SST	May	5	ESDS	-0,420
cmc2	cmc2_sst_hcst_Apric_5-7_1991-2020	SST	MJJ	4	ESDS	-0,419
gfdl	gfdl_sst_hcst_Apric_8-10_1991-2020	SST	ASO	1	Cessation date	-0,415
cmc2	cmc2_sst_hcst_Apric_10_1991	SST	Oct	6	Cessation date	-0,415
gfdl	gfdl_sst_hcst_Apric_9-11_1991-2020	SST	SON	1	Cessation date	-0,413
gfdl	gfdl_sst_hcst_Apric_9-11_1991-2020	SST	SON	4	Cessation date	-0,413
nmme	nmme_sst_hcst_Apric_7-9_1991-2020	SST	JAS	3	Cessation date	-0,413
cfsv2	cfsv2_sst_hcst_Apric_9_1991	SST	Sept	4	Cessation date	-0,413
ncar_ccsm4	ncar_ccsm4_sst_hcst_Apric_9_1991	SST	Sept	1	Cessation date	-0,413
cmc1	cmc1_precip_hcst_Apric_8-10_1991-2020	precip	ASO	7	Cessation date	-0,413
nasa	nasa_sst_hcst_Apric_9-11_1991-2020	SST	SON	2	Cessation date	-0,412
ncar_ccsm4	ncar_ccsm4_sst_hcst_Apric_7-9_1991-2020	SST	JAS	1	Cessation date	-0,412

cmc2	cmc2_sst_hcst_Apric_10_1991	SST	Oct	4	Cessation date	-0,412
gfdl	gfdl_sst_hcst_Apric_10_1991	SST	Oct	2	Cessation date	-0,412
gfdl	gfdl_sst_hcst_Apric_8-10_1991-2020	SST	ASO	2	Cessation date	-0,411
gfdl	gfdl_sst_hcst_Apric_10_1991	SST	Oct	1	Cessation date	-0,411
ncar_ccsm4	ncar_ccsm4_sst_hcst_Apric_8_1991	SST	Aug	1	Cessation date	-0,411
ncar_ccsm4	ncar_ccsm4_sst_hcst_Apric_10_1991	SST	Oct	1	Cessation date	-0,411
cmc1	cmc1_sst_hcst_Apric_8-10_1991-2020	SST	ASO	2	Cessation date	-0,410
ncar_ccsm4	ncar_ccsm4_sst_hcst_Apric_8-10_1991-2020	SST	ASO	1	Cessation date	-0,410
ncar_ccsm4	ncar_ccsm4_sst_hcst_Apric_8_1991	SST	Aug	2	LSDS	-0,414
cfsv2	cfsv2_sst_hcst_Apric_8-10_1991-2020	SST	ASO	1	LSDS	-0,413
nasa	nasa_sst_hcst_Apric_8-10_1991-2020	SST	ASO	4	LSDS	-0,413
cfsv2	cfsv2_sst_hcst_Apric_10_1991	SST	Oct	1	LSDS	-0,413
ncar_ccsm4	ncar_ccsm4_sst_hcst_Apric_9-11_1991-2020	SST	SON	6	LSDS	-0,412
cmc1	cmc1_sst_hcst_Apric_10_1991	SST	Oct	6	LSDS	-0,412
cmc2	cmc2_sst_hcst_Apric_10_1991	SST	Oct	4	LSDS	-0,412
nasa	nasa_sst_hcst_Apric_8_1991	SST	Aug	1	LSDS	-0,412
nmme	nmme_sst_hcst_Apric_8_1991	SST	Aug	1	LSDS	-0,412
cfsv2	cfsv2_sst_hcst_Apric_7-9_1991-2020	SST	JAS	4	LSDS	-0,411
cfsv2	cfsv2_sst_hcst_Apric_9-11_1991-2020	SST	SON	1	LSDS	-0,411
nasa	nasa_sst_hcst_Apric_7-9_1991-2020	SST	JAS	1	LSDS	-0,411
nasa	nasa_sst_hcst_Apric_8-10_1991-2020	SST	ASO	2	LSDS	-0,411
gfdl	gfdl_sst_hcst_Apric_9_1991	SST	Sept	2	LSDS	-0,411
nmme	nmme_sst_hcst_Apric_8_1991	SST	Aug	4	LSDS	-0,411
nasa	nasa_sst_hcst_Apric_10_1991	SST	Oct	1	LSDS	-0,410
cfsv2	cfsv2_sst_hcst_Apric_8-10_1991-2020	SST	ASO	6	LSDS	-0,409
cmc1	cmc1_sst_hcst_Apric_7-9_1991-2020	SST	JAS	6	LSDS	-0,409
nmme	nmme_sst_hcst_Apric_5-7_1991-2020	SST	MJJ	4	Onset date	-0,397
cfsv2	cfsv2_sst_hcst_Apric_7_1991	SST	July	3	Onset date	-0,397
cmc1	cmc1_sst_hcst_Apric_6_1991	SST	June	3	Onset date	-0,397
ncar_ccsm4	ncar_ccsm4_sst_hcst_Apric_6_1991	SST	June	3	Onset date	-0,397
ncar_ccsm4	ncar_ccsm4_sst_hcst_Apric_6_1991	SST	June	6	Onset date	-0,397

nmme	nmme_sst_hcst_Apric_7_1991	SST	July	4	Onset date	-0,397
cmc1	cmc1_sst_hcst_Apric_5-7_1991-2020	SST	MJJ	3	Onset date	-0,396
cmc1	cmc1_sst_hcst_Apric_7_1991	SST	July	3	Onset date	-0,396
cmc2	cmc2_sst_hcst_Apric_7_1991	SST	July	3	Onset date	-0,396
nmme	nmme_sst_hcst_Apric_7_1991	SST	July	3	Onset date	-0,396
ncar_ccsm4	ncar_ccsm4_sst_hcst_Apric_6-8_1991-2020	SST	JJA	3	Onset date	-0,395
nmme	nmme_sst_hcst_Apric_6_1991	SST	June	5	Onset date	-0,395
cfsv2	cfsv2_sst_hcst_Apric_6_1991	SST	June	2	ESDS	-0,419
nasa	nasa_sst_hcst_Apric_5_1991	SST	May	2	ESDS	-0,419
nmme	nmme_sst_hcst_Apric_5_1991	SST	May	2	ESDS	-0,419
gfdl	gfdl_sst_hcst_Apric_6-8_1991-2020	SST	JJA	3	ESDS	-0,418
gfdl	gfdl_sst_hcst_Apric_6-8_1991-2020	SST	JJA	5	ESDS	-0,418
nmme	nmme_sst_hcst_Apric_6_1991	SST	June	6	ESDS	-0,418
cmc2	cmc2_precip_hcst_Apric_6_1991	precip	June	7	ESDS	-0,418
cmc2	cmc2_sst_hcst_Apric_6_1991	SST	June	4	ESDS	-0,417
gfdl	gfdl_precip_hcst_Apric_6_1991	precip	June	7	ESDS	-0,417
cfsv2	cfsv2_sst_hcst_Apric_5-7_1991-2020	SST	MJJ	6	ESDS	-0,416
cfsv2	cfsv2_sst_hcst_Apric_7_1991	SST	July	6	ESDS	-0,416
gfdl	gfdl_sst_hcst_Apric_5-7_1991-2020	SST	MJJ	6	ESDS	-0,415
cmc1	cmc1_sst_hcst_Apric_10_1991	SST	Oct	1	Cessation date	-0,410
gfdl	gfdl_sst_hcst_Apric_10_1991	SST	Oct	4	Cessation date	-0,410
cmc1	cmc1_sst_hcst_Apric_8-10_1991-2020	SST	ASO	1	Cessation date	-0,409
gfdl	gfdl_sst_hcst_Apric_7-9_1991-2020	SST	JAS	2	Cessation date	-0,409
cmc1	cmc1_sst_hcst_Apric_10_1991	SST	Oct	2	Cessation date	-0,409
gfdl	gfdl_sst_hcst_Apric_8_1991	SST	Aug	2	Cessation date	-0,409
ncar_ccsm4	ncar_ccsm4_sst_hcst_Apric_9-11_1991-2020	SST	SON	1	Cessation date	-0,408
cmc1	cmc1_sst_hcst_Apric_9_1991	SST	Sept	1	Cessation date	-0,408
ncar_ccsm4	ncar_ccsm4_sst_hcst_Apric_8_1991	SST	Aug	3	Cessation date	-0,408
nmme	nmme_sst_hcst_Apric_9_1991	SST	Sept	3	Cessation date	-0,408
cfsv2	cfsv2_precip_hcst_Apric_10_1991	precip	Oct	7	Cessation date	-0,408
nasa	nasa_sst_hcst_Apric_9-11_1991-2020	SST	SON	5	Cessation date	-0,407

gfdl	gfdl_sst_hcst_Apric_9_1991	SST	Sept	2	Cessation date	-0,406
nmme	nmme_sst_hcst_Apric_8_1991	SST	Aug	4	Cessation date	-0,406
cmc1	cmc1_sst_hcst_Apric_8-10_1991-2020	SST	ASO	6	Cessation date	-0,405
cmc1	cmc1_sst_hcst_Apric_9-11_1991-2020	SST	SON	1	Cessation date	-0,404
cmc1	cmc1_sst_hcst_Apric_9-11_1991-2020	SST	SON	2	Cessation date	-0,404
cmc1	cmc1_sst_hcst_Apric_10_1991	SST	Oct	6	Cessation date	-0,403
cmc1	cmc1_sst_hcst_Apric_9-11_1991-2020	SST	SON	6	LSDS	-0,409
nasa	nasa_sst_hcst_Apric_8-10_1991-2020	SST	ASO	1	LSDS	-0,409
nasa	nasa_sst_hcst_Apric_9_1991	SST	Sept	1	LSDS	-0,409
nasa	nasa_sst_hcst_Apric_10_1991	SST	Oct	2	LSDS	-0,409
nasa	nasa_sst_hcst_Apric_7-9_1991-2020	SST	JAS	2	LSDS	-0,408
cmc1	cmc1_sst_hcst_Apric_9_1991	SST	Sept	6	LSDS	-0,408
nasa	nasa_sst_hcst_Apric_9_1991	SST	Sept	2	LSDS	-0,408
nasa	nasa_sst_hcst_Apric_9_1991	SST	Sept	5	LSDS	-0,408
ncar_ccsm4	ncar_ccsm4_sst_hcst_Apric_10_1991	SST	Oct	6	LSDS	-0,408
nmme	nmme_sst_hcst_Apric_8_1991	SST	Aug	2	LSDS	-0,408
nmme	nmme_sst_hcst_Apric_10_1991	SST	Oct	6	LSDS	-0,408
cmc1	cmc1_sst_hcst_Apric_8-10_1991-2020	SST	ASO	6	LSDS	-0,407
cmc2	cmc2_sst_hcst_Apric_9-11_1991-2020	SST	SON	6	LSDS	-0,407
gfdl	gfdl_sst_hcst_Apric_8-10_1991-2020	SST	ASO	2	LSDS	-0,407
gfdl	gfdl_sst_hcst_Apric_9-11_1991-2020	SST	SON	6	LSDS	-0,407
nasa	nasa_sst_hcst_Apric_9-11_1991-2020	SST	SON	1	LSDS	-0,407
nasa	nasa_sst_hcst_Apric_9-11_1991-2020	SST	SON	6	LSDS	-0,407
nmme	nmme_sst_hcst_Apric_7-9_1991-2020	SST	JAS	2	LSDS	-0,407
nmme	nmme_precip_hcst_Apric_5-7_1991-2020	precip	MJJ	7	Onset date	-0,395
nmme	nmme_sst_hcst_Apric_5-7_1991-2020	SST	MJJ	3	Onset date	-0,394
cfsv2	cfsv2_sst_hcst_Apric_7_1991	SST	July	5	Onset date	-0,394
nasa	nasa_sst_hcst_Apric_5_1991	SST	May	4	Onset date	-0,394
nasa	nasa_sst_hcst_Apric_7_1991	SST	July	5	Onset date	-0,394
cfsv2	cfsv2_sst_hcst_Apric_5-7_1991-2020	SST	MJJ	5	Onset date	-0,393
cmc2	cmc2_sst_hcst_Apric_6_1991	SST	June	3	Onset date	-0,393

nasa	nasa_sst_hcst_Apric_7_1991	SST	July	3	Onset date	-0,393
cfsv2	cfsv2_sst_hcst_Apric_5-7_1991-2020	SST	MJJ	3	Onset date	-0,392
nasa	nasa_precip_hcst_Apric_5_1991	precip	May	7	Onset date	-0,392
cmc1	cmc1_sst_hcst_Apric_6-8_1991-2020	SST	JJA	3	Onset date	-0,391
nmme	nmme_sst_hcst_Apric_6-8_1991-2020	SST	JJA	3	Onset date	-0,391
gfdl	gfdl_sst_hcst_Apric_5_1991	SST	May	4	ESDS	-0,414
gfdl	gfdl_sst_hcst_Apric_6_1991	SST	June	4	ESDS	-0,414
nasa	nasa_sst_hcst_Apric_6_1991	SST	June	6	ESDS	-0,414
ncar_ccsm4	ncar_ccsm4_sst_hcst_Apric_5_1991	SST	May	2	ESDS	-0,414
nasa	nasa_precip_hcst_Apric_6_1991	precip	June	7	ESDS	-0,414
cfsv2	cfsv2_sst_hcst_Apric_6-8_1991-2020	SST	JJA	6	ESDS	-0,413
cmc2	cmc2_sst_hcst_Apric_6-8_1991-2020	SST	JJA	3	ESDS	-0,413
cfsv2	cfsv2_sst_hcst_Apric_5_1991	SST	May	1	ESDS	-0,413
cmc1	cmc1_sst_hcst_Apric_6_1991	SST	June	2	ESDS	-0,413
gfdl	gfdl_sst_hcst_Apric_7_1991	SST	July	6	ESDS	-0,413
cmc1	cmc1_sst_hcst_Apric_5-7_1991-2020	SST	MJJ	4	ESDS	-0,412
cfsv2	cfsv2_sst_hcst_Apric_7_1991	SST	July	3	ESDS	-0,412
gfdl	gfdl_sst_hcst_Apric_9_1991	SST	Sept	3	Cessation date	-0,402
cmc1	cmc1_sst_hcst_Apric_9-11_1991-2020	SST	SON	6	Cessation date	-0,400
gfdl	gfdl_sst_hcst_Apric_8-10_1991-2020	SST	ASO	5	Cessation date	-0,399
ncar_ccsm4	ncar_ccsm4_sst_hcst_Apric_8_1991	SST	Aug	2	Cessation date	-0,399
cmc1	cmc1_sst_hcst_Apric_10_1991	SST	Oct	5	Cessation date	-0,397
cmc2	cmc2_precip_hcst_Apric_7-9_1991-2020	precip	JAS	7	Cessation date	-0,397
cmc2	cmc2_sst_hcst_Apric_8-10_1991-2020	SST	ASO	6	Cessation date	-0,396
cfsv2	cfsv2_sst_hcst_Apric_9_1991	SST	Sept	1	Cessation date	-0,396
gfdl	gfdl_sst_hcst_Apric_8_1991	SST	Aug	3	Cessation date	-0,396
nasa	nasa_sst_hcst_Apric_7-9_1991-2020	SST	JAS	3	Cessation date	-0,395
cfsv2	cfsv2_sst_hcst_Apric_7-9_1991-2020	SST	JAS	4	Cessation date	-0,391
cmc1	cmc1_sst_hcst_Apric_7-9_1991-2020	SST	JAS	5	Cessation date	-0,391
cmc1	cmc1_sst_hcst_Apric_8-10_1991-2020	SST	ASO	5	Cessation date	-0,391
nmme	nmme_sst_hcst_Apric_8-10_1991-2020	SST	ASO	3	Cessation date	-0,391

cfsv2	cfsv2_sst_hcst_Apric_8_1991	SST	Aug	4	Cessation date	-0,391
gfdl	gfdl_sst_hcst_Apric_7-9_1991-2020	SST	JAS	5	Cessation date	-0,390
nasa	nasa_sst_hcst_Apric_9_1991	SST	Sept	3	Cessation date	-0,390
cfsv2	cfsv2_precip_hcst_Apric_8-10_1991-2020	precip	ASO	7	Cessation date	-0,390
gfdl	gfdl_sst_hcst_Apric_9_1991	SST	Sept	5	LSDS	-0,407
nmme	nmme_sst_hcst_Apric_8_1991	SST	Aug	3	LSDS	-0,407
ncar_ccsm4	ncar_ccsm4_sst_hcst_Apric_9-11_1991-2020	SST	SON	3	LSDS	-0,406
cfsv2	cfsv2_sst_hcst_Apric_9_1991	SST	Sept	3	LSDS	-0,406
cmc2	cmc2_sst_hcst_Apric_8_1991	SST	Aug	2	LSDS	-0,406
cfsv2	cfsv2_sst_hcst_Apric_7-9_1991-2020	SST	JAS	3	LSDS	-0,405
gfdl	gfdl_sst_hcst_Apric_8_1991	SST	Aug	1	LSDS	-0,405
gfdl	gfdl_sst_hcst_Apric_10_1991	SST	Oct	2	LSDS	-0,405
nmme	nmme_sst_hcst_Apric_9_1991	SST	Sept	2	LSDS	-0,405
nmme	nmme_sst_hcst_Apric_10_1991	SST	Oct	4	LSDS	-0,405
cmc1	cmc1_sst_hcst_Apric_9-11_1991-2020	SST	SON	4	LSDS	-0,404
ncar_ccsm4	ncar_ccsm4_sst_hcst_Apric_8-10_1991-2020	SST	ASO	6	LSDS	-0,404
ncar_ccsm4	ncar_ccsm4_sst_hcst_Apric_8_1991	SST	Aug	1	LSDS	-0,404
nasa	nasa_precip_hcst_Apric_8_1991	precip	Aug	7	LSDS	-0,404
gfdl	gfdl_sst_hcst_Apric_7-9_1991-2020	SST	JAS	4	LSDS	-0,403
gfdl	gfdl_sst_hcst_Apric_9-11_1991-2020	SST	SON	2	LSDS	-0,403
gfdl	gfdl_sst_hcst_Apric_8_1991	SST	Aug	5	LSDS	-0,403
cmc2	cmc2_precip_hcst_Apric_10_1991	precip	Oct	7	LSDS	-0,403
cfsv2	cfsv2_sst_hcst_Apric_5_1991	SST	May	4	Onset date	-0,391
cfsv2	cfsv2_sst_hcst_Apric_6-8_1991-2020	SST	JJA	5	Onset date	-0,390
ncar_ccsm4	ncar_ccsm4_sst_hcst_Apric_6-8_1991-2020	SST	JJA	1	Onset date	-0,390
ncar_ccsm4	ncar_ccsm4_sst_hcst_Apric_6-8_1991-2020	SST	JJA	4	Onset date	-0,390
cfsv2	cfsv2_sst_hcst_Apric_6_1991	SST	June	3	Onset date	-0,390
cmc1	cmc1_sst_hcst_Apric_5_1991	SST	May	4	Onset date	-0,390
nmme	nmme_sst_hcst_Apric_5_1991	SST	May	4	Onset date	-0,390
nmme	nmme_sst_hcst_Apric_6_1991	SST	June	3	Onset date	-0,390
cfsv2	cfsv2_sst_hcst_Apric_6-8_1991-2020	SST	JJA	1	Onset date	-0,389

nmme	nmme_sst_hcst_Apric_6-8_1991-2020	SST	JJA	4	Onset date	-0,389
gfdl	gfdl_sst_hcst_Apric_6_1991	SST	June	4	Onset date	-0,389
nmme	nmme_sst_hcst_Apric_5_1991	SST	May	5	Onset date	-0,388
nmme	nmme_sst_hcst_Apric_5_1991	SST	May	6	Onset date	-0,388
gfdl	gfdl_sst_hcst_Apric_6-8_1991-2020	SST	JJA	3	Onset date	-0,387
nasa	nasa_sst_hcst_Apric_5-7_1991-2020	SST	MJJ	3	Onset date	-0,387
nasa	nasa_sst_hcst_Apric_6-8_1991-2020	SST	JJA	3	Onset date	-0,387
cmc2	cmc2_sst_hcst_Apric_5_1991	SST	May	4	Onset date	-0,387
cfsv2	cfsv2_sst_hcst_Apric_6_1991	SST	June	5	Onset date	-0,386
cmc2	cmc2_precip_hcst_Apric_6-8_1991-2020	precip	JJA	7	ESDS	-0,412
cfsv2	cfsv2_sst_hcst_Apric_5_1991	SST	May	5	ESDS	-0,411
nasa	nasa_sst_hcst_Apric_6_1991	SST	June	2	ESDS	-0,411
cmc2	cmc2_precip_hcst_Apric_5-7_1991-2020	precip	MJJ	7	ESDS	-0,411
gfdl	gfdl_sst_hcst_Apric_6-8_1991-2020	SST	JJA	6	ESDS	-0,410
cmc2	cmc2_sst_hcst_Apric_5-7_1991-2020	SST	MJJ	3	ESDS	-0,409
ncar_ccsm4	ncar_ccsm4_sst_hcst_Apric_5_1991	SST	May	5	ESDS	-0,409
gfdl	gfdl_sst_hcst_Apric_6_1991	SST	June	5	ESDS	-0,408
cfsv2	cfsv2_sst_hcst_Apric_6_1991	SST	June	3	ESDS	-0,407
ncar_ccsm4	ncar_ccsm4_sst_hcst_Apric_6_1991	SST	June	6	ESDS	-0,407
nmme	nmme_sst_hcst_Apric_5_1991	SST	May	1	ESDS	-0,407
cfsv2	cfsv2_sst_hcst_Apric_5-7_1991-2020	SST	MJJ	3	ESDS	-0,406
cmc2	cmc2_sst_hcst_Apric_7_1991	SST	July	3	ESDS	-0,406
nasa	nasa_sst_hcst_Apric_6_1991	SST	June	4	ESDS	-0,405
ncar_ccsm4	ncar_ccsm4_sst_hcst_Apric_5_1991	SST	May	1	ESDS	-0,405
cmc2	cmc2_sst_hcst_Apric_6-8_1991-2020	SST	JJA	4	ESDS	-0,404
cmc2	cmc2_sst_hcst_Apric_5_1991	SST	May	5	ESDS	-0,404
gfdl	gfdl_sst_hcst_Apric_5_1991	SST	May	2	ESDS	-0,404
cfsv2	cfsv2_sst_hcst_Apric_8_1991	SST	Aug	5	Cessation date	-0,389
cmc1	cmc1_sst_hcst_Apric_9_1991	SST	Sept	5	Cessation date	-0,389
cfsv2	cfsv2_sst_hcst_Apric_8_1991	SST	Aug	3	Cessation date	-0,388
nasa	nasa_sst_hcst_Apric_9-11_1991-2020	SST	SON	3	Cessation date	-0,387

nmme	nmme_sst_hcst_Apric_10_1991	SST	Oct	3	Cessation date	-0,387
cmc2	cmc2_sst_hcst_Apric_9-11_1991-2020	SST	SON	6	Cessation date	-0,386
cfsv2	cfsv2_sst_hcst_Apric_9_1991	SST	Sept	2	Cessation date	-0,386
cmc1	cmc1_sst_hcst_Apric_7-9_1991-2020	SST	JAS	6	Cessation date	-0,385
gfdl	gfdl_sst_hcst_Apric_7-9_1991-2020	SST	JAS	3	Cessation date	-0,385
nasa	nasa_sst_hcst_Apric_8-10_1991-2020	SST	ASO	3	Cessation date	-0,384
cfsv2	cfsv2_sst_hcst_Apric_8_1991	SST	Aug	2	Cessation date	-0,384
cfsv2	cfsv2_sst_hcst_Apric_7-9_1991-2020	SST	JAS	1	Cessation date	-0,383
cfsv2	cfsv2_sst_hcst_Apric_8_1991	SST	Aug	1	Cessation date	-0,383
cfsv2	cfsv2_sst_hcst_Apric_7-9_1991-2020	SST	JAS	2	Cessation date	-0,382
cfsv2	cfsv2_sst_hcst_Apric_10_1991	SST	Oct	2	Cessation date	-0,382
nasa	nasa_precip_hcst_Apric_8-10_1991-2020	precip	ASO	7	Cessation date	-0,382
cmc1	cmc1_sst_hcst_Apric_8_1991	SST	Aug	5	Cessation date	-0,381
nasa	nasa_sst_hcst_Apric_10_1991	SST	Oct	3	Cessation date	-0,381
cmc2	cmc2_sst_hcst_Apric_8-10_1991-2020	SST	ASO	6	LSDS	-0,402
nmme	nmme_sst_hcst_Apric_8-10_1991-2020	SST	ASO	2	LSDS	-0,402
nasa	nasa_sst_hcst_Apric_10_1991	SST	Oct	5	LSDS	-0,402
nasa	nasa_precip_hcst_Apric_8-10_1991-2020	precip	ASO	7	LSDS	-0,402
gfdl	gfdl_sst_hcst_Apric_9_1991	SST	Sept	4	LSDS	-0,401
gfdl	gfdl_sst_hcst_Apric_10_1991	SST	Oct	4	LSDS	-0,401
nmme	nmme_sst_hcst_Apric_10_1991	SST	Oct	2	LSDS	-0,401
nmme	nmme_sst_hcst_Apric_9-11_1991-2020	SST	SON	2	LSDS	-0,400
cfsv2	cfsv2_sst_hcst_Apric_9_1991	SST	Sept	1	LSDS	-0,400
cmc2	cmc2_sst_hcst_Apric_8_1991	SST	Aug	4	LSDS	-0,400
cfsv2	cfsv2_precip_hcst_Apric_7-9_1991-2020	precip	JAS	7	LSDS	-0,400
gfdl	gfdl_sst_hcst_Apric_8-10_1991-2020	SST	ASO	4	LSDS	-0,399
nmme	nmme_sst_hcst_Apric_7-9_1991-2020	SST	JAS	1	LSDS	-0,399
cmc2	cmc2_sst_hcst_Apric_8_1991	SST	Aug	5	LSDS	-0,399
nasa	nasa_sst_hcst_Apric_8-10_1991-2020	SST	ASO	6	LSDS	-0,398
nmme	nmme_sst_hcst_Apric_8-10_1991-2020	SST	ASO	6	LSDS	-0,398
gfdl	gfdl_sst_hcst_Apric_8_1991	SST	Aug	4	LSDS	-0,398

cmc1	cmc1_precip_hcst_Apric_7-9_1991-2020	precip	JAS	7	LSDS	-0,397
nasa	nasa_sst_hcst_Apric_5_1991	SST	May	3	Onset date	-0,386
nasa	nasa_sst_hcst_Apric_5-7_1991-2020	SST	MJJ	4	Onset date	-0,385
cmc1	cmc1_sst_hcst_Apric_5_1991	SST	May	3	Onset date	-0,385
nmme	nmme_sst_hcst_Apric_5_1991	SST	May	3	Onset date	-0,385
gfdl	gfdl_sst_hcst_Apric_7_1991	SST	July	3	Onset date	-0,384
cfsv2	cfsv2_sst_hcst_Apric_5_1991	SST	May	3	Onset date	-0,383
cmc2	cmc2_sst_hcst_Apric_5-7_1991-2020	SST	MJJ	6	Onset date	-0,382
gfdl	gfdl_sst_hcst_Apric_5-7_1991-2020	SST	MJJ	3	Onset date	-0,381
nasa	nasa_sst_hcst_Apric_6_1991	SST	June	3	Onset date	-0,381
gfdl	gfdl_precip_hcst_Apric_6_1991	precip	June	7	Onset date	-0,381
cfsv2	cfsv2_sst_hcst_Apric_6-8_1991-2020	SST	JJA	2	Onset date	-0,380
cfsv2	cfsv2_sst_hcst_Apric_6-8_1991-2020	SST	JJA	3	Onset date	-0,380
gfdl	gfdl_sst_hcst_Apric_5_1991	SST	May	4	Onset date	-0,380
nasa	nasa_precip_hcst_Apric_5-7_1991-2020	precip	MJJ	7	Onset date	-0,380
ncar_ccsm4	ncar_ccsm4_precip_hcst_Apric_5_1991	precip	May	7	Onset date	-0,380
ncar_ccsm4	ncar_ccsm4_sst_hcst_Apric_6-8_1991-2020	SST	JJA	2	Onset date	-0,379
ncar_ccsm4	ncar_ccsm4_sst_hcst_Apric_5_1991	SST	May	5	Onset date	-0,379
ncar_ccsm4	ncar_ccsm4_sst_hcst_Apric_6_1991	SST	June	4	Onset date	-0,379
ncar_ccsm4	ncar_ccsm4_sst_hcst_Apric_6_1991	SST	June	5	ESDS	-0,404
cfsv2	cfsv2_precip_hcst_Apric_5-7_1991-2020	precip	MJJ	7	ESDS	-0,404
cfsv2	cfsv2_sst_hcst_Apric_6-8_1991-2020	SST	JJA	3	ESDS	-0,403
ncar_ccsm4	ncar_ccsm4_sst_hcst_Apric_6-8_1991-2020	SST	JJA	6	ESDS	-0,403
cmc2	cmc2_sst_hcst_Apric_5_1991	SST	May	1	ESDS	-0,403
cmc2	cmc2_sst_hcst_Apric_6_1991	SST	June	3	ESDS	-0,403
ncar_ccsm4	ncar_ccsm4_sst_hcst_Apric_5-7_1991-2020	SST	MJJ	6	ESDS	-0,402
cmc2	cmc2_sst_hcst_Apric_5_1991	SST	May	3	ESDS	-0,402
cmc2	cmc2_sst_hcst_Apric_7_1991	SST	July	4	ESDS	-0,402
nasa	nasa_sst_hcst_Apric_5_1991	SST	May	1	ESDS	-0,402
ncar_ccsm4	ncar_ccsm4_sst_hcst_Apric_7_1991	SST	July	4	ESDS	-0,402
cmc1	cmc1_precip_hcst_Apric_5-7_1991-2020	precip	MJJ	7	ESDS	-0,402

nasa	nasa_sst_hcst_Apric_5-7_1991-2020	SST	MJJ	2	ESDS	-0,401
nasa	nasa_sst_hcst_Apric_7_1991	SST	July	2	ESDS	-0,401
ncar_ccsm4	ncar_ccsm4_sst_hcst_Apric_5_1991	SST	May	3	ESDS	-0,401
nmme	nmme_sst_hcst_Apric_5_1991	SST	May	4	ESDS	-0,401
nasa	nasa_sst_hcst_Apric_5-7_1991-2020	SST	MJJ	4	ESDS	-0,400
cfsv2	cfsv2_sst_hcst_Apric_6_1991	SST	June	1	ESDS	-0,400
cfsv2	cfsv2_sst_hcst_Apric_8-10_1991-2020	SST	ASO	1	Cessation date	-0,380
cmc2	cmc2_sst_hcst_Apric_10_1991	SST	Oct	3	Cessation date	-0,380
gfdl	gfdl_sst_hcst_Apric_10_1991	SST	Oct	3	Cessation date	-0,380
nasa	nasa_sst_hcst_Apric_10_1991	SST	Oct	5	Cessation date	-0,380
gfdl	gfdl_sst_hcst_Apric_8-10_1991-2020	SST	ASO	3	Cessation date	-0,379
cfsv2	cfsv2_precip_hcst_Apric_9-11_1991-2020	precip	SON	7	Cessation date	-0,379
cfsv2	cfsv2_sst_hcst_Apric_8-10_1991-2020	SST	ASO	2	Cessation date	-0,378
cfsv2	cfsv2_sst_hcst_Apric_10_1991	SST	Oct	1	Cessation date	-0,378
nasa	nasa_precip_hcst_Apric_7-9_1991-2020	precip	JAS	7	Cessation date	-0,378
nmme	nmme_sst_hcst_Apric_9-11_1991-2020	SST	SON	3	Cessation date	-0,377
cmc2	cmc2_sst_hcst_Apric_10_1991	SST	Oct	5	Cessation date	-0,377
cfsv2	cfsv2_sst_hcst_Apric_7-9_1991-2020	SST	JAS	3	Cessation date	-0,376
nmme	nmme_sst_hcst_Apric_8_1991	SST	Aug	2	Cessation date	-0,376
nmme	nmme_precip_hcst_Apric_8-10_1991-2020	precip	ASO	7	Cessation date	-0,376
cfsv2	cfsv2_precip_hcst_Apric_8_1991	precip	Aug	7	Cessation date	-0,375
cfsv2	cfsv2_sst_hcst_Apric_9_1991	SST	Sept	3	Cessation date	-0,373
cfsv2	cfsv2_sst_hcst_Apric_10_1991	SST	Oct	3	Cessation date	-0,373
cfsv2	cfsv2_sst_hcst_Apric_9-11_1991-2020	SST	SON	2	Cessation date	-0,372
cmc2	cmc2_sst_hcst_Apric_9_1991	SST	Sept	5	LSDS	-0,396
nasa	nasa_sst_hcst_Apric_8_1991	SST	Aug	2	LSDS	-0,396
ncar_ccsm4	ncar_ccsm4_sst_hcst_Apric_9_1991	SST	Sept	6	LSDS	-0,395
nmme	nmme_sst_hcst_Apric_9_1991	SST	Sept	1	LSDS	-0,395
nmme	nmme_sst_hcst_Apric_9_1991	SST	Sept	4	LSDS	-0,395
cfsv2	cfsv2_precip_hcst_Apric_8-10_1991-2020	precip	ASO	7	LSDS	-0,395
nasa	nasa_sst_hcst_Apric_8-10_1991-2020	SST	ASO	5	LSDS	-0,394

ncar_ccsm4	ncar_ccsm4_sst_hcst_Apric_7-9_1991-2020	SST	JAS	2	LSDS	-0,394
nmme	nmme_precip_hcst_Apric_9-11_1991-2020	precip	SON	7	LSDS	-0,394
gfdl	gfdl_sst_hcst_Apric_9-11_1991-2020	SST	SON	4	LSDS	-0,393
nmme	nmme_sst_hcst_Apric_7-9_1991-2020	SST	JAS	4	LSDS	-0,393
nmme	nmme_sst_hcst_Apric_8-10_1991-2020	SST	ASO	1	LSDS	-0,393
cfsv2	cfsv2_sst_hcst_Apric_8_1991	SST	Aug	4	LSDS	-0,393
nasa	nasa_sst_hcst_Apric_10_1991	SST	Oct	6	LSDS	-0,393
gfdl	gfdl_sst_hcst_Apric_9-11_1991-2020	SST	SON	3	LSDS	-0,392
ncar_ccsm4	ncar_ccsm4_sst_hcst_Apric_7-9_1991-2020	SST	JAS	6	LSDS	-0,392
nmme	nmme_sst_hcst_Apric_9-11_1991-2020	SST	SON	1	LSDS	-0,392
nmme	nmme_sst_hcst_Apric_10_1991	SST	Oct	1	LSDS	-0,392
cmc1	cmc1_sst_hcst_Apric_6-8_1991-2020	SST	JJA	1	Onset date	-0,378
gfdl	gfdl_sst_hcst_Apric_5_1991	SST	May	3	Onset date	-0,378
cfsv2	cfsv2_sst_hcst_Apric_6-8_1991-2020	SST	JJA	4	Onset date	-0,377
gfdl	gfdl_sst_hcst_Apric_5-7_1991-2020	SST	MJJ	4	Onset date	-0,377
cfsv2	cfsv2_sst_hcst_Apric_6_1991	SST	June	4	Onset date	-0,377
ncar_ccsm4	ncar_ccsm4_sst_hcst_Apric_5_1991	SST	May	3	Onset date	-0,377
nasa	nasa_precip_hcst_Apric_6_1991	precip	June	7	Onset date	-0,377
nmme	nmme_sst_hcst_Apric_6-8_1991-2020	SST	JJA	5	Onset date	-0,376
cmc1	cmc1_sst_hcst_Apric_5_1991	SST	May	5	Onset date	-0,376
cmc2	cmc2_sst_hcst_Apric_7_1991	SST	July	4	Onset date	-0,376
ncar_ccsm4	ncar_ccsm4_sst_hcst_Apric_5_1991	SST	May	4	Onset date	-0,376
cmc2	cmc2_precip_hcst_Apric_7_1991	precip	July	7	Onset date	-0,376
nmme	nmme_precip_hcst_Apric_6_1991	precip	June	7	Onset date	-0,375
cmc2	cmc2_sst_hcst_Apric_5_1991	SST	May	3	Onset date	-0,374
cmc2	cmc2_sst_hcst_Apric_7_1991	SST	July	6	Onset date	-0,374
cfsv2	cfsv2_sst_hcst_Apric_5-7_1991-2020	SST	MJJ	4	Onset date	-0,373
cfsv2	cfsv2_sst_hcst_Apric_7_1991	SST	July	4	Onset date	-0,373
gfdl	gfdl_sst_hcst_Apric_6_1991	SST	June	3	Onset date	-0,373
nmme	nmme_precip_hcst_Apric_6_1991	precip	June	7	ESDS	-0,400
cmc2	cmc2_sst_hcst_Apric_6_1991	SST	June	2	ESDS	-0,399

cmc2	cmc2_precip_hcst_Apric_7_1991	precip	July	7	ESDS	-0,399
nasa	nasa_sst_hcst_Apric_6-8_1991-2020	SST	JJA	2	ESDS	-0,398
cmc1	cmc1_sst_hcst_Apric_6_1991	SST	June	1	ESDS	-0,398
ncar_ccsm4	ncar_ccsm4_sst_hcst_Apric_7_1991	SST	July	6	ESDS	-0,398
cmc1	cmc1_sst_hcst_Apric_6-8_1991-2020	SST	JJA	1	ESDS	-0,397
ncar_ccsm4	ncar_ccsm4_sst_hcst_Apric_5-7_1991-2020	SST	MJJ	4	ESDS	-0,397
gfdl	gfdl_sst_hcst_Apric_5-7_1991-2020	SST	MJJ	5	ESDS	-0,396
cfsv2	cfsv2_sst_hcst_Apric_5_1991	SST	May	3	ESDS	-0,396
ncar_ccsm4	ncar_ccsm4_precip_hcst_Apric_5-7_1991-2020	precip	MJJ	7	ESDS	-0,396
nmme	nmme_sst_hcst_Apric_6_1991	SST	June	2	ESDS	-0,395
nmme	nmme_sst_hcst_Apric_7_1991	SST	July	4	ESDS	-0,395
cmc1	cmc1_precip_hcst_Apric_7_1991	precip	July	7	ESDS	-0,395
nmme	nmme_sst_hcst_Apric_6-8_1991-2020	SST	JJA	3	ESDS	-0,394
cfsv2	cfsv2_precip_hcst_Apric_7_1991	precip	July	7	ESDS	-0,394
cmc1	cmc1_sst_hcst_Apric_5_1991	SST	May	4	ESDS	-0,393
nasa	nasa_sst_hcst_Apric_6_1991	SST	June	1	ESDS	-0,393
cfsv2	cfsv2_sst_hcst_Apric_9-11_1991-2020	SST	SON	3	Cessation date	-0,372
nmme	nmme_sst_hcst_Apric_9_1991	SST	Sept	2	Cessation date	-0,372
cfsv2	cfsv2_sst_hcst_Apric_9-11_1991-2020	SST	SON	1	Cessation date	-0,371
cfsv2	cfsv2_sst_hcst_Apric_9-11_1991-2020	SST	SON	6	Cessation date	-0,371
gfdl	gfdl_sst_hcst_Apric_9-11_1991-2020	SST	SON	3	Cessation date	-0,371
ncar_ccsm4	ncar_ccsm4_sst_hcst_Apric_7-9_1991-2020	SST	JAS	3	Cessation date	-0,371
nmme	nmme_sst_hcst_Apric_7-9_1991-2020	SST	JAS	2	Cessation date	-0,371
nmme	nmme_precip_hcst_Apric_7-9_1991-2020	precip	JAS	7	Cessation date	-0,371
cmc1	cmc1_sst_hcst_Apric_8_1991	SST	Aug	6	Cessation date	-0,370
nmme	nmme_sst_hcst_Apric_10_1991	SST	Oct	2	Cessation date	-0,370
nmme	nmme_precip_hcst_Apric_8_1991	precip	Aug	7	Cessation date	-0,370
cmc2	cmc2_sst_hcst_Apric_9_1991	SST	Sept	6	Cessation date	-0,369
cfsv2	cfsv2_sst_hcst_Apric_8-10_1991-2020	SST	ASO	3	Cessation date	-0,368
nmme	nmme_sst_hcst_Apric_8-10_1991-2020	SST	ASO	2	Cessation date	-0,368
nmme	nmme_sst_hcst_Apric_9-11_1991-2020	SST	SON	2	Cessation date	-0,368

nasa	nasa_precip_hcst_Apric_10_1991	precip	Oct	7	Cessation date	-0,367
cfsv2	cfsv2_sst_hcst_Apric_9_1991	SST	Sept	6	Cessation date	-0,366
nasa	nasa_sst_hcst_Apric_8_1991	SST	Aug	6	Cessation date	-0,366
cmc2	cmc2_sst_hcst_Apric_7-9_1991-2020	SST	JAS	5	LSDS	-0,391
gfdl	gfdl_sst_hcst_Apric_7-9_1991-2020	SST	JAS	1	LSDS	-0,391
cmc1	cmc1_sst_hcst_Apric_8_1991	SST	Aug	6	LSDS	-0,391
cmc1	cmc1_sst_hcst_Apric_8_1991	SST	Aug	5	LSDS	-0,390
ncar_ccsm4	ncar_ccsm4_sst_hcst_Apric_9_1991	SST	Sept	2	LSDS	-0,390
cmc1	cmc1_sst_hcst_Apric_9-11_1991-2020	SST	SON	2	LSDS	-0,389
cmc2	cmc2_sst_hcst_Apric_9_1991	SST	Sept	6	LSDS	-0,389
cmc1	cmc1_sst_hcst_Apric_9-11_1991-2020	SST	SON	1	LSDS	-0,387
nasa	nasa_sst_hcst_Apric_7-9_1991-2020	SST	JAS	6	LSDS	-0,387
ncar_ccsm4	ncar_ccsm4_sst_hcst_Apric_8-10_1991-2020	SST	ASO	2	LSDS	-0,387
cfsv2	cfsv2_precip_hcst_Apric_10_1991	precip	Oct	7	LSDS	-0,387
nmme	nmme_sst_hcst_Apric_9-11_1991-2020	SST	SON	4	LSDS	-0,386
gfdl	gfdl_sst_hcst_Apric_9_1991	SST	Sept	1	LSDS	-0,386
ncar_ccsm4	ncar_ccsm4_sst_hcst_Apric_10_1991	SST	Oct	2	LSDS	-0,386
cmc1	cmc1_sst_hcst_Apric_8-10_1991-2020	SST	ASO	2	LSDS	-0,385
gfdl	gfdl_sst_hcst_Apric_8-10_1991-2020	SST	ASO	1	LSDS	-0,385
gfdl	gfdl_sst_hcst_Apric_8-10_1991-2020	SST	ASO	3	LSDS	-0,385
ncar_ccsm4	ncar_ccsm4_sst_hcst_Apric_7-9_1991-2020	SST	JAS	1	LSDS	-0,385
gfdl	gfdl_sst_hcst_Apric_7_1991	SST	July	2	Onset date	-0,372
nasa	nasa_sst_hcst_Apric_7_1991	SST	July	6	Onset date	-0,372
nmme	nmme_precip_hcst_Apric_5_1991	precip	May	7	Onset date	-0,372
gfdl	gfdl_sst_hcst_Apric_6-8_1991-2020	SST	JJA	4	Onset date	-0,371
gfdl	gfdl_sst_hcst_Apric_5-7_1991-2020	SST	MJJ	2	Onset date	-0,370
cmc2	cmc2_precip_hcst_Apric_6_1991	precip	June	7	Onset date	-0,370
gfdl	gfdl_sst_hcst_Apric_7_1991	SST	July	4	Onset date	-0,369
ncar_ccsm4	ncar_ccsm4_precip_hcst_Apric_6-8_1991-2020	precip	JJA	7	Onset date	-0,368
gfdl	gfdl_precip_hcst_Apric_5_1991	precip	May	7	Onset date	-0,367
cmc1	cmc1_sst_hcst_Apric_5-7_1991-2020	SST	MJJ	4	Onset date	-0,366

cfsv2	cfsv2_precip_hcst_Apric_6_1991	precip	June	7	Onset date	-0,366
ncar_ccsm4	ncar_ccsm4_sst_hcst_Apric_5-7_1991-2020	SST	MJJ	5	Onset date	-0,365
nasa	nasa_precip_hcst_Apric_6-8_1991-2020	precip	JJA	7	Onset date	-0,365
nmme	nmme_precip_hcst_Apric_6-8_1991-2020	precip	JJA	7	Onset date	-0,365
cmc2	cmc2_sst_hcst_Apric_6-8_1991-2020	SST	JJA	4	Onset date	-0,364
cfsv2	cfsv2_sst_hcst_Apric_6_1991	SST	June	1	Onset date	-0,364
cfsv2	cfsv2_sst_hcst_Apric_6_1991	SST	June	2	Onset date	-0,364
ncar_ccsm4	ncar_ccsm4_sst_hcst_Apric_7_1991	SST	July	5	Onset date	-0,364
cmc1	cmc1_sst_hcst_Apric_5-7_1991-2020	SST	MJJ	2	ESDS	-0,392
nmme	nmme_sst_hcst_Apric_6_1991	SST	June	4	ESDS	-0,392
cmc1	cmc1_sst_hcst_Apric_6-8_1991-2020	SST	JJA	2	ESDS	-0,391
nmme	nmme_sst_hcst_Apric_7_1991	SST	July	3	ESDS	-0,391
cmc1	cmc1_sst_hcst_Apric_7_1991	SST	July	2	ESDS	-0,390
gfdl	gfdl_sst_hcst_Apric_5_1991	SST	May	5	ESDS	-0,390
nmme	nmme_sst_hcst_Apric_5-7_1991-2020	SST	MJJ	4	ESDS	-0,388
nmme	nmme_sst_hcst_Apric_5-7_1991-2020	SST	MJJ	3	ESDS	-0,387
gfdl	gfdl_sst_hcst_Apric_7_1991	SST	July	3	ESDS	-0,387
cmc1	cmc1_sst_hcst_Apric_5-7_1991-2020	SST	MJJ	1	ESDS	-0,386
nasa	nasa_sst_hcst_Apric_6-8_1991-2020	SST	JJA	1	ESDS	-0,386
nmme	nmme_sst_hcst_Apric_5_1991	SST	May	3	ESDS	-0,386
cmc1	cmc1_sst_hcst_Apric_6_1991	SST	June	5	ESDS	-0,385
cmc1	cmc1_sst_hcst_Apric_7_1991	SST	July	1	ESDS	-0,385
nmme	nmme_precip_hcst_Apric_5_1991	precip	May	7	ESDS	-0,385
cfsv2	cfsv2_sst_hcst_Apric_5-7_1991-2020	SST	MJJ	2	ESDS	-0,384
cfsv2	cfsv2_sst_hcst_Apric_6-8_1991-2020	SST	JJA	1	ESDS	-0,384
cfsv2	cfsv2_sst_hcst_Apric_7_1991	SST	July	2	ESDS	-0,384
nmme	nmme_sst_hcst_Apric_9_1991	SST	Sept	1	Cessation date	-0,365
cfsv2	cfsv2_sst_hcst_Apric_7-9_1991-2020	SST	JAS	6	Cessation date	-0,364
cmc1	cmc1_sst_hcst_Apric_9-11_1991-2020	SST	SON	5	Cessation date	-0,363
nmme	nmme_sst_hcst_Apric_7-9_1991-2020	SST	JAS	1	Cessation date	-0,362
nmme	nmme_precip_hcst_Apric_9_1991	precip	Sept	7	Cessation date	-0,362

ncar_ccsm4	ncar_ccsm4_sst_hcst_Apric_9_1991	SST	Sept	3	Cessation date	-0,361
nmme	nmme_sst_hcst_Apric_8_1991	SST	Aug	1	Cessation date	-0,361
nmme	nmme_sst_hcst_Apric_10_1991	SST	Oct	1	Cessation date	-0,361
nmme	nmme_sst_hcst_Apric_8-10_1991-2020	SST	ASO	1	Cessation date	-0,360
cmc2	cmc2_sst_hcst_Apric_7-9_1991-2020	SST	JAS	6	Cessation date	-0,359
cfsv2	cfsv2_sst_hcst_Apric_8_1991	SST	Aug	6	Cessation date	-0,358
nmme	nmme_sst_hcst_Apric_9-11_1991-2020	SST	SON	1	Cessation date	-0,357
cmc1	cmc1_sst_hcst_Apric_9_1991	SST	Sept	6	Cessation date	-0,357
cfsv2	cfsv2_sst_hcst_Apric_8-10_1991-2020	SST	ASO	6	Cessation date	-0,356
nasa	nasa_precip_hcst_Apric_9_1991	precip	Sept	7	Cessation date	-0,356
nmme	nmme_sst_hcst_Apric_10_1991	SST	Oct	6	Cessation date	-0,355
gfdl	gfdl_sst_hcst_Apric_9-11_1991-2020	SST	SON	6	Cessation date	-0,352
cmc2	cmc2_sst_hcst_Apric_8_1991	SST	Aug	4	Cessation date	-0,351
gfdl	gfdl_sst_hcst_Apric_10_1991	SST	Oct	3	LSDS	-0,385
cmc1	cmc1_sst_hcst_Apric_9-11_1991-2020	SST	SON	5	LSDS	-0,384
gfdl	gfdl_sst_hcst_Apric_8-10_1991-2020	SST	ASO	5	LSDS	-0,384
gfdl	gfdl_sst_hcst_Apric_9-11_1991-2020	SST	SON	1	LSDS	-0,384
cmc1	cmc1_sst_hcst_Apric_8_1991	SST	Aug	2	LSDS	-0,384
gfdl	gfdl_sst_hcst_Apric_10_1991	SST	Oct	1	LSDS	-0,384
cmc1	cmc1_sst_hcst_Apric_7-9_1991-2020	SST	JAS	2	LSDS	-0,383
cmc2	cmc2_sst_hcst_Apric_8-10_1991-2020	SST	ASO	5	LSDS	-0,383
ncar_ccsm4	ncar_ccsm4_sst_hcst_Apric_9-11_1991-2020	SST	SON	2	LSDS	-0,383
nmme	nmme_sst_hcst_Apric_8-10_1991-2020	SST	ASO	4	LSDS	-0,383
ncar_ccsm4	ncar_ccsm4_sst_hcst_Apric_9_1991	SST	Sept	1	LSDS	-0,383
cfsv2	cfsv2_precip_hcst_Apric_9-11_1991-2020	precip	SON	7	LSDS	-0,383
nasa	nasa_precip_hcst_Apric_9-11_1991-2020	precip	SON	7	LSDS	-0,383
cmc1	cmc1_precip_hcst_Apric_10_1991	precip	Oct	7	LSDS	-0,383
cmc1	cmc1_sst_hcst_Apric_10_1991	SST	Oct	2	LSDS	-0,382
cfsv2	cfsv2_precip_hcst_Apric_8_1991	precip	Aug	7	LSDS	-0,382
cmc1	cmc1_sst_hcst_Apric_8-10_1991-2020	SST	ASO	1	LSDS	-0,381
nasa	nasa_sst_hcst_Apric_9_1991	SST	Sept	6	LSDS	-0,381

cmc1	cmc1_precip_hcst_Apric_6_1991	precip	June	7	Onset date	-0,364
cmc1	cmc1_sst_hcst_Apric_5-7_1991-2020	SST	MJJ	1	Onset date	-0,362
cmc2	cmc2_precip_hcst_Apric_5_1991	precip	May	7	Onset date	-0,362
cfsv2	cfsv2_sst_hcst_Apric_5_1991	SST	May	1	Onset date	-0,361
cfsv2	cfsv2_sst_hcst_Apric_5_1991	SST	May	2	Onset date	-0,361
cmc1	cmc1_sst_hcst_Apric_7_1991	SST	July	1	Onset date	-0,361
gfdl	gfdl_sst_hcst_Apric_5-7_1991-2020	SST	MJJ	5	Onset date	-0,360
cmc1	cmc1_sst_hcst_Apric_5_1991	SST	May	6	Onset date	-0,360
gfdl	gfdl_sst_hcst_Apric_5_1991	SST	May	5	Onset date	-0,360
cmc2	cmc2_precip_hcst_Apric_5-7_1991-2020	precip	MJJ	7	Onset date	-0,360
cfsv2	cfsv2_sst_hcst_Apric_5-7_1991-2020	SST	MJJ	2	Onset date	-0,359
nasa	nasa_sst_hcst_Apric_5_1991	SST	May	6	Onset date	-0,358
nmme	nmme_sst_hcst_Apric_6-8_1991-2020	SST	JJA	1	Onset date	-0,357
gfdl	gfdl_precip_hcst_Apric_5-7_1991-2020	precip	MJJ	7	Onset date	-0,357
cfsv2	cfsv2_sst_hcst_Apric_7_1991	SST	July	2	Onset date	-0,356
cmc2	cmc2_sst_hcst_Apric_5_1991	SST	May	5	Onset date	-0,356
gfdl	gfdl_sst_hcst_Apric_7_1991	SST	July	5	Onset date	-0,356
cfsv2	cfsv2_sst_hcst_Apric_5-7_1991-2020	SST	MJJ	1	Onset date	-0,355
gfdl	gfdl_precip_hcst_Apric_6-8_1991-2020	precip	JJA	7	ESDS	-0,384
nasa	nasa_sst_hcst_Apric_5-7_1991-2020	SST	MJJ	1	ESDS	-0,383
ncar_ccsm4	ncar_ccsm4_sst_hcst_Apric_5_1991	SST	May	4	ESDS	-0,383
ncar_ccsm4	ncar_ccsm4_sst_hcst_Apric_7_1991	SST	July	5	ESDS	-0,382
ncar_ccsm4	ncar_ccsm4_precip_hcst_Apric_6_1991	precip	June	7	ESDS	-0,382
nasa	nasa_sst_hcst_Apric_5_1991	SST	May	4	ESDS	-0,381
cfsv2	cfsv2_sst_hcst_Apric_6-8_1991-2020	SST	JJA	2	ESDS	-0,380
gfdl	gfdl_sst_hcst_Apric_5-7_1991-2020	SST	MJJ	3	ESDS	-0,380
cmc1	cmc1_precip_hcst_Apric_6-8_1991-2020	precip	JJA	7	ESDS	-0,380
ncar_ccsm4	ncar_ccsm4_sst_hcst_Apric_6-8_1991-2020	SST	JJA	4	ESDS	-0,379
cmc1	cmc1_sst_hcst_Apric_6_1991	SST	June	4	ESDS	-0,379
nasa	nasa_sst_hcst_Apric_7_1991	SST	July	1	ESDS	-0,379
cmc2	cmc2_sst_hcst_Apric_6_1991	SST	June	5	ESDS	-0,378

ncar_ccsm4	ncar_ccsm4_sst_hcst_Apric_6_1991	SST	June	3	ESDS	-0,378
nmme	nmme_sst_hcst_Apric_6_1991	SST	June	1	ESDS	-0,378
nmme	nmme_sst_hcst_Apric_6_1991	SST	June	3	ESDS	-0,378
nmme	nmme_sst_hcst_Apric_6-8_1991-2020	SST	JJA	4	ESDS	-0,377
cfsv2	cfsv2_sst_hcst_Apric_5-7_1991-2020	SST	MJJ	1	ESDS	-0,375
nasa	nasa_sst_hcst_Apric_9-11_1991-2020	SST	SON	4	Cessation date	-0,350
ncar_ccsm4	ncar_ccsm4_sst_hcst_Apric_9-11_1991-2020	SST	SON	5	Cessation date	-0,350
nasa	nasa_sst_hcst_Apric_7-9_1991-2020	SST	JAS	6	Cessation date	-0,348
cfsv2	cfsv2_sst_hcst_Apric_10_1991	SST	Oct	6	Cessation date	-0,346
nmme	nmme_precip_hcst_Apric_10_1991	precip	Oct	7	Cessation date	-0,343
nasa	nasa_sst_hcst_Apric_8-10_1991-2020	SST	ASO	5	Cessation date	-0,342
gfdl	gfdl_sst_hcst_Apric_9_1991	SST	Sept	5	Cessation date	-0,341
nmme	nmme_sst_hcst_Apric_9-11_1991-2020	SST	SON	6	Cessation date	-0,339
cmc2	cmc2_sst_hcst_Apric_8_1991	SST	Aug	2	Cessation date	-0,336
nasa	nasa_sst_hcst_Apric_9-11_1991-2020	SST	SON	6	Cessation date	-0,334
ncar_ccsm4	ncar_ccsm4_sst_hcst_Apric_8-10_1991-2020	SST	ASO	3	Cessation date	-0,333
nmme	nmme_sst_hcst_Apric_8-10_1991-2020	SST	ASO	6	Cessation date	-0,333
cmc2	cmc2_sst_hcst_Apric_9_1991	SST	Sept	2	Cessation date	-0,333
cmc2	cmc2_sst_hcst_Apric_7-9_1991-2020	SST	JAS	2	Cessation date	-0,332
cmc2	cmc2_sst_hcst_Apric_8-10_1991-2020	SST	ASO	1	Cessation date	-0,331
cmc2	cmc2_sst_hcst_Apric_8-10_1991-2020	SST	ASO	2	Cessation date	-0,331
cmc2	cmc2_sst_hcst_Apric_9-11_1991-2020	SST	SON	1	Cessation date	-0,331
cmc2	cmc2_sst_hcst_Apric_9-11_1991-2020	SST	SON	2	Cessation date	-0,331
ncar_ccsm4	ncar_ccsm4_sst_hcst_Apric_8-10_1991-2020	SST	ASO	1	LSDS	-0,380
cmc1	cmc1_sst_hcst_Apric_9_1991	SST	Sept	2	LSDS	-0,380
cmc1	cmc1_sst_hcst_Apric_10_1991	SST	Oct	1	LSDS	-0,380
cmc2	cmc2_sst_hcst_Apric_10_1991	SST	Oct	3	LSDS	-0,380
gfdl	gfdl_sst_hcst_Apric_9_1991	SST	Sept	3	LSDS	-0,380
cmc1	cmc1_sst_hcst_Apric_7-9_1991-2020	SST	JAS	1	LSDS	-0,379
gfdl	gfdl_sst_hcst_Apric_7-9_1991-2020	SST	JAS	3	LSDS	-0,379
nasa	nasa_sst_hcst_Apric_9-11_1991-2020	SST	SON	4	LSDS	-0,379

nmme	nmme_sst_hcst_Apric_7-9_1991-2020	SST	JAS	6	LSDS	-0,379
cmc1	cmc1_sst_hcst_Apric_8_1991	SST	Aug	1	LSDS	-0,379
gfdl	gfdl_sst_hcst_Apric_10_1991	SST	Oct	6	LSDS	-0,379
ncar_ccsm4	ncar_ccsm4_sst_hcst_Apric_10_1991	SST	Oct	1	LSDS	-0,379
cmc2	cmc2_precip_hcst_Apric_7-9_1991-2020	precip	JAS	7	LSDS	-0,379
cmc1	cmc1_sst_hcst_Apric_9_1991	SST	Sept	1	LSDS	-0,378
ncar_ccsm4	ncar_ccsm4_sst_hcst_Apric_8_1991	SST	Aug	6	LSDS	-0,378
nmme	nmme_sst_hcst_Apric_9_1991	SST	Sept	6	LSDS	-0,378
cmc1	cmc1_precip_hcst_Apric_9_1991	precip	Sept	7	LSDS	-0,378
cmc2	cmc2_precip_hcst_Apric_9_1991	precip	Sept	7	LSDS	-0,378
ncar_ccsm4	ncar_ccsm4_sst_hcst_Apric_7_1991	SST	July	1	Onset date	-0,355
ncar_ccsm4	ncar_ccsm4_sst_hcst_Apric_5-7_1991-2020	SST	MJJ	1	Onset date	-0,354
cmc1	cmc1_sst_hcst_Apric_6_1991	SST	June	1	Onset date	-0,354
nasa	nasa_sst_hcst_Apric_6-8_1991-2020	SST	JJA	1	Onset date	-0,353
cmc1	cmc1_sst_hcst_Apric_7_1991	SST	July	4	Onset date	-0,352
gfdl	gfdl_sst_hcst_Apric_6_1991	SST	June	5	Onset date	-0,352
ncar_ccsm4	ncar_ccsm4_sst_hcst_Apric_5_1991	SST	May	1	Onset date	-0,352
nmme	nmme_sst_hcst_Apric_5-7_1991-2020	SST	MJJ	1	Onset date	-0,351
gfdl	gfdl_sst_hcst_Apric_6_1991	SST	June	1	Onset date	-0,351
cmc1	cmc1_sst_hcst_Apric_6-8_1991-2020	SST	JJA	2	Onset date	-0,350
nasa	nasa_sst_hcst_Apric_6_1991	SST	June	6	Onset date	-0,350
ncar_ccsm4	ncar_ccsm4_sst_hcst_Apric_7_1991	SST	July	2	Onset date	-0,350
ncar_ccsm4	ncar_ccsm4_sst_hcst_Apric_5-7_1991-2020	SST	MJJ	2	Onset date	-0,349
ncar_ccsm4	ncar_ccsm4_sst_hcst_Apric_6-8_1991-2020	SST	JJA	5	Onset date	-0,349
cmc2	cmc2_sst_hcst_Apric_6_1991	SST	June	6	Onset date	-0,348
cmc1	cmc1_sst_hcst_Apric_5_1991	SST	May	1	Onset date	-0,346
ncar_ccsm4	ncar_ccsm4_sst_hcst_Apric_5_1991	SST	May	2	Onset date	-0,346
cmc1	cmc1_sst_hcst_Apric_6-8_1991-2020	SST	JJA	4	Onset date	-0,344
cmc1	cmc1_sst_hcst_Apric_6-8_1991-2020	SST	JJA	3	ESDS	-0,375
ncar_ccsm4	ncar_ccsm4_sst_hcst_Apric_5-7_1991-2020	SST	MJJ	5	ESDS	-0,375
cfsv2	cfsv2_sst_hcst_Apric_5_1991	SST	May	4	ESDS	-0,375

ncar_ccsm4	ncar_ccsm4_sst_hcst_Apric_7_1991	SST	July	3	ESDS	-0,375
ncar_ccsm4	ncar_ccsm4_sst_hcst_Apric_6-8_1991-2020	SST	JJA	3	ESDS	-0,374
cfsv2	cfsv2_sst_hcst_Apric_6_1991	SST	June	4	ESDS	-0,374
nasa	nasa_sst_hcst_Apric_5_1991	SST	May	3	ESDS	-0,374
gfdl	gfdl_sst_hcst_Apric_5_1991	SST	May	3	ESDS	-0,373
ncar_ccsm4	ncar_ccsm4_sst_hcst_Apric_5-7_1991-2020	SST	MJJ	3	ESDS	-0,372
cmc1	cmc1_sst_hcst_Apric_5_1991	SST	May	3	ESDS	-0,372
ncar_ccsm4	ncar_ccsm4_sst_hcst_Apric_6_1991	SST	June	2	ESDS	-0,371
cfsv2	cfsv2_sst_hcst_Apric_7_1991	SST	July	1	ESDS	-0,370
cmc1	cmc1_sst_hcst_Apric_7_1991	SST	July	3	ESDS	-0,369
gfdl	gfdl_sst_hcst_Apric_6_1991	SST	June	1	ESDS	-0,369
ncar_ccsm4	ncar_ccsm4_sst_hcst_Apric_6_1991	SST	June	1	ESDS	-0,368
cmc2	cmc2_sst_hcst_Apric_5-7_1991-2020	SST	MJJ	2	ESDS	-0,367
cmc2	cmc2_sst_hcst_Apric_7_1991	SST	July	2	ESDS	-0,366
cmc1	cmc1_sst_hcst_Apric_5-7_1991-2020	SST	MJJ	3	ESDS	-0,365
nasa	nasa_sst_hcst_Apric_8-10_1991-2020	SST	ASO	6	Cessation date	-0,331
nasa	nasa_sst_hcst_Apric_10_1991	SST	Oct	4	Cessation date	-0,328
cmc2	cmc2_sst_hcst_Apric_7-9_1991-2020	SST	JAS	1	Cessation date	-0,327
nasa	nasa_sst_hcst_Apric_8_1991	SST	Aug	2	Cessation date	-0,327
cmc2	cmc2_sst_hcst_Apric_8_1991	SST	Aug	6	Cessation date	-0,326
nasa	nasa_sst_hcst_Apric_10_1991	SST	Oct	6	Cessation date	-0,326
ncar_ccsm4	ncar_ccsm4_sst_hcst_Apric_10_1991	SST	Oct	3	Cessation date	-0,326
cmc2	cmc2_sst_hcst_Apric_8_1991	SST	Aug	1	Cessation date	-0,325
cmc2	cmc2_sst_hcst_Apric_9_1991	SST	Sept	1	Cessation date	-0,325
gfdl	gfdl_sst_hcst_Apric_8-10_1991-2020	SST	ASO	6	Cessation date	-0,321
ncar_ccsm4	ncar_ccsm4_sst_hcst_Apric_9-11_1991-2020	SST	SON	4	Cessation date	-0,321
nasa	nasa_sst_hcst_Apric_9_1991	SST	Sept	2	Cessation date	-0,318
nasa	nasa_sst_hcst_Apric_9_1991	SST	Sept	1	Cessation date	-0,317
gfdl	gfdl_sst_hcst_Apric_10_1991	SST	Oct	6	Cessation date	-0,316
nmme	nmme_sst_hcst_Apric_7-9_1991-2020	SST	JAS	6	Cessation date	-0,315
nmme	nmme_sst_hcst_Apric_9_1991	SST	Sept	6	Cessation date	-0,315

nasa	nasa_sst_hcst_Apric_7-9_1991-2020	SST	JAS	2	Cessation date	-0,314
ncar_ccsm4	ncar_ccsm4_sst_hcst_Apric_9-11_1991-2020	SST	SON	3	Cessation date	-0,314
ncar_ccsm4	ncar_ccsm4_sst_hcst_Apric_9-11_1991-2020	SST	SON	1	LSDS	-0,377
cmc2	cmc2_sst_hcst_Apric_10_1991	SST	Oct	5	LSDS	-0,377
cmc2	cmc2_sst_hcst_Apric_7-9_1991-2020	SST	JAS	6	LSDS	-0,376
cmc2	cmc2_sst_hcst_Apric_8_1991	SST	Aug	3	LSDS	-0,376
gfdl	gfdl_sst_hcst_Apric_8_1991	SST	Aug	3	LSDS	-0,375
nasa	nasa_sst_hcst_Apric_8_1991	SST	Aug	6	LSDS	-0,375
gfdl	gfdl_sst_hcst_Apric_8-10_1991-2020	SST	ASO	6	LSDS	-0,374
gfdl	gfdl_sst_hcst_Apric_10_1991	SST	Oct	5	LSDS	-0,374
cfsv2	cfsv2_sst_hcst_Apric_8_1991	SST	Aug	3	LSDS	-0,373
cmc2	cmc2_sst_hcst_Apric_7-9_1991-2020	SST	JAS	3	LSDS	-0,372
cfsv2	cfsv2_sst_hcst_Apric_9_1991	SST	Sept	6	LSDS	-0,372
cmc1	cmc1_sst_hcst_Apric_10_1991	SST	Oct	5	LSDS	-0,372
cfsv2	cfsv2_sst_hcst_Apric_7-9_1991-2020	SST	JAS	6	LSDS	-0,371
cmc2	cmc2_sst_hcst_Apric_8-10_1991-2020	SST	ASO	3	LSDS	-0,371
cmc1	cmc1_sst_hcst_Apric_7-9_1991-2020	SST	JAS	5	LSDS	-0,370
gfdl	gfdl_sst_hcst_Apric_9-11_1991-2020	SST	SON	5	LSDS	-0,370
nasa	nasa_sst_hcst_Apric_9-11_1991-2020	SST	SON	5	LSDS	-0,370
gfdl	gfdl_precip_hcst_Apric_10_1991	precip	Oct	7	LSDS	-0,370
cmc1	cmc1_sst_hcst_Apric_6_1991	SST	June	6	Onset date	-0,344
cmc1	cmc1_sst_hcst_Apric_6_1991	SST	June	2	Onset date	-0,343
ncar_ccsm4	ncar_ccsm4_sst_hcst_Apric_6_1991	SST	June	1	Onset date	-0,343
ncar_ccsm4	ncar_ccsm4_sst_hcst_Apric_6_1991	SST	June	2	Onset date	-0,343
cfsv2	cfsv2_sst_hcst_Apric_7_1991	SST	July	1	Onset date	-0,342
cmc1	cmc1_sst_hcst_Apric_5-7_1991-2020	SST	MJJ	2	Onset date	-0,341
cmc1	cmc1_sst_hcst_Apric_5_1991	SST	May	2	Onset date	-0,339
nmme	nmme_precip_hcst_Apric_7_1991	precip	July	7	Onset date	-0,339
nasa	nasa_sst_hcst_Apric_5-7_1991-2020	SST	MJJ	1	Onset date	-0,337
cmc1	cmc1_sst_hcst_Apric_7_1991	SST	July	2	Onset date	-0,337
nmme	nmme_sst_hcst_Apric_5_1991	SST	May	1	Onset date	-0,337

gfdl	gfdl_sst_hcst_Apric_6_1991	SST	June	2	Onset date	-0,335
nasa	nasa_sst_hcst_Apric_7_1991	SST	July	1	Onset date	-0,335
nasa	nasa_sst_hcst_Apric_6-8_1991-2020	SST	JJA	2	Onset date	-0,334
gfdl	gfdl_sst_hcst_Apric_5_1991	SST	May	1	Onset date	-0,333
cmc2	cmc2_sst_hcst_Apric_6-8_1991-2020	SST	JJA	2	Onset date	-0,332
nmme	nmme_sst_hcst_Apric_7_1991	SST	July	1	Onset date	-0,332
cmc2	cmc2_precip_hcst_Apric_6-8_1991-2020	precip	JJA	7	Onset date	-0,332
cfsv2	cfsv2_precip_hcst_Apric_5_1991	precip	May	7	ESDS	-0,365
gfdl	gfdl_sst_hcst_Apric_7_1991	SST	July	5	ESDS	-0,364
nasa	nasa_precip_hcst_Apric_6-8_1991-2020	precip	JJA	7	ESDS	-0,363
cmc2	cmc2_sst_hcst_Apric_5-7_1991-2020	SST	MJJ	5	ESDS	-0,362
ncar_ccsm4	ncar_ccsm4_sst_hcst_Apric_6-8_1991-2020	SST	JJA	1	ESDS	-0,362
cfsv2	cfsv2_sst_hcst_Apric_6_1991	SST	June	5	ESDS	-0,362
cmc2	cmc2_sst_hcst_Apric_6_1991	SST	June	1	ESDS	-0,362
cmc1	cmc1_precip_hcst_Apric_5_1991	precip	May	7	ESDS	-0,362
nmme	nmme_sst_hcst_Apric_6-8_1991-2020	SST	JJA	1	ESDS	-0,360
gfdl	gfdl_sst_hcst_Apric_6-8_1991-2020	SST	JJA	2	ESDS	-0,359
ncar_ccsm4	ncar_ccsm4_sst_hcst_Apric_6-8_1991-2020	SST	JJA	5	ESDS	-0,359
nmme	nmme_sst_hcst_Apric_7_1991	SST	July	2	ESDS	-0,359
nmme	nmme_sst_hcst_Apric_5-7_1991-2020	SST	MJJ	2	ESDS	-0,358
cmc1	cmc1_sst_hcst_Apric_6_1991	SST	June	3	ESDS	-0,358
gfdl	gfdl_sst_hcst_Apric_5_1991	SST	May	1	ESDS	-0,357
cmc2	cmc2_sst_hcst_Apric_6-8_1991-2020	SST	JJA	2	ESDS	-0,356
gfdl	gfdl_sst_hcst_Apric_7_1991	SST	July	2	ESDS	-0,356
cmc2	cmc2_sst_hcst_Apric_6-8_1991-2020	SST	JJA	5	ESDS	-0,355
gfdl	gfdl_sst_hcst_Apric_9_1991	SST	Sept	6	Cessation date	-0,314
nmme	nmme_sst_hcst_Apric_8_1991	SST	Aug	6	Cessation date	-0,313
gfdl	gfdl_sst_hcst_Apric_7-9_1991-2020	SST	JAS	6	Cessation date	-0,311
nasa	nasa_sst_hcst_Apric_9_1991	SST	Sept	6	Cessation date	-0,311
cmc2	cmc2_precip_hcst_Apric_8-10_1991-2020	precip	ASO	7	Cessation date	-0,311
nasa	nasa_sst_hcst_Apric_10_1991	SST	Oct	2	Cessation date	-0,310

cmc2	cmc2_sst_hcst_Apric_8_1991	SST	Aug	5	Cessation date	-0,309
ncar_ccsm4	ncar_ccsm4_sst_hcst_Apric_8_1991	SST	Aug	6	Cessation date	-0,308
nasa	nasa_sst_hcst_Apric_7-9_1991-2020	SST	JAS	1	Cessation date	-0,305
nasa	nasa_sst_hcst_Apric_8-10_1991-2020	SST	ASO	4	Cessation date	-0,305
nasa	nasa_sst_hcst_Apric_10_1991	SST	Oct	1	Cessation date	-0,305
nasa	nasa_sst_hcst_Apric_8-10_1991-2020	SST	ASO	1	Cessation date	-0,304
nasa	nasa_sst_hcst_Apric_8-10_1991-2020	SST	ASO	2	Cessation date	-0,304
gfdl	gfdl_sst_hcst_Apric_8_1991	SST	Aug	6	Cessation date	-0,304
ncar_ccsm4	ncar_ccsm4_sst_hcst_Apric_8-10_1991-2020	SST	ASO	5	Cessation date	-0,303
nasa	nasa_sst_hcst_Apric_8_1991	SST	Aug	1	Cessation date	-0,301
nasa	nasa_sst_hcst_Apric_9-11_1991-2020	SST	SON	1	Cessation date	-0,298
nasa	nasa_sst_hcst_Apric_8_1991	SST	Aug	4	Cessation date	-0,298
ncar_ccsm4	ncar_ccsm4_precip_hcst_Apric_8-10_1991-2020	precip	ASO	7	LSDS	-0,369
cmc2	cmc2_sst_hcst_Apric_9-11_1991-2020	SST	SON	3	LSDS	-0,368
nmme	nmme_precip_hcst_Apric_8-10_1991-2020	precip	ASO	7	LSDS	-0,368
cfsv2	cfsv2_precip_hcst_Apric_9_1991	precip	Sept	7	LSDS	-0,368
cmc2	cmc2_sst_hcst_Apric_9-11_1991-2020	SST	SON	5	LSDS	-0,367
cmc2	cmc2_sst_hcst_Apric_9_1991	SST	Sept	3	LSDS	-0,367
nmme	nmme_sst_hcst_Apric_8_1991	SST	Aug	6	LSDS	-0,367
gfdl	gfdl_sst_hcst_Apric_9_1991	SST	Sept	6	LSDS	-0,366
cmc1	cmc1_precip_hcst_Apric_8-10_1991-2020	precip	ASO	7	LSDS	-0,365
gfdl	gfdl_sst_hcst_Apric_7-9_1991-2020	SST	JAS	6	LSDS	-0,364
cmc1	cmc1_sst_hcst_Apric_8-10_1991-2020	SST	ASO	5	LSDS	-0,363
cmc1	cmc1_precip_hcst_Apric_8_1991	precip	Aug	7	LSDS	-0,363
nmme	nmme_sst_hcst_Apric_9-11_1991-2020	SST	SON	5	LSDS	-0,361
cfsv2	cfsv2_sst_hcst_Apric_9_1991	SST	Sept	4	LSDS	-0,361
gfdl	gfdl_sst_hcst_Apric_8_1991	SST	Aug	6	LSDS	-0,361
cmc2	cmc2_sst_hcst_Apric_8_1991	SST	Aug	6	LSDS	-0,359
gfdl	gfdl_precip_hcst_Apric_9-11_1991-2020	precip	SON	7	LSDS	-0,358
cfsv2	cfsv2_sst_hcst_Apric_8_1991	SST	Aug	6	LSDS	-0,357
nmme	nmme_sst_hcst_Apric_6-8_1991-2020	SST	JJA	2	Onset date	-0,331

cmc2	cmc2_sst_hcst_Apric_5_1991	SST	May	1	Onset date	-0,330
gfdl	gfdl_sst_hcst_Apric_6_1991	SST	June	3	ESDS	-0,355
gfdl	gfdl_sst_hcst_Apric_6-8_1991-2020	SST	JJA	1	ESDS	-0,353
ncar_ccsm4	ncar_ccsm4_sst_hcst_Apric_10_1991	SST	Oct	5	Cessation date	-0,298
cfsv2	cfsv2_precip_hcst_Apric_7-9_1991-2020	precip	JAS	7	Cessation date	-0,297
cmc2	cmc2_precip_hcst_Apric_9-11_1991-2020	precip	SON	7	Cessation date	-0,297
ncar_ccsm4	ncar_ccsm4_precip_hcst_Apric_9-11_1991-2020	precip	SON	7	LSDS	-0,356
cfsv2	cfsv2_sst_hcst_Apric_8_1991	SST	Aug	5	LSDS	-0,352
cmc1	cmc1_sst_hcst_Apric_9_1991	SST	Sept	5	LSDS	-0,351
nmme	nmme_sst_hcst_Apric_5_1991	SST	May	2	Onset date	-0,330
cfsv2	cfsv2_precip_hcst_Apric_5_1991	precip	May	7	Onset date	-0,330
nmme	nmme_sst_hcst_Apric_6-8_1991-2020	SST	JJA	2	ESDS	-0,353
cfsv2	cfsv2_sst_hcst_Apric_7_1991	SST	July	4	ESDS	-0,353
cmc2	cmc2_precip_hcst_Apric_10_1991	precip	Oct	7	Cessation date	-0,296
cmc2	cmc2_sst_hcst_Apric_9_1991	SST	Sept	5	Cessation date	-0,294
ncar_ccsm4	ncar_ccsm4_sst_hcst_Apric_8_1991	SST	Aug	4	Cessation date	-0,294
gfdl	gfdl_precip_hcst_Apric_9_1991	precip	Sept	7	LSDS	-0,350
nmme	nmme_precip_hcst_Apric_10_1991	precip	Oct	7	LSDS	-0,350
nmme	nmme_sst_hcst_Apric_8_1991	SST	Aug	5	LSDS	-0,348
nmme	nmme_sst_hcst_Apric_6_1991	SST	June	1	Onset date	-0,329
cmc2	cmc2_sst_hcst_Apric_5_1991	SST	May	6	Onset date	-0,325
cmc2	cmc2_sst_hcst_Apric_7_1991	SST	July	5	ESDS	-0,352
cfsv2	cfsv2_sst_hcst_Apric_5-7_1991-2020	SST	MJJ	4	ESDS	-0,351
gfdl	gfdl_precip_hcst_Apric_9-11_1991-2020	precip	SON	7	Cessation date	-0,294
gfdl	gfdl_precip_hcst_Apric_8_1991	precip	Aug	7	Cessation date	-0,293
nasa	nasa_sst_hcst_Apric_9_1991	SST	Sept	4	Cessation date	-0,288
ncar_ccsm4	ncar_ccsm4_sst_hcst_Apric_8_1991	SST	Aug	4	LSDS	-0,346
ncar_ccsm4	ncar_ccsm4_sst_hcst_Apric_9_1991	SST	Sept	4	LSDS	-0,346
ncar_ccsm4	ncar_ccsm4_precip_hcst_Apric_7-9_1991-2020	precip	JAS	7	LSDS	-0,346
cmc2	cmc2_sst_hcst_Apric_7_1991	SST	July	1	Onset date	-0,324
nasa	nasa_sst_hcst_Apric_5_1991	SST	May	1	Onset date	-0,324

gfdl	gfdl_sst_hcst_Apric_5-7_1991-2020	SST	MJJ	2	ESDS	-0,351
cmc1	cmc1_sst_hcst_Apric_5-7_1991-2020	SST	MJJ	5	ESDS	-0,350
cmc2	cmc2_sst_hcst_Apric_7-9_1991-2020	SST	JAS	5	Cessation date	-0,281
ncar_ccsm4	ncar_ccsm4_sst_hcst_Apric_10_1991	SST	Oct	6	Cessation date	-0,278
cmc2	cmc2_sst_hcst_Apric_9_1991	SST	Sept	4	Cessation date	-0,276
gfdl	gfdl_precip_hcst_Apric_8-10_1991-2020	precip	ASO	7	LSDS	-0,345
gfdl	gfdl_precip_hcst_Apric_7-9_1991-2020	precip	JAS	7	LSDS	-0,344
ncar_ccsm4	ncar_ccsm4_sst_hcst_Apric_9_1991	SST	Sept	5	LSDS	-0,343
nasa	nasa_sst_hcst_Apric_6_1991	SST	June	1	Onset date	-0,324
nmme	nmme_sst_hcst_Apric_6_1991	SST	June	2	Onset date	-0,324
nmme	nmme_sst_hcst_Apric_7_1991	SST	July	1	ESDS	-0,347
ncar_ccsm4	ncar_ccsm4_sst_hcst_Apric_5-7_1991-2020	SST	MJJ	1	ESDS	-0,346
ncar_ccsm4	ncar_ccsm4_precip_hcst_Apric_9_1991	precip	Sept	7	Cessation date	-0,276
ncar_ccsm4	ncar_ccsm4_sst_hcst_Apric_7-9_1991-2020	SST	JAS	5	Cessation date	-0,275
cfsv2	cfsv2_precip_hcst_Apric_9_1991	precip	Sept	7	Cessation date	-0,275
ncar_ccsm4	ncar_ccsm4_sst_hcst_Apric_8_1991	SST	Aug	5	LSDS	-0,342
cmc1	cmc1_precip_hcst_Apric_9-11_1991-2020	precip	SON	7	LSDS	-0,342
nmme	nmme_precip_hcst_Apric_9_1991	precip	Sept	7	LSDS	-0,341
cmc2	cmc2_sst_hcst_Apric_6-8_1991-2020	SST	JJA	1	Onset date	-0,323
cmc2	cmc2_sst_hcst_Apric_5_1991	SST	May	2	Onset date	-0,323
ncar_ccsm4	ncar_ccsm4_sst_hcst_Apric_7_1991	SST	July	1	ESDS	-0,346
ncar_ccsm4	ncar_ccsm4_sst_hcst_Apric_6_1991	SST	June	4	ESDS	-0,345
ncar_ccsm4	ncar_ccsm4_sst_hcst_Apric_8-10_1991-2020	SST	ASO	4	Cessation date	-0,274
ncar_ccsm4	ncar_ccsm4_sst_hcst_Apric_7-9_1991-2020	SST	JAS	6	Cessation date	-0,273
ncar_ccsm4	ncar_ccsm4_sst_hcst_Apric_9_1991	SST	Sept	6	Cessation date	-0,273
cfsv2	cfsv2_sst_hcst_Apric_8-10_1991-2020	SST	ASO	4	LSDS	-0,337
nmme	nmme_sst_hcst_Apric_8-10_1991-2020	SST	ASO	5	LSDS	-0,336
ncar_ccsm4	ncar_ccsm4_sst_hcst_Apric_7-9_1991-2020	SST	JAS	4	LSDS	-0,333
gfdl	gfdl_sst_hcst_Apric_5_1991	SST	May	2	Onset date	-0,322
cmc2	cmc2_sst_hcst_Apric_6_1991	SST	June	5	Onset date	-0,320
nasa	nasa_precip_hcst_Apric_5_1991	precip	May	7	ESDS	-0,345

cmc2	cmc2_sst_hcst_Apric_5-7_1991-2020	SST	MJJ	1	ESDS	-0,344
ncar_ccsm4	ncar_ccsm4_sst_hcst_Apric_9_1991	SST	Sept	5	Cessation date	-0,271
cmc2	cmc2_sst_hcst_Apric_7-9_1991-2020	SST	JAS	4	Cessation date	-0,270
ncar_ccsm4	ncar_ccsm4_sst_hcst_Apric_7-9_1991-2020	SST	JAS	4	Cessation date	-0,269
ncar_ccsm4	ncar_ccsm4_sst_hcst_Apric_7-9_1991-2020	SST	JAS	5	LSDS	-0,333
nmme	nmme_sst_hcst_Apric_10_1991	SST	Oct	5	LSDS	-0,333
cfsv2	cfsv2_sst_hcst_Apric_9-11_1991-2020	SST	SON	4	LSDS	-0,331
cmc2	cmc2_sst_hcst_Apric_5-7_1991-2020	SST	MJJ	1	Onset date	-0,318
cmc2	cmc2_sst_hcst_Apric_6_1991	SST	June	2	Onset date	-0,318
nasa	nasa_sst_hcst_Apric_5_1991	SST	May	2	Onset date	-0,317
ncar_ccsm4	ncar_ccsm4_sst_hcst_Apric_6-8_1991-2020	SST	JJA	2	ESDS	-0,344
ncar_ccsm4	ncar_ccsm4_precip_hcst_Apric_6-8_1991-2020	precip	JJA	7	ESDS	-0,344
gfdl	gfdl_precip_hcst_Apric_5_1991	precip	May	7	ESDS	-0,343
ncar_ccsm4	ncar_ccsm4_sst_hcst_Apric_8_1991	SST	Aug	5	Cessation date	-0,267
ncar_ccsm4	ncar_ccsm4_sst_hcst_Apric_10_1991	SST	Oct	4	Cessation date	-0,266
ncar_ccsm4	ncar_ccsm4_sst_hcst_Apric_8-10_1991-2020	SST	ASO	6	Cessation date	-0,263
nmme	nmme_precip_hcst_Apric_7-9_1991-2020	precip	JAS	7	LSDS	-0,331
cfsv2	cfsv2_sst_hcst_Apric_7-9_1991-2020	SST	JAS	5	LSDS	-0,330
nmme	nmme_sst_hcst_Apric_7-9_1991-2020	SST	JAS	5	LSDS	-0,330
cmc1	cmc1_precip_hcst_Apric_5-7_1991-2020	precip	MJJ	7	Onset date	-0,316
nasa	nasa_sst_hcst_Apric_5-7_1991-2020	SST	MJJ	2	Onset date	-0,315
nmme	nmme_sst_hcst_Apric_5-7_1991-2020	SST	MJJ	2	Onset date	-0,315
cmc2	cmc2_sst_hcst_Apric_6-8_1991-2020	SST	JJA	1	ESDS	-0,342
gfdl	gfdl_sst_hcst_Apric_5-7_1991-2020	SST	MJJ	1	ESDS	-0,341
cmc2	cmc2_sst_hcst_Apric_7_1991	SST	July	1	ESDS	-0,339
nasa	nasa_sst_hcst_Apric_7-9_1991-2020	SST	JAS	5	Cessation date	-0,258
ncar_ccsm4	ncar_ccsm4_precip_hcst_Apric_10_1991	precip	Oct	7	Cessation date	-0,258
ncar_ccsm4	ncar_ccsm4_sst_hcst_Apric_9-11_1991-2020	SST	SON	6	Cessation date	-0,257
ncar_ccsm4	ncar_ccsm4_precip_hcst_Apric_10_1991	precip	Oct	7	LSDS	-0,329
cfsv2	cfsv2_sst_hcst_Apric_10_1991	SST	Oct	4	LSDS	-0,327
nmme	nmme_sst_hcst_Apric_9_1991	SST	Sept	5	LSDS	-0,325

nmme	nmme_sst_hcst_Apric_7_1991	SST	July	2	Onset date	-0,315
cmc2	cmc2_sst_hcst_Apric_7_1991	SST	July	2	Onset date	-0,314
nasa	nasa_sst_hcst_Apric_7_1991	SST	July	2	Onset date	-0,314
cmc1	cmc1_sst_hcst_Apric_7_1991	SST	July	5	ESDS	-0,338
ncar_ccsm4	ncar_ccsm4_sst_hcst_Apric_7_1991	SST	July	2	ESDS	-0,337
ncar_ccsm4	ncar_ccsm4_sst_hcst_Apric_5-7_1991-2020	SST	MJJ	2	ESDS	-0,336
gfdl	gfdl_precip_hcst_Apric_8-10_1991-2020	precip	ASO	7	Cessation date	-0,257
cmc2	cmc2_sst_hcst_Apric_8-10_1991-2020	SST	ASO	4	Cessation date	-0,255
nasa	nasa_sst_hcst_Apric_7-9_1991-2020	SST	JAS	4	Cessation date	-0,252
ncar_ccsm4	ncar_ccsm4_precip_hcst_Apric_9_1991	precip	Sept	7	LSDS	-0,322
cmc2	cmc2_precip_hcst_Apric_8_1991	precip	Aug	7	LSDS	-0,320
ncar_ccsm4	ncar_ccsm4_precip_hcst_Apric_8_1991	precip	Aug	7	LSDS	-0,320
nasa	nasa_sst_hcst_Apric_6_1991	SST	June	2	Onset date	-0,313
cmc1	cmc1_precip_hcst_Apric_6-8_1991-2020	precip	JJA	7	Onset date	-0,313
cmc2	cmc2_sst_hcst_Apric_5-7_1991-2020	SST	MJJ	2	Onset date	-0,311
gfdl	gfdl_sst_hcst_Apric_7_1991	SST	July	1	ESDS	-0,333
nmme	nmme_sst_hcst_Apric_5-7_1991-2020	SST	MJJ	1	ESDS	-0,332
cfsv2	cfsv2_precip_hcst_Apric_6-8_1991-2020	precip	JJA	7	ESDS	-0,329
ncar_ccsm4	ncar_ccsm4_sst_hcst_Apric_9_1991	SST	Sept	4	Cessation date	-0,252
cmc2	cmc2_sst_hcst_Apric_8-10_1991-2020	SST	ASO	5	Cessation date	-0,250
cmc2	cmc2_sst_hcst_Apric_9-11_1991-2020	SST	SON	4	Cessation date	-0,247
cfsv2	cfsv2_sst_hcst_Apric_9-11_1991-2020	SST	SON	5	LSDS	-0,318
ncar_ccsm4	ncar_ccsm4_sst_hcst_Apric_8-10_1991-2020	SST	ASO	5	LSDS	-0,317
cfsv2	cfsv2_sst_hcst_Apric_8-10_1991-2020	SST	ASO	5	LSDS	-0,316
cmc1	cmc1_sst_hcst_Apric_6_1991	SST	June	5	Onset date	-0,311
cmc1	cmc1_precip_hcst_Apric_7_1991	precip	July	7	Onset date	-0,301
cmc2	cmc2_sst_hcst_Apric_7_1991	SST	July	5	Onset date	-0,300
cmc1	cmc1_sst_hcst_Apric_6-8_1991-2020	SST	JJA	5	ESDS	-0,328
ncar_ccsm4	ncar_ccsm4_precip_hcst_Apric_7_1991	precip	July	7	ESDS	-0,324
gfdl	gfdl_sst_hcst_Apric_6_1991	SST	June	2	ESDS	-0,320
ncar_ccsm4	ncar_ccsm4_precip_hcst_Apric_9-11_1991-2020	precip	SON	7	Cessation date	-0,246

ncar_ccsm4	ncar_ccsm4_precip_hcst_Apric_7-9_1991-2020	precip	JAS	7	Cessation date	-0,242
gfdl	gfdl_precip_hcst_Apric_7-9_1991-2020	precip	JAS	7	Cessation date	-0,238
ncar_ccsm4	ncar_ccsm4_sst_hcst_Apric_10_1991	SST	Oct	4	LSDS	-0,316
ncar_ccsm4	ncar_ccsm4_sst_hcst_Apric_8-10_1991-2020	SST	ASO	4	LSDS	-0,314
ncar_ccsm4	ncar_ccsm4_sst_hcst_Apric_10_1991	SST	Oct	5	LSDS	-0,313
cmc2	cmc2_sst_hcst_Apric_5-7_1991-2020	SST	MJJ	5	Onset date	-0,298
cmc2	cmc2_sst_hcst_Apric_6-8_1991-2020	SST	JJA	5	Onset date	-0,288
cmc1	cmc1_sst_hcst_Apric_5-7_1991-2020	SST	MJJ	5	Onset date	-0,282
cfsv2	cfsv2_sst_hcst_Apric_5-7_1991-2020	SST	MJJ	5	ESDS	-0,318
ncar_ccsm4	ncar_ccsm4_precip_hcst_Apric_5_1991	precip	May	7	ESDS	-0,318
cfsv2	cfsv2_sst_hcst_Apric_7_1991	SST	July	5	ESDS	-0,310
nasa	nasa_sst_hcst_Apric_8_1991	SST	Aug	5	Cessation date	-0,232
ncar_ccsm4	ncar_ccsm4_precip_hcst_Apric_8-10_1991-2020	precip	ASO	7	Cessation date	-0,232
gfdl	gfdl_precip_hcst_Apric_9_1991	precip	Sept	7	Cessation date	-0,228
gfdl	gfdl_precip_hcst_Apric_8_1991	precip	Aug	7	LSDS	-0,313
cfsv2	cfsv2_sst_hcst_Apric_10_1991	SST	Oct	5	LSDS	-0,311
nmme	nmme_precip_hcst_Apric_8_1991	precip	Aug	7	LSDS	-0,309
cmc1	cmc1_sst_hcst_Apric_6-8_1991-2020	SST	JJA	5	Onset date	-0,282
cmc1	cmc1_sst_hcst_Apric_7_1991	SST	July	5	Onset date	-0,263
cmc2	cmc2_sst_hcst_Apric_6_1991	SST	June	1	Onset date	-0.321
cfsv2	cfsv2_sst_hcst_Apric_6-8_1991-2020	SST	JJA	4	ESDS	-0,306
cfsv2	cfsv2_sst_hcst_Apric_6-8_1991-2020	SST	JJA	5	ESDS	-0,293
ncar_ccsm4	ncar_ccsm4_sst_hcst_Apric_5_1991	SST	May	6	ESDS	0,424
gfdl	gfdl_precip_hcst_Apric_10_1991	precip	Oct	7	Cessation date	-0,218
cmc2	cmc2_sst_hcst_Apric_9-11_1991-2020	SST	SON	5	Cessation date	-0,213
ncar_ccsm4	ncar_ccsm4_precip_hcst_Apric_8_1991	precip	Aug	7	Cessation date	0,301
ncar_ccsm4	ncar_ccsm4_sst_hcst_Apric_9-11_1991-2020	SST	SON	5	LSDS	-0,304
nasa	nasa_sst_hcst_Apric_9-11_1991-2020	SST	SON	2	LSDS	-0,298
ncar_ccsm4	ncar_ccsm4_sst_hcst_Apric_9-11_1991-2020	SST	SON	4	LSDS	-0,225

Appendix D: Correlation coefficients from the regression between the actual onset dates and the rainfall totals over various time windows within the season at station level in Niger

Appendix D (1/7)

RR totals' period	Abala			Abalak			Aguie			Ayarou		
	p-value	r-value	rsquare	p-value	r-value	rsquare	p-value	r-value	rsquare	p-value	r-value	rsquare
May	0,0002	-0,5506	0,3032	0,0004	-0,5264	0,2771	0,0000	-0,7088	0,5024	0,0066	-0,4177	0,1744
Jun	0,0039	-0,4411	0,1946	0,0016	-0,4764	0,2270	0,0134	-0,3833	0,1469	0,0085	-0,4058	0,1646
Jul	0,0797	-0,2769	0,0767	0,1897	-0,2090	0,0437	0,6370	0,0759	0,0058	0,3382	-0,1534	0,0235
Aug	0,8067	-0,0394	0,0016	0,2111	0,1995	0,0398	0,0616	0,2945	0,0867	0,8460	-0,0313	0,0010
MJ	0,0000	-0,5938	0,3526	0,0000	-0,6756	0,4564	0,0000	-0,6914	0,4781	0,0001	-0,5681	0,3227
JJ	0,0034	-0,4469	0,1997	0,0013	-0,4846	0,2349	0,3396	-0,1530	0,0234	0,0615	-0,2946	0,0868
JA	0,2642	-0,1785	0,0319	0,6887	0,0645	0,0042	0,1335	0,2383	0,0568	0,5311	-0,1007	0,0101
AMJ	0,0000	-0,5944	0,3534	0,0000	-0,6514	0,4243	0,0000	-0,6834	0,4670	0,0001	-0,5649	0,3191
MJJ	0,0001	-0,5611	0,3148	0,0000	-0,6174	0,3812	0,0122	-0,3878	0,1504	0,0084	-0,4061	0,1650
JJA	0,0623	-0,2938	0,0863	0,5086	-0,1062	0,0113	0,6566	0,0716	0,0051	0,2287	-0,1922	0,0369
JAS	0,4366	-0,1249	0,0156	0,6631	0,0701	0,0049	0,1130	0,2513	0,0631	0,6496	-0,0731	0,0053
Year	0,0650	-0,2909	0,0846	0,3926	-0,1371	0,0188	0,8643	-0,0275	0,0008	0,2528	-0,1828	0,0334

RR totals' period	Bankilare			Beylande			Birni N'Gaoure			Birni N'Konni		
	p-value	r-value	rsquare	p-value	r-value	rsquare	p-value	r-value	rsquare	p-value	r-value	rsquare
May	0,2050	-0,2021	0,0409	0,0000	-0,7420	0,5505	0,0038	-0,4417	0,1951	0,0003	-0,5412	0,2929
Jun	0,0002	-0,5523	0,3050	0,0370	-0,3269	0,1068	0,0627	-0,2933	0,0860	0,1036	-0,2578	0,0665
Jul	0,6189	-0,0800	0,0064	0,0328	-0,3341	0,1116	0,2543	-0,1822	0,0332	0,9852	0,0030	0,0000
Aug	0,1482	-0,2299	0,0529	0,2842	0,1713	0,0293	0,2978	-0,1666	0,0278	0,2929	0,1683	0,0283
MJ	0,0002	-0,5466	0,2988	0,0000	-0,6863	0,4710	0,0021	-0,4672	0,2183	0,0002	-0,5484	0,3008
JJ	0,0144	-0,3795	0,1441	0,0067	-0,4170	0,1739	0,0430	-0,3176	0,1009	0,3445	-0,1514	0,0229
JA	0,1597	-0,2237	0,0501	0,6295	-0,0776	0,0060	0,1361	-0,2368	0,0561	0,3792	0,1410	0,0199
AMJ	0,0001	-0,5816	0,3382	0,0000	-0,7048	0,4968	0,0016	-0,4784	0,2289	0,0000	-0,6495	0,4219
MJJ	0,0115	-0,3911	0,1530	0,0000	-0,6230	0,3882	0,0069	-0,4157	0,1728	0,0176	-0,3691	0,1362
JJA	0,0157	-0,3751	0,1407	0,2666	-0,1776	0,0315	0,0379	-0,3254	0,1059	0,8462	0,0312	0,0010
JAS	0,1860	-0,2107	0,0444	0,7314	-0,0553	0,0031	0,6083	-0,0824	0,0068	0,3977	0,1357	0,0184
Year	0,0311	-0,3372	0,1137	0,0380	-0,3252	0,1058	0,0967	-0,2630	0,0691	0,5999	-0,0844	0,0071

Appendix D (2/7)

RR totals' period	Bouza			Dakoro			Dan Issa			Dargol		
	p-value	r-value	rsquare	p-value	r-value	rsquare	p-value	r-value	rsquare	p-value	r-value	rsquare
May	0,0002	-0,5516	0,3043	0,0880	-0,2698	0,0728	0,0002	-0,5475	0,2997	0,0002	-0,5535	0,3064
Jun	0,1228	-0,2449	0,0600	0,0015	-0,4810	0,2314	0,0567	-0,3000	0,0900	0,0043	-0,4364	0,1904
Jul	0,0903	-0,2680	0,0718	0,0866	-0,2710	0,0734	0,9051	0,0192	0,0004	0,9785	-0,0043	0,0000
Aug	0,0391	-0,3236	0,1047	0,5164	-0,1043	0,0109	0,5382	0,0990	0,0098	0,0942	-0,2649	0,0702
MJ	0,0001	-0,5806	0,3371	0,0002	-0,5443	0,2962	0,0001	-0,5682	0,3229	0,0001	-0,5720	0,3272
JJ	0,0293	-0,3407	0,1160	0,0018	-0,4735	0,2242	0,5168	-0,1042	0,0109	0,2201	-0,1957	0,0383
JA	0,0095	-0,4004	0,1604	0,1428	-0,2329	0,0543	0,6364	0,0761	0,0058	0,2253	-0,1936	0,0375
AMJ	0,0000	-0,6642	0,4412	0,0002	-0,5473	0,2996	0,0000	-0,6331	0,4008	0,0001	-0,5822	0,3389
MJJ	0,0002	-0,5459	0,2980	0,0003	-0,5362	0,2875	0,0776	-0,2787	0,0777	0,0708	-0,2851	0,0813
JJA	0,0024	-0,4608	0,2123	0,0172	-0,3701	0,1370	0,9813	-0,0038	0,0000	0,0668	-0,2891	0,0836
JAS	0,0360	-0,3285	0,1079	0,0961	-0,2634	0,0694	0,5910	0,0864	0,0075	0,2663	-0,1777	0,0316
Year	0,0003	-0,5395	0,2910	0,0039	-0,4416	0,1950	0,5309	-0,1007	0,0101	0,0271	-0,3453	0,1192

RR totals' period	Diffa			Dioundou			Dogondoutchi			Dosso		
	p-value	r-value	rsquare	p-value	r-value	rsquare	p-value	r-value	rsquare	p-value	r-value	rsquare
May	0,0000	-0,6389	0,4082	0,0000	-0,6081	0,3697	0,0008	-0,5052	0,2552	0,0000	-0,6072	0,3687
Jun	0,0007	-0,5061	0,2561	0,1490	-0,2295	0,0527	0,0014	-0,4826	0,2329	0,0327	-0,3342	0,1117
Jul	0,3547	-0,1483	0,0220	0,7416	-0,0531	0,0028	0,7223	-0,0572	0,0033	0,4479	-0,1218	0,0148
Aug	0,3765	-0,1418	0,0201	0,6309	-0,0773	0,0060	0,0146	0,3786	0,1433	0,6867	0,0649	0,0042
MJ	0,0000	-0,7030	0,4942	0,0002	-0,5492	0,3016	0,0000	-0,6434	0,4140	0,0000	-0,6088	0,3706
JJ	0,0120	-0,3886	0,1510	0,2138	-0,1984	0,0393	0,0088	-0,4038	0,1630	0,0529	-0,3045	0,0927
JA	0,2117	-0,1993	0,0397	0,5598	-0,0938	0,0088	0,0752	0,2809	0,0789	0,9209	-0,0160	0,0003
AMJ	0,0000	-0,6927	0,4799	0,0000	-0,6619	0,4382	0,0000	-0,6183	0,3822	0,0000	-0,6469	0,4185
MJJ	0,0012	-0,4868	0,2370	0,0035	-0,4451	0,1981	0,0001	-0,5722	0,3274	0,0019	-0,4700	0,2209
JJA	0,0258	-0,3479	0,1211	0,2804	-0,1727	0,0298	0,6877	0,0647	0,0042	0,4055	-0,1335	0,0178
JAS	0,2041	-0,2025	0,0410	0,6974	-0,0626	0,0039	0,0820	0,2749	0,0756	0,9879	0,0024	0,0000
Year	0,0190	-0,3649	0,1332	0,0066	-0,4178	0,1745	0,3170	-0,1602	0,0257	0,1440	-0,2322	0,0539

Appendix D (3/7)

RR totals' period	Falmeye			Filingue			Gaya			Gazaoua		
	p-value	r-value	rsquare	p-value	r-value	rsquare	p-value	r-value	rsquare	p-value	r-value	rsquare
May	0,0002	-0,5543	0,3072	0,0022	-0,4652	0,2164	0,0495	-0,3088	0,0953	0,0002	-0,5531	0,3059
Jun	0,7879	-0,0433	0,0019	0,0180	-0,3678	0,1353	0,6599	-0,0708	0,0050	0,0127	-0,3860	0,1490
Jul	0,8329	0,0340	0,0012	0,5166	-0,1042	0,0109	0,7963	0,0416	0,0017	0,3779	-0,1414	0,0200
Aug	0,4335	-0,1257	0,0158	0,2159	0,1975	0,0390	0,2965	0,1671	0,0279	0,6148	-0,0810	0,0066
MJ	0,0241	-0,3518	0,1238	0,0006	-0,5147	0,2649	0,1163	-0,2491	0,0621	0,0000	-0,6033	0,3639
JJ	0,9860	0,0028	0,0000	0,1130	-0,2513	0,0632	0,9499	-0,0101	0,0001	0,0598	-0,2965	0,0879
JA	0,6790	-0,0666	0,0044	0,6890	0,0644	0,0042	0,3666	0,1447	0,0209	0,4016	-0,1346	0,0181
AMJ	0,0010	-0,4952	0,2452	0,0008	-0,5054	0,2554	0,0149	-0,3778	0,1427	0,0001	-0,5847	0,3419
MJJ	0,2061	-0,2017	0,0407	0,0160	-0,3739	0,1398	0,3106	-0,1623	0,0263	0,0034	-0,4474	0,2001
JJA	0,6153	-0,0809	0,0065	0,7698	-0,0471	0,0022	0,4911	0,1106	0,0122	0,1218	-0,2455	0,0603
JAS	0,6980	-0,0625	0,0039	0,6543	0,0721	0,0052	0,2707	0,1761	0,0310	0,6550	-0,0719	0,0052
Year	0,1843	-0,2115	0,0447	0,3302	-0,1560	0,0243	0,7902	-0,0429	0,0018	0,1150	-0,2500	0,0625

RR totals' period	Goudoumaria			Goure			Guecheme			Guidan Roundji		
	p-value	r-value	rsquare	p-value	r-value	rsquare	p-value	r-value	rsquare	p-value	r-value	rsquare
May	0,8519	-0,0301	0,0009	0,0704	-0,2854	0,0815	0,0003	-0,5329	0,2840	0,0033	-0,4485	0,2012
Jun	0,0001	-0,5706	0,3255	0,0000	-0,6643	0,4413	0,1193	-0,2471	0,0611	0,0079	-0,4092	0,1674
Jul	0,1754	-0,2158	0,0466	0,7692	-0,0473	0,0022	0,4823	0,1129	0,0127	0,3527	-0,1489	0,0222
Aug	0,0560	-0,3008	0,0905	0,3444	-0,1515	0,0229	0,4784	-0,1139	0,0130	0,9160	0,0170	0,0003
MJ	0,0005	-0,5171	0,2674	0,0000	-0,7229	0,5226	0,0017	-0,4749	0,2255	0,0001	-0,5741	0,3296
JJ	0,0209	-0,3598	0,1294	0,0004	-0,5284	0,2792	0,8164	-0,0374	0,0014	0,0287	-0,3418	0,1168
JA	0,0639	-0,2921	0,0853	0,3620	-0,1461	0,0213	0,9217	-0,0158	0,0003	0,6915	-0,0639	0,0041
AMJ	0,0007	-0,5088	0,2589	0,0000	-0,7085	0,5019	0,0005	-0,5174	0,2677	0,0000	-0,6227	0,3878
MJJ	0,0205	-0,3608	0,1301	0,0000	-0,5929	0,3516	0,1213	-0,2458	0,0604	0,0027	-0,4570	0,2088
JJA	0,0176	-0,3690	0,1362	0,0147	-0,3785	0,1433	0,5573	-0,0944	0,0089	0,2575	-0,1810	0,0328
JAS	0,0304	-0,3385	0,1146	0,3565	-0,1478	0,0218	0,7291	-0,0558	0,0031	0,4599	-0,1187	0,0141
Year	0,0075	-0,4116	0,1694	0,0119	-0,3892	0,1515	0,1180	-0,2480	0,0615	0,0445	-0,3155	0,0995

Appendix D (4/7)

RR totals' period	Illela			Kao			Kornaka			Loga		
	p-value	r-value	rsquare	p-value	r-value	rsquare	p-value	r-value	rsquare	p-value	r-value	rsquare
May	0,0012	-0,4888	0,2389	0,0010	-0,4966	0,2466	0,6659	-0,0695	0,0048	0,0019	-0,4716	0,2224
Jun	0,1237	-0,2443	0,0597	0,0098	-0,3990	0,1592	0,0148	-0,3780	0,1429	0,0092	-0,4020	0,1616
Jul	0,8279	-0,0350	0,0012	0,8481	-0,0309	0,0010	0,8785	-0,0246	0,0006	0,6676	-0,0691	0,0048
Aug	0,1521	0,2277	0,0519	0,0474	-0,3115	0,0970	0,6247	-0,0787	0,0062	0,9498	0,0102	0,0001
MJ	0,0001	-0,5741	0,3295	0,0001	-0,5742	0,3297	0,0236	-0,3529	0,1246	0,0001	-0,5795	0,3358
JJ	0,3223	-0,1585	0,0251	0,1649	-0,2211	0,0489	0,3184	-0,1598	0,0255	0,0983	-0,2617	0,0685
JA	0,2773	0,1737	0,0302	0,1211	-0,2459	0,0605	0,7150	-0,0588	0,0035	0,8445	-0,0316	0,0010
AMJ	0,0001	-0,5611	0,3148	0,0000	-0,6040	0,3648	0,0304	-0,3385	0,1146	0,0000	-0,6379	0,4070
MJJ	0,0079	-0,4090	0,1673	0,0262	-0,3471	0,1205	0,2868	-0,1704	0,0290	0,0010	-0,4963	0,2463
JJA	0,6094	0,0822	0,0068	0,0383	-0,3248	0,1055	0,3818	-0,1403	0,0197	0,2921	-0,1686	0,0284
JAS	0,3149	0,1609	0,0259	0,1523	-0,2276	0,0518	0,9171	-0,0168	0,0003	0,4074	0,1329	0,0177
Year	0,3547	-0,1483	0,0220	0,0320	-0,3356	0,1126	0,5784	-0,0894	0,0080	0,0478	-0,3110	0,0967

RR totals' period	Bankilare			Beylande			Birni N'Gaoure			Birni N'Konni		
	p-value	r-value	rsquare	p-value	r-value	rsquare	p-value	r-value	rsquare	p-value	r-value	rsquare
May	0,2050	-0,2021	0,0409	0,0000	-0,7420	0,5505	0,0038	-0,4417	0,1951	0,0003	-0,5412	0,2929
Jun	0,0002	-0,5523	0,3050	0,0370	-0,3269	0,1068	0,0627	-0,2933	0,0860	0,1036	-0,2578	0,0665
Jul	0,6189	-0,0800	0,0064	0,0328	-0,3341	0,1116	0,2543	-0,1822	0,0332	0,9852	0,0030	0,0000
Aug	0,1482	-0,2299	0,0529	0,2842	0,1713	0,0293	0,2978	-0,1666	0,0278	0,2929	0,1683	0,0283
MJ	0,0002	-0,5466	0,2988	0,0000	-0,6863	0,4710	0,0021	-0,4672	0,2183	0,0002	-0,5484	0,3008
JJ	0,0144	-0,3795	0,1441	0,0067	-0,4170	0,1739	0,0430	-0,3176	0,1009	0,3445	-0,1514	0,0229
JA	0,1597	-0,2237	0,0501	0,6295	-0,0776	0,0060	0,1361	-0,2368	0,0561	0,3792	0,1410	0,0199
AMJ	0,0001	-0,5816	0,3382	0,0000	-0,7048	0,4968	0,0016	-0,4784	0,2289	0,0000	-0,6495	0,4219
MJJ	0,0115	-0,3911	0,1530	0,0000	-0,6230	0,3882	0,0069	-0,4157	0,1728	0,0176	-0,3691	0,1362
JJA	0,0157	-0,3751	0,1407	0,2666	-0,1776	0,0315	0,0379	-0,3254	0,1059	0,8462	0,0312	0,0010
JAS	0,1860	-0,2107	0,0444	0,7314	-0,0553	0,0031	0,6083	-0,0824	0,0068	0,3977	0,1357	0,0184
Year	0,0311	-0,3372	0,1137	0,0380	-0,3252	0,1058	0,0967	-0,2630	0,0691	0,5999	-0,0844	0,0071

Appendix D (5/7)

RR totals' period	Madaoua			Madarounfa			Magaria			Maine Soroa		
	p-value	r-value	rsquare	p-value	r-value	rsquare	p-value	r-value	rsquare	p-value	r-value	rsquare
May	0,0002	-0,5427	0,2945	0,0003	-0,5368	0,2882	0,0007	-0,5093	0,2594	0,3076	-0,1633	0,0267
Jun	0,0360	-0,3285	0,1079	0,4845	-0,1123	0,0126	0,0000	-0,6127	0,3754	0,0000	-0,6786	0,4606
Jul	0,4018	-0,1345	0,0181	0,3536	0,1487	0,0221	0,5575	-0,0943	0,0089	0,5388	-0,0988	0,0098
Aug	0,6091	-0,0823	0,0068	0,6388	-0,0755	0,0057	0,0750	-0,2811	0,0790	0,2293	-0,1919	0,0368
MJ	0,0001	-0,5735	0,3289	0,0011	-0,4907	0,2408	0,0000	-0,6680	0,4462	0,0000	-0,7019	0,4927
JJ	0,1252	-0,2434	0,0592	0,5520	0,0956	0,0091	0,0019	-0,4699	0,2208	0,0139	-0,3812	0,1453
JA	0,3990	-0,1353	0,0183	0,6620	0,0704	0,0050	0,0929	-0,2659	0,0707	0,1900	-0,2089	0,0436
AMJ	0,0004	-0,5304	0,2813	0,0001	-0,5757	0,3314	0,0000	-0,6739	0,4542	0,0000	-0,7092	0,5029
MJJ	0,0072	-0,4137	0,1711	0,3309	-0,1557	0,0243	0,0002	-0,5522	0,3049	0,0108	-0,3941	0,1553
JJA	0,1837	-0,2118	0,0449	0,8304	0,0345	0,0012	0,0014	-0,4825	0,2328	0,0119	-0,3892	0,1515
JAS	0,5424	-0,0979	0,0096	0,5564	0,0946	0,0089	0,1801	-0,2135	0,0456	0,1114	-0,2524	0,0637
Year	0,1025	-0,2587	0,0669	0,4087	-0,1326	0,0176	0,0017	-0,4750	0,2256	0,0104	-0,3958	0,1567

RR totals' period	Maradi Aero			Matameye			Mayahi			Myrriah		
	p-value	r-value	rsquare	p-value	r-value	rsquare	p-value	r-value	rsquare	p-value	r-value	rsquare
May	0,0001	-0,5597	0,3133	0,0004	-0,5232	0,2737	0,0001	-0,5692	0,3240	0,0109	-0,3935	0,1548
Jun	0,0308	-0,3377	0,1141	0,0138	-0,3818	0,1457	0,0001	-0,5890	0,3469	0,0004	-0,5302	0,2811
Jul	0,1567	-0,2253	0,0508	0,1931	-0,2075	0,0430	0,1524	0,2276	0,0518	0,1630	0,2220	0,0493
Aug	0,1011	0,2597	0,0674	0,3862	0,1390	0,0193	0,3626	0,1459	0,0213	0,3974	0,1357	0,0184
MJ	0,0000	-0,6133	0,3762	0,0000	-0,6235	0,3887	0,0000	-0,7450	0,5550	0,0001	-0,5686	0,3233
JJ	0,0222	-0,3563	0,1269	0,0314	-0,3365	0,1133	0,5476	-0,0967	0,0093	0,6036	-0,0835	0,0070
JA	0,8200	0,0367	0,0013	0,7110	-0,0597	0,0036	0,1205	0,2463	0,0607	0,1340	0,2380	0,0567
AMJ	0,0000	-0,5982	0,3579	0,0000	-0,6150	0,3782	0,0000	-0,7363	0,5421	0,0001	-0,5741	0,3296
MJJ	0,0003	-0,5346	0,2858	0,0011	-0,4929	0,2429	0,0910	-0,2674	0,0715	0,3299	-0,1561	0,0244
JJA	0,5335	-0,1001	0,0100	0,2648	-0,1783	0,0318	0,7953	0,0418	0,0017	0,7854	0,0439	0,0019
JAS	0,5664	0,0922	0,0085	0,7742	-0,0462	0,0021	0,0758	0,2803	0,0786	0,0689	0,2870	0,0824
Year	0,3463	-0,1509	0,0228	0,0916	-0,2669	0,0712	0,8950	0,0213	0,0005	0,6484	0,0734	0,0054

Appendix D (6/7)

RR totals' period	N'guigmi			Niamey Aero			Niamey Ville			Ouallam		
	p-value	r-value	rsquare	p-value	r-value	rsquare	p-value	r-value	rsquare	p-value	r-value	rsquare
May	0,6101	-0,0820	0,0067	0,0623	-0,2938	0,0863	0,0002	-0,5489	0,3012	0,0000	-0,6165	0,3800
Jun	0,0004	-0,5312	0,2822	0,0379	-0,3254	0,1059	0,0235	-0,3531	0,1247	0,0004	-0,5252	0,2758
Jul	0,4115	-0,1318	0,0174	0,3575	0,1475	0,0217	0,4507	0,1211	0,0147	0,5253	-0,1021	0,0104
Aug	0,4399	-0,1240	0,0154	0,7702	-0,0471	0,0022	0,6788	-0,0667	0,0044	0,5538	0,0952	0,0091
MJ	0,0007	-0,5096	0,2597	0,0171	-0,3705	0,1373	0,0006	-0,5135	0,2637	0,0000	-0,6427	0,4130
JJ	0,0497	-0,3085	0,0952	0,6149	-0,0809	0,0066	0,4359	-0,1251	0,0156	0,0188	-0,3654	0,1335
JA	0,2872	-0,1703	0,0290	0,7629	0,0486	0,0024	0,8469	0,0311	0,0010	0,9810	-0,0038	0,0000
AMJ	0,0012	-0,4880	0,2382	0,0015	-0,4790	0,2295	0,0000	-0,6278	0,3942	0,0000	-0,6463	0,4178
MJJ	0,0489	-0,3096	0,0958	0,2801	-0,1728	0,0298	0,0798	-0,2768	0,0766	0,0013	-0,4841	0,2344
JJA	0,0610	-0,2951	0,0871	0,5727	-0,0907	0,0082	0,4128	-0,1314	0,0173	0,1872	-0,2101	0,0442
JAS	0,1695	-0,2187	0,0478	0,7611	0,0490	0,0024	0,9508	-0,0099	0,0001	0,9046	-0,0193	0,0004
Year	0,0488	-0,3097	0,0959	0,2792	-0,1731	0,0300	0,1145	-0,2503	0,0627	0,0365	-0,3276	0,1074

RR totals' period	Say			Tahoua Aero			Tchintabaraden			Tera		
	p-value	r-value	rsquare	p-value	r-value	rsquare	p-value	r-value	rsquare	p-value	r-value	rsquare
May	0,0001	-0,5760	0,3318	0,0369	-0,3271	0,1070	0,0017	-0,4744	0,2250	0,0005	-0,5202	0,2706
Jun	0,0003	-0,5417	0,2934	0,0946	-0,2645	0,0700	0,0001	-0,5609	0,3146	0,0038	-0,4421	0,1955
Jul	0,3960	-0,1361	0,0185	0,3358	-0,1542	0,0238	0,0814	-0,2754	0,0758	0,4021	-0,1344	0,0181
Aug	0,5312	0,1007	0,0101	0,0499	0,3082	0,0950	0,6938	-0,0634	0,0040	0,7076	-0,0604	0,0036
MJ	0,0000	-0,6933	0,4807	0,0037	-0,4433	0,1965	0,0000	-0,7358	0,5413	0,0000	-0,6900	0,4761
JJ	0,0076	-0,4110	0,1689	0,0948	-0,2644	0,0699	0,0023	-0,4633	0,2146	0,0181	-0,3675	0,1351
JA	0,8876	0,0228	0,0005	0,3038	0,1646	0,0271	0,1354	-0,2372	0,0563	0,5009	-0,1082	0,0117
AMJ	0,0000	-0,7431	0,5521	0,0041	-0,4384	0,1922	0,0000	-0,7347	0,5397	0,0000	-0,6450	0,4161
MJJ	0,0002	-0,5518	0,3044	0,0215	-0,3581	0,1282	0,0001	-0,5732	0,3285	0,0001	-0,5676	0,3222
JJA	0,3800	-0,1408	0,0198	0,6696	0,0687	0,0047	0,0080	-0,4084	0,1668	0,1645	-0,2212	0,0489
JAS	0,7469	0,0520	0,0027	0,7163	0,0585	0,0034	0,1617	-0,2227	0,0496	0,4071	-0,1330	0,0177
Year	0,1994	-0,2046	0,0419	0,5237	-0,1025	0,0105	0,0023	-0,4636	0,2149	0,0564	-0,3003	0,0902

Appendix D (7/7)

RR totals' period	Tessaoua			Tibiri Douchi			Tillabery			Torodi		
	p-value	r-value	rsquare	p-value	r-value	rsquare	p-value	r-value	rsquare	p-value	r-value	rsquare
May	0,2405	-0,1875	0,0351	0,0002	-0,5462	0,2983	0,0382	-0,3249	0,1055	0,0017	-0,4746	0,2253
Jun	0,0717	-0,2842	0,0808	0,0003	-0,5337	0,2848	0,2584	-0,1806	0,0326	0,1206	-0,2463	0,0607
Jul	0,0958	-0,2636	0,0695	0,7402	0,0534	0,0029	0,7985	0,0411	0,0017	0,1561	0,2256	0,0509
Aug	0,1018	-0,2591	0,0672	0,1504	-0,2287	0,0523	0,7036	0,0613	0,0038	0,9011	-0,0200	0,0004
MJ	0,0451	-0,3147	0,0991	0,0000	-0,6704	0,4495	0,0617	-0,2944	0,0866	0,0036	-0,4441	0,1972
JJ	0,0179	-0,3680	0,1354	0,0754	-0,2807	0,0788	0,7657	-0,0480	0,0023	0,9322	0,0137	0,0002
JA	0,0426	-0,3183	0,1013	0,3323	-0,1553	0,0241	0,6725	0,0681	0,0046	0,5892	0,0869	0,0075
AMJ	0,0411	-0,3204	0,1026	0,0000	-0,6917	0,4784	0,0731	-0,2829	0,0800	0,0001	-0,5618	0,3156
MJJ	0,0084	-0,4062	0,1650	0,0014	-0,4822	0,2325	0,4439	-0,1229	0,0151	0,2654	-0,1780	0,0317
JJA	0,0179	-0,3682	0,1355	0,0273	-0,3448	0,1189	0,9611	0,0079	0,0001	0,9607	-0,0079	0,0001
JAS	0,0844	-0,2728	0,0744	0,8652	-0,0274	0,0007	0,6097	0,0821	0,0067	0,1945	0,2068	0,0428
Year	0,0146	-0,3789	0,1436	0,0284	-0,3426	0,1173	0,9306	-0,0140	0,0002	0,7000	-0,0620	0,0038

RR totals' period	Toukounous			Zinder Aero		
	p-value	r-value	rsquare	p-value	r-value	rsquare
May	0,7318	0,0552	0,0030	0,0000	-0,6666	0,4444
Jun	0,0002	-0,5483	0,3007	0,0010	-0,4954	0,2454
Jul	0,3328	-0,1551	0,0241	0,9763	-0,0048	0,0000
Aug	0,5046	0,1072	0,0115	0,5318	0,1005	0,0101
MJ	0,0037	-0,4429	0,1962	0,0000	-0,6521	0,4252
JJ	0,0077	-0,4104	0,1684	0,1053	-0,2566	0,0659
JA	0,9673	-0,0066	0,0000	0,6830	0,0657	0,0043
AMJ	0,0037	-0,4435	0,1967	0,0000	-0,6461	0,4175
MJJ	0,0078	-0,4100	0,1681	0,0131	-0,3844	0,1477
JJA	0,1684	-0,2193	0,0481	0,5153	-0,1046	0,0109
JAS	0,6693	-0,0688	0,0047	0,2464	0,1852	0,0343
Year	0,1341	-0,2379	0,0566	0,6924	-0,0637	0,0041

